Appendix-2 Attachment-1
Tube-to-TSP wear depth diagram for Unit-2/3

1. Introduction

This attachment provides the tube-to-TSP wear depth at each TSP elevation for SONGS-2/3 RSGs.

2. Tube-to-TSP wear depth

The following figures provide the tube-to-TSP wear depth in %. Note that the figures do not include the tubes with the wear in U-bend region.

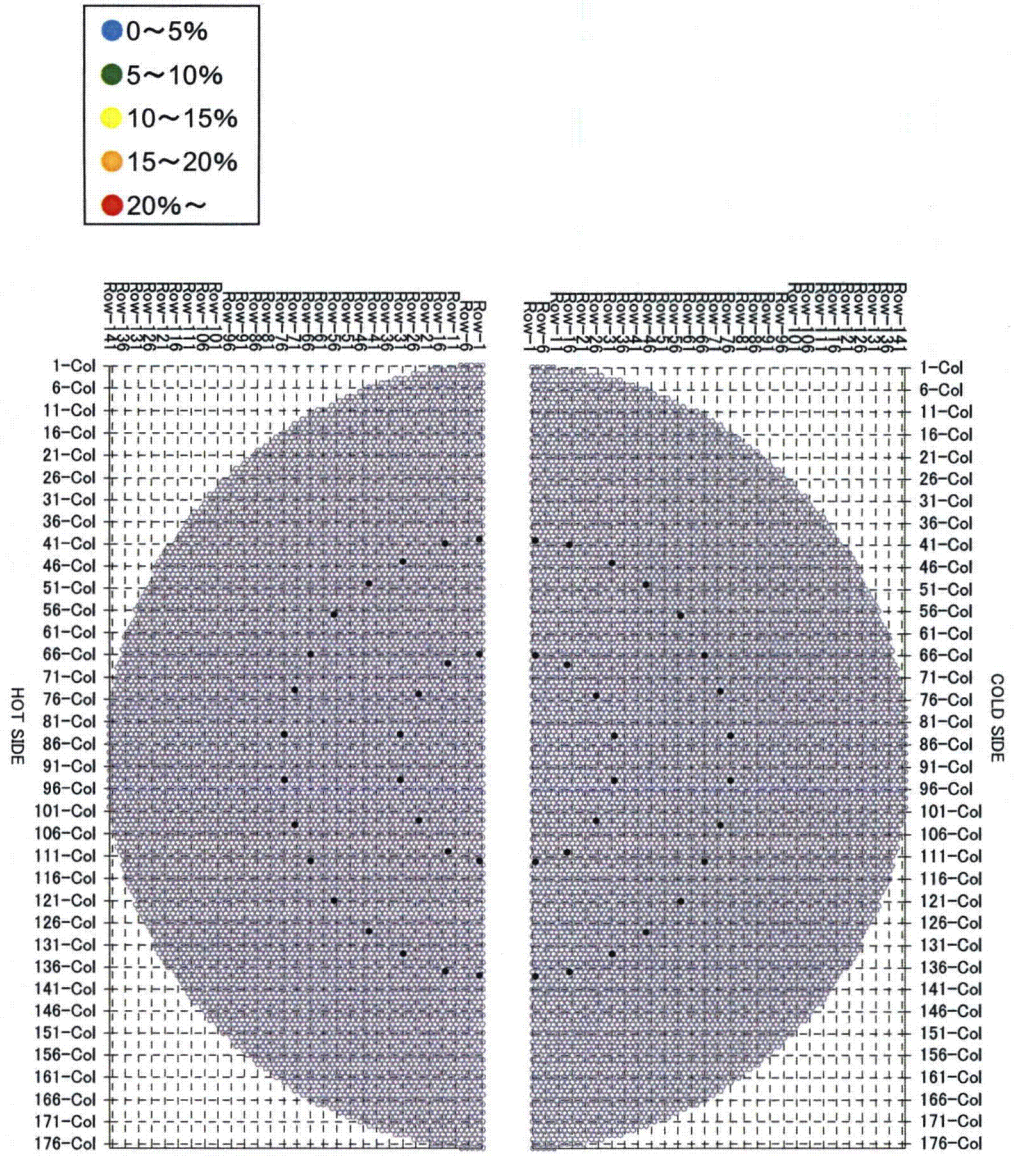

2A_#1TSP

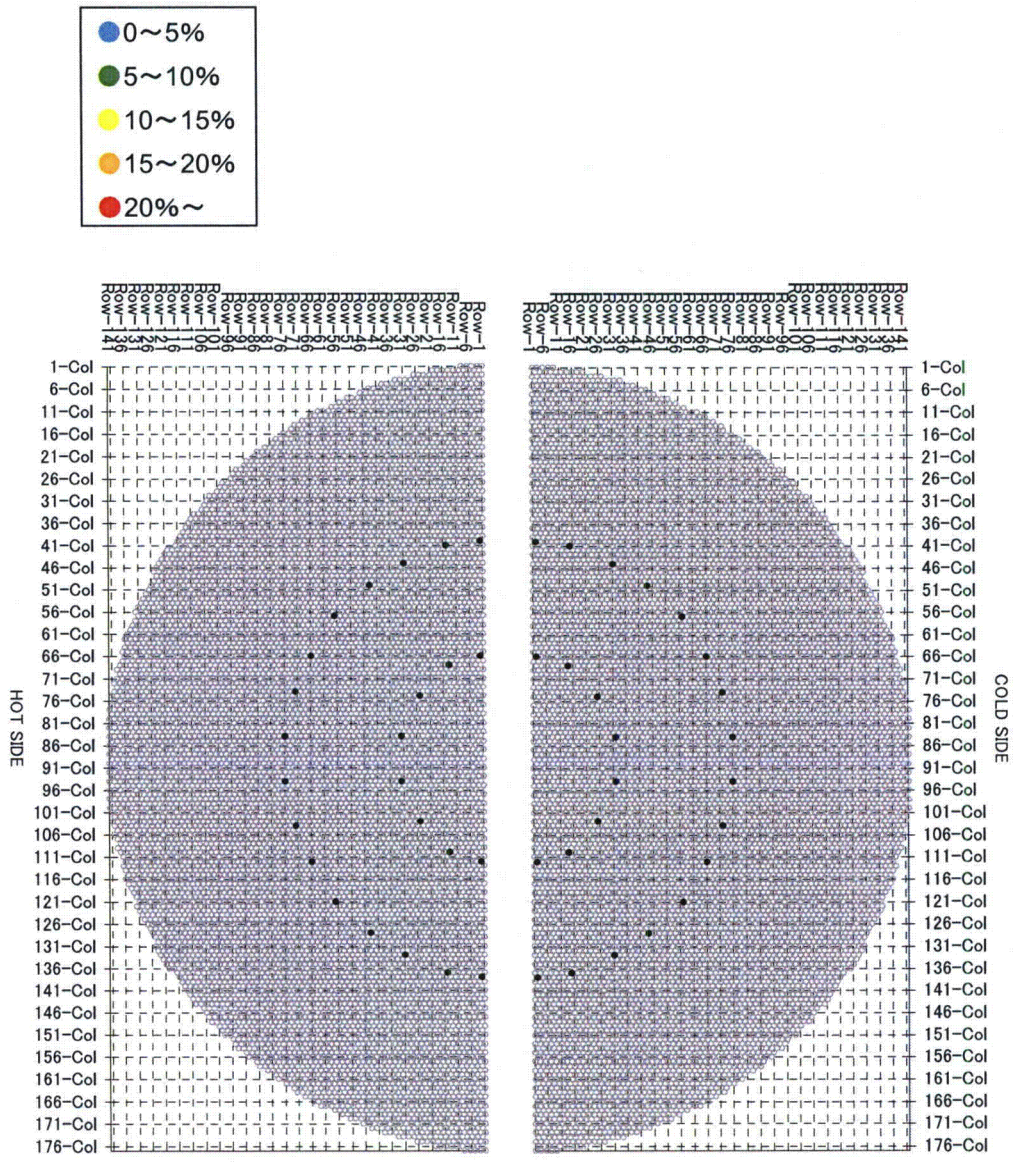

2A_#2TSP

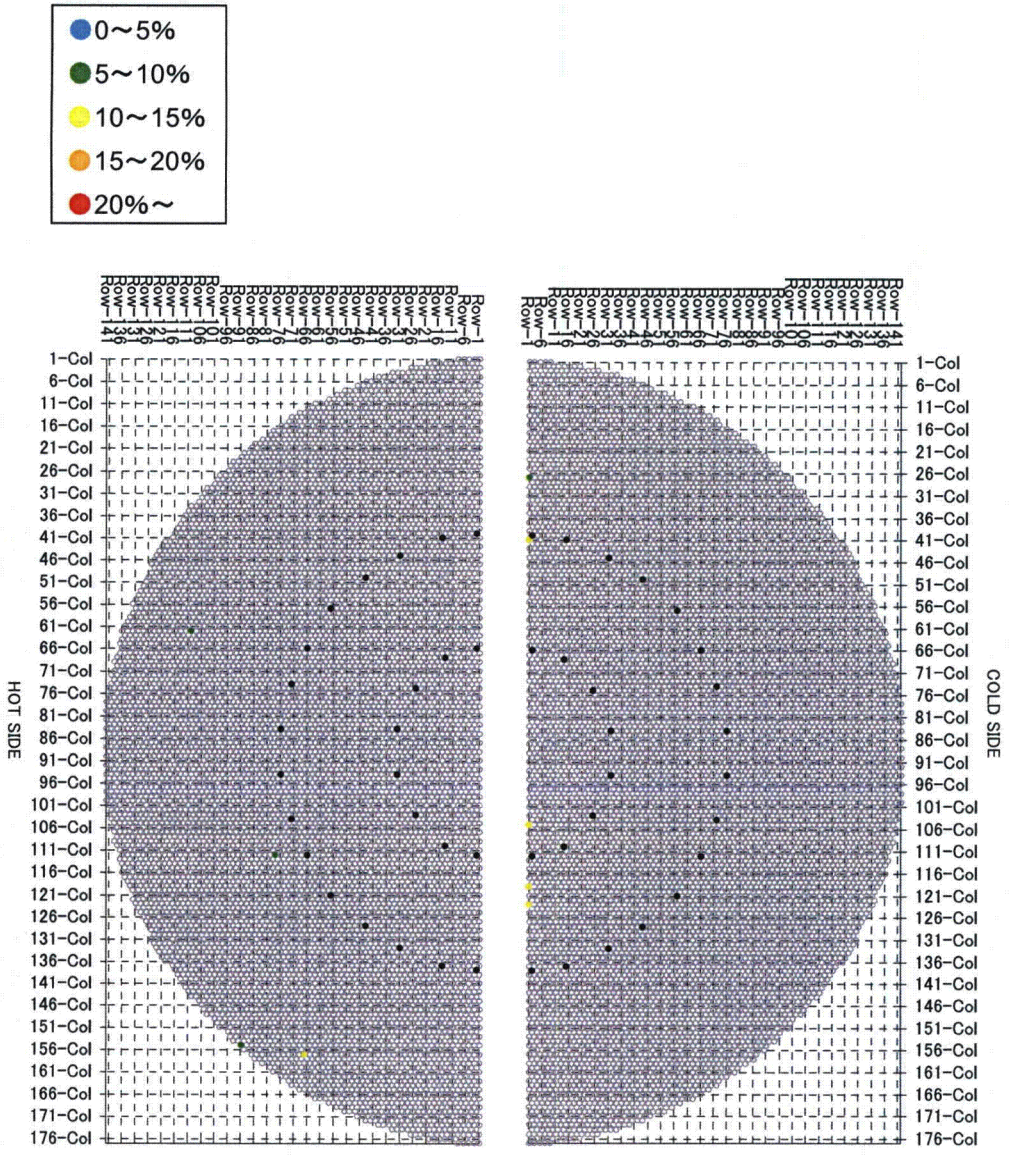

2A_#3TSP

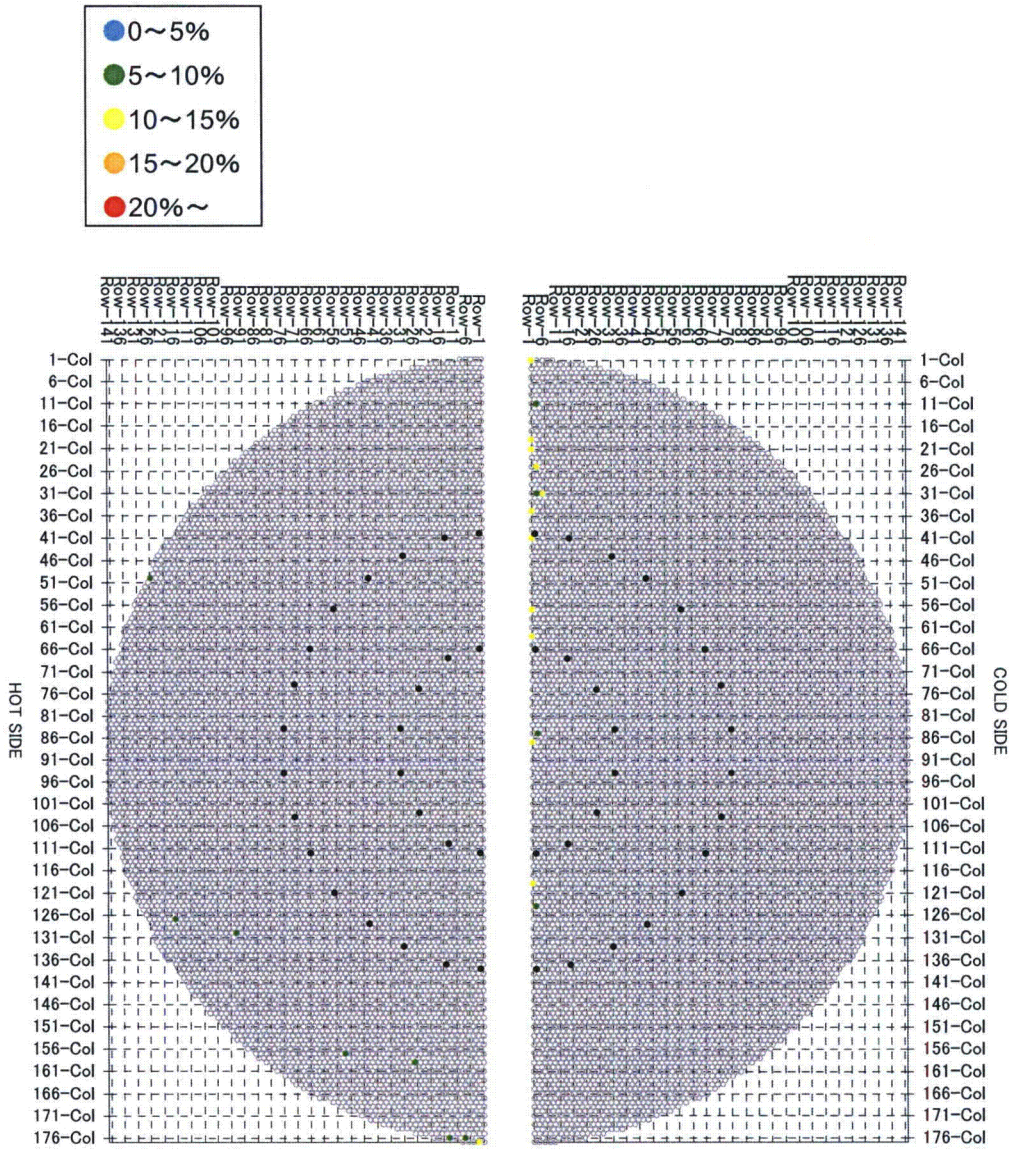
0～5%
5～10%
10～15%
15～20%
20%～
HOT SIDE
COLD SIDE
1-Col
6-Col
11-Col
16-Col
21-Col
26-Col
31-Col
36-Col
41-Col
46-Col
51-Col
56-Col
61-Col
66-Col
71-Col
76-Col
81-Col
86-Col
91-Col
96-Col
101-Col
106-Col
111-Col
116-Col
121-Col
126-Col
131-Col
136-Col
141-Col
146-Col
151-Col
156-Col
161-Col
166-Col
171-Col
176-Col

2A_#4TSP

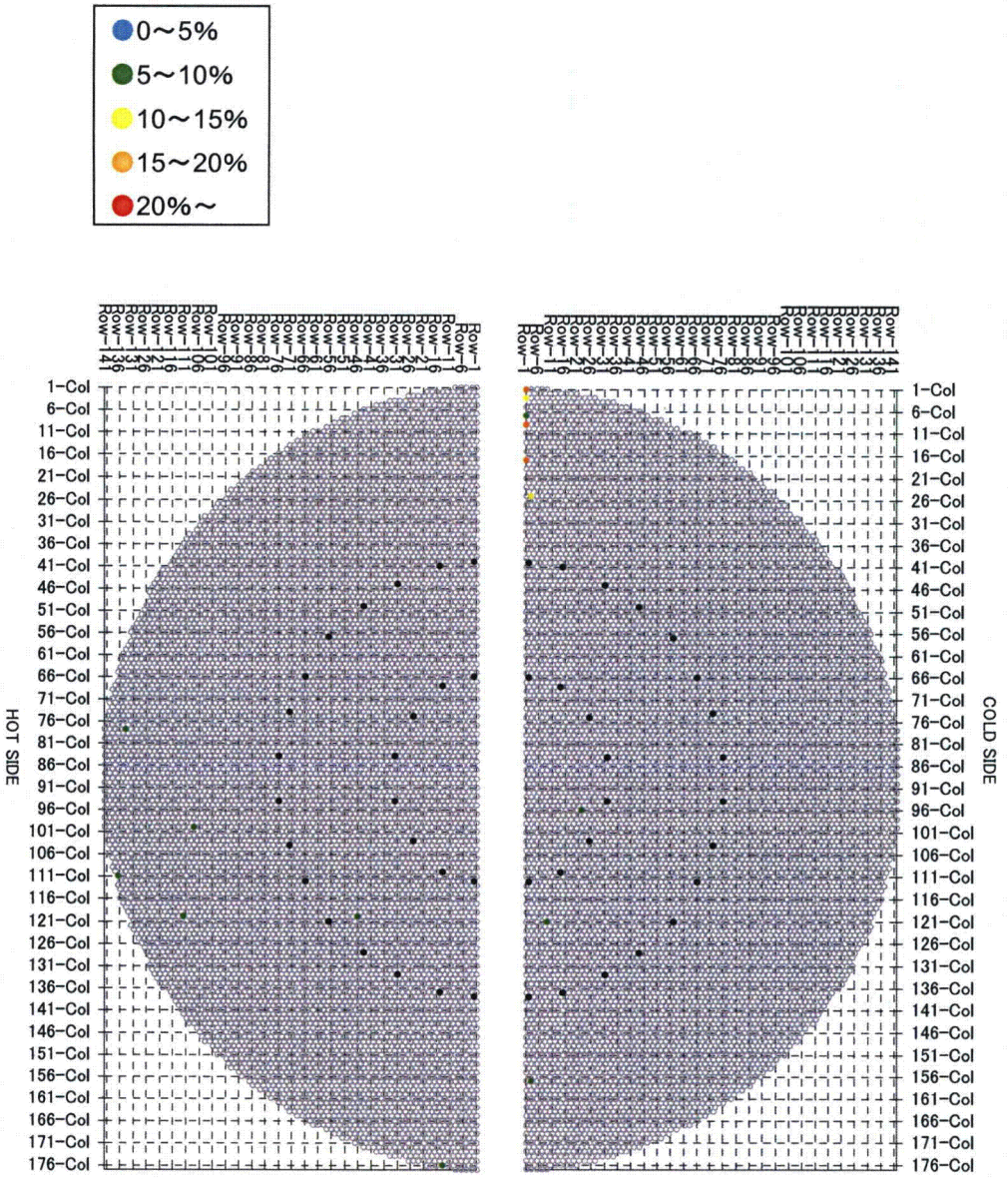

2A_#5TSP

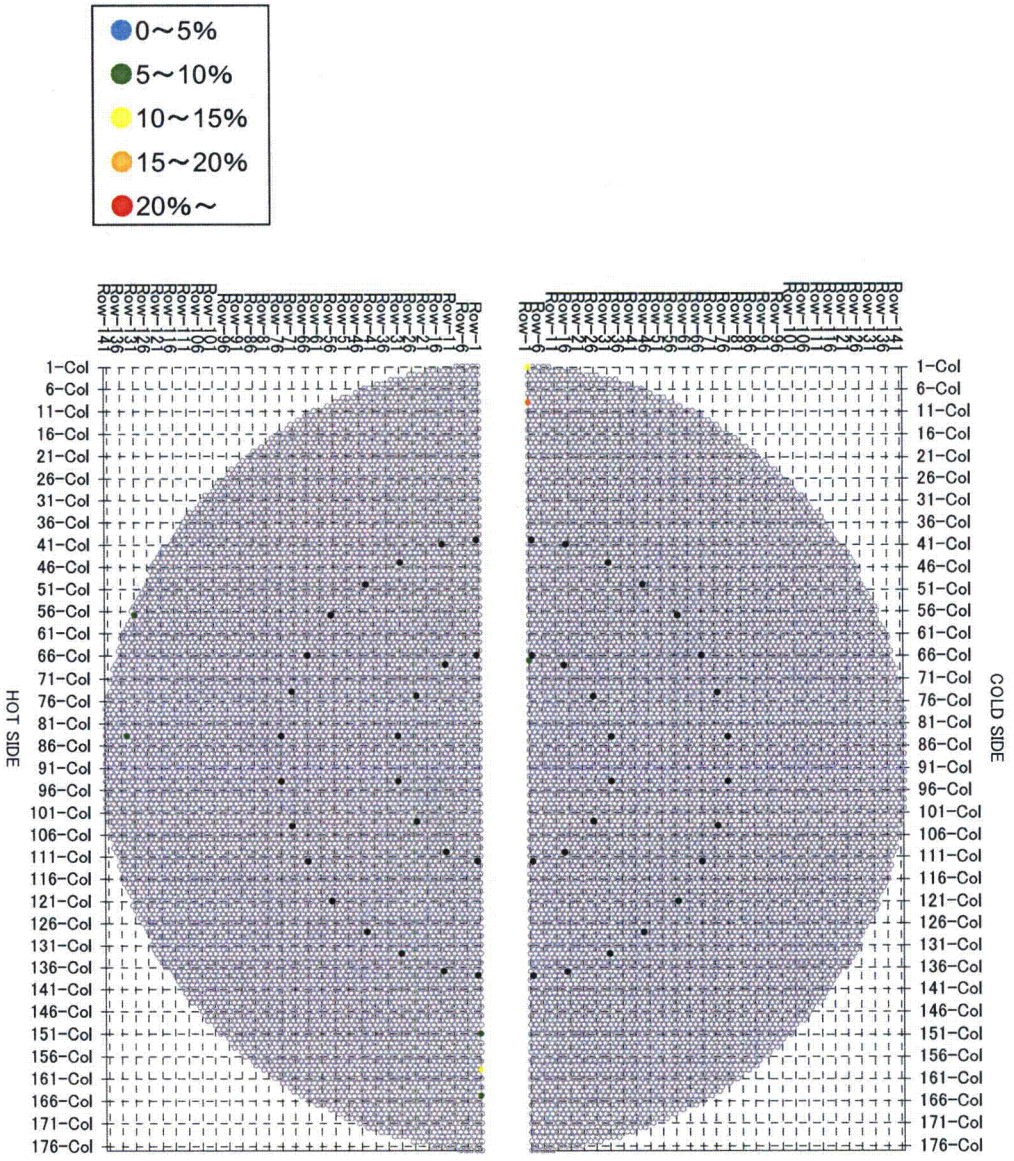

2A_#6TSP

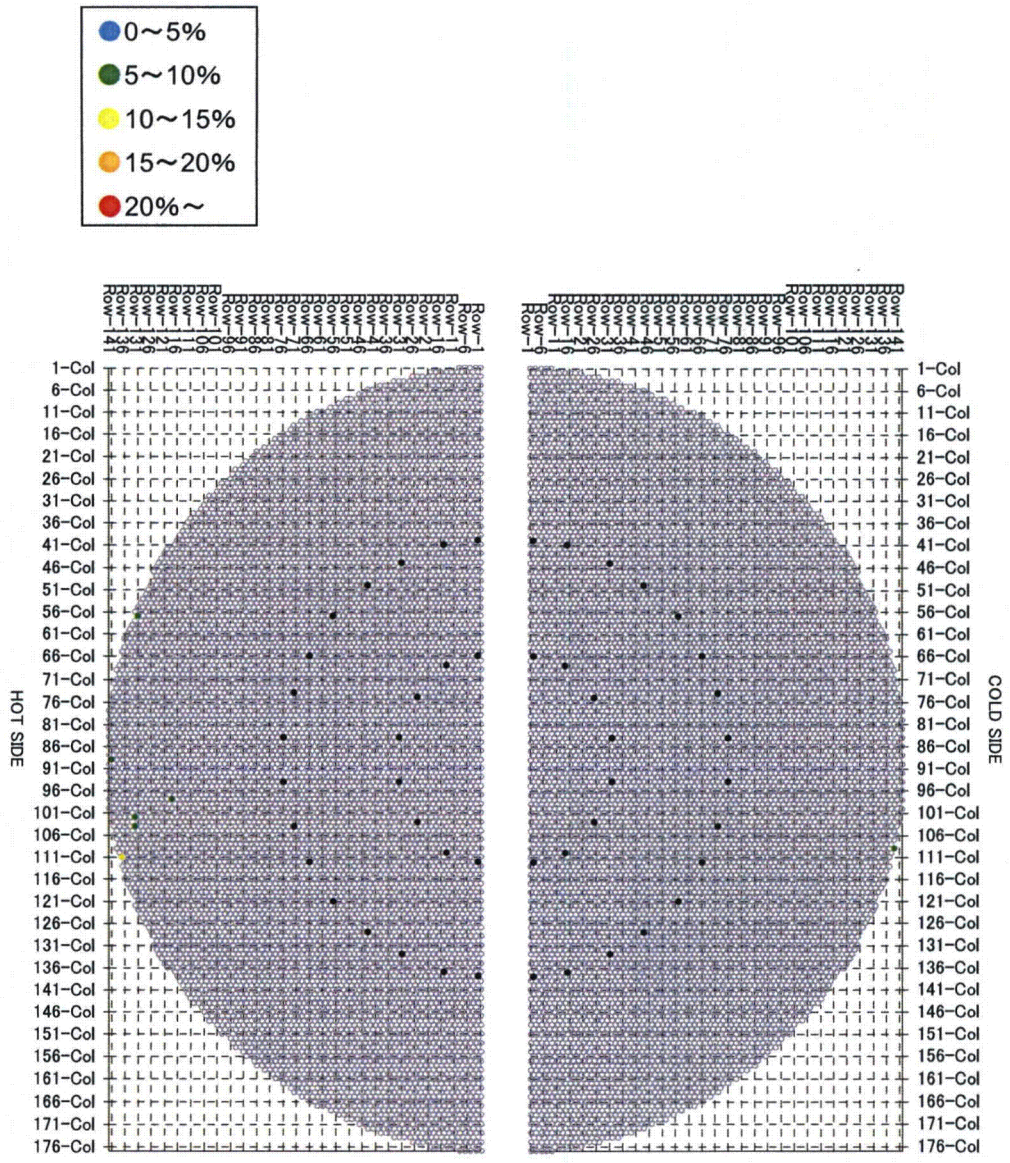
0～5%
5～10%
10～15%
15～20%
20%～
HOT SIDE
COLD SIDE
1-Col
6-Col
11-Col
16-Col
21-Col
26-Col
31-Col
36-Col
41-Col
46-Col
51-Col
56-Col
61-Col
66-Col
71-Col
76-Col
81-Col
86-Col
91-Col
96-Col
101-Col
106-Col
111-Col
116-Col
121-Col
126-Col
131-Col
136-Col
141-Col
146-Col
151-Col
156-Col
161-Col
166-Col
171-Col
176-Col

2A_#7TSP

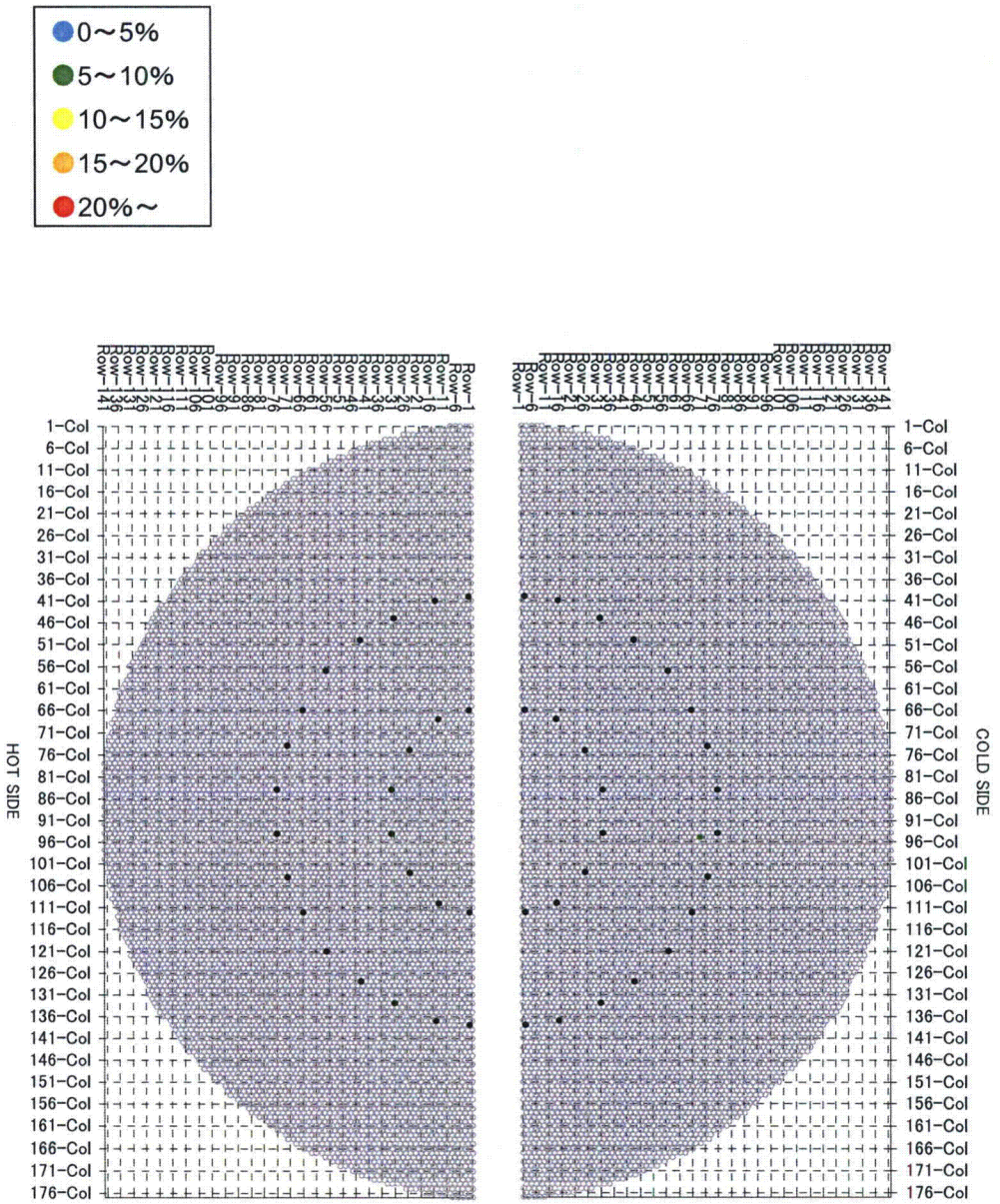

2B_#1TSP

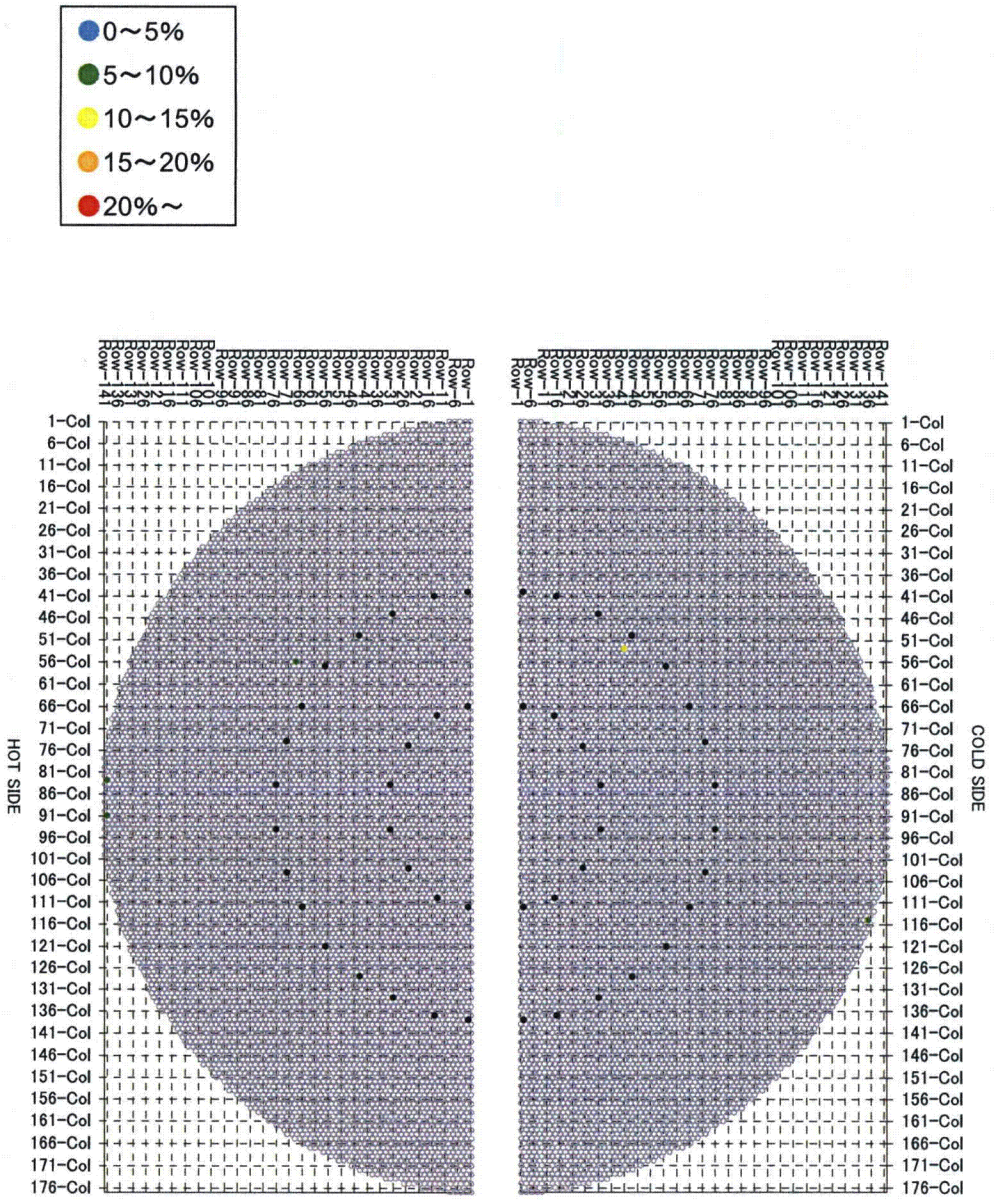

2B_#2TSP

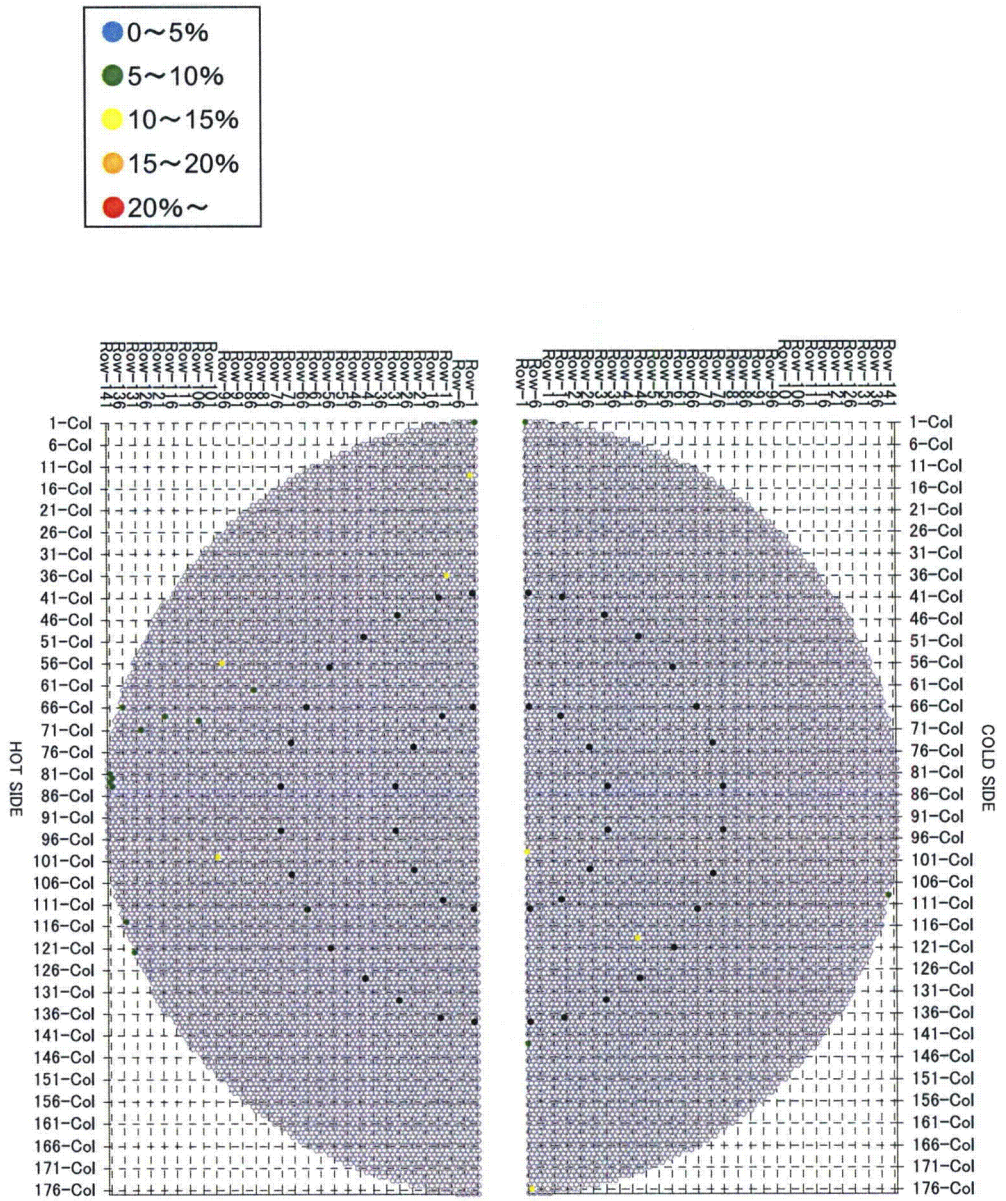

2B_#3TSP

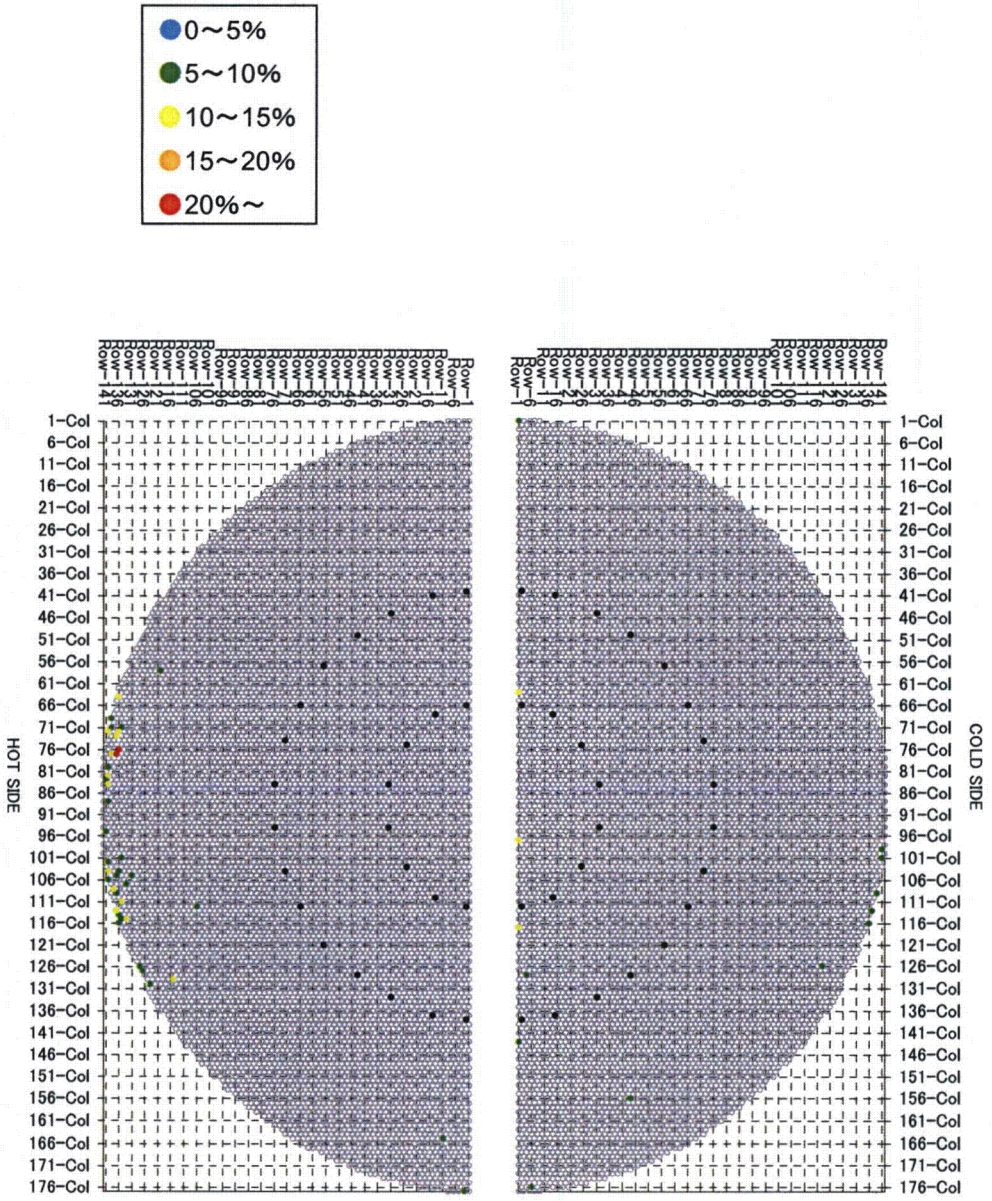

2B_#4TSP

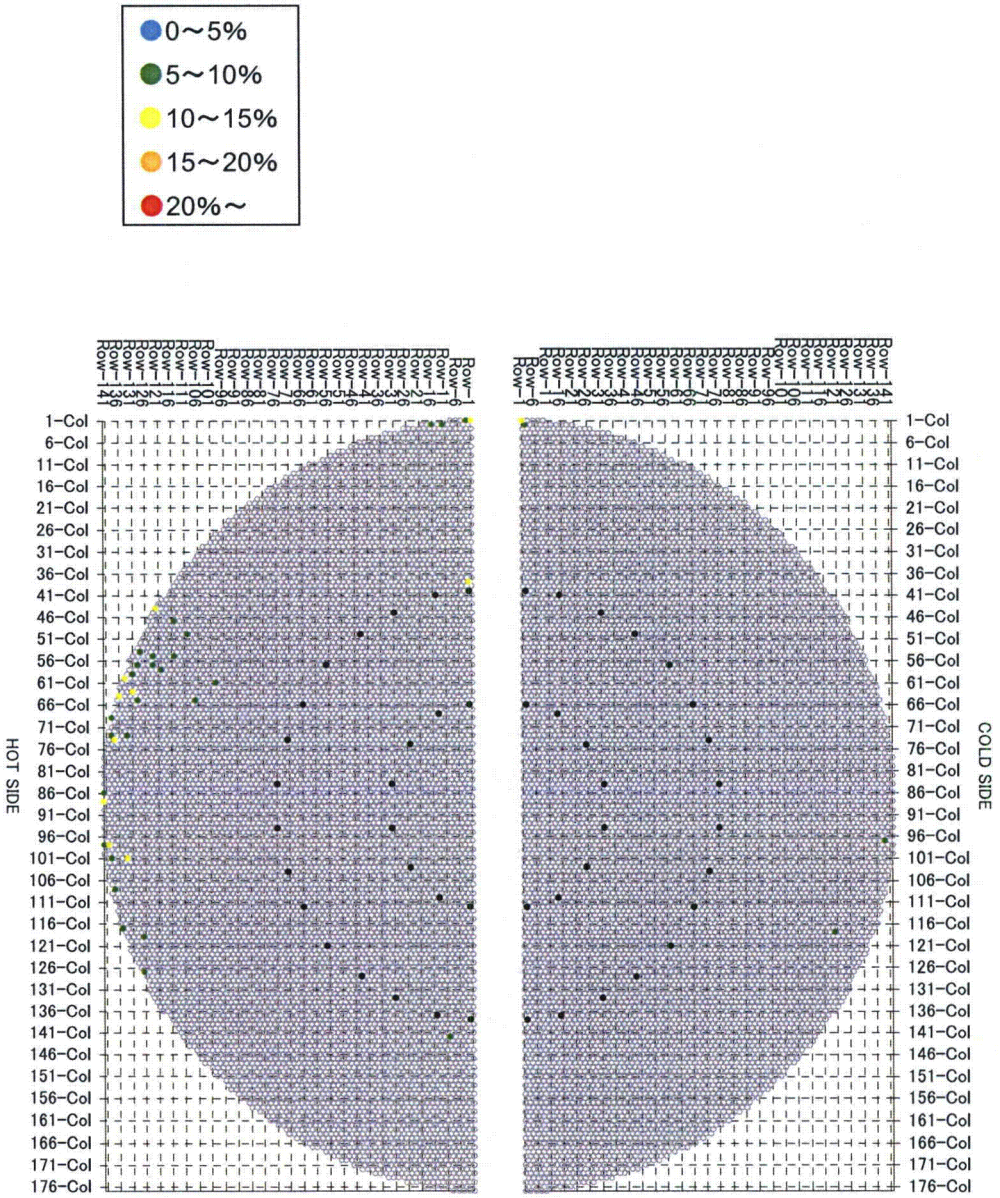

2B_#5TSP

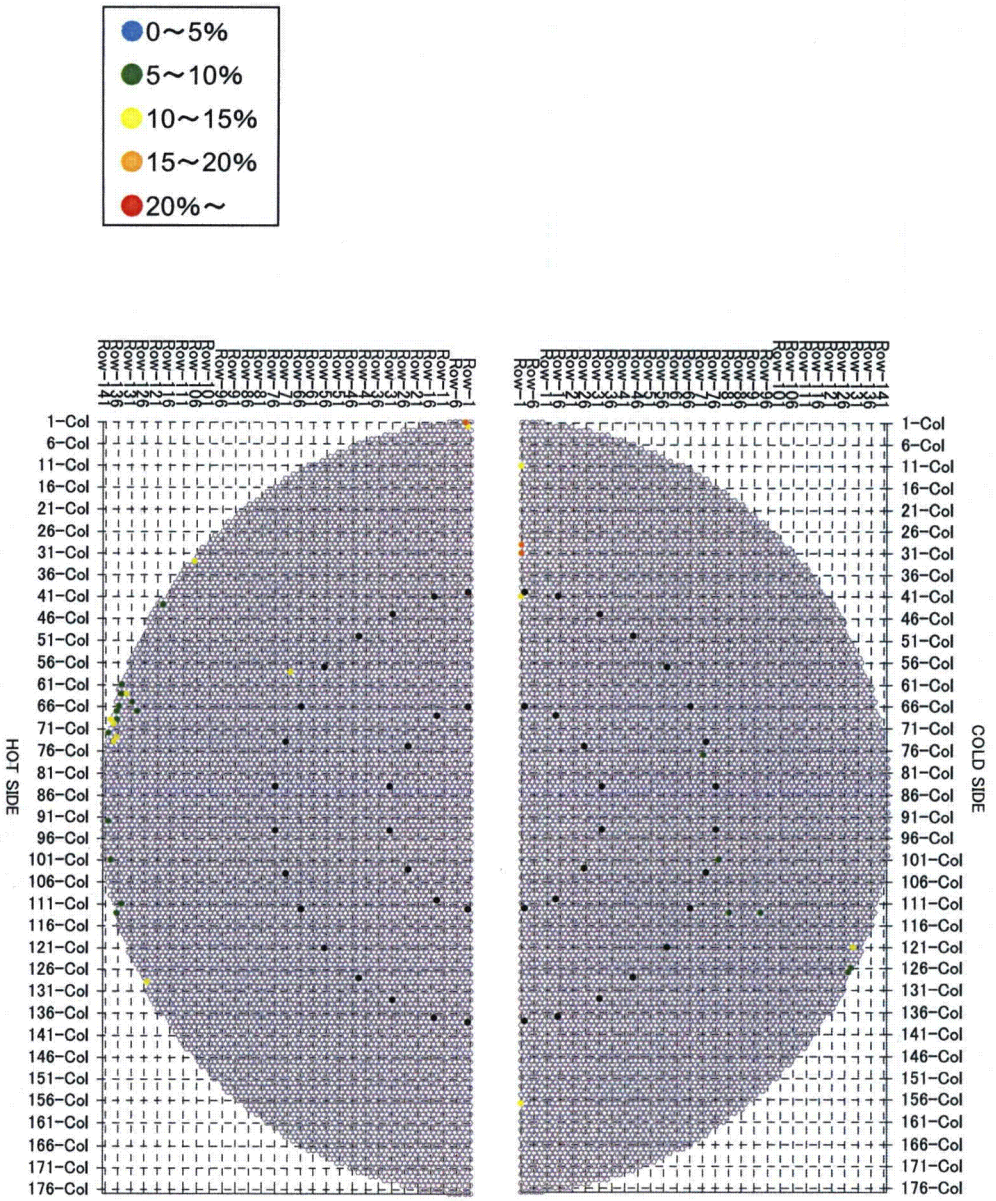
0～5%
5～10%
10～15%
15～20%
20%～
HOT SIDE
COLD SIDE
1-Col
6-Col
11-Col
16-Col
21-Col
26-Col
31-Col
36-Col
41-Col
46-Col
51-Col
56-Col
61-Col
66-Col
71-Col
76-Col
81-Col
86-Col
91-Col
96-Col
101-Col
106-Col
111-Col
116-Col
121-Col
126-Col
131-Col
136-Col
141-Col
146-Col
151-Col
156-Col
161-Col
166-Col
171-Col
176-Col

2B_#6TSP

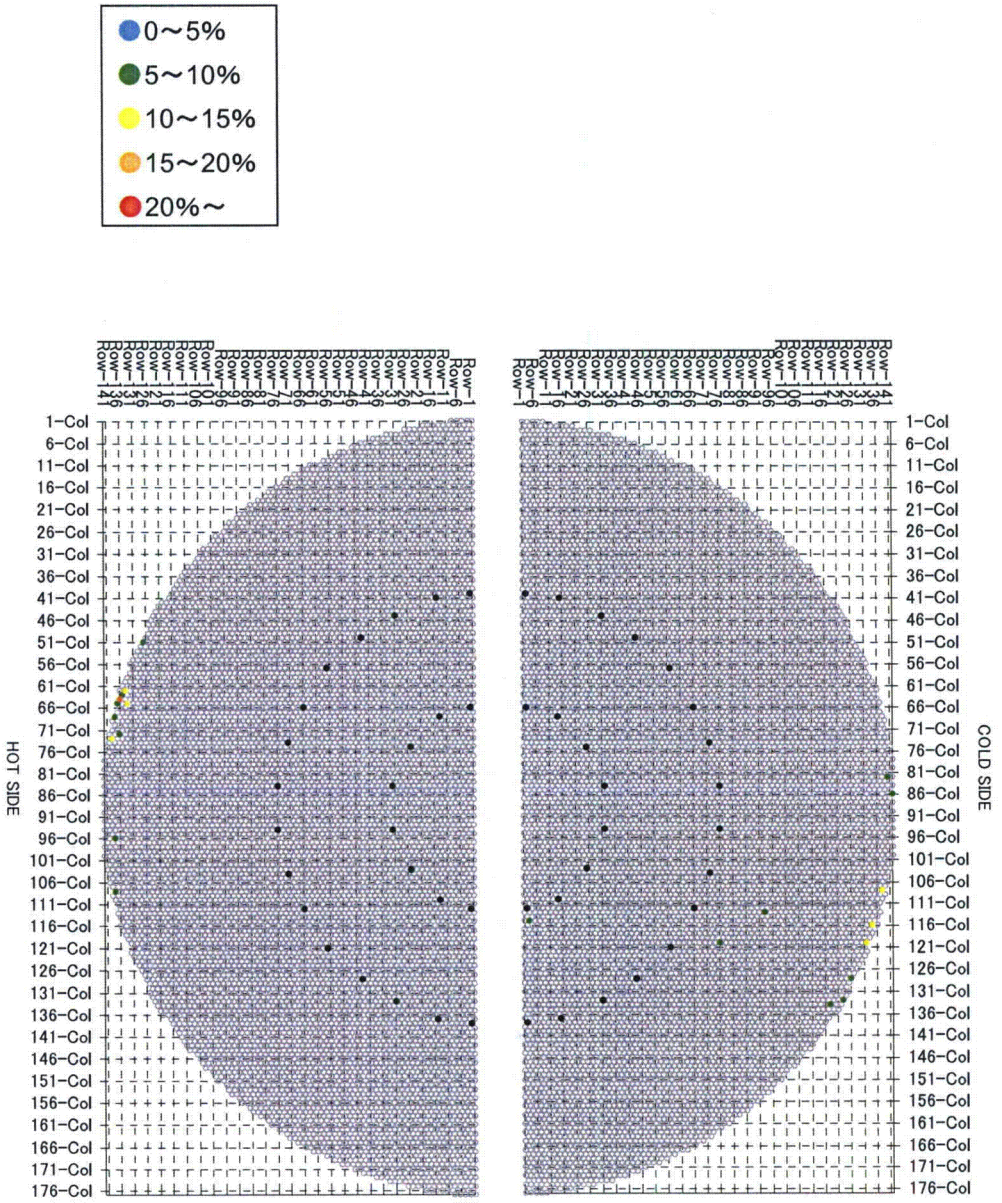

2B_#7TSP

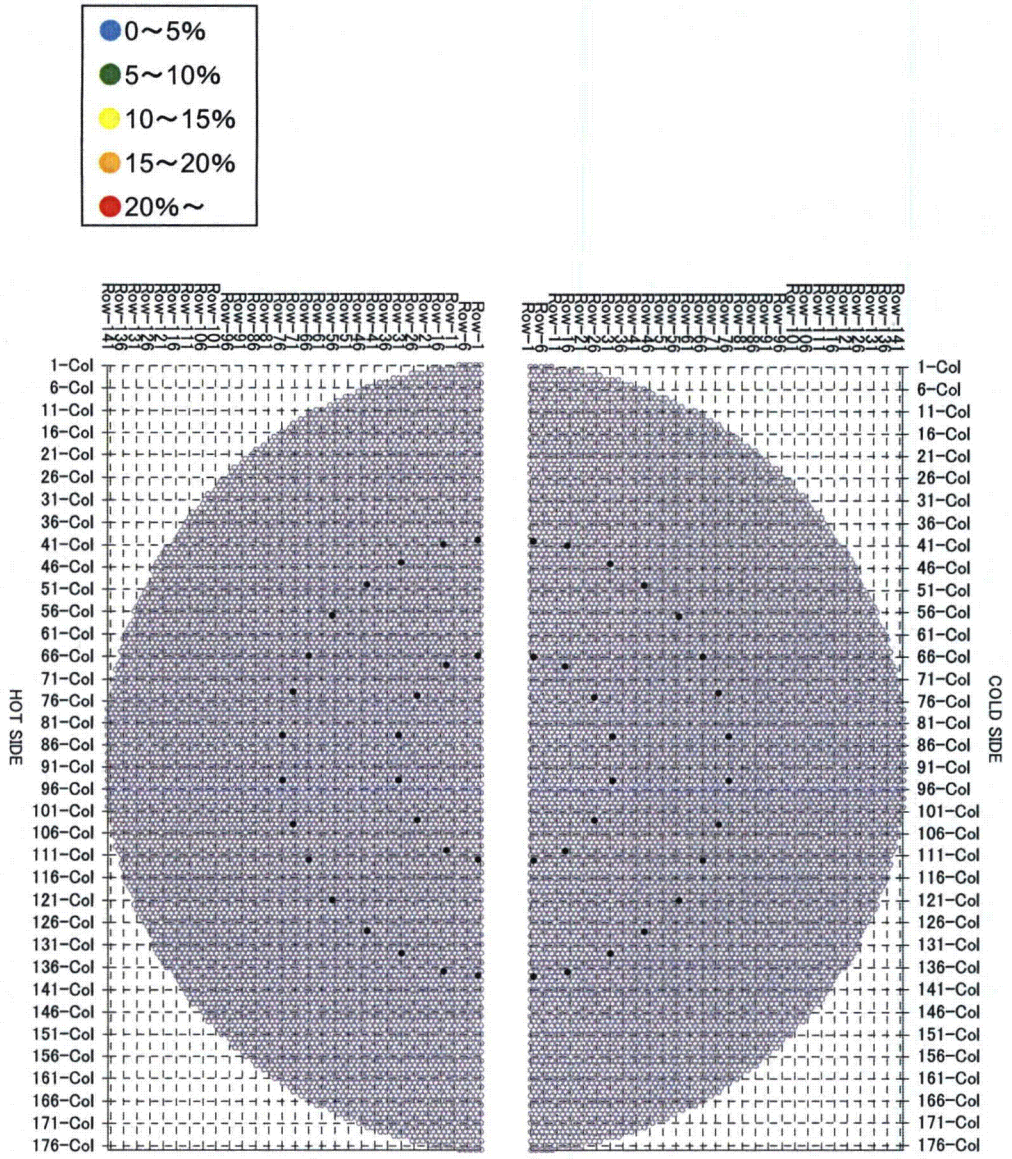

3A_#1TSP

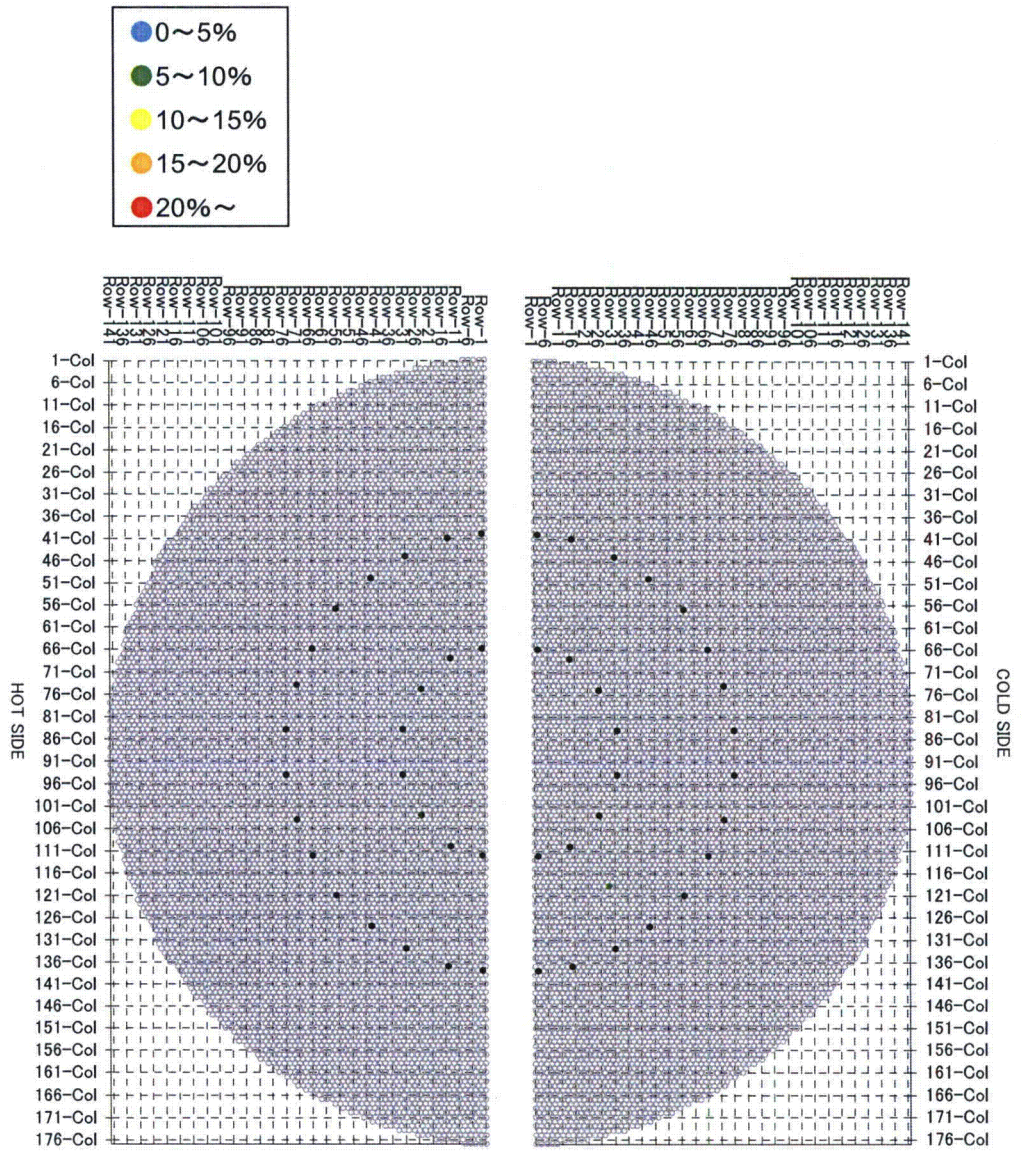

3A_#2TSP

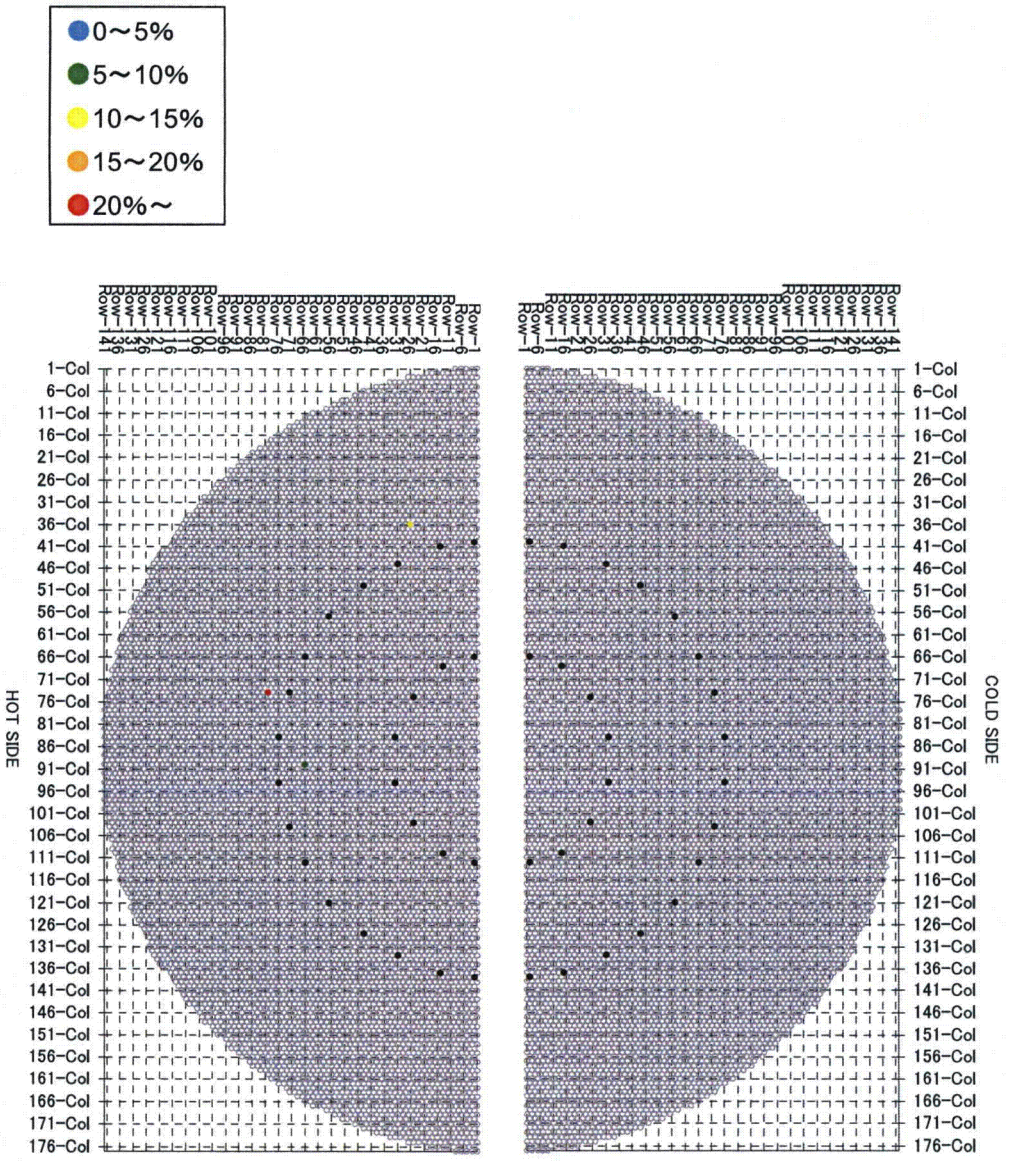

3A_#3TSP

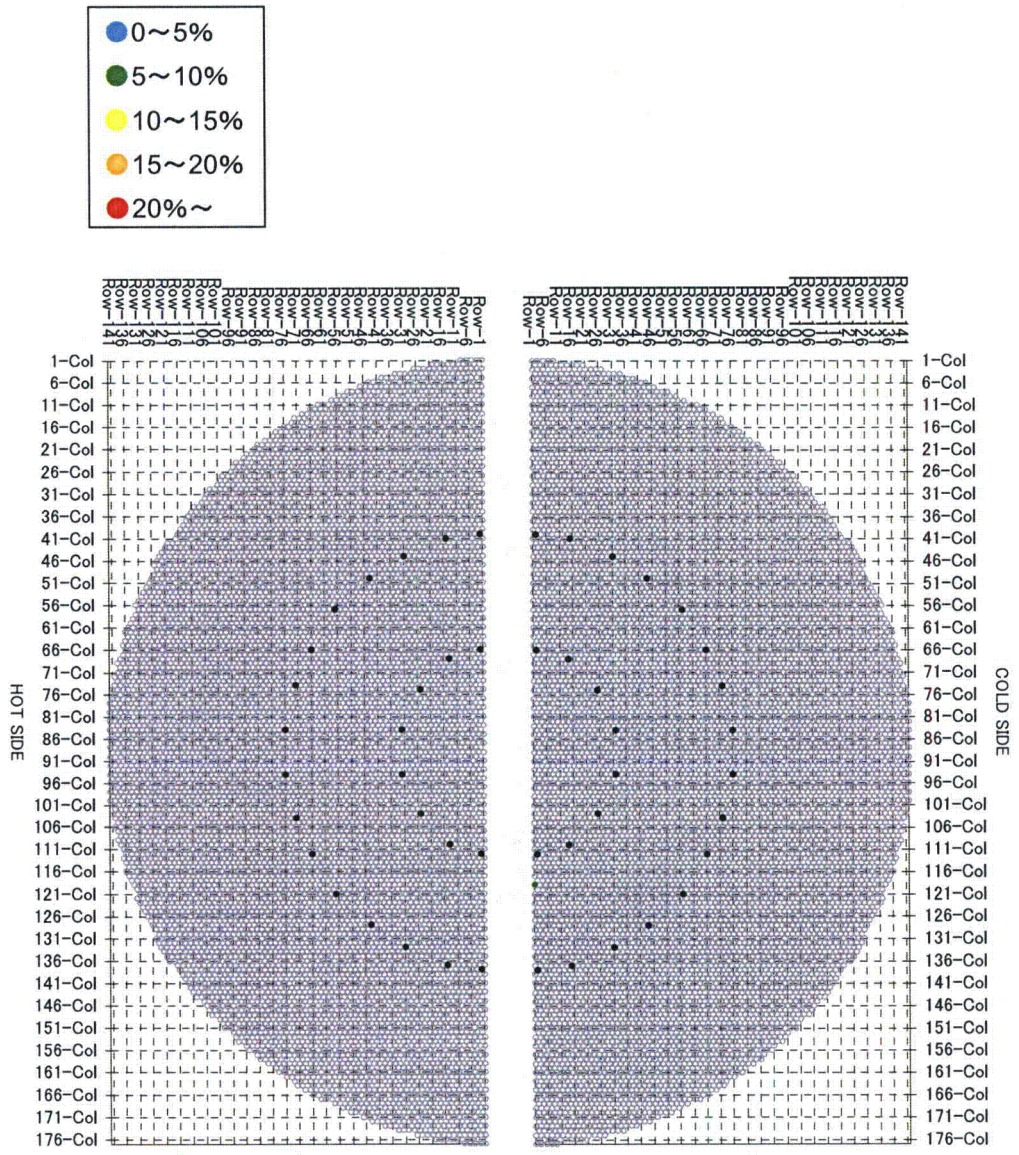

3A_#4TSP

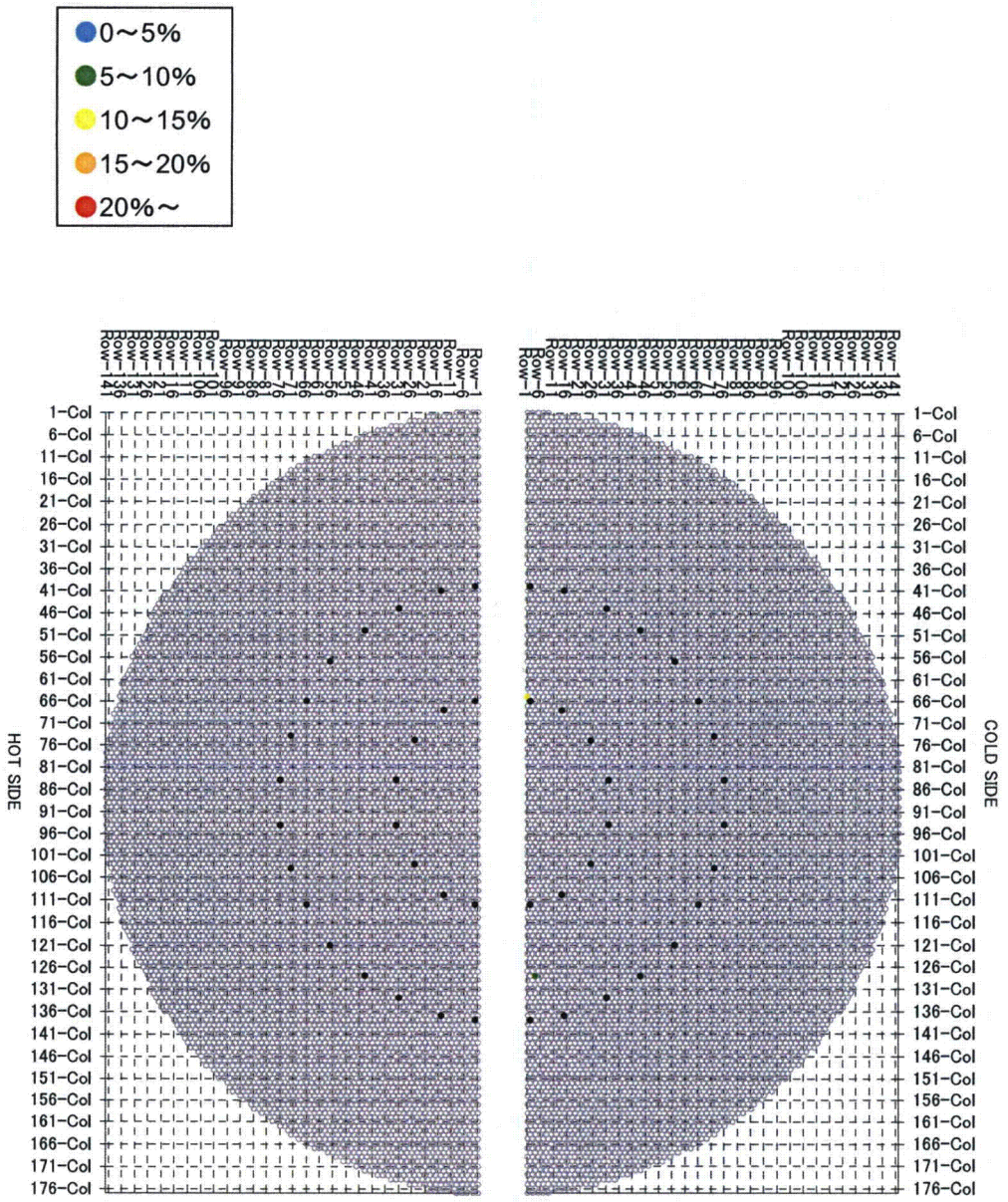

3A_#5TSP

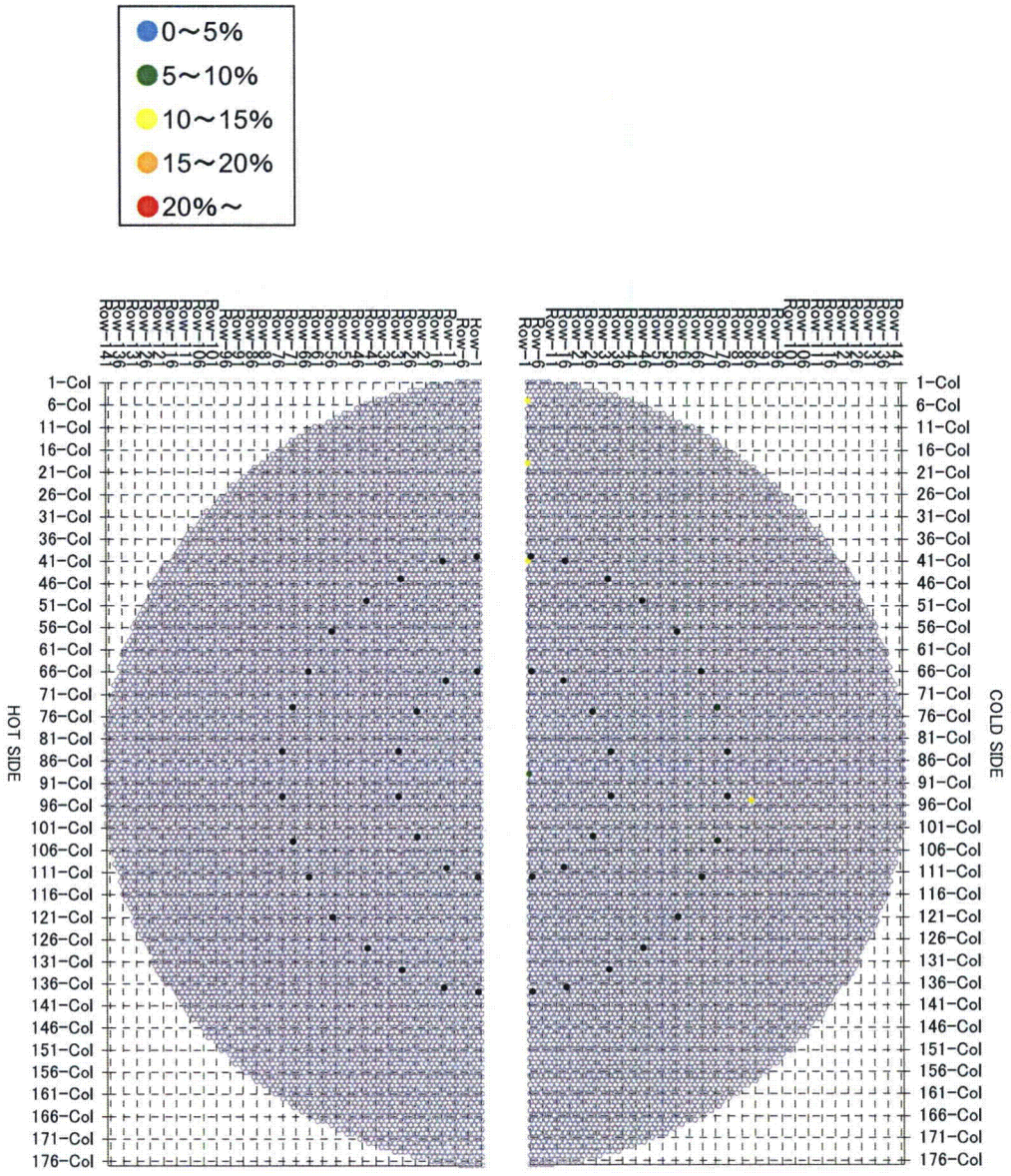

3A_#6TSP

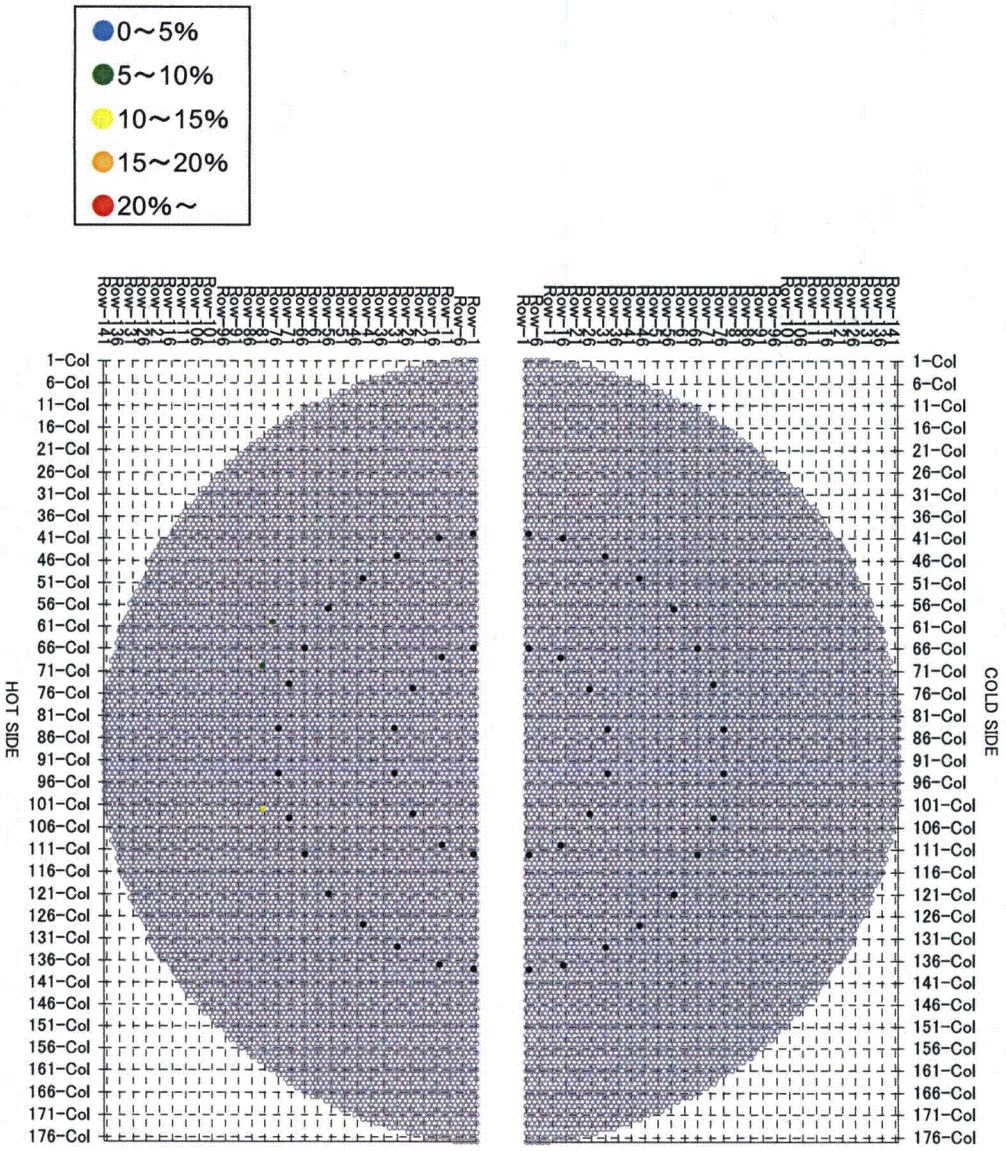
0～5%
5～10%
10～15%
15～20%
20%～
HOT SIDE
COLD SIDE
1-Col
6-Col
11-Col
16-Col
21-Col
26-Col
31-Col
36-Col
41-Col
46-Col
51-Col
56-Col
61-Col
66-Col
71-Col
76-Col
81-Col
86-Col
91-Col
96-Col
101-Col
106-Col
111-Col
116-Col
121-Col
126-Col
131-Col
136-Col
141-Col
146-Col
151-Col
156-Col
161-Col
166-Col
171-Col
176-Col

3A_#7TSP

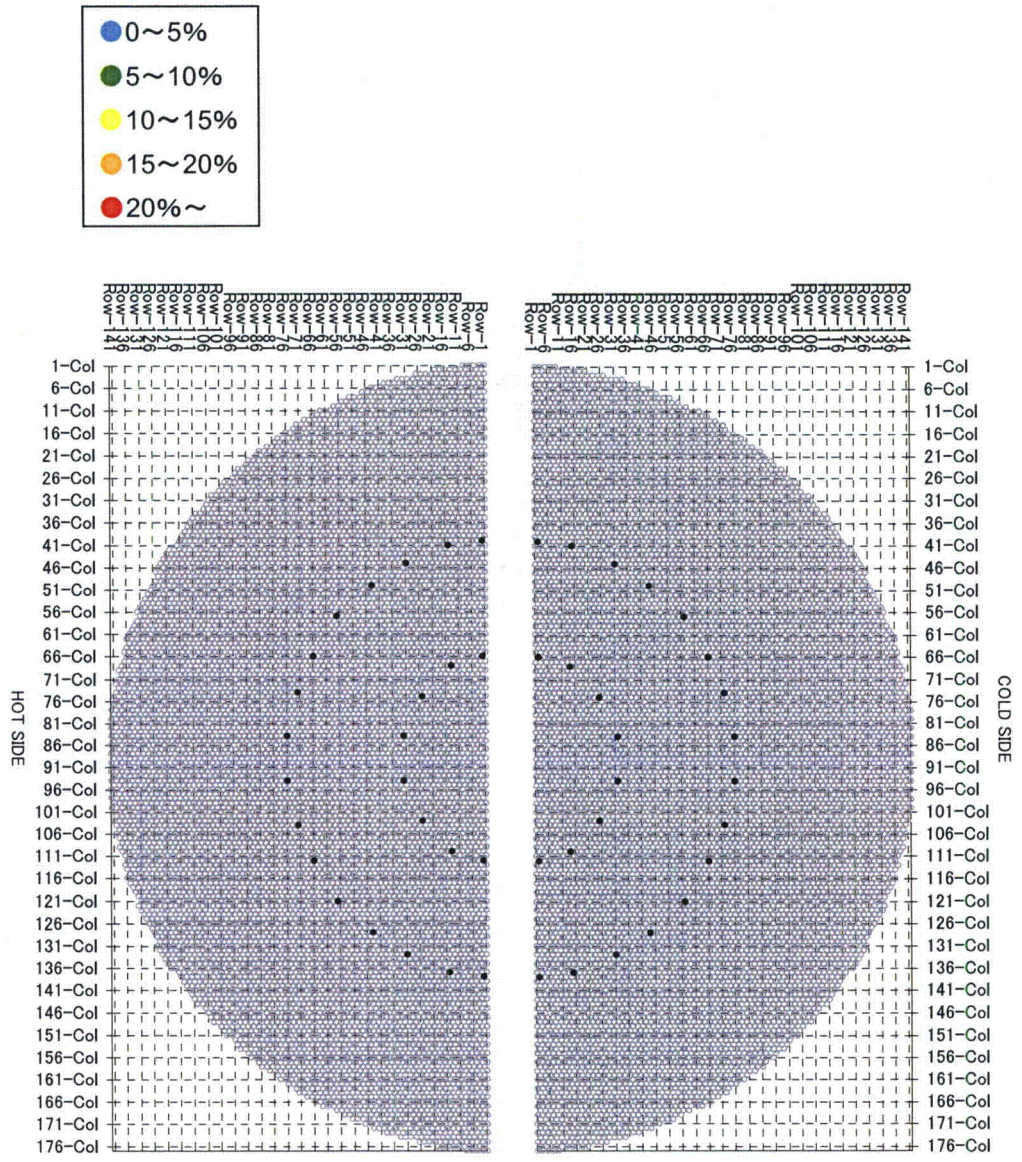

3B_#1TSP

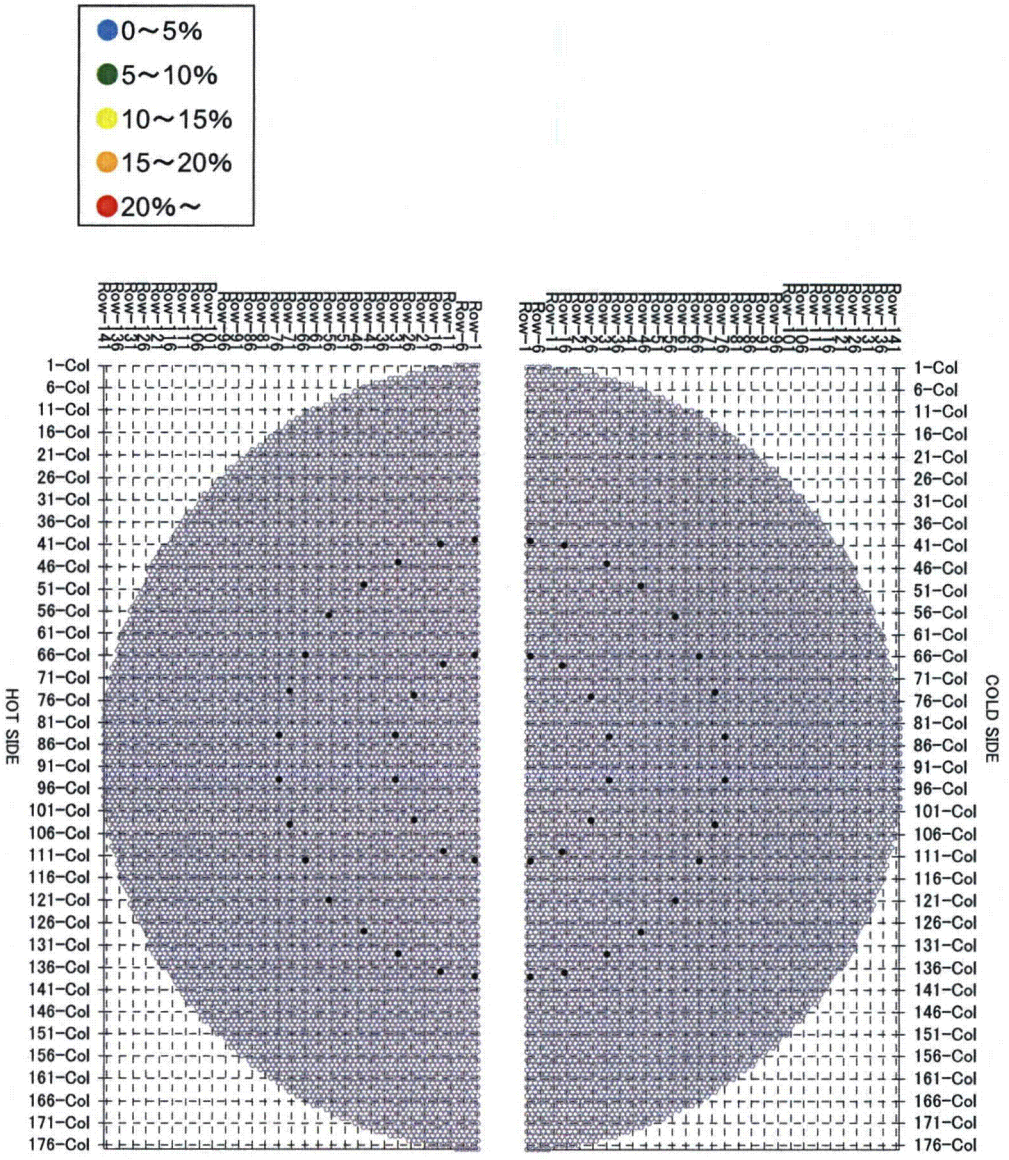

3B_#2TSP

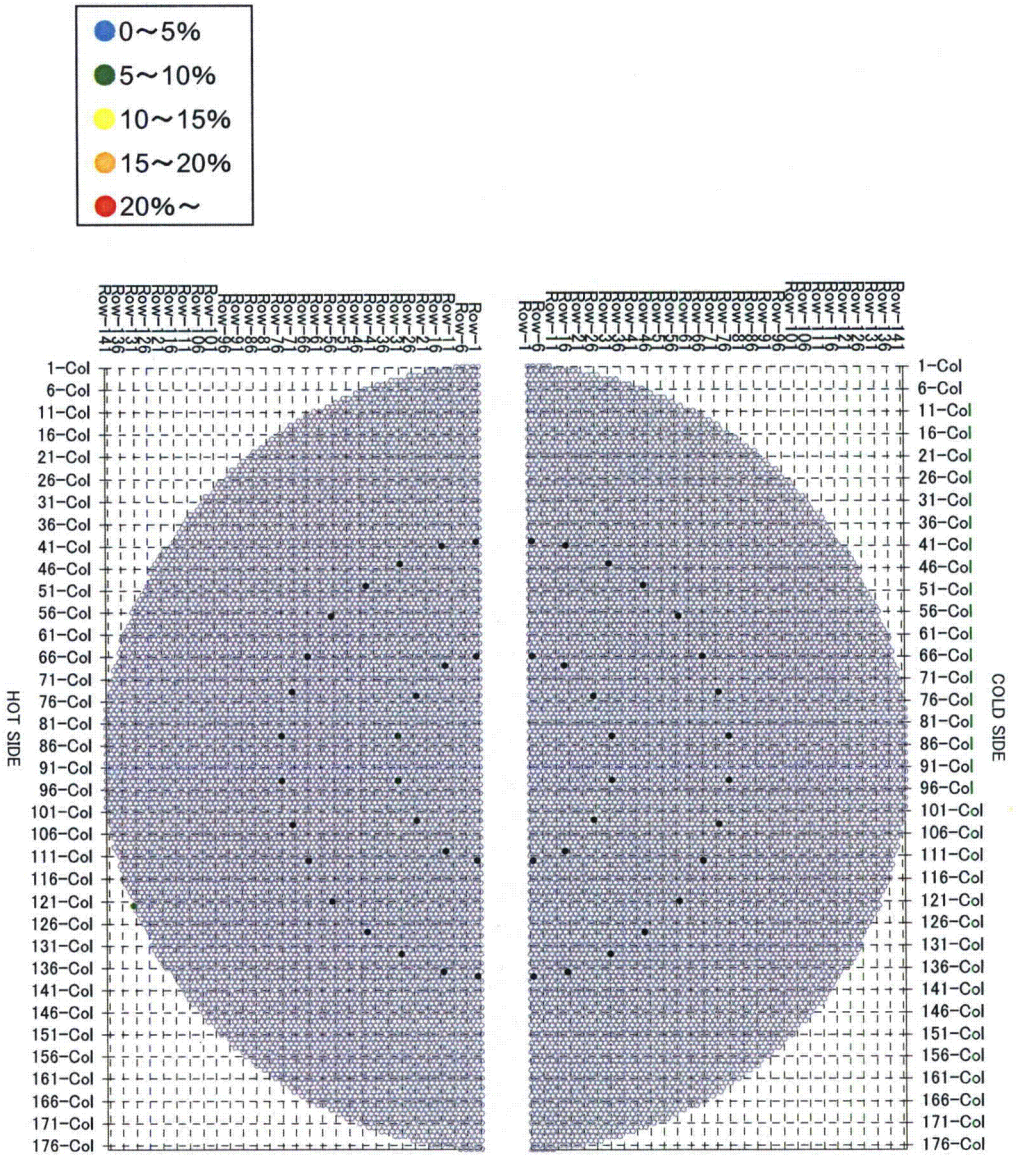

3B_#3TSP

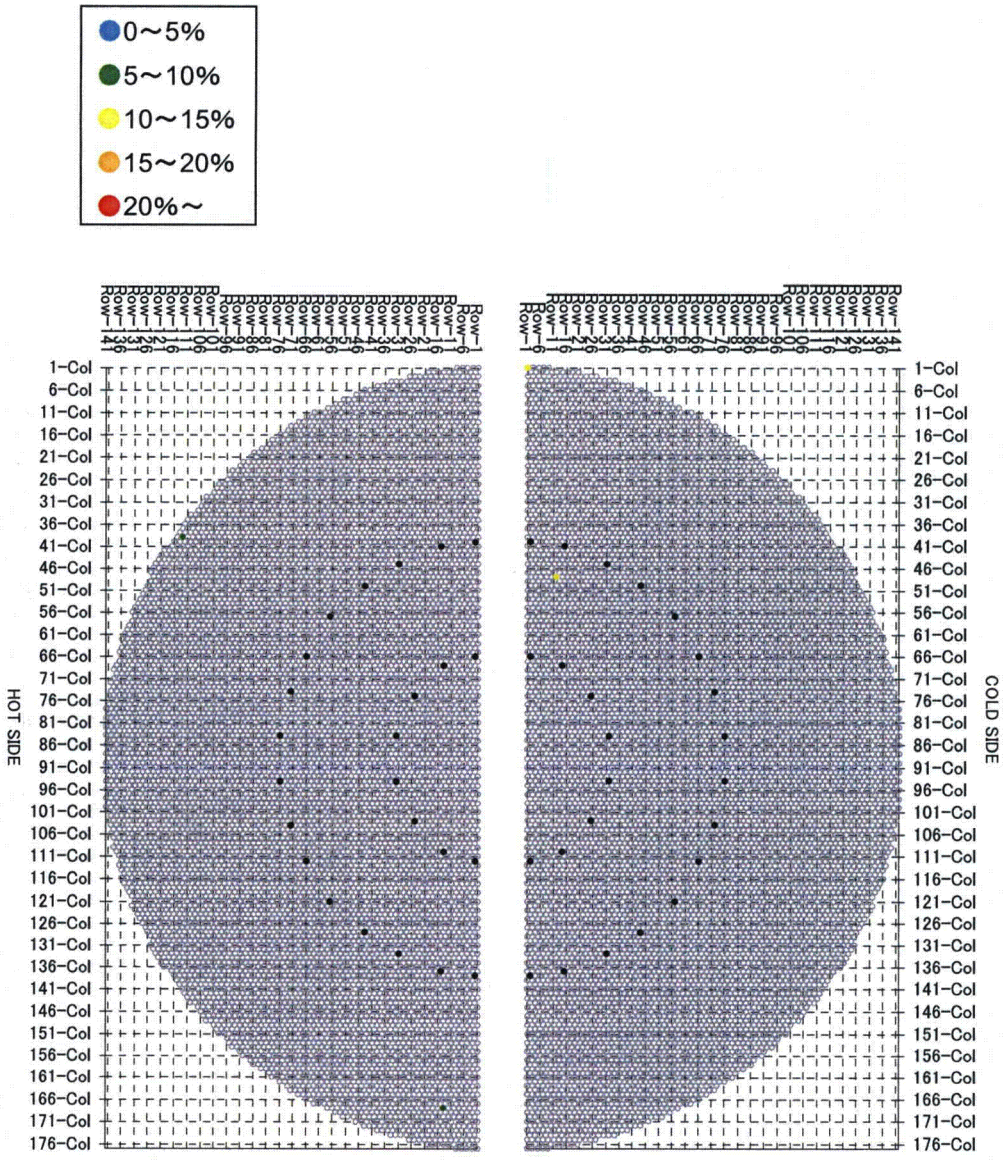

3B_#4TSP

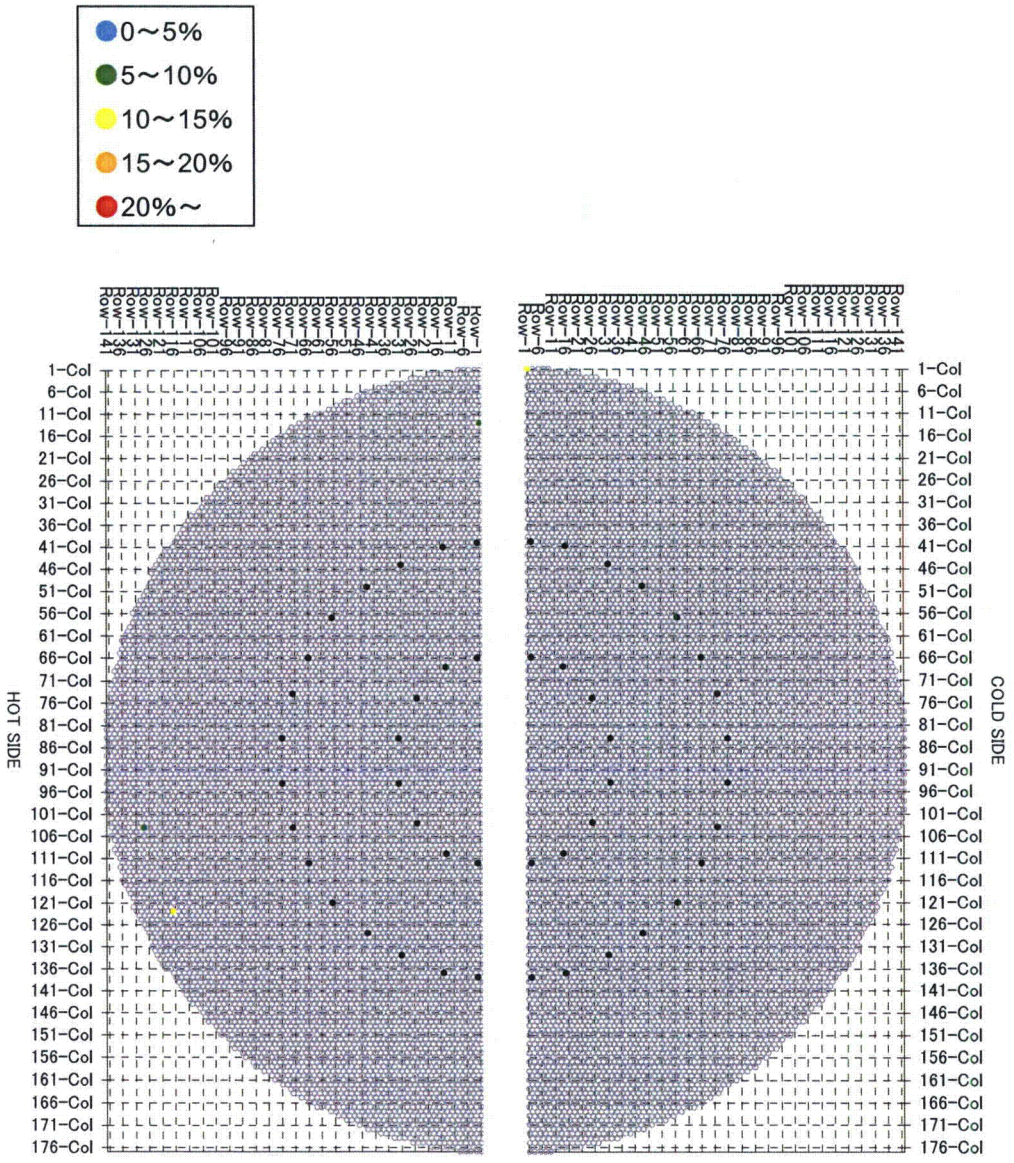

3B_#5TSP

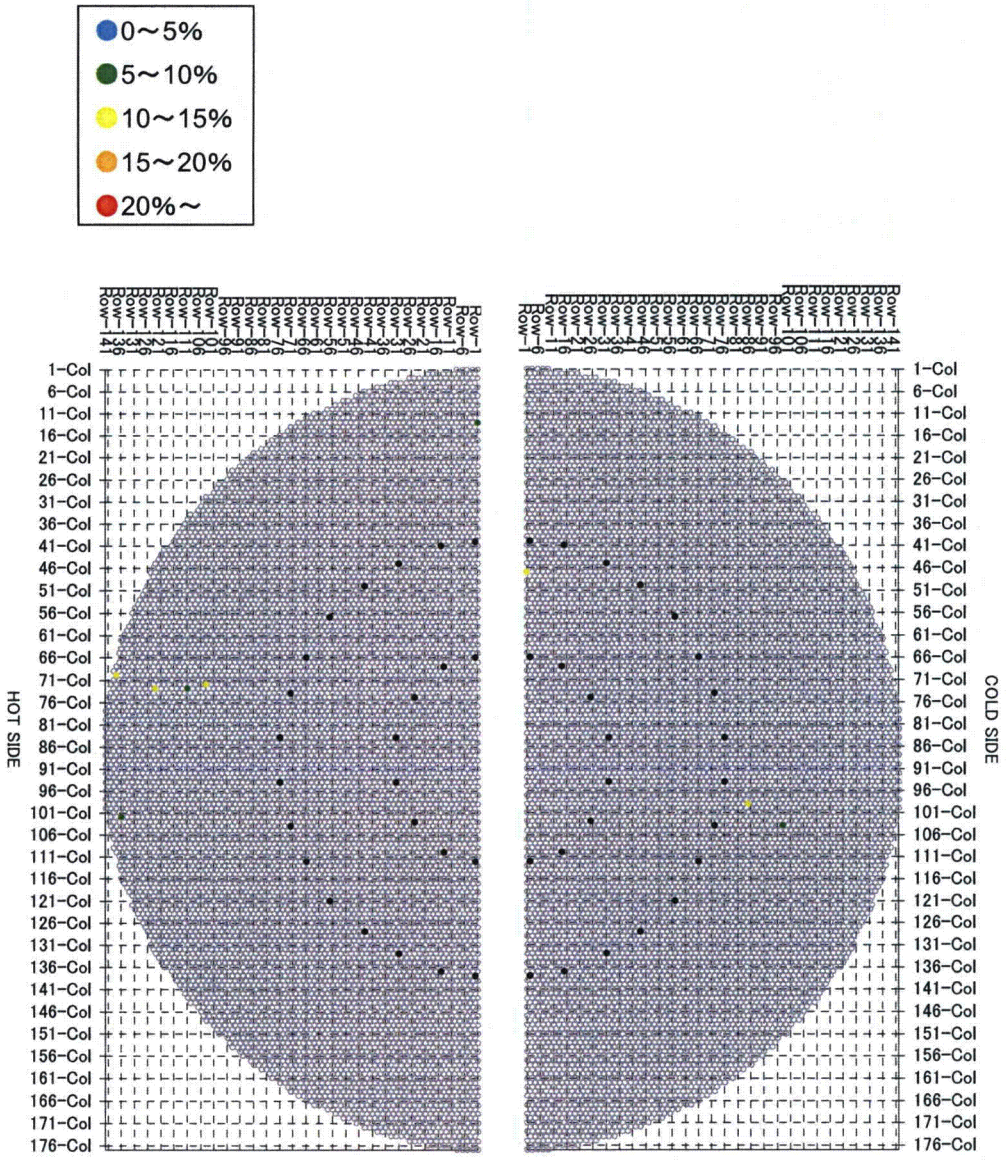

3B_#6TSP

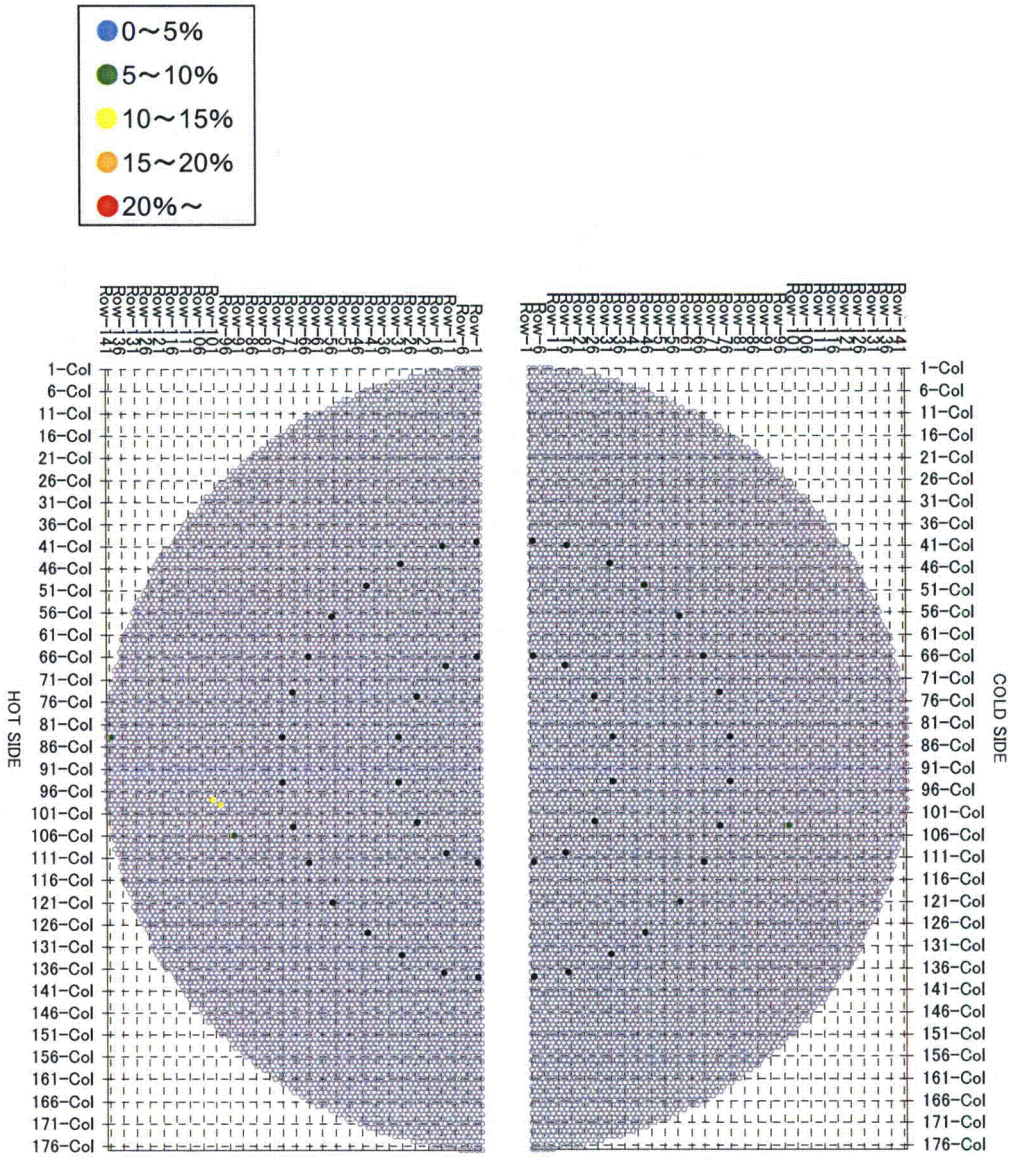

3B_#7TSP

Appendix-2 Attachment-2
Flow velocity data of analysis by ATHOS/SGAP for Unit-2/3

1. Introduction

This attachment provides the data of flow velocity above tube sheet and at each TSPs analyzed by ATHOS/SGAP computer code.

2. Flow velocity data

The following tables provide the data of flow velocity above tube sheet and at each TSPs (#1 ~#7TSP). These data indicate superficial velocities in horizontal sections. The directions of these velocities are shown in figs. 5-24~5-31 in Appendix-2. Symbols IX and IY show the position of cells in horizontal sections (shown in following figure).

Position of cells

Velocity above tube sheet (1/2)

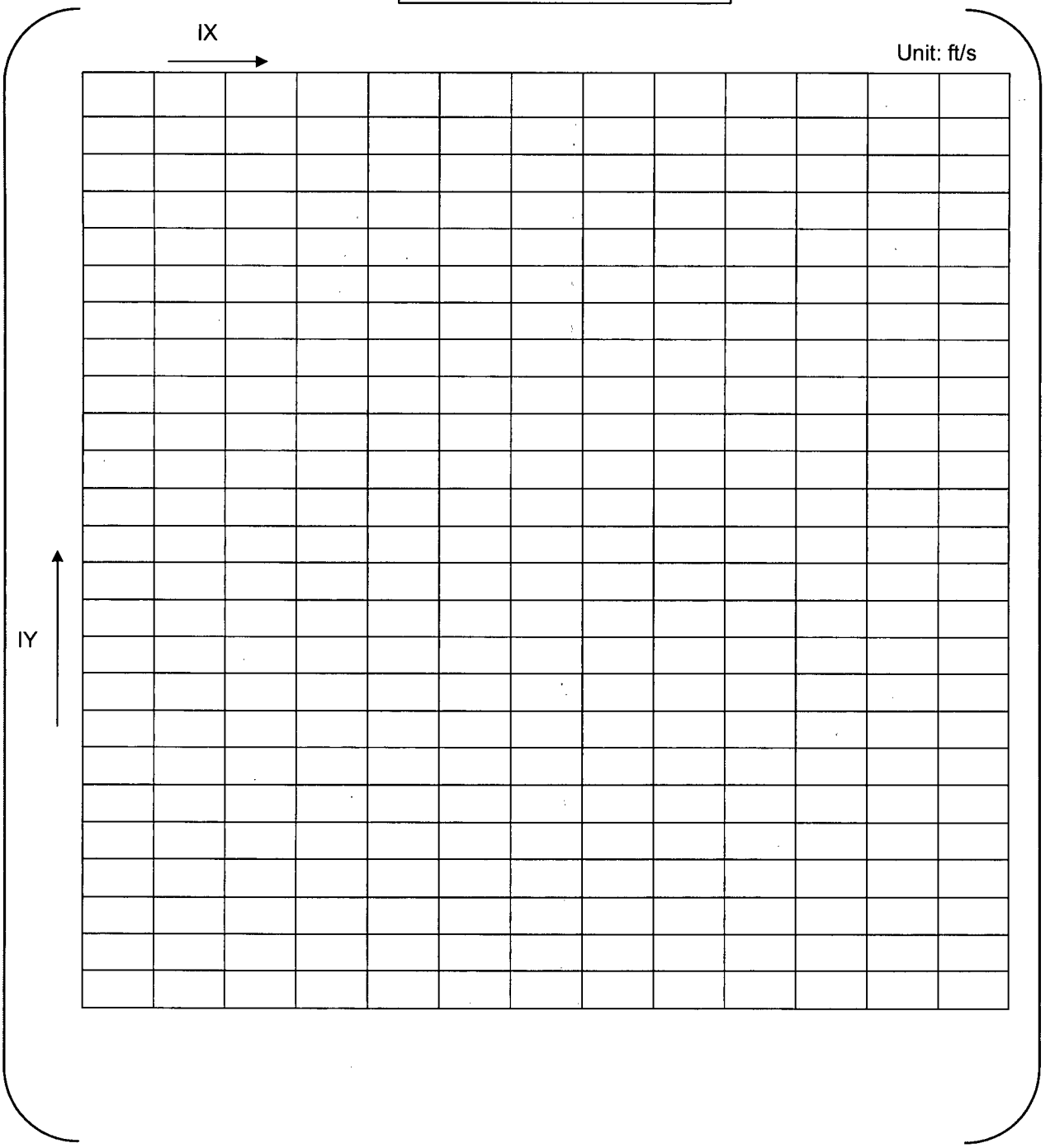

Velocity above tube sheet (2/2)

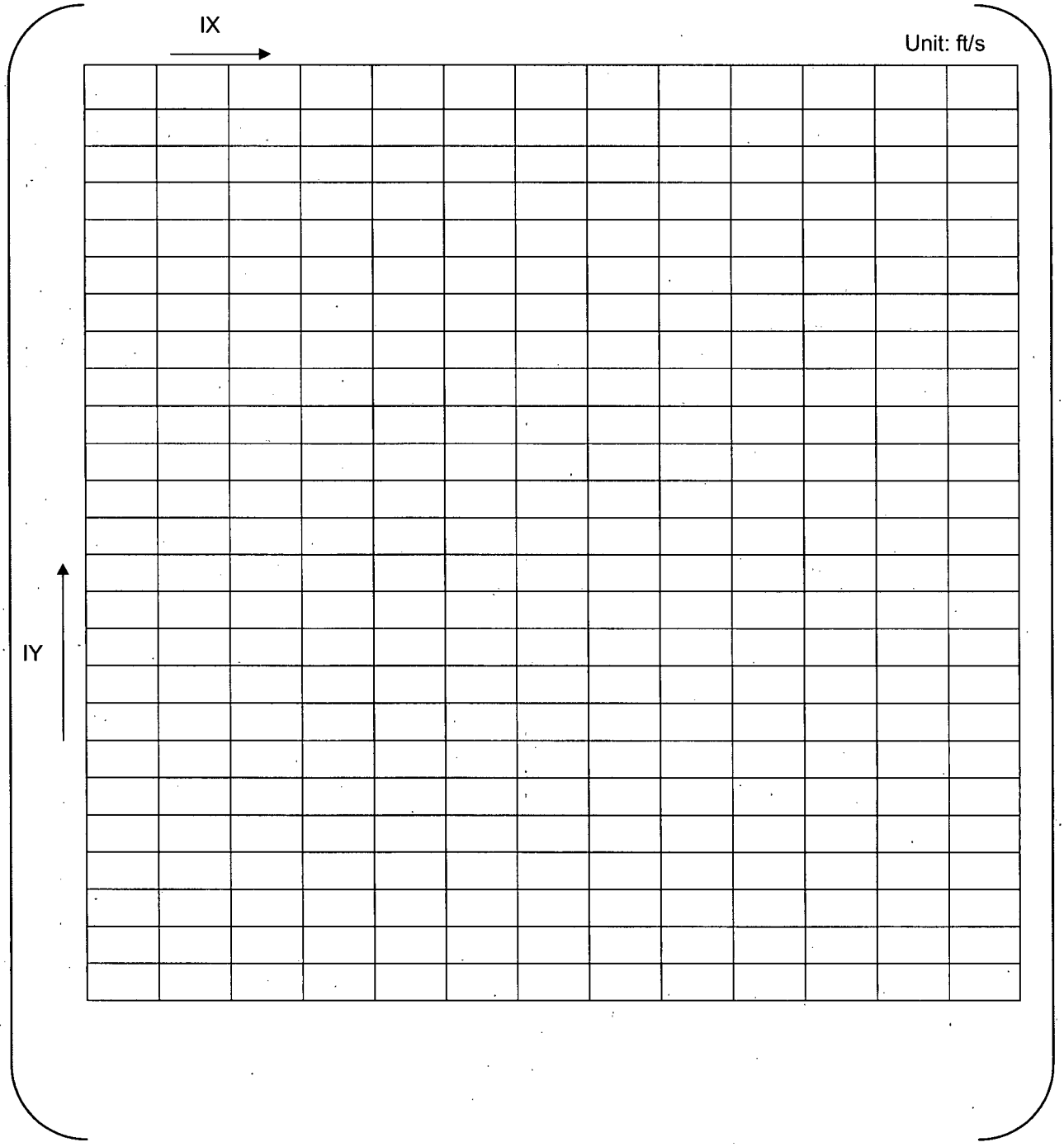

Velocity at #1TSP (1/2)

IX

Unit: ft/s

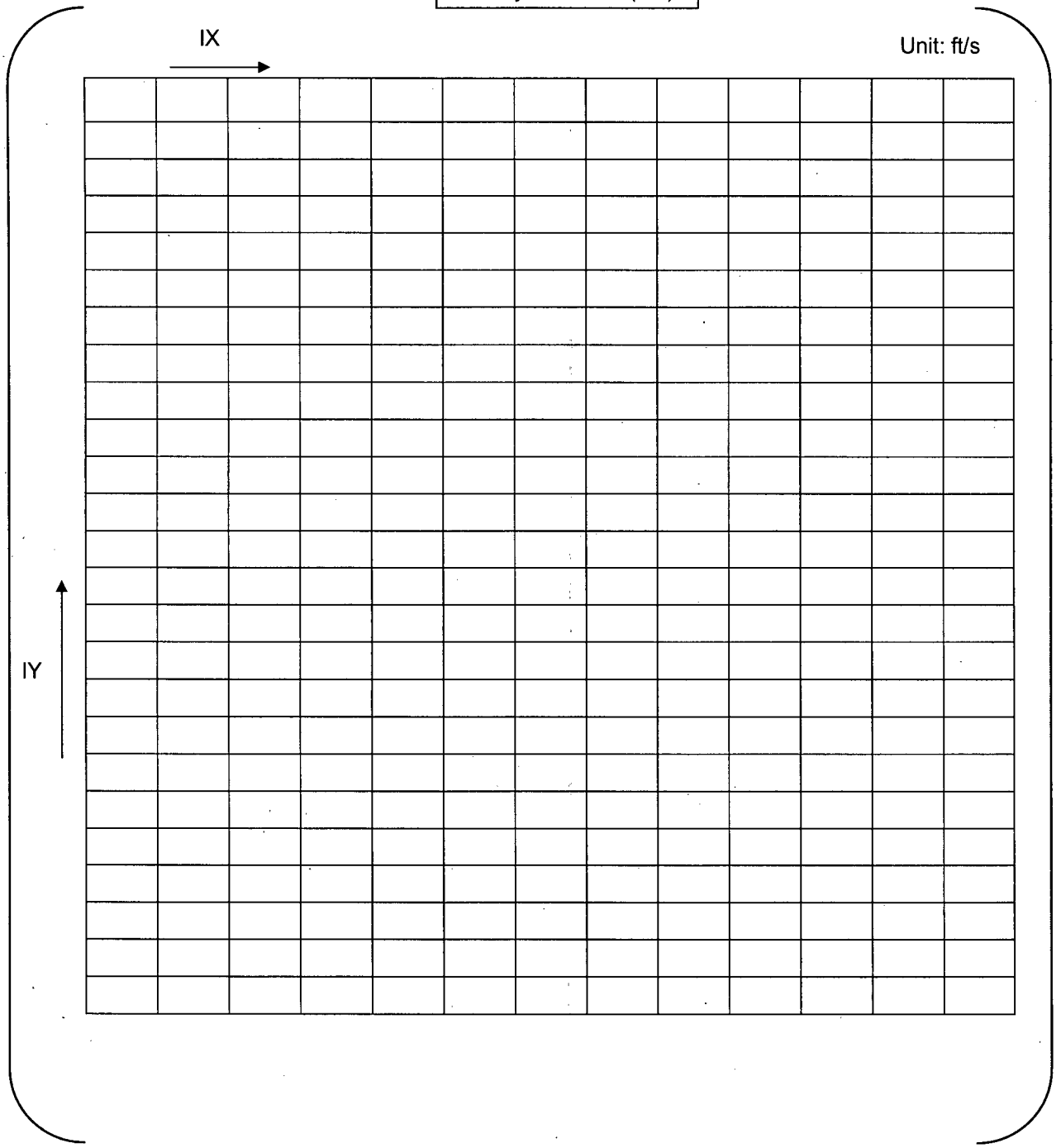

IY

Velocity at #1TSP (2/2)

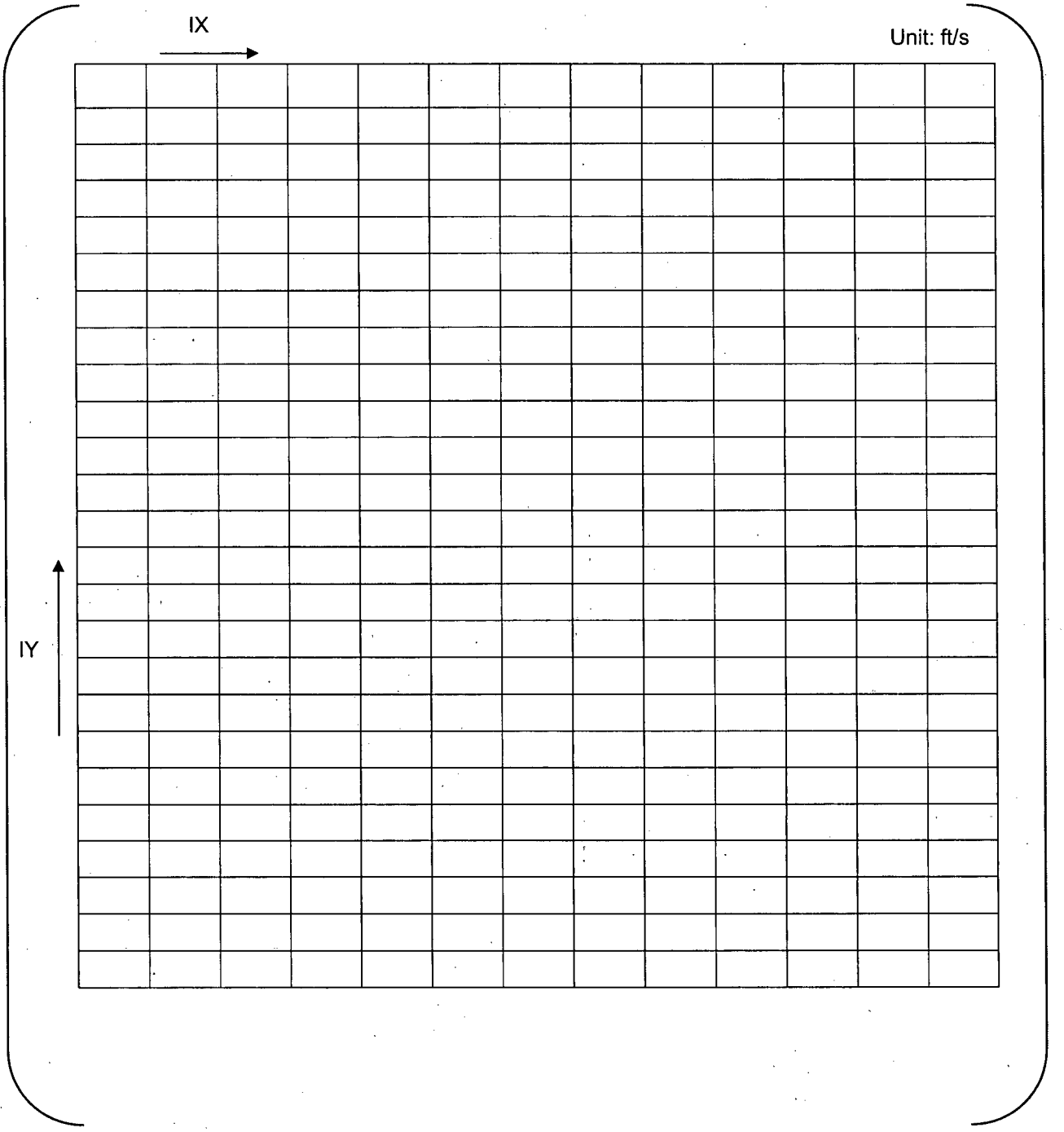

Velocity at #2TSP (1/2)

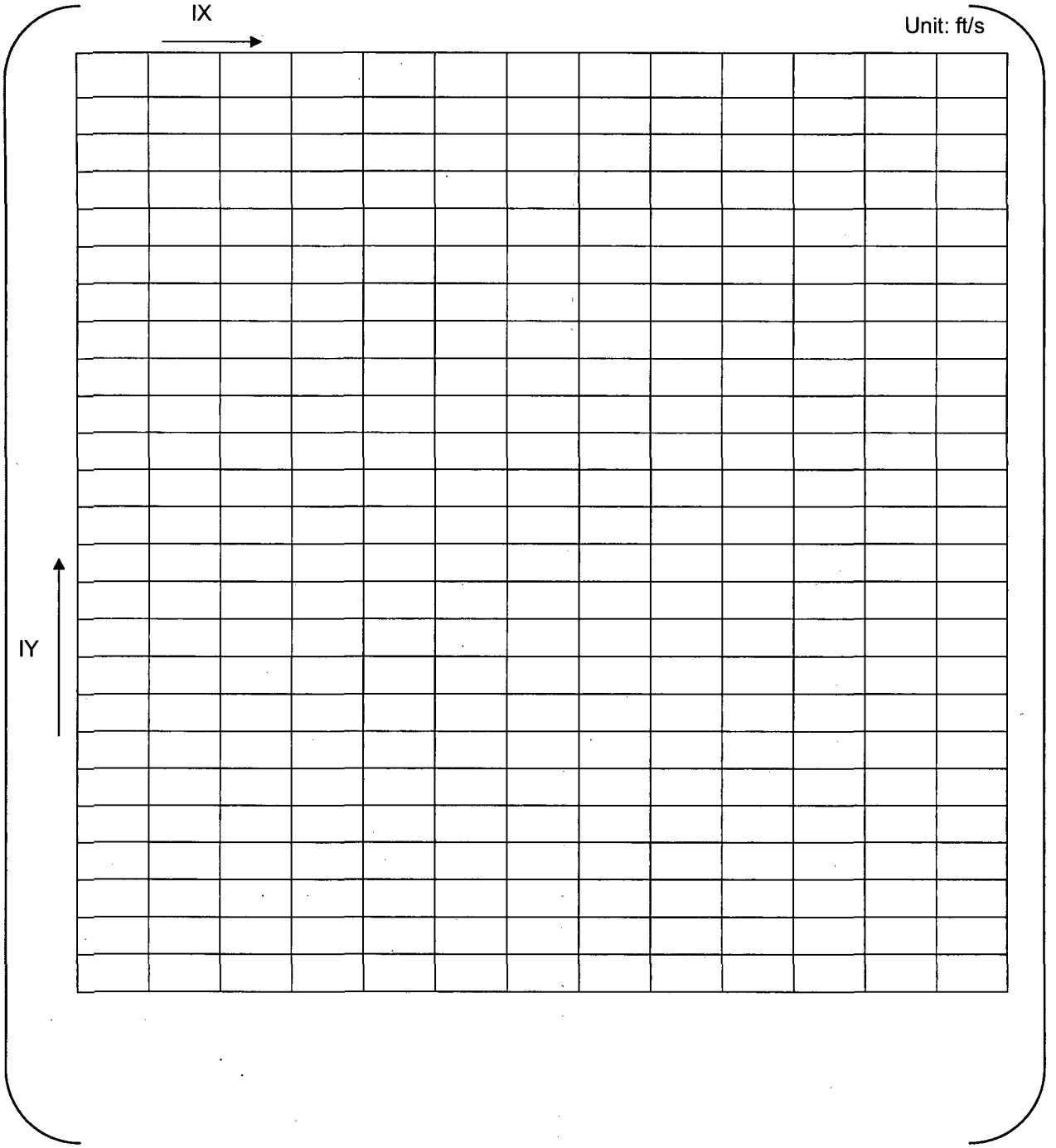

Velocity at #2TSP (2/2)

IX

Unit: ft/s

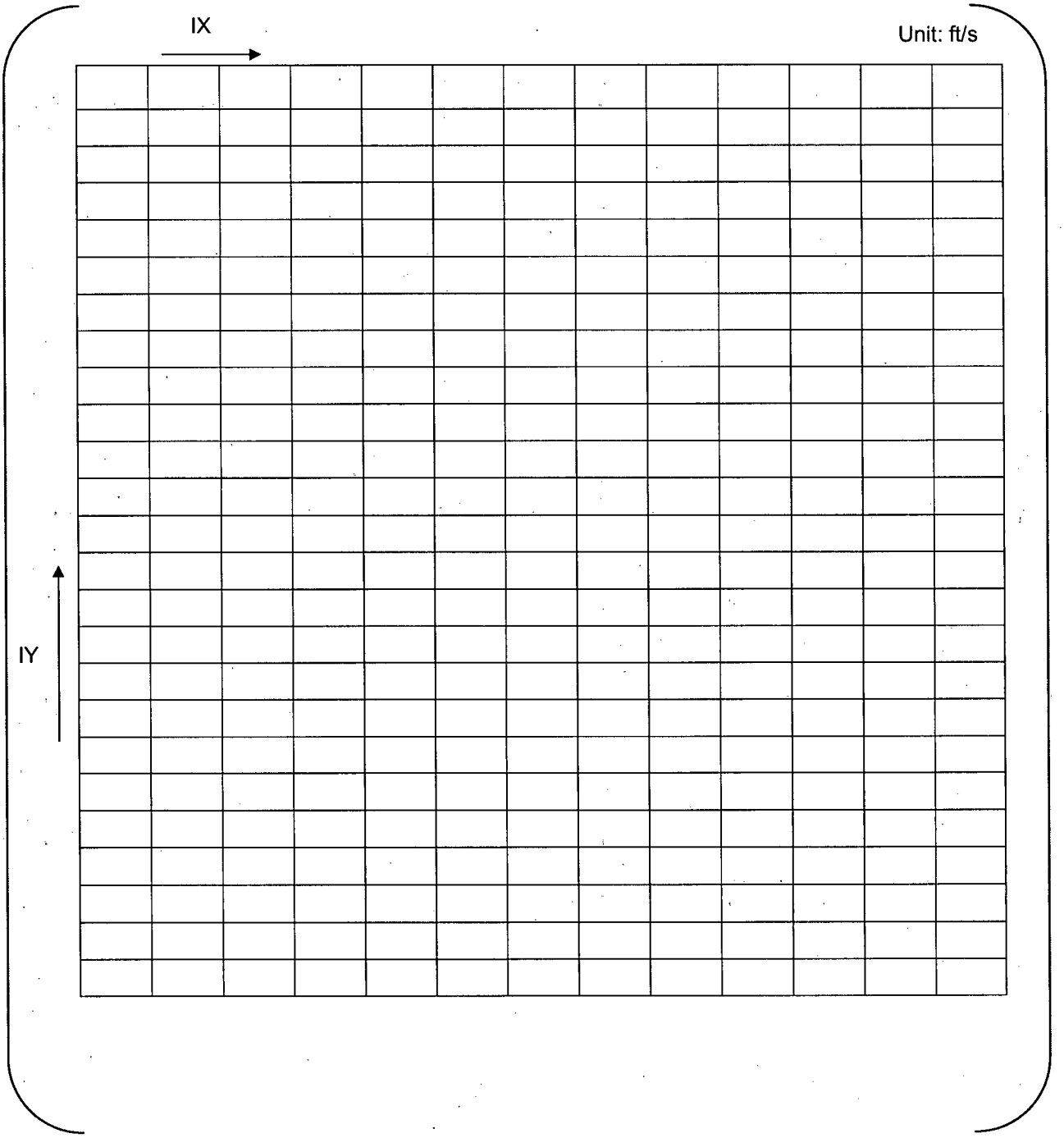

IY

Velocity at #3TSP (1/2)

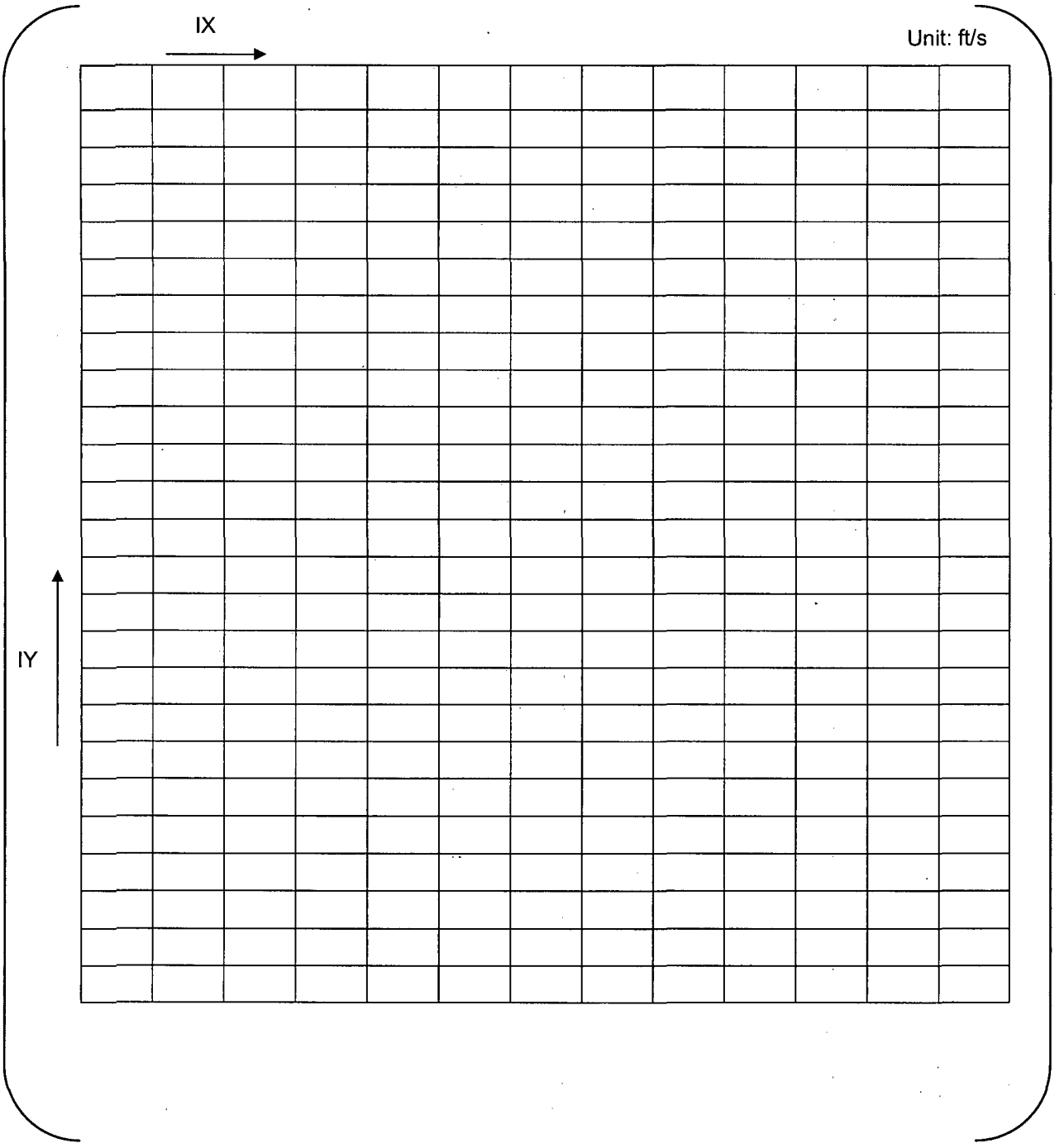

Velocity at #3TSP (2/2)

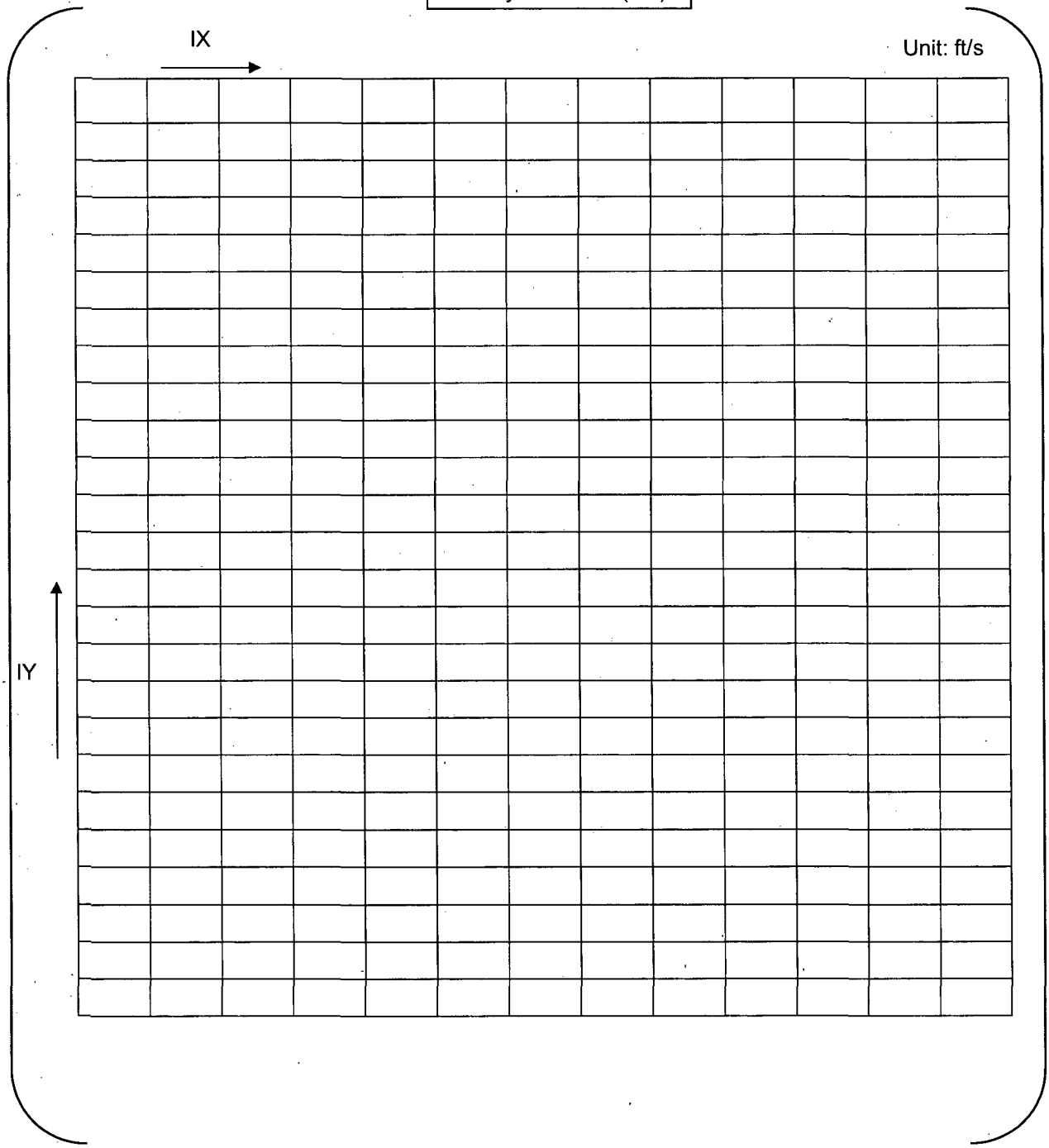

Velocity at #4TSP (1/2)

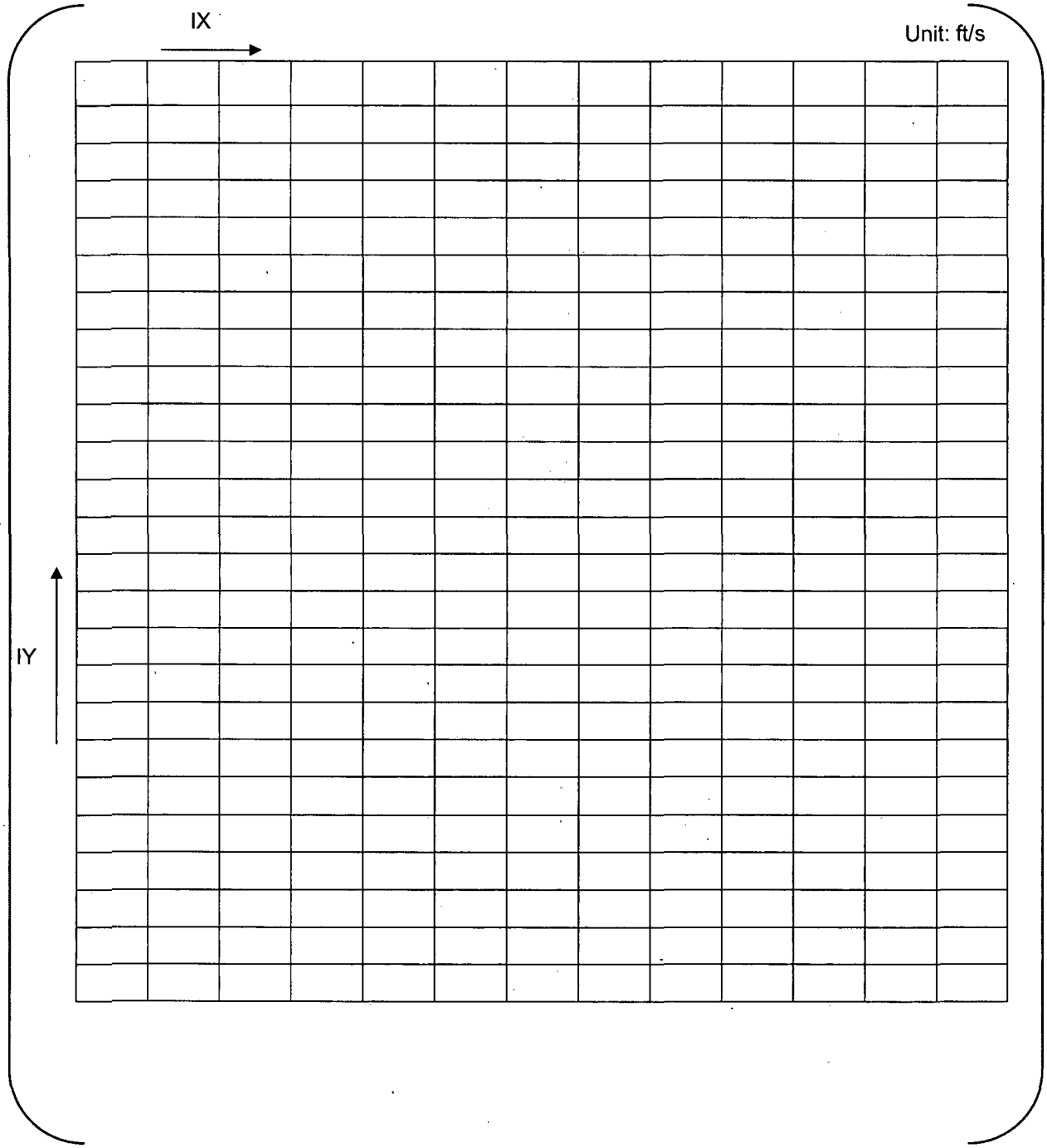

Velocity at #4TSP (2/2)

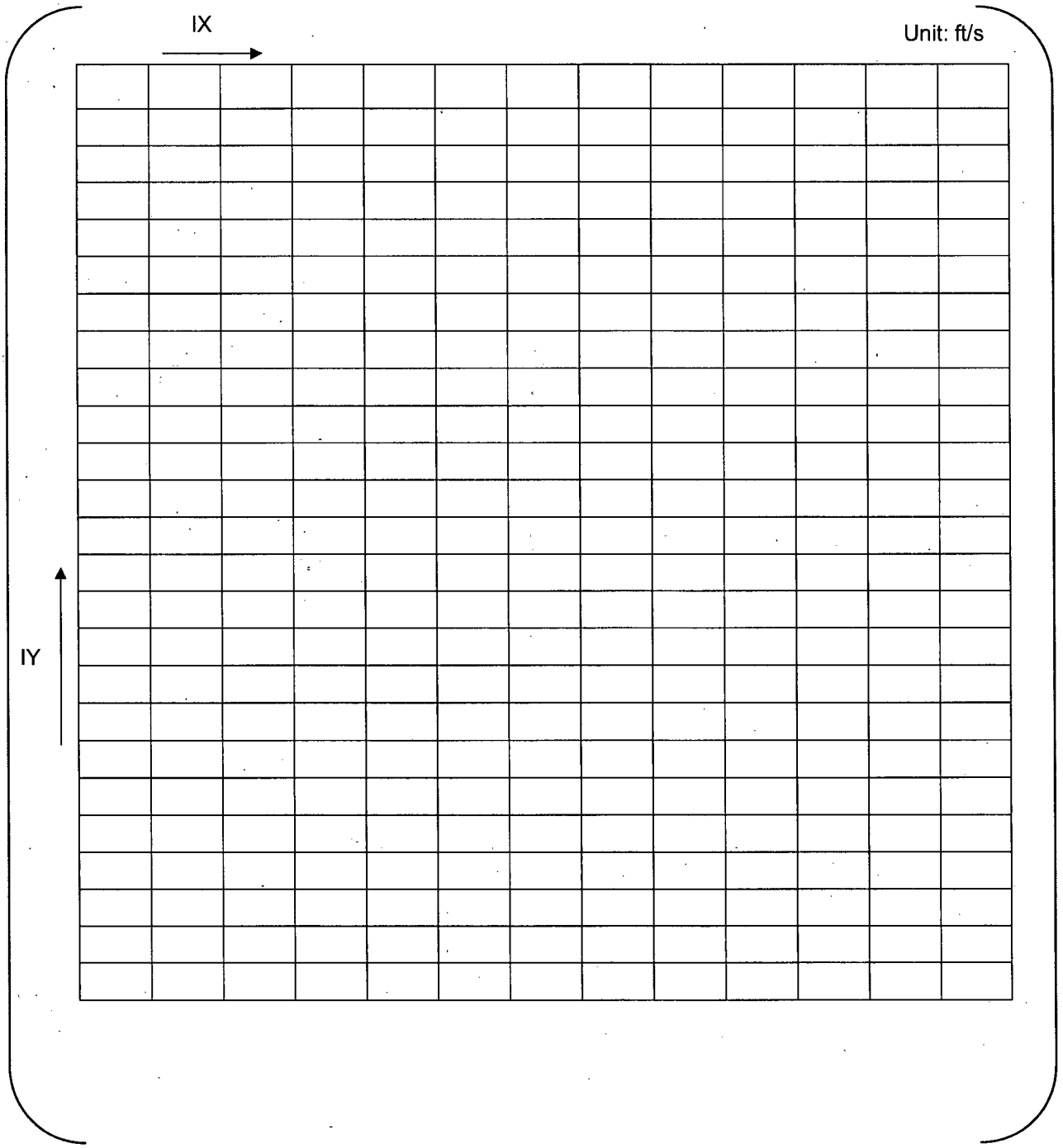

Velocity at #5TSP (1/2)

IX

Unit: ft/s

IY

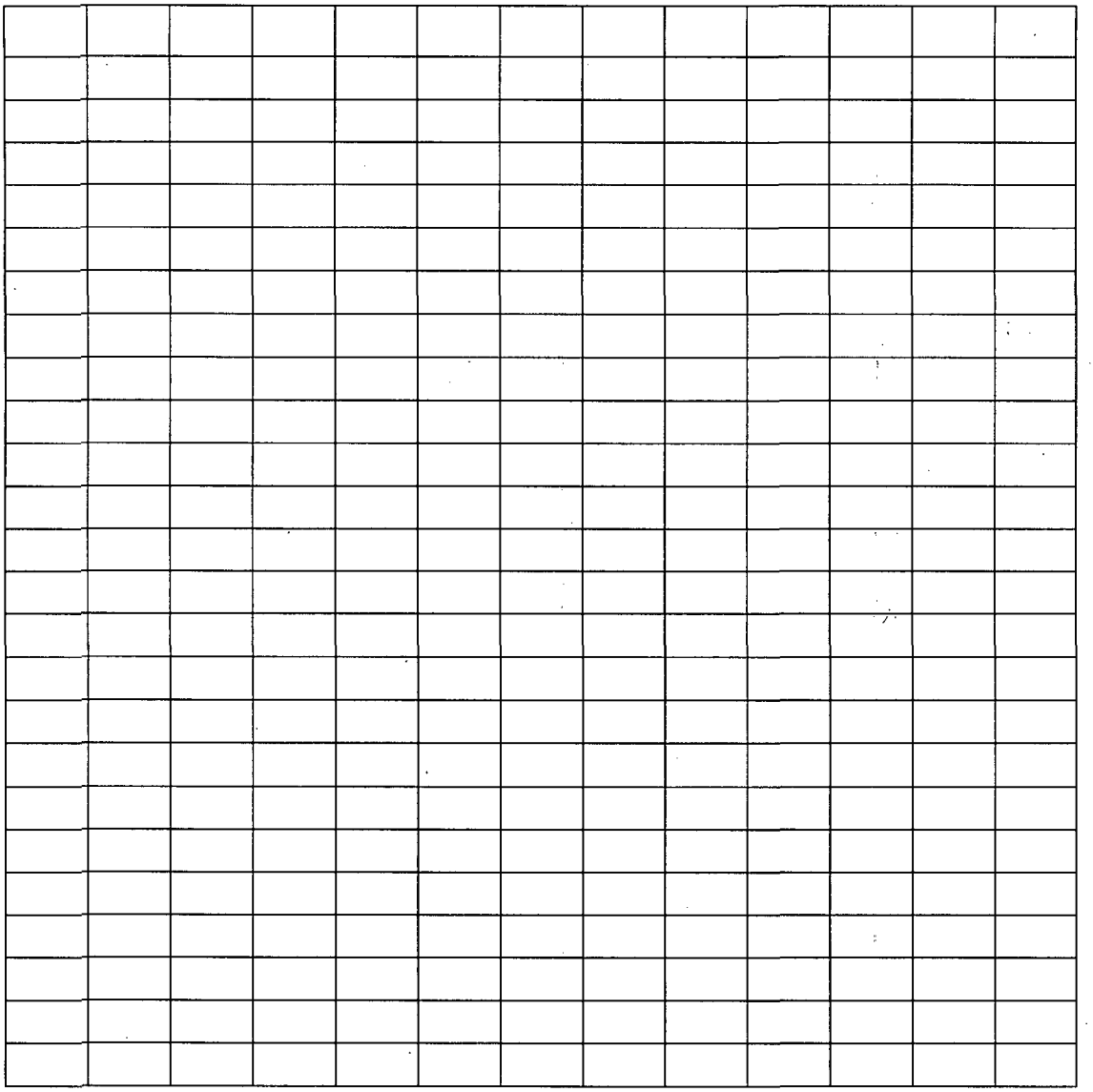

Velocity at #5TSP (2/2)

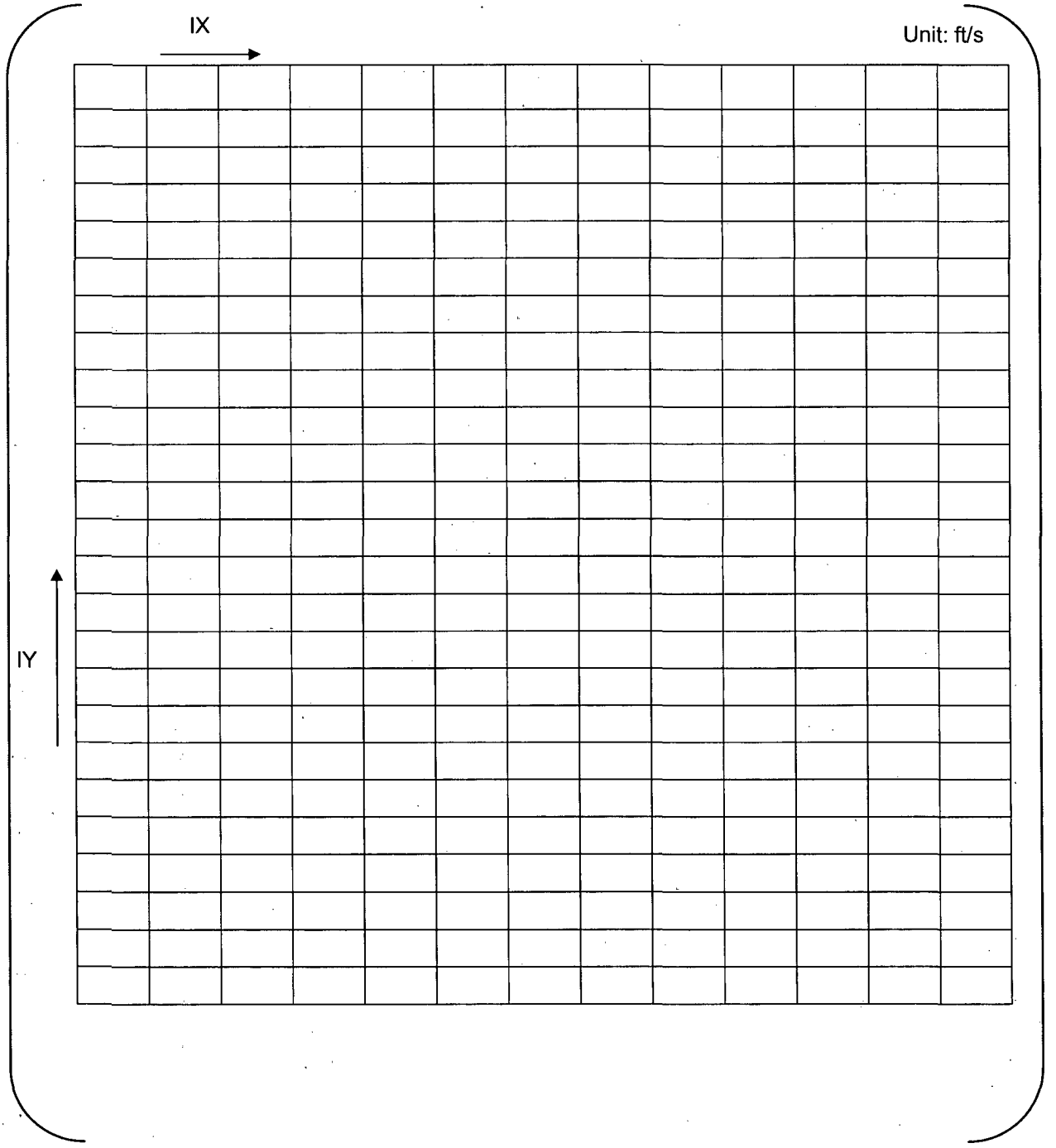

Velocity at #6TSP (1/2)

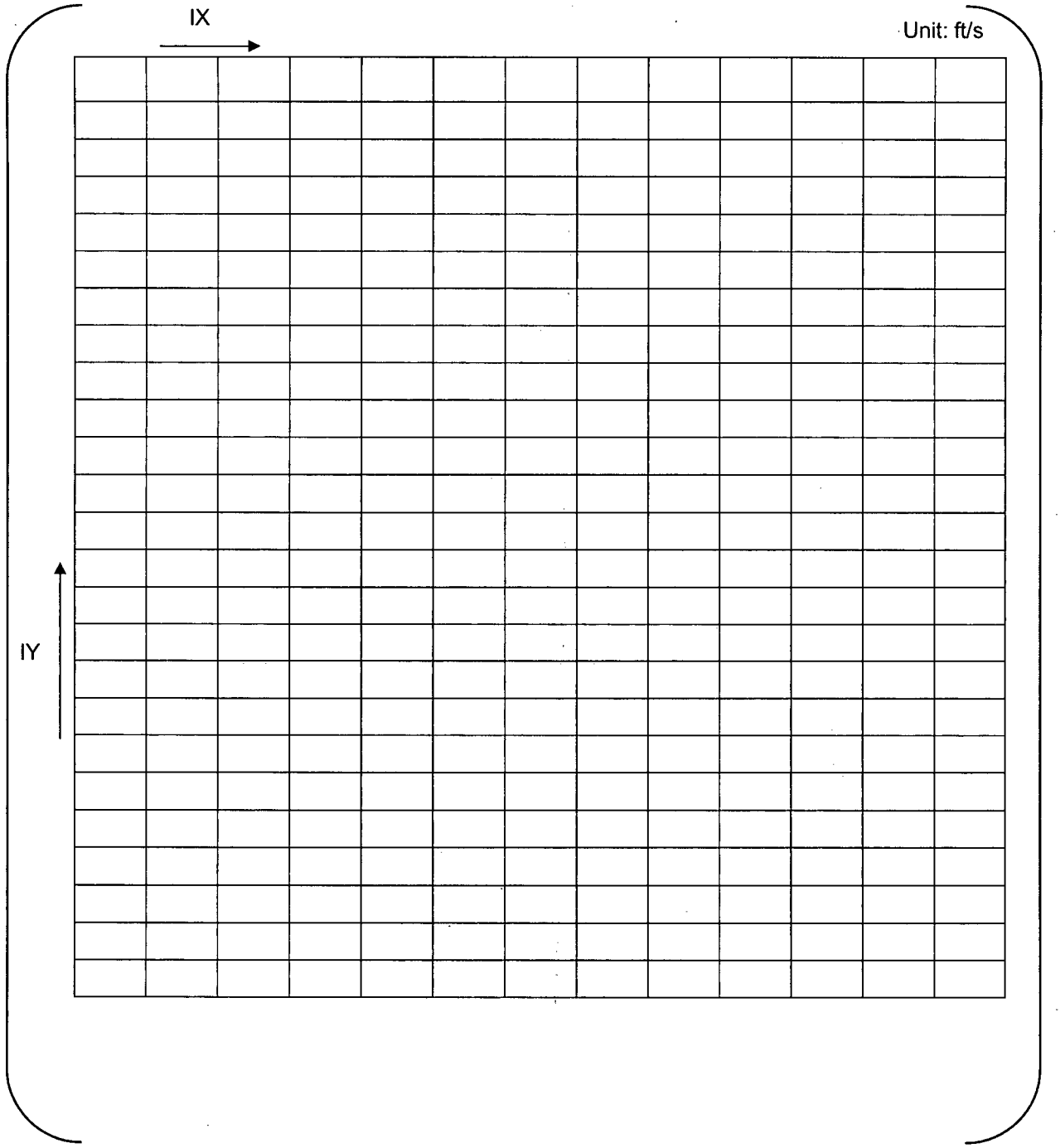

Velocity at #6TSP (2/2)

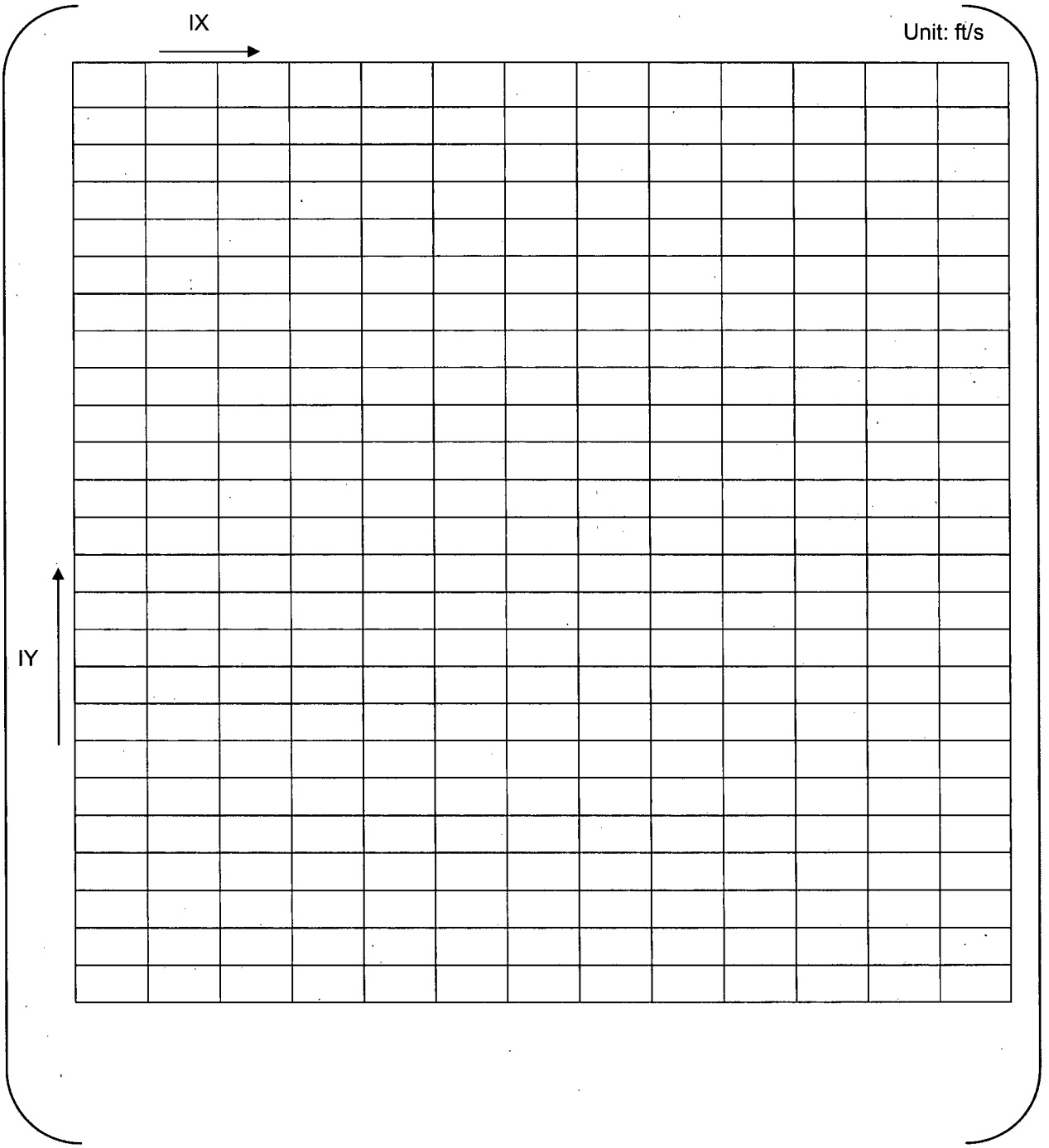

Velocity at #7TSP (1/2)

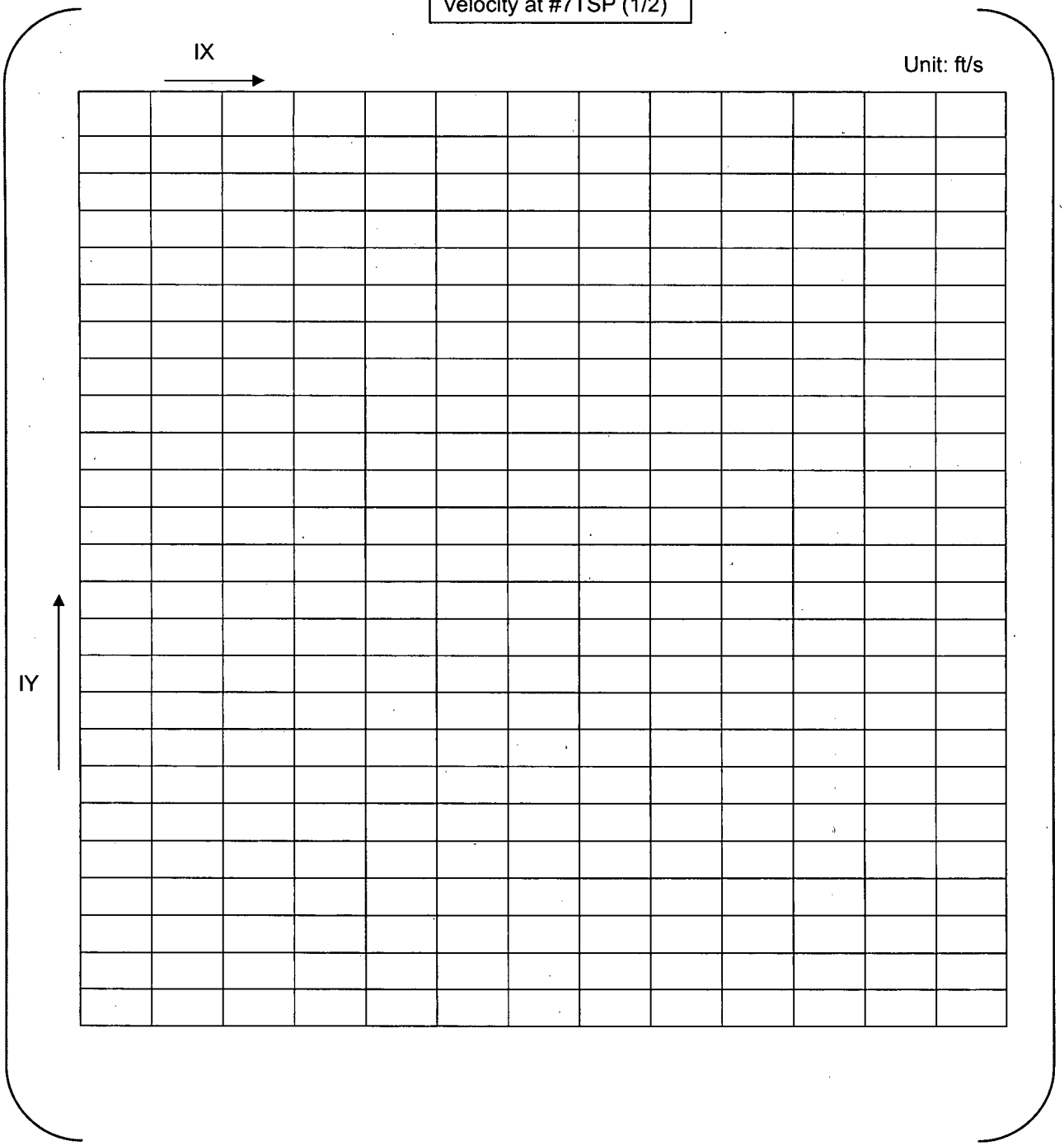

Velocity at #7TSP (2/2)

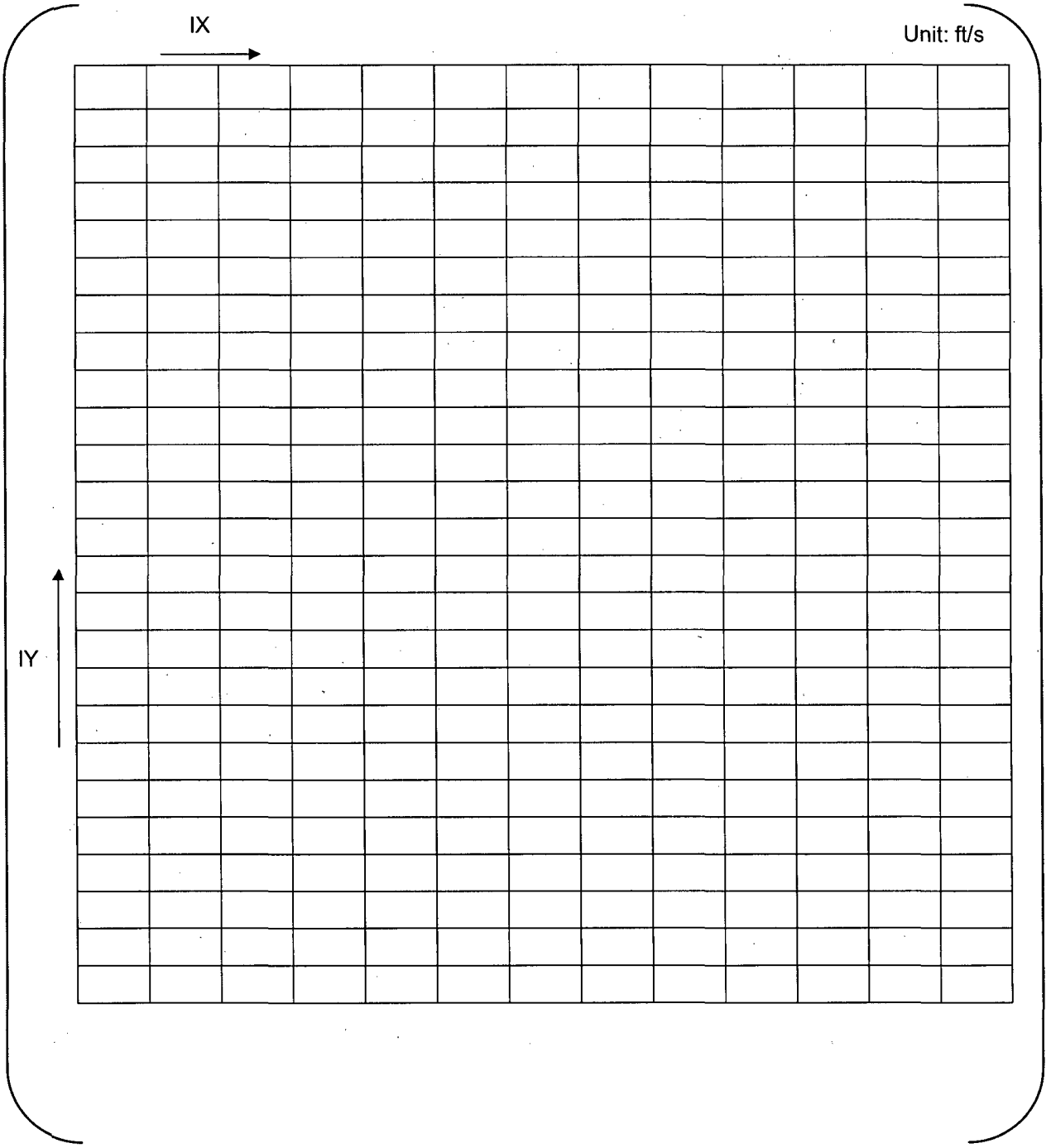

Appendix-2A
Random Vibration Evaluation of Tube Straight Portion for Unit-2/3

1. Purpose

Tube-to-tube support plate (TSP) wears at tube straight portions are detected in SONGS-2/3 RSGs. It is possible that the cause of the wears is the random vibration mechanism. The purpose of study provided in appendix-2A is to evaluate the possibility of random vibration of the tube straight portion, through the thermal and hydraulic calculations by ATHOS/SGAP computer code and vibration calculations by IVHET computer code.

2. Conclusion

The tube wear depth for Row1 Column1 tube is calculated with assuming the tube-to-TSP contact force of[ ]. Since contact force due to the thermal expansion is 0.6N which can be variable because of manufacturing tolerances and fluid forces, the contact is a parameter for this case study[ ].

The nonlinear analysis predicts that the contact force of 1.5N results in tube wear depth of 2 ~Approx.20%, which is similar to the tube inspection results 0~19%. This parametric study implies that the random vibration mechanism is the probable cause of tube-to-TSP wear and the contact force at the locations where wear indications are detected happened to be larger than the locations where no indication is detected.

Table 2-1 Parameter survey result

Case	Wear depth	Note
Calculation	Approx. 2~20%	Contact force of[ ]is assumed.
Tube inspection	0~19%	

3. Assumption

The following assumptions are used in the tube vibration calculations.

1) The tube vibration is calculated based on the assumption that the cause of tube vibration is the tube cross flow and axial flow.

2) Since there are clearances between tubes and tube holes of TSPs, the tube support conditions are uncertain. However, most tube-to-TSP contact points are considered to be effective supports because of the differential thermal expansion of the tubesheet and TSPs (Refer to Assumption of Appendix-2). TSPs supports are generally expected to be in contact with the tubes.

   For the tube-to-TSP contact point without tube-to-TSP wear identification, the tube is assumed to be in contact with the TSP (zero touch condition). For the contact point with tube-to-TSP wear indication, the contact force is considered.

3) The tube-to-TSP contact force ranging [ ] is assumed. Since the contact force due to the thermal expansion is [ ], the contact force [ ] is considered to be in the realistic range.

4) For the conservative evaluation, the large random excitation forces due to the flows are used in the vibration analysis.

4. Acceptance criteria

There is no acceptance criterion because the purpose of the parametric survey is to trace the tube-to-TSP wear depth, which is identified by the tube inspection.

5. Design input

The nominal dimensions are obtained from the design drawings (Ref.3 to 20) and the manufacturing tolerances are not considered.

Flow characteristics are obtained from 3 dimensional thermal and hydraulic analysis (See Appendix-12) .Flow velocity, density, void fraction and hydrodynamic pressure are evaluated for Row 1 Column 1 tube (Fig. 5-1). The reason of selection of the tube is provided in section 6.3.

The velocity, density distribution and volume flow rate quality for tube straight portion are provided in Fig.5-2 and 5-3.

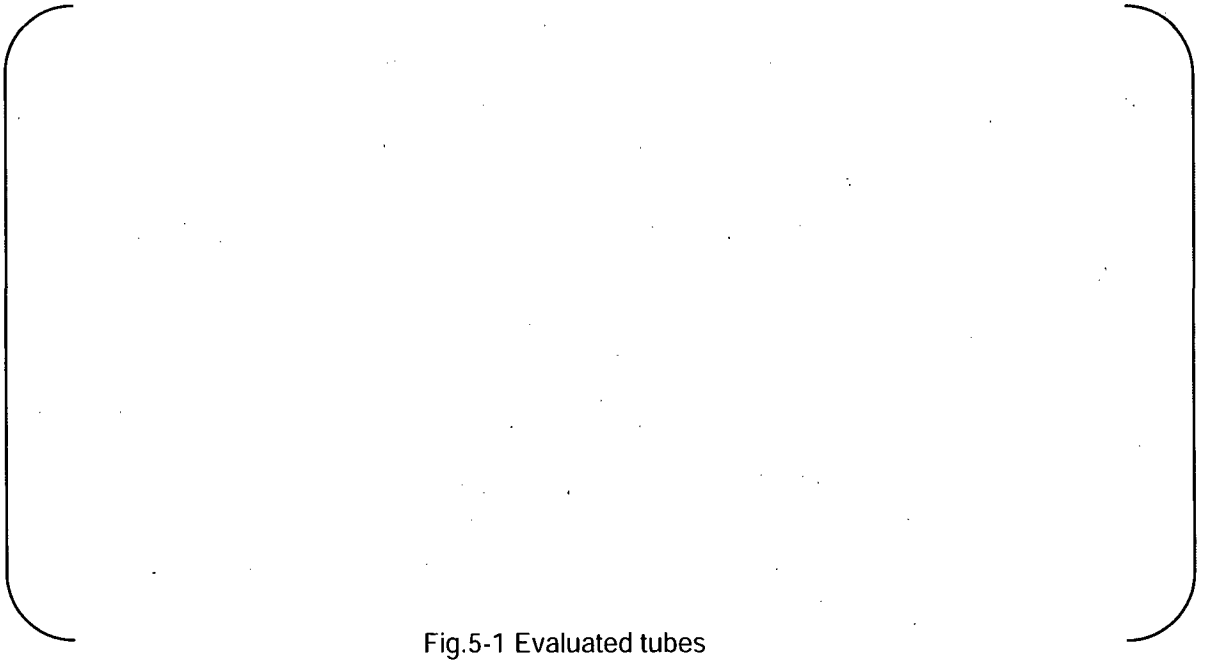

Fig.5-1 Evaluated tubes

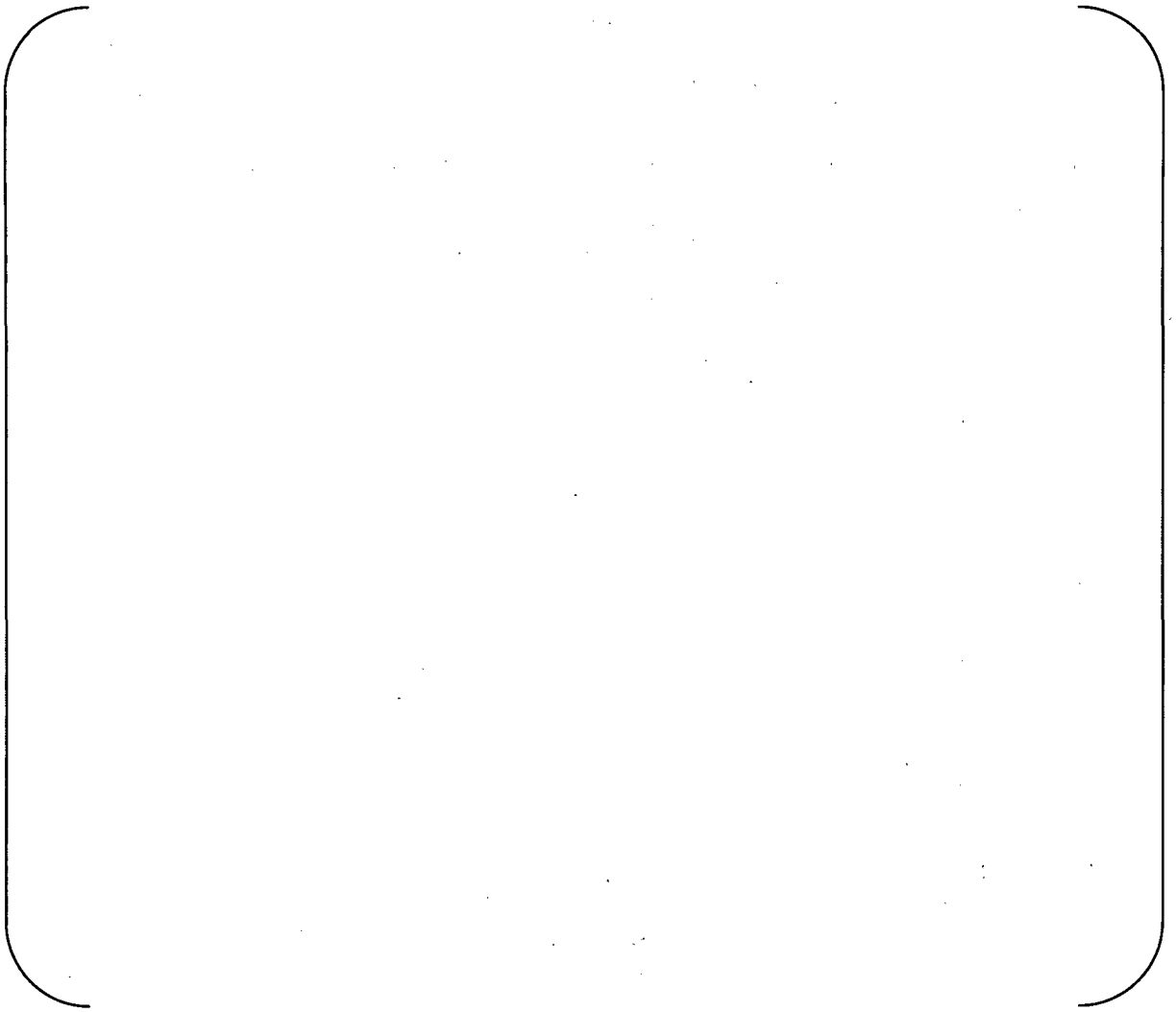

Fig 5-2 Flow distribution

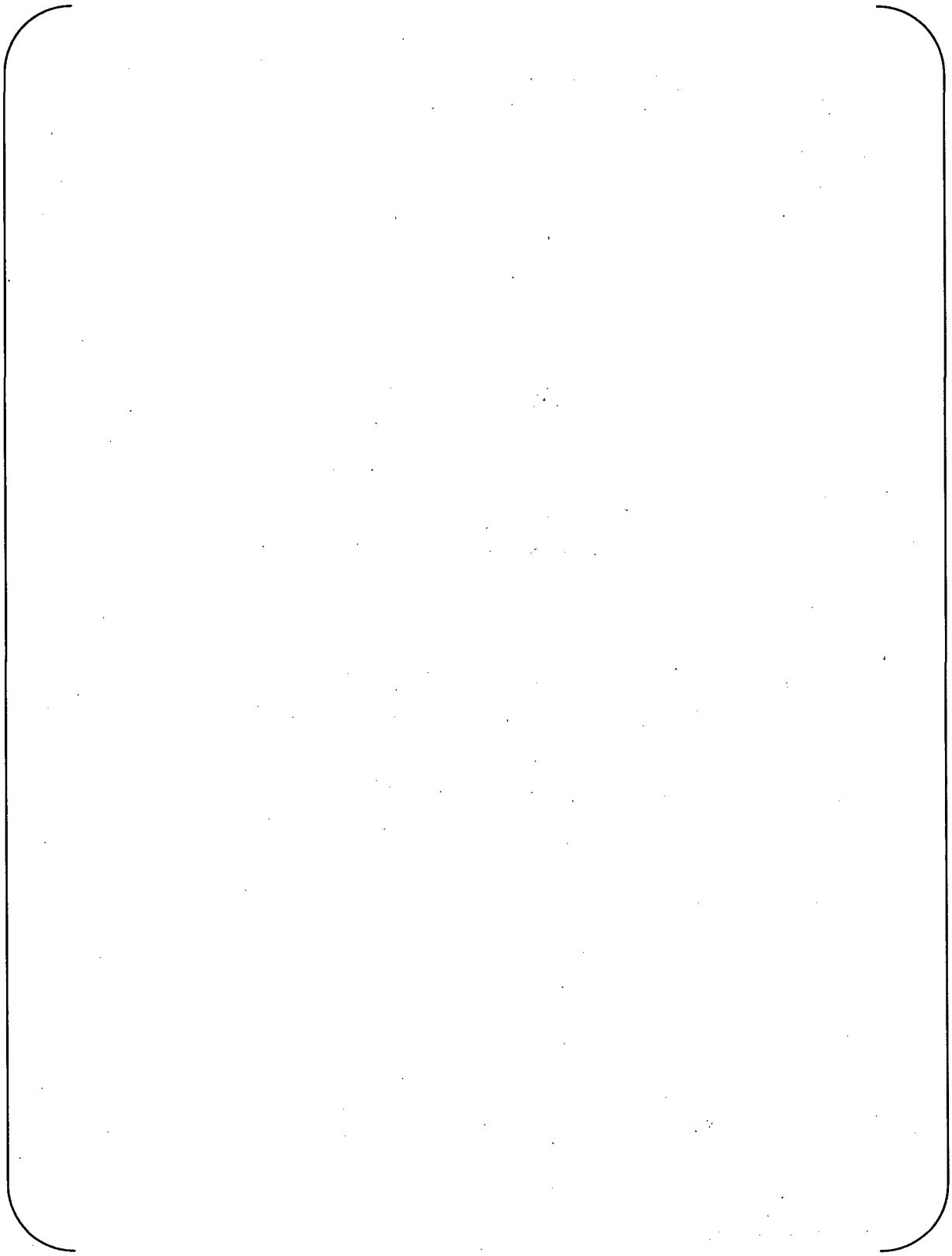

Fig 5-3 density and flow velocity multiplied

6. Methodology

6.1 Outline of analysis

Based on the design input of the operating conditions, the calculation of the circulation ratio is performed by evaluating the pressure loss and the recirculation head with SSPC, which is a 1 dimensional Thermal and Hydraulic parameter calculation code (Ref.21). Using ATHOS/SGAP, the thermal hydraulic analysis is performed to obtain the 3 dimensional flow distribution that includes the flow velocity, the flow density, and the void fraction (See Appendix-12). Then, IVHET is used to evaluate the non-linear tube vibration. The evaluation process is shown in Fig.6-1.

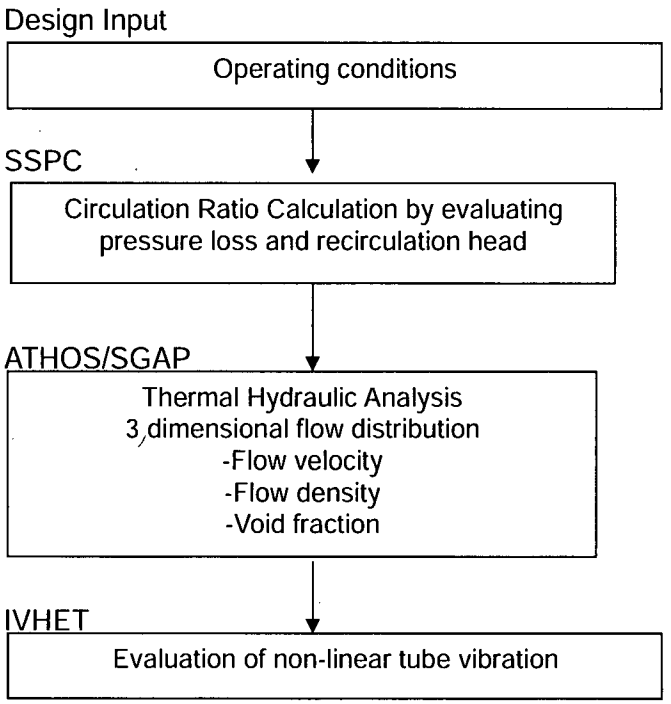

Fig.6-1 Flow of the evaluation

6.2 Evaluation Parameters

In general, larger thermal power is more severe for vibration, because the steam flow rate increases. At constant thermal power, lower steam pressure is more severe for vibration than higher pressure, because ρU^2 increases - (the lower ρ causes the higher U).
Basic parameters required for calculations are shown in Table 6-1.

Table 6-1 Basic parameters for calculation

	Condition of Cycle 16
Plugging	[
T_{cold} (°F)	
T_{hot} (Tsg-in) (°F)	
$T_{sg\text{-}out}$ (°F)	
$T_{feedwater}$ (°F)	
Saturation Steam Pressure (psia)	
Steam Mass Flow (lb/hr)	
Circulation ratio	
Thermal power (MWt/SG)	]

6.3 Selection of tubes to be evaluated

In all SGs, tube-to-TSP wear is present in many Row 1 tubes that border on the tube-free-lane. In this case study, the Row1 Column1 tube is used for the evaluation in order to compare the actual ECT inspection results of R1C1 of 2A-SG and 2B-SG, which are selected as worse cases.

Table 6-2 Tube-to-TSP wear depth of Row1 Column1 of 2B-SG

Unit (%)

SG	01H	02H	03H	04H	05H	06H	07H	07C	06C	05C	04C	03C	02C	01C
2A	[													]
2B	[													]

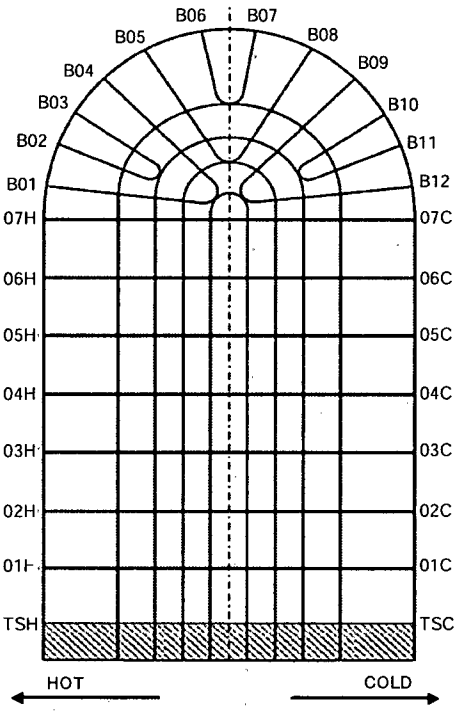

6.4 Random excitation force

The random excitation forces due to the cross flow and axial flow are considered.

(1) Random excitation force due to the cross flow

The random excitation force due to the cross flow is calculated based on Fig.6-2 [22]. Since the "envelop spectrum" in the figure 6-2 is used, the random excitation force is overestimated. The following equation is used for the calculation.

$$\Phi_{cross} = (\rho g D_w D)^2 \cdot \left(\frac{D_w}{U}\right) \cdot \Phi_E$$

$$\Phi_E = \begin{cases} 10 f_r^{-0.5} & ; \ f_r < 0.06 \\ (2\times 10^{-3}) f_r^{-3.5} & ; \ f_r > 0.06 \end{cases}, \quad f_r = \frac{f D_w}{U_{mean}}, \quad D_w = \frac{0.1D}{\sqrt{1-\beta_{mean}}}$$

where

Φ_{cross} : Power spectrum density of fluid force per unit length (cross flow)

D : Tube outer diameter

ρ : Density at each element

U : Flow force at each element

U_{mean} : Average flow velocity between each span

β_{mean} : Average volume flow velocity quality between each span

g : Gravity acceleration

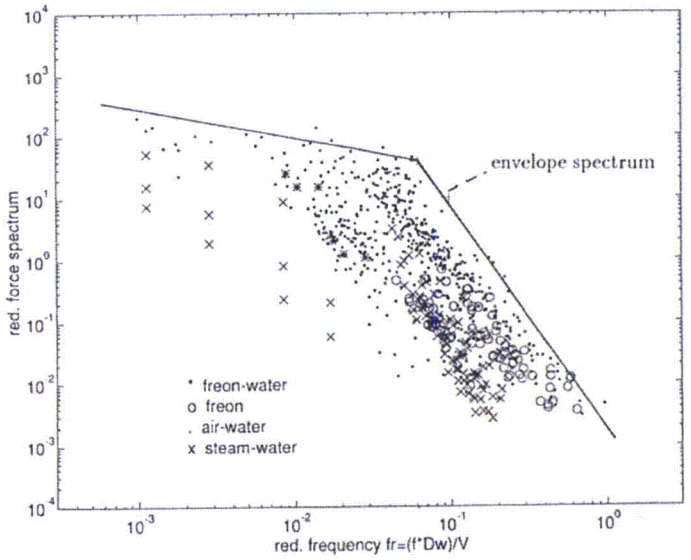

Fig 6-2 Power spectrum density of random excitation force due to the cross flow

(2) Random excitation force due to the axial flow

The random excitation force due to the axial flow is calculated based on Fig.6-3 [23]. Since the design guideline covering most data is used, the random excitation force is overestimated. The following equation is used for the calculation.

$$\Phi_{axial} = (2.0 \times 10^{-7}) \times (\rho UD)^2$$

where

Φ_{axial} : Power spectrum density of fluid force per unit length (axial flow)

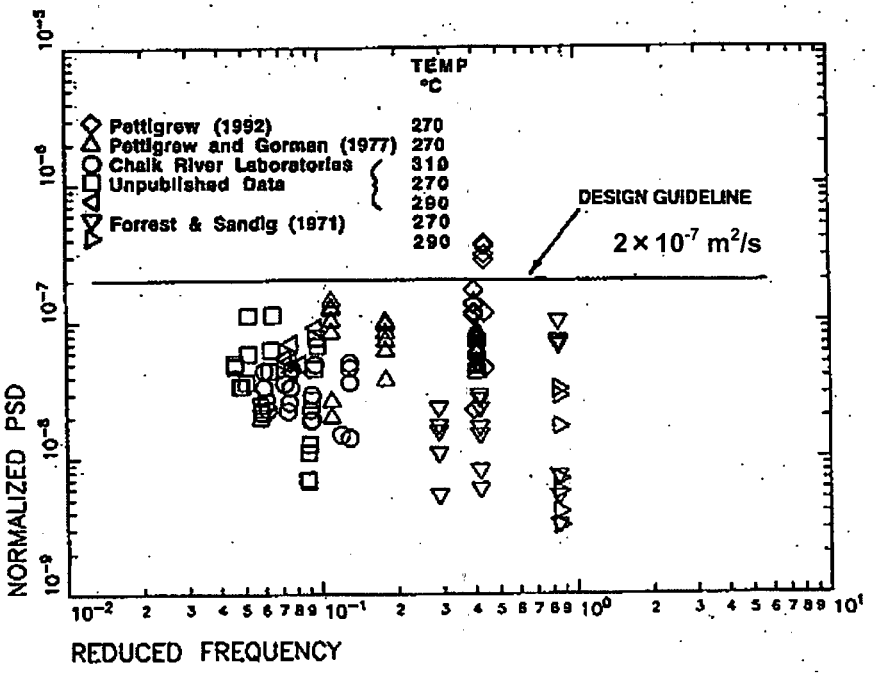

Fig 6-3 Power spectrum density of random excitation force due to the axial flow

7. Results

The vibration analysis results are provided in Fig.7-1. The parametric survey of the contact force shows that the contact force of[ ] gives the tube wear depth is[ ], which is similar to the tube inspection results[ ].

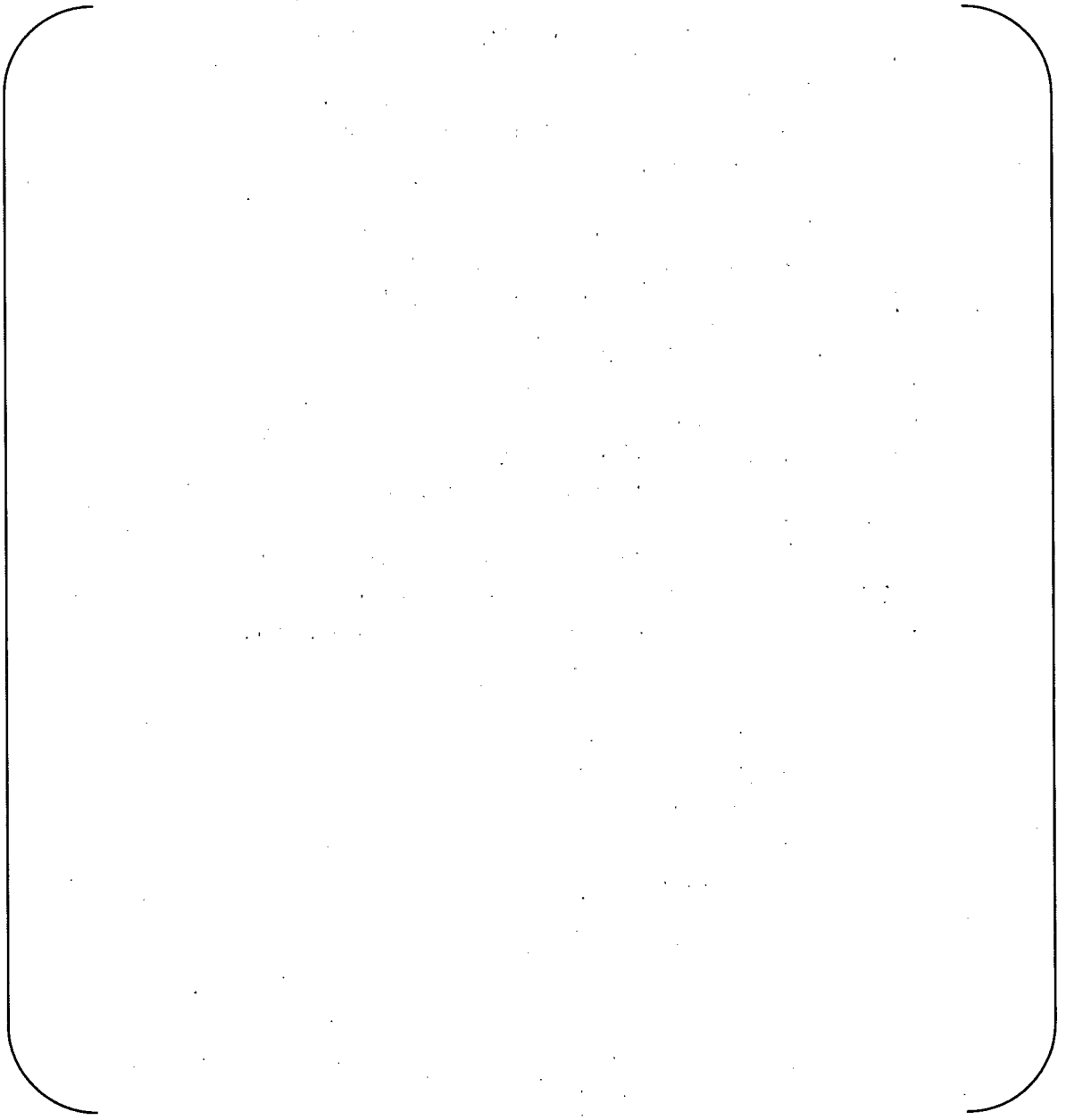

Fig 7-1 Wear depth of analysis result

8. References

1) Deleted
2) Deleted
3) L5-04FU001 the latest revision, Component and Outline Drawing 1/3
4) L5-04FU002 the latest revision, Component and Outline Drawing 2/3
5) L5-04FU003 the latest revision, Component and Outline Drawing 3/3
6) L5-04FU021 the latest revision, Tube Sheet and Extension Ring 1/3
7) L5-04FU022 the latest revision, Tube Sheet and Extension Ring 2/3
8) L5-04FU023 the latest revision, Tube Sheet and Extension Ring 3/3
9) L5-04FU051 the latest revision, Tube Bundle 1/3
10) L5-04FU052 the latest revision, Tube Bundle 2/3
11) L5-04FU053 the latest revision, Tube Bundle 3/3
12) L5-04FU111 the latest revision, AVB assembly 1/9
13) L5-04FU112 the latest revision, AVB assembly 2/9
14) L5-04FU113 the latest revision, AVB assembly 3/9
15) L5-04FU114 the latest revision, AVB assembly 4/9
16) L5-04FU115 the latest revision, AVB assembly 5/9
17) L5-04FU116 the latest revision, AVB assembly 6/9
18) L5-04FU117 the latest revision, AVB assembly 7/9
19) L5-04FU118 the latest revision, AVB assembly 8/9
20) L5-04FU119 the latest revision, AVB assembly 9/9
21) L5-04GA510 the latest revision, Thermal and Hydraulic Parametric Calculations
22) "Flow~Induced Vibration", 107-117 P.W. Bearman (Edit)
23) " Two-Phase Flow-Induced Vibration : An Overview", Journal of Pressure Vessel Technology 1994 , Vol.116, 233-253 M. J. Pettigrew, C. E. Taylor

Appendix-3
FEI Evaluation of Tube U-bend Portion for Unit-2/3

1. Purpose

The analysis is conducted for 100% reactor power, zero plugged tubes and all AVB supports being active to evaluate design conditions of the RSGs in the first operating period.

The purpose of this appendix is to provide a fluid elastic instability evaluation of out-of-plane direction for the tubes of the San Onofre Units 2 and 3 Replacement Steam Generators (RSGs) in accordance with Section III Appendix N, Article N-1330 based on U-bend flow conditions from the ATHOS/SGAP (EPRI) thermal-hydraulic analysis code instead of the evaluation based on the flow conditions obtained from FIT-III during the RSG design stage (Ref.1).

2. Conclusion

The fluid elastic stability ratios are confirmed to be less than 1.0 at full power and with all AVBs active to satisfy the criteria of ASME Section III Appendix N, Article N-1330. This conclusion applies to all of the steam generator tubes. The results for the most limiting tubes are shown in Table 2-1 and indicate the occurrence of tube out-of-plane FEI is very unlikely when the gap between tube and AVB is very small and the AVB support point is active in the tube out-of-plane direction.

Table 2-1 Fluid Elastic Stability Ratios for the Limiting Tubes

Row	Column	Damping ratio	Critical Factor	Natural frequency f (Hz)	Critical Flow velocity Uc (ft/s)	Effective flow Velocity Ue (ft/s)	Stability ratio
142	88	1.5%*	2.4*				
47	89						
47	7						
26	88						
26	4						
14	88						
14	2						
1	89						
1	1						

Note*: Values recommended by ASME Section III Appendix N, Article N-1331.3

3. Assumption

(1) Nominal tube thickness and nominal tube length are used in the evaluation model because the effect of the tolerances of these dimensions on the natural frequency is negligible.

(2) Contact condition between tube and tube support plate is pin-supported. Fixed supported condition at No. 1 TSP is added.

(3) Contact condition between tube and active support points by the anti-vibration bar (AVB) is pin-supported. And all points are active.

(4) Modulus of elasticity of tube is interpolated based on the tube average temperature of $\frac{T_{av}+T_s}{2}$ from table of ASME Boiler and Pressure Vessel Code, Sec II, Materials, 1998 Edition, 2000 addenda (Ref.23).

Where,

T_{av} : Primary side average temperature (°F)

T_s : Secondary side temperature (°F)

(5) Tube has the virtual added mass supposing the fluid-structure interaction (FSI) effect as shown in the following formula (Ref.24).

$$m_v = \frac{\pi D_o^2 \rho_o}{4}\left\{\frac{(D_e/D_o)^2+1}{(D_e/D_o)^2-1}\right\} \text{(lbm/ft)} \quad \cdots\cdots (1)$$

$$D_e/D_o = \left(1+\frac{1}{2}P/D_o\right)P/D_o \quad \cdots\cdots (2)$$

Where,

m_v : Virtual added mass per unit length due to FSI effect;

ρ_o : Average density of water outside the tube;

D_o : Tube outside diameter

P : Tube pitch.

9

4. Acceptance criteria

The ASME Section III, Appendix N (Ref. 22) methodology and acceptance criteria are used for this analysis. The acceptance criterion is that the effective flow velocity across the tubes be no greater than the Appendix N critical flow velocity. The ratio of these two velocities may not exceed 1.0. The ASME methodology includes conservatisms to account for practical design variability.

5. Design Inputs

The nominal tube dimensions are used in the analysis and are obtained from the design drawings (Ref. 3 to 20). Manufacturing tolerances are not considered.

The basic operating parameters required for the calculations are shown in Table 5-1 (see Appendix-12 for details).

Table 5-1 Basic parameters

Number of tubes plugged	
Thermal power (MWt/SG)	
T_{cold} (°F)	
T_{hot} (Tsg-in) (°F)	
$T_{feedwater}$ (°F)	
Saturation Steam Pressure (psia)	
Steam Mass Flow (lb/hr)	
Circulation ratio	

(Note) The primary inlet temperature range is [ ]°F. It is conservative for this analysis to use the lower inlet temperature ([ ]°F) because it produces a lower secondary pressure and a higher steam flow velocity.

The tubes selected for evaluation are listed in Table 5-2, which are the same tubes evaluated during the RSG design stage (Ref.1). These tubes have longer support spans, lower damping and higher flow excitation than others.

Table 5-2 Evaluated Tubes

Row	Column
142	88 (Center)
47	89 (Center)
47	7 (Outer-most)
26	88 (Center)
26	4 (Outer-most)
14	88 (Center)
14	2 (Outer-most)
1	89 (Center)
1	1 (Outer-most)

The flow conditions (flow velocity*, flow density and void fraction) applied to these limiting tubes are shown in Fig. 5-1 through 5-5. The ATHOS flow conditions are only applied over the U-bend portion of the tube. The structural model for the U-tubes includes the full tube length including the straight legs, but no cross flow velocities are applied to the straight legs.

Note)

*: Flow velocity shown in Fig. 5-1 through 5-5 indicates the gap velocity in normal direction to tube in-plane.

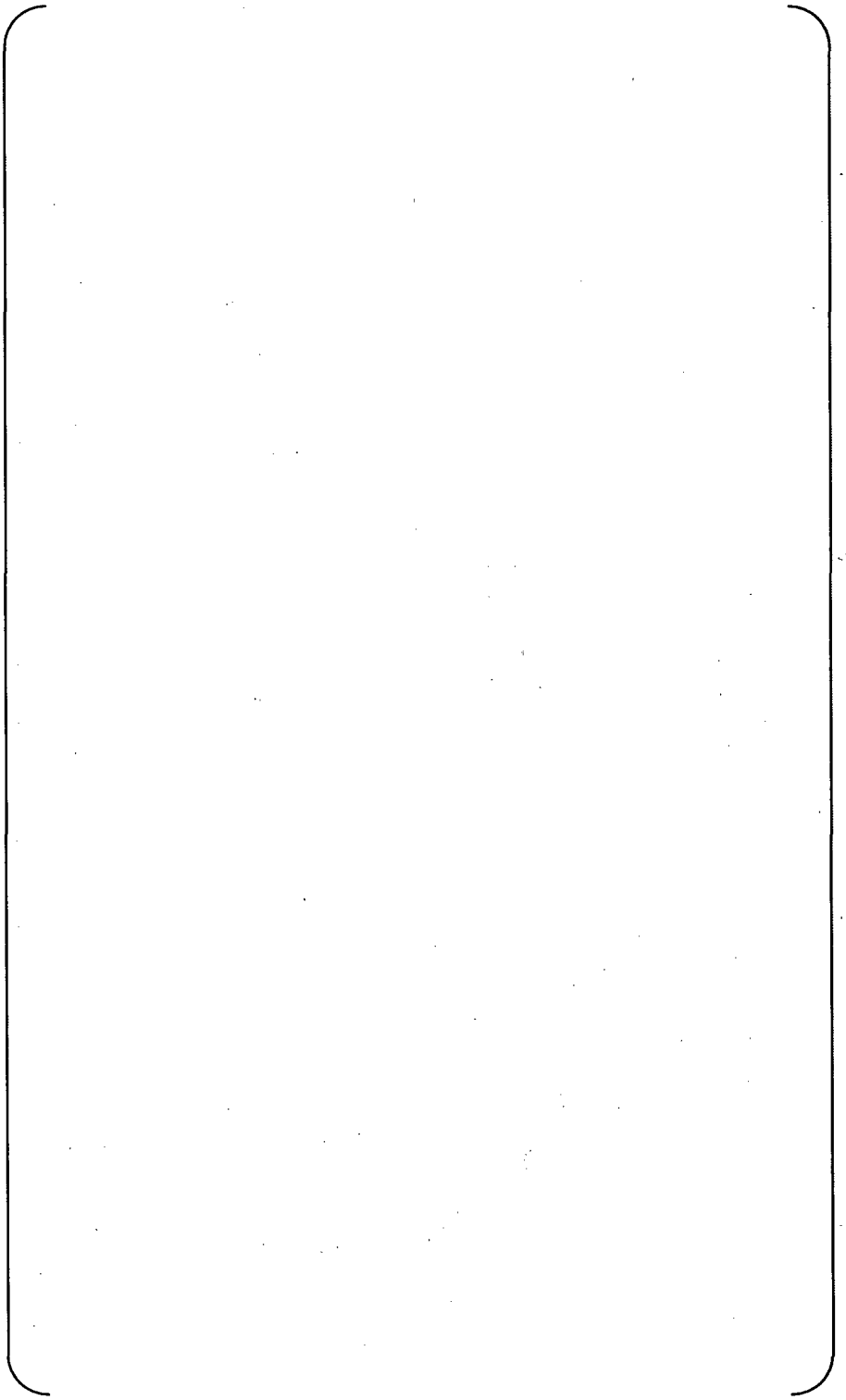

Fig.5-1 Flow distribution of Row 142 Col 88

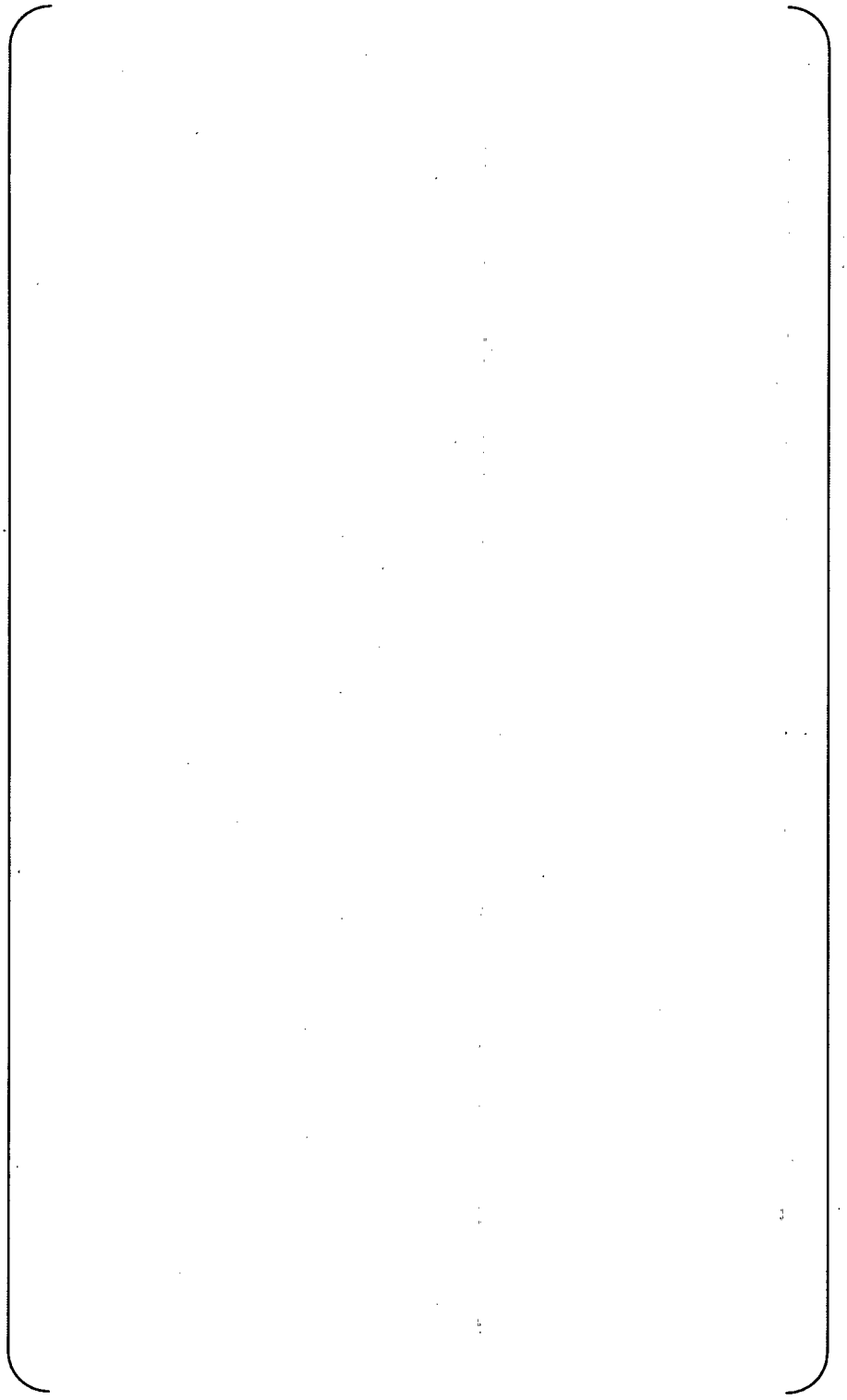

Fig.5-2 Flow distribution of Row 47, Columns 89 and 7

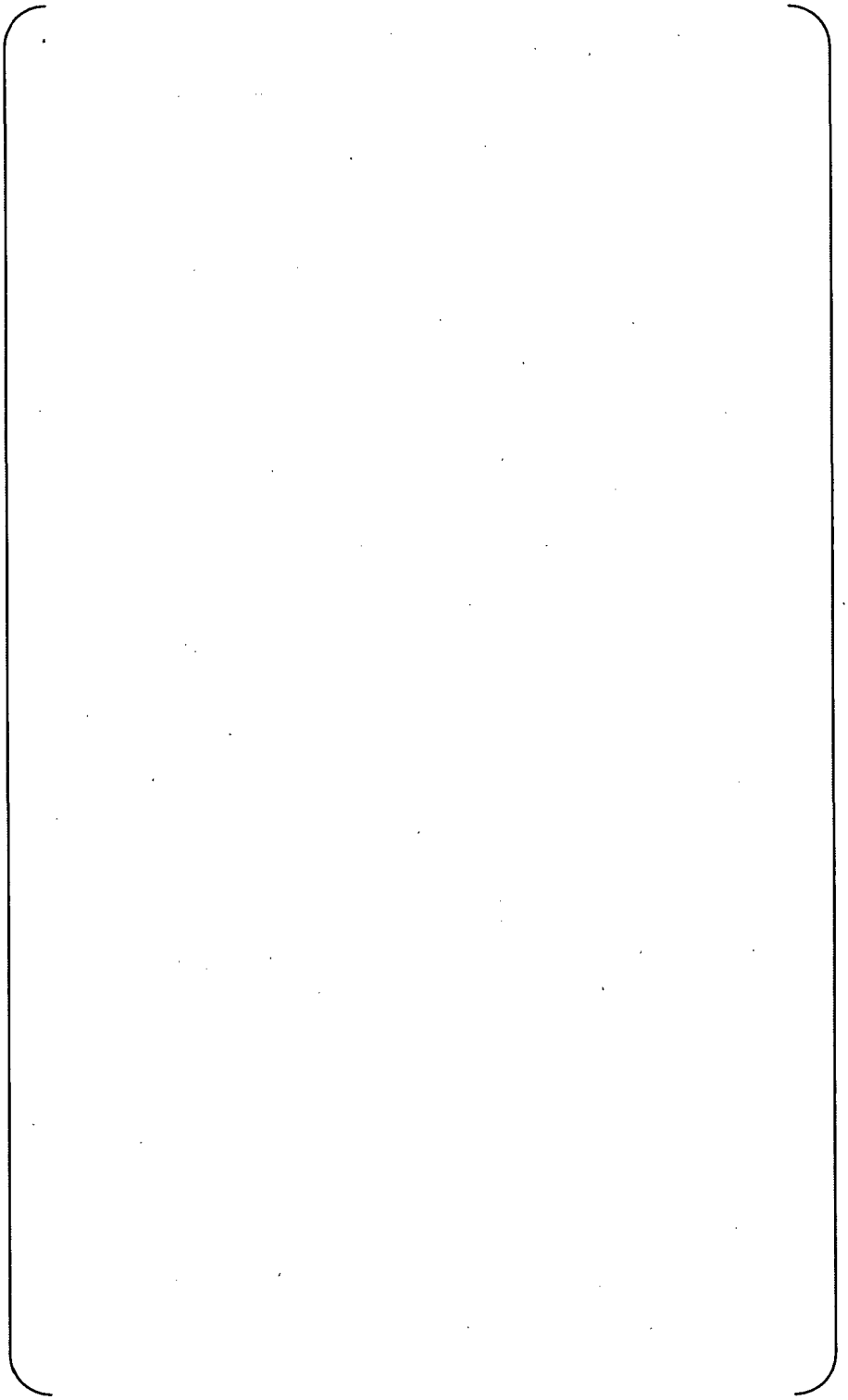

Fig.5-3 Flow distribution of Row 26, Columns 88 and 4

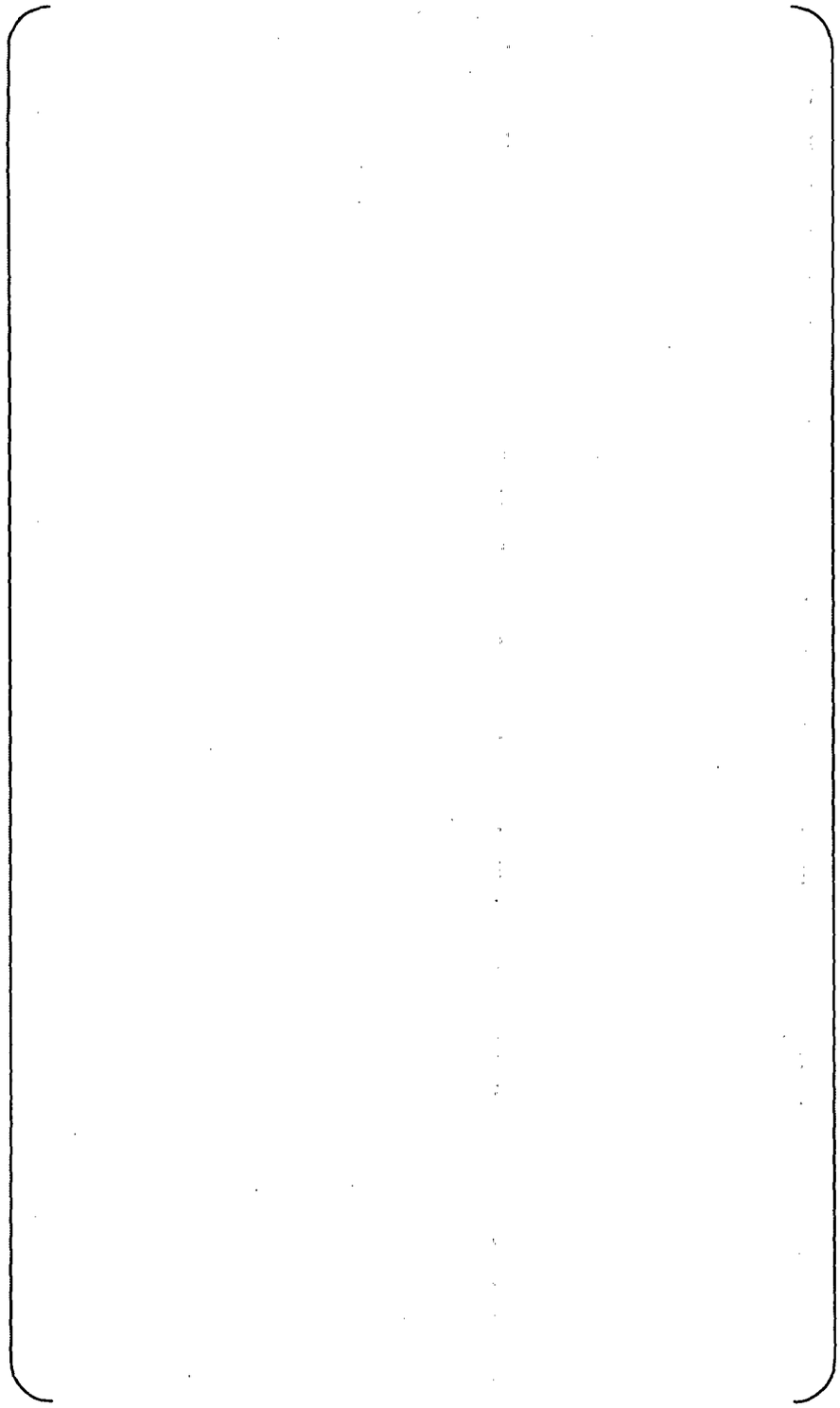

Fig.5-4 Flow distribution of Row 14, Columns 88 and 2

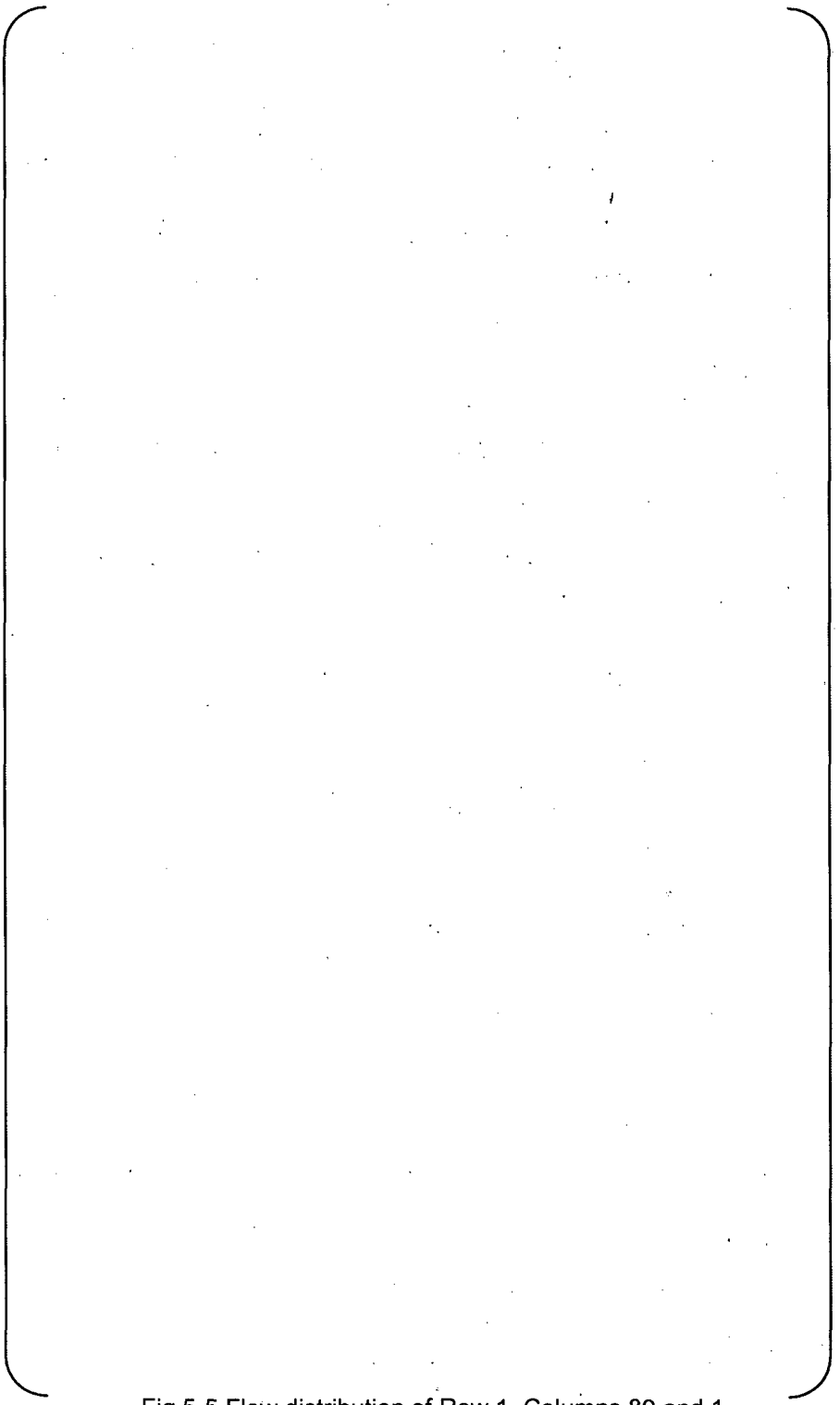

Fig.5-5 Flow distribution of Row 1, Columns 89 and 1

6. Methodology

The term "fluid elastic instability" is generally used to refer to self-excited vibration of tube bundles due to cross flow. In 1969, Connors disclosed the presence of this phenomenon for the first time (Ref.25).

Causes of fluid elastic instability are considered to be the absorption of flow energy due to the interaction of fluid and structure. This phenomenon occurs on tube bundles, and is subjected to effects of tube bundle array. Thus, it is experimentally attempted to determine the criticality of occurrence in various tube bundle arrays.

The critical flow velocity U_c for generating fluid elastic instability is obtained in the following Connors' formula (Ref.25). This formula is employed in the TEMA (Standards of the Tubular Exchanger Manufactures Association), which is the industrial design standard in the United States.

$$\frac{U_c}{fD_o} = K\left[\frac{m_0\delta}{\rho_o D_o^{\,2}}\right]^{1/2} \quad \cdots\cdots (3)$$

Where,

U_c	: Critical flow velocity
f	: Tube natural frequency
D_o	: Tube outside diameter
K	: Critical factor
m_0	: Average tube mass per unit length
δ	: Tube logarithmic decrement(= $2\pi h$)
h	: Damping ratio
ρ_o	: Density of water outside the tube

The critical flow velocity U_c in eq. (3) is evaluated in case of tube vibration of single degree of freedom system with uniform cross flow along the tube axis. In actual tube, however, the vibration of the tube supported by the tube support plate is multi degrees of freedom system with beam type of vibration modes. Therefore, considering the vibration mode and fluid distribution, the effective flow velocity U_{en} is evaluated in the following formula.

$$U_{en} = \left[\frac{\int_0^L \frac{\rho(x)}{\rho_O} \cdot U(x)^2 \cdot \phi_n(x)^2 dx}{\int_0^L \frac{m(x)}{m_O} \cdot \phi_n(x)^2 dx}\right]^{1/2} \quad \cdots\cdots (4)$$

Where,

U_{en}	: Nth mode effective flow velocity
$\varphi_n(x)$	: Nth vibration mode
$\rho(x)$	: Fluid density distribution of water outside the tube in tube axis direction
$m(x)$	: Tube mass distribution per unit length in tube axis direction
$U(x)$	: Flow velocity distribution orthogonal to tube axis in tube axis direction
x	: Coordinate component along tube axis
ρ_o	: Average density of water outside the tube
m_o	: Average tube mass per unit length
L	: Tube length

The stability ratio is determined as follows in each vibration mode by calculating the ratio of eq. (3) and eq. (4).

$$SR_n = \frac{U_{en}}{U_{cn}} \quad \cdots\cdots (5)$$

where,

$$\frac{U_{cn}}{f_n \cdot D_o} = K\left[\frac{m_0 \delta}{\rho_o D_o^{\,2}}\right]^{1/2} \quad \cdots\cdots (6)$$

This value is called the n-th mode stability ratio SR_n, and if $SR_n > 1$, fluid elastic instability occurs. Generally, the maximum stability ratio in each mode is called the stability ratio of the tube, which is simply expressed as SR.

Evaluation of occurrence of fluid elastic instability in U-tubes is carried out in the following steps :

① Using a 1-dimensional Thermal and Hydraulic parameter code (SSPC), determine the tube bundle circulation ratio and other secondary side operating conditions for the normal operating condition (Ref.21).

② Using the flow analysis code (ATHOS/SGAP), determine the distributions of flow velocity U(x) and density of the fluid ρ(x) along the tube axis.

③ For the damping ratio h and critical factor K, the suggested values based on ASME Sec III Appendix N-1330 are used, and from eqs. (3) ~ (5) stability ratio is evaluated (Ref.24).

The critical factor K=2.4 in eq. (3) gives a conservative criteria for avoiding fluid-elastic instabilities of tube arrays. Also, the damping ratio h= 1.5% for wet steam or liquid is used. Natural frequencies, vibration mode and stability ratio are calculated by vibration analysis code FIVATS.

Figure 6-1 describes this process.

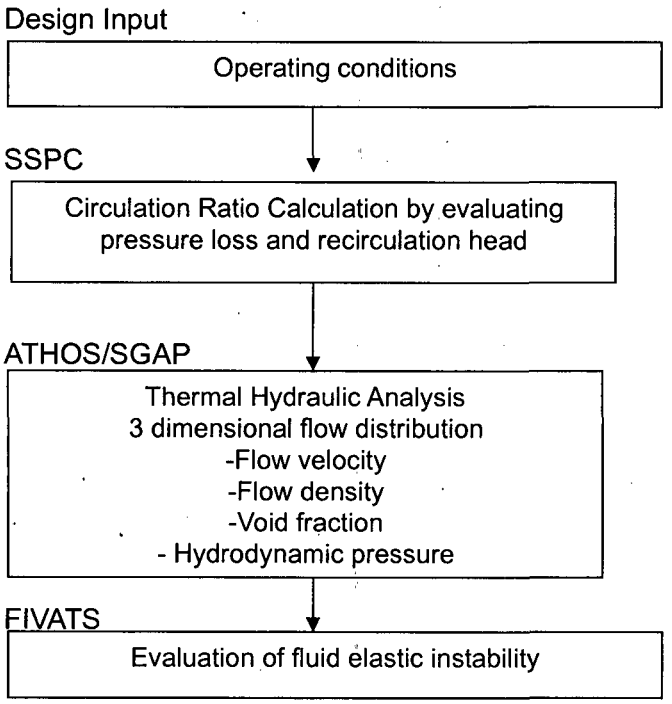

Fig.6-1 Steps in the Analysis Process

7. Results

All of the stability ratios are less than the limiting value of 1.0. The results are summarized in Table 7-1. Figures 7-1 to 7-9 show examples of the tube vibration mode shapes that are associated with the maximum stability ratio for each tube.

Table 7-1 Vibration Analysis Results (1/4)

Table 7-1 Vibration Analysis Results (2/4)

Table 7-1 Vibration Analysis Results (3/4)

Table 7-1 Vibration Analysis Results (4/4)

MODE	FREQ.(HZ)	Uc (ft/s)	Ue(ft/s)	SR
1				
2				
3				
4				
5				
6				
7				
8				
9				
10				
11				
12				
13				
14				
15				
16				
17				
18				
19				
20				
21				
22				
23				
24				
25				
26				
27				
28				
29				
30				

Fig. 7-1 Vibration mode diagram for Row 142 Column 88

MODE	FREQ.(HZ)	Uc (ft/s)	Ue(ft/s)	SR
1				
2				
3				
4				
5				
6				
7				
8				
9				
10				
11				
12				
13				
14				
15				
16				
17				
18				
19				
20				
21				
22				
23				
24				
25				
26				
27				
28				
29				
30				

Fig. 7-2 Vibration mode diagram for Row 47 Column 89

MODE	FREQ.(HZ)	Uc (ft/s)	Ue(ft/s)	SR
1				
2				
3				
4				
5				
6				
7				
8				
9				
10				
11				
12				
13				
14				
15				
16				
17				
18				
19				
20				
21				
22				
23				
24				
25				
26				
27				
28				
29				
30				

Fig. 7-3 Vibration mode diagram for Row 47 Column 7

MODE	FREQ.(HZ)	Uc (ft/s)	Ue(ft/s)	SR
1				
2				
3				
4				
5				
6				
7				
8				
9				
10				
11				
12				
13				
14				
15				
16				
17				
18				
19				
20				
21				
22				
23				
24				
25				
26				
27				
28				
29				
30				

Fig. 7-4 Vibration mode diagram for Row 26 Column 88

MODE	FREQ.(HZ)	Uc (ft/s)	Ue(ft/s)	SR
1				
2				
3				
4				
5				
6				
7				
8				
9				
10				
11				
12				
13				
14				
15				
16				
17				
18				
19				
20				
21				
22				
23				
24				
25				
26				
27				
28				
29				
30				

Fig. 7-5 Vibration mode diagram for Row 26 Column 4

MODE	FREQ.(HZ)	Uc (ft/s)	Ue(ft/s)	SR
1				
2				
3				
4				
5				
6				
7				
8				
9				
10				
11				
12				
13				
14				
15				
16				
17				
18				
19				
20				
21				
22				
23				
24				
25				
26				
27				
28				
29				
30				

Fig. 7-6 Vibration mode diagram for Row 14 Column 88

MODE	FREQ.(HZ)	Uc (ft/s)	Ue(ft/s)	SR
1				
2				
3				
4				
5				
6				
7				
8				
9				
10				
11				
12				
13				
14				
15				
16				
17				
18				
19				
20				
21				
22				
23				
24				
25				
26				
27				
28				
29				
30				

Fig. 7-7 Vibration mode diagram for Row 14 Column 2

MODE	FREQ.(HZ)	Uc (ft/s)	Ue(ft/s)	SR
1				
2				
3				
4				
5				
6				
7				
8				
9				
10				
11				
12				
13				
14				
15				
16				
17				
18				
19				
20				
21				
22				
23				
24				
25				
26				
27				
28				
29				
30				

Fig. 7-8 Vibration mode diagram for Row 1 Column 89

MODE	FREQ.(HZ)	Uc (ft/s)	Ue(ft/s)	SR
1				
2				
3				
4				
5				
6				
7				
8				
9				
10				
11				
12				
13				
14				
15				
16				
17				
18				
19				
20				
21				
22				
23				
24				
25				
26				
27				
28				
29				
30				

Fig. 7-9 Vibration mode diagram for Row 1 Column 1

8. References

1) L5-04GA504 the latest revision, Evaluation of Tube Vibration
2) Deleted
3) L5-04FU001 the latest revision, Component and Outline Drawing 1/3
4) L5-04FU002 the latest revision, Component and Outline Drawing 2/3
5) L5-04FU003 the latest revision, Component and Outline Drawing 3/3
6) L5-04FU021 the latest revision, Tube Sheet and Extension Ring 1/3
7) L5-04FU022 the latest revision, Tube Sheet and Extension Ring 2/3
8) L5-04FU023 the latest revision, Tube Sheet and Extension Ring 3/3
9) L5-04FU051 the latest revision, Tube Bundle 1/3
10) L5-04FU052 the latest revision, Tube Bundle 2/3
11) L5-04FU053 the latest revision, Tube Bundle 3/3
12) L5-04FU111 the latest revision, AVB assembly 1/9
13) L5-04FU112 the latest revision, AVB assembly 2/9
14) L5-04FU113 the latest revision, AVB assembly 3/9
15) L5-04FU114 the latest revision, AVB assembly 4/9
16) L5-04FU115 the latest revision, AVB assembly 5/9
17) L5-04FU116 the latest revision, AVB assembly 6/9
18) L5-04FU117 the latest revision, AVB assembly 7/9
19) L5-04FU118 the latest revision, AVB assembly 8/9
20) L5-04FU119 the latest revision, AVB assembly 9/9
21) L5-04GA510 the latest revision, Thermal and Hydraulic Parametric Calculations
22) ASME Boiler and Pressure Vessel Code, Section III, 1998 edition, 2000 addenda
23) ASME Boiler and Pressure Vessel Code, Sec II, Materials, 1998 Edition through 2000 addenda.
24) Blevins, R. D., "Flow-induced Vibration", Krieger Publishing Company.
25) Connors, H.J., Fluid Elastic Vibration of Tube Arrays Excited by Cross Flow, ASME Annual Meeting, 1970.

Appendix-4
Investigation of Unit-2/3 Manufacturing and Inspection Records

1. Purpose

The purpose of this appendix is to investigate the manufacturing history of the Unit-2 and Unit-3 steam generators to identify differences in dimensions, materials, fabrication processes and inspections that may have a relationship to the differences in U-bend degradation patterns.

2. Conclusion

The major differences between the Unit-2 and Unit-3 steam generators are listed below. The influences of these differences are evaluated in Section 5.2.3 of the main report.

(1) Number of Rotations due to Divider Plate Repair
(2) Number of Hydrostatic Tests
(3) Dimensional Control of Tubes and AVBs

Attachment-1: Difference of fabrication and transportation between Unit-2 and Unit-3 (1/4)

Category		Item	Unit-2	Unit-3	Effect to the final AVB structure assembly and tube bundle (especialy tube-to-AVB gap)
Design	Material	Mechanical property of AVB	All tensile test and hardness test results are within specification for all AVB material for all units.		There is no remarkable difference on any test results.
		Outer diameter of tube (G value)			Standard deviation of G value for Unit-3 RSGs were smaller than that for Unit-2 RSGs. However, difference of the tube dimensions are small between all four SGs, as the tube diameters are within the [ ] and the standard deviation is within [ ]
Fabrication & Inspection	Tube insertion	Number of tubing operators			No impact is assumed at the point of this difference.
		Number of manual adjustment of U-bend portion during tubing installation (in case the gap between the tubes are small)			Number of manual adjustment of U-bent portion for Unit-3 is smaller than that for Unit-2, therefore configuration of U-bent tube for Unit-3 RSGs is better than that for Unit-2.
	AVB assembly	AVB manufacturer, fabrication sequence, and procedure			There is no difference.
		Thickness of AVBs before installation			The difference of thickness of AVBs are small between all four SGs, as the thickness are within [ ] with standard deviations between [ ]

Note *) For Unit-3, [ ]N pressing was used for AVB bend nose portion after bending in order to control the twist and flatness of AVB more precisely, while [ ]N pressing was used for Unit-2 as described in Appendix-9.

Attachment-1: Difference of fabrication and transportation between Unit-2 and Unit-3 (2/4)

Category		Item	Unit-2	Unit-3	Effect to the final AVB structure assembly and tube bundle (especialy tube-to-AVB gap)
Fabrication & Inspection	AVB assembly	Procedure of AVB assembling (Insertion, welding and fixuring the bridge and retainer bar)			The approved procedure(document) was revised up from Unit-2A to Unit-3B. Those for Unit-2A are different from those for the others. However, there is no remarkable difference for Unit-2B and Unit-3 RSGs at the point of the basic manners for AVB assembly.
		Situation and condition of fixturing AVBs at tubes with tie ropes or temporary fixturing equipments			Same manners are applied to all units.
		Size of spacer block used for welding AVBs to retaining bar			Size of spacer for Unit-2A is different from that for the others. Therefore there is no difference for Unit-2B and Unit-3 RSGs.
		AVB assembly rotations			This operation might have led to some differnce. AVB assembly rotations for Unit-2A is different from that for the others. Therefore there is no remarkable difference for Unit-2B and Unit-3 RSGs.
		Fillet weld size between retaining bars and end-caps			There is no remarkable difference.
		Increased weld size between AVB and retaining bar			There is no remarkable difference.
		Re-insertion of AVBs			This operation was applied only for Unit-2A. There is no remarkable difference for Unit-2B and Unit-3 RSGs.
		Re-welding retaining bars and end-caps after helium leak tests			This operation was applied only for Unit-2A. There is no remarkable difference for Unit-2B and Unit-3 RSGs.

Attachment-1: Difference of fabrication and transportation between Unit-2 and Unit-3 (3/4)

Category		Item	Unit-2	Unit-3	Effect to the final AVB structure assembly and tube bundle (especialy tube-to-AVB gap)
Fabrication & Inspection	AVB assembly	Welding position for the bridge and retainer bar assembling			Welding position for Unit-2A is different from that for the others. Therefore there is no difference for Unit-2B and Unit-3 RSGs.
		Tube-to-AVB Gap measurement results at outermost tubes			These AVB-to-tube gaps were smaller in Unit-3 than in Unit-2.
		Time of tying retaining bar to tube for prevention of pulling AVB out			This difference influenced the number of shell rotations - Unit 2 RSGs were rotated 60 more times than Unit 3 RSGs. Shell rotations are assumed to not impact the tube-to-AVB gap* size.
	Tube support plate	Tolerance for pitch of the upper most tube support plate			Same tolerances are applied to all units.
	Transition wrapper welding	Time of transition wrapper welding			This difference influenced the number of shell rotations - Unit 2 RSGs were rotated 15 more times than Unit 3 RSGs. Shell rotations are assumed to not impact the tube-to-AVB gap.*
	Helium leak test	Condition of helium leak test			This difference influenced the number of shell rotations - Unit 2 RSGs were rotated 20 more times than Unit 3 RSGs. Shell rotations are assumed to not impact the tube-to-AVB gap.*
	Tube expansion	Hydro/mechanical tube expansion			There is no difference.
	Final dryer vane jacking (tightening)	Time of final dryer vane jacking (tightening)			This difference influenced the number of shell rotations - Unit 2 RSGs were rotated 30 more times than Unit 3 RSGs. Shell rotations are assumed to not impact the tube-to-AVB gap.*
	Bundle rotations after completion of AVB assembly (excluding divider plate repair)	Bundle rotations after completion of AVB assembly (excluding divider plate repair)			No impact is assumed for the point of this difference.

Note) See Appendix-5 for details

Attachment-1: Difference of fabrication and transportation between Unit-2 and Unit-3 (4/4)

Category		Item	Unit-2	Unit-3	Effect to the final AVB structure assembly and tube bundle (especialy tube-to-AVB gap)
Fabrication & Inspection	Bundle rotations for divider plate repair	Bundle rotations for divider plate repair			This difference influenced the number of shell rotations - Unit 2 RSGs were rotated 30 more times than Unit 3 RSGs. Shell rotations are assumed to not impact the tube-to-AVB gap*
	Hydrostatic test	Number of times water was poured into the shell for the hydrostatic test, and number of hydrostatic test			It is confirmed by deformation analysis result no remarkable enlargement of tube-to-AVB gap is caused by this operation.
	Heat treatment after AVB structure assembling	Tubesheet to Channel Head welding & PWHT for divider plate repair			No impact is assumed for the point of this difference.
	Channel head removal from tubesheet	Channel head removal by flame cutting for divider plate repair			No impact is assumed for the point of this difference.
	Tube PSI	Time and situation of tube PSI			Indications of tube PSI results is not changed compared with latest ECT results. Therefore no impact is assumed at the point of this difference.
Others	Transport	Position of the shell during transport			No impact is assumed for the point of this difference.
		Accelerations during transport			There is no remarkable difference.
		Nitrogen recharge system			There is no remarkable difference.
		Ship name			There is no remarkable difference.
		Tugboat company			There is no remarkable difference.
		Barge support stand			There is no remarkable difference.
		Off load duration			There is no remarkable difference.
		Transportation time			There is no remarkable difference.
		Platform trailers			There is no remarkable difference.

Note) See Appendix-5 for details

Attachment-2: Difference of fabrication history between Unit-2 and Unit-3 (1/3)

N/R: Number of Rotation, N/L: Number of Loading, SUM: Summation

Attachment-2: Difference of fabrication history between Unit-2 and Unit-3 (2/3)

N/R: Number of Rotation, N/L: Number of Loading, SUM: Summation

Attachment-2: Difference of fabrication history between Unit-2 and Unit-3 (3/3)

Attachment-3: Detail investigation of AVB assembly

Appendix-5
Analytical Simulation of Tube Bundle Rotation and Hydro Static Test

1. Purpose

The purpose of this evaluation is to analytically simulate the SONGS SG U-bend to evaluate the behavior of the tube-to-AVB gaps during gravitational sagging, shop rotation, and primary hydrotest.

2. *Conclusion*

2.1 Bundle Rotation

The tube-to-AVB gaps near the center columns increase by [ ] mm in one rotation. If this gap is postulated to occur at each rotation (which it doesn't), the total gap growth for 300 rotations would be [ ] mm, which is negligible. In the analyses, small plastic deformation occurred in limited portion, AVB outside the bundle. This small plastic strain level can not cause permanent deformation.

The tube-to-AVB gaps in the outer columns increase by [ ] in the first rotation; but do not repeat or grow significantly during additional rotations. The difference of the tube-to-AVB gaps between Unit-2 and 3 due to the number of SG rotations is not judged to be significant, even if it is postulated that the increased gaps in the outer columns were redistributed to the center.

The gaps generated by the pressure tests are also determined to be negligible so the difference of the tube-to-AVB gaps between Unit-2 and 3 due to the number of pressure tests is negligible.

3. Assumption

1) Nominal dimensions are used for analysis model.
2) The initial value of the tube-to-AVB gaps is assumed to be zero.
3) The tube pitch is assumed to be the same as the tube hole pitch of the TSP.

4. Acceptance Criteria

The tube-to-AVB gaps are evaluated to determine if they get larger during SG shop rotations or during pressure tests. The results of the analysis are compared to see if there is a significant difference between Unit-2 and Unit-3.

Table 4-1 Difference between Unit-2 and 3 during fabrication

Unit	Number of SG rotations	Number of pressure tests or times the bundle was filled with water
2	[ ]	2A & 2B: 1
3	[ ]	3A: 3, 3B: 2

5. Design Inputs

5.1 Geometry

The nominal tube bundle dimensions are obtained from the design drawings

6. Methodology

6.1 Analysis model

The ABAQUS finite element program is used to perform the analysis. The model includes the tubes, AVBs, retaining bars, retainer bars, and bridges. The modeling assumptions are shown in Table 6.1-1 and Figure 6.1-1. The model is shown in Figure 6.1-2. The TSPs are treated as pinned supports. The tubes at the TSP #6 elevation are prevented from displacing in the lateral and axial directions but are free to rotate. The tubes at the TSP #7 elevation are restrained against lateral displacement but are free to displace axially and to rotate. It is appropriate not to simulate initial gaps between TSP and tubes, because all tubes laterally displace just same amount of initial gap in the case of cantilevered U-bend, and the tube pitch is not changed. Modeling the top two TSPs is sufficient to produce a reasonable replication of the cantilevered U-bend.

Table 6.1-1 Condition of analysis models (1/2)

Analysis	Elastic —Plastic	Element					
		Tube	AVB	Retaining bars	Bridges	Retainer bars	Water
(1) Validation of analysis model	[						]
(2) Simulation of SG rotation							
(3) Simulation of pressure testing	[						]

Table 6.1-1 Condition of analysis models (2/2)

Analysis	Friction Coefficient (*1)	Boundary condition		
		Contact condition		Fastening condition
		Tubes - AVB	Tubes - Retaining bars	Retainer bars - Tube
(1) Validation of analysis model	[			]
(2) Simulation of SG rotation				
(3) Simulation of pressure testing	[			]

Note 1) See Fig. 6.1-1.

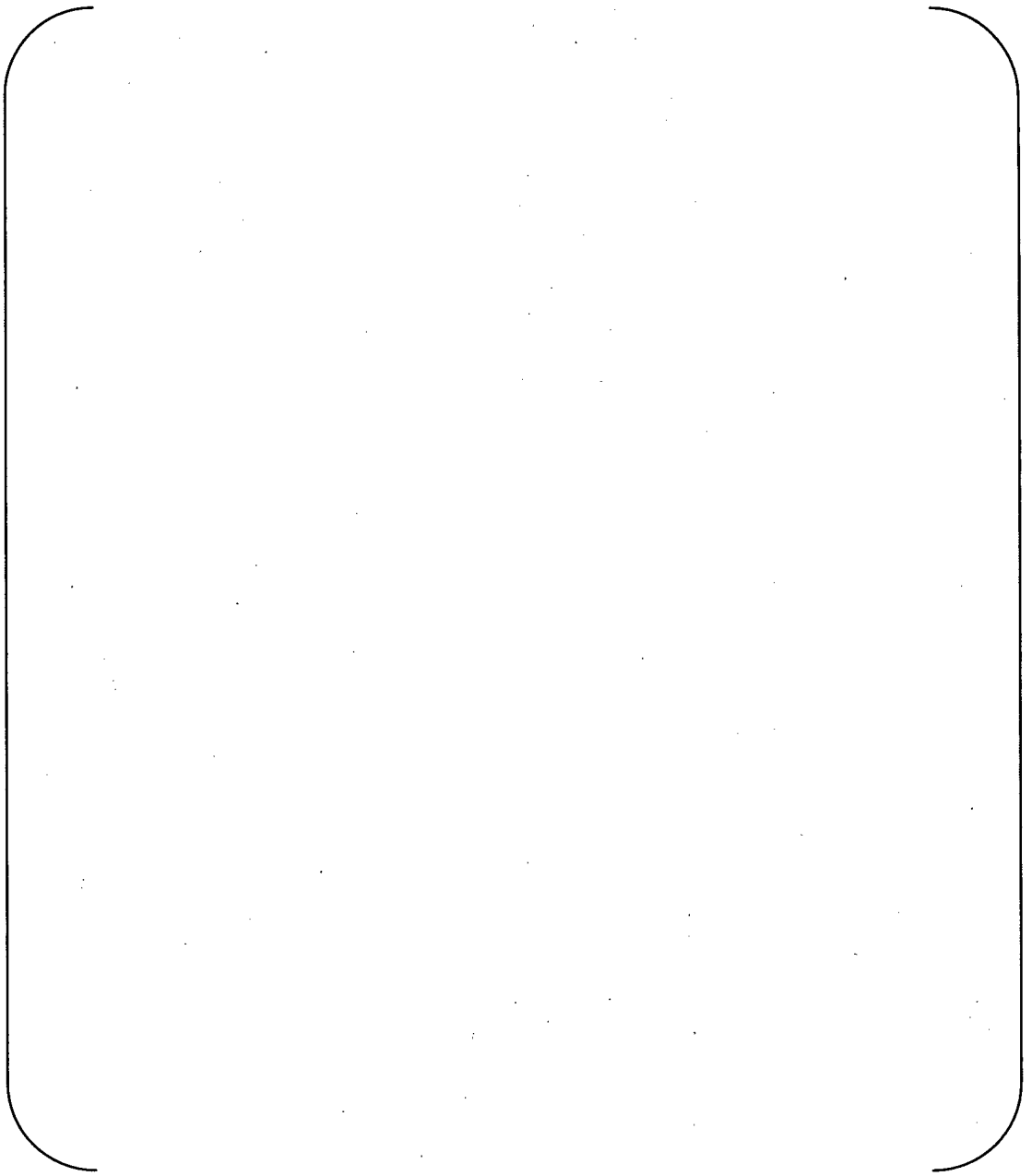

Fig. 6.1-1 Friction coefficient between Inconel 690 and 405 S.S

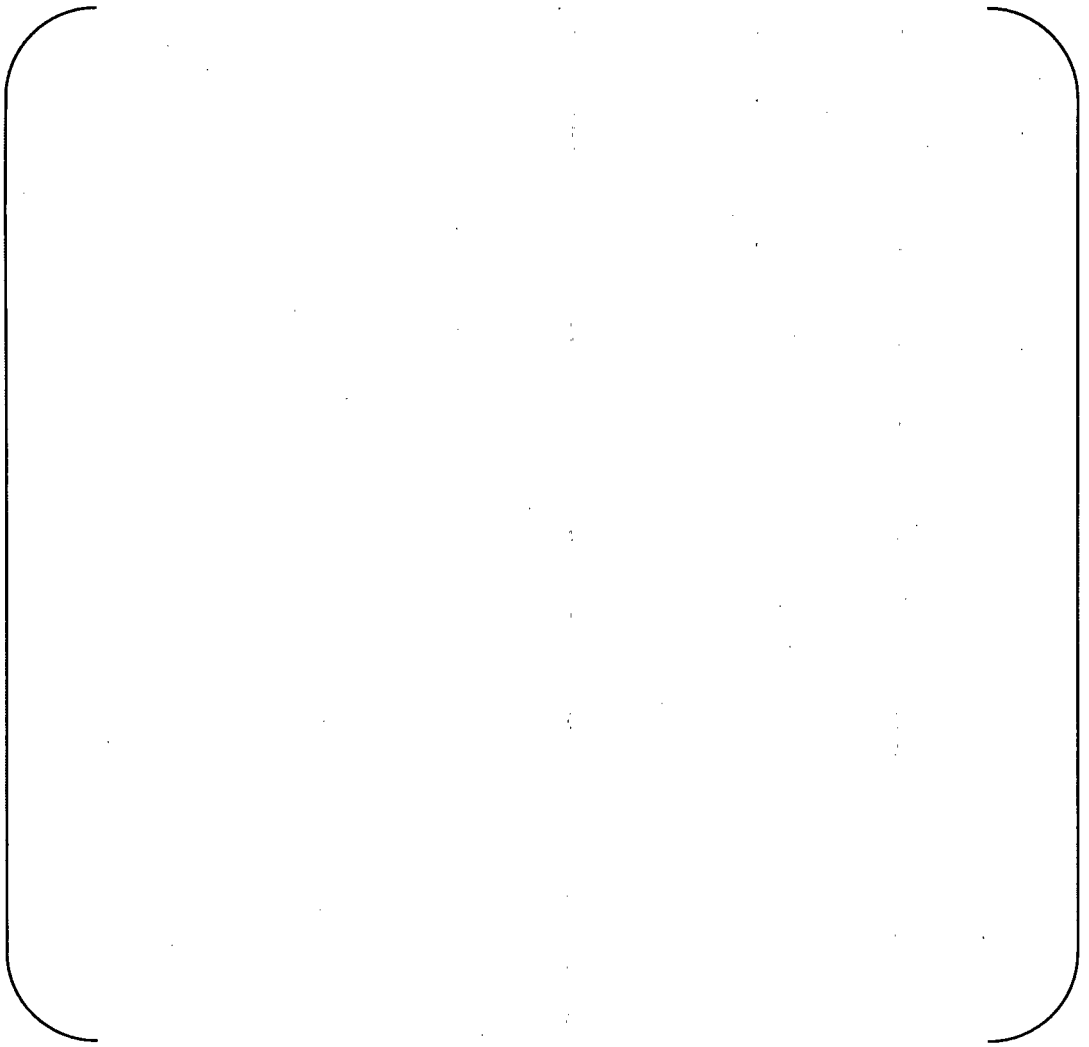

Fig. 6.1-2 Analysis Model

6.2 Evaluation cases

The following three cases were evaluated.

(i) U-bend Sagging to validate the analytical model
(ii) Simulation of bundle rotation
(iii) Simulation of hydrostatic pressure testing

6.2.1 Validation of Analytical Model

A simulation of the U-bend sag due to gravity was performed to compare to measurements made during manufacture to validate the analytical model. Gravity (1G) in the out-of-plane direction (i.e. with the U-tubes in the horizontal plane, perpendicular to the floor) produced sagging that was measured at the tips of AVBs #41 and #69. A one-half model of that shown in Figure 6.1-2 was used taking advantage of symmetry. Since the measurements were taken before the retaining bars, retainer bars, and bridges were installed, those features were excluded from the model.

6.2.2 Simulation of Bundle Rotation

Since the objective of this evaluation is the tube-to-AVB gaps, bundle rotation was simulated by cycling a gravity load from plus to minus with the bundle oriented in the out-of-plane direction. A zero gravity load step was performed between each gravity load reversal. The following diagram describes this load cycle.

0G → +1G → 0G → -1G → 0G → +1G → ...

This model includes the retainer bars, the retaining bars, and the bridges. Figure 6.2.2-1 shows the model and load sequence. Refer to Table 6.1-1 for additional information about this simulation.

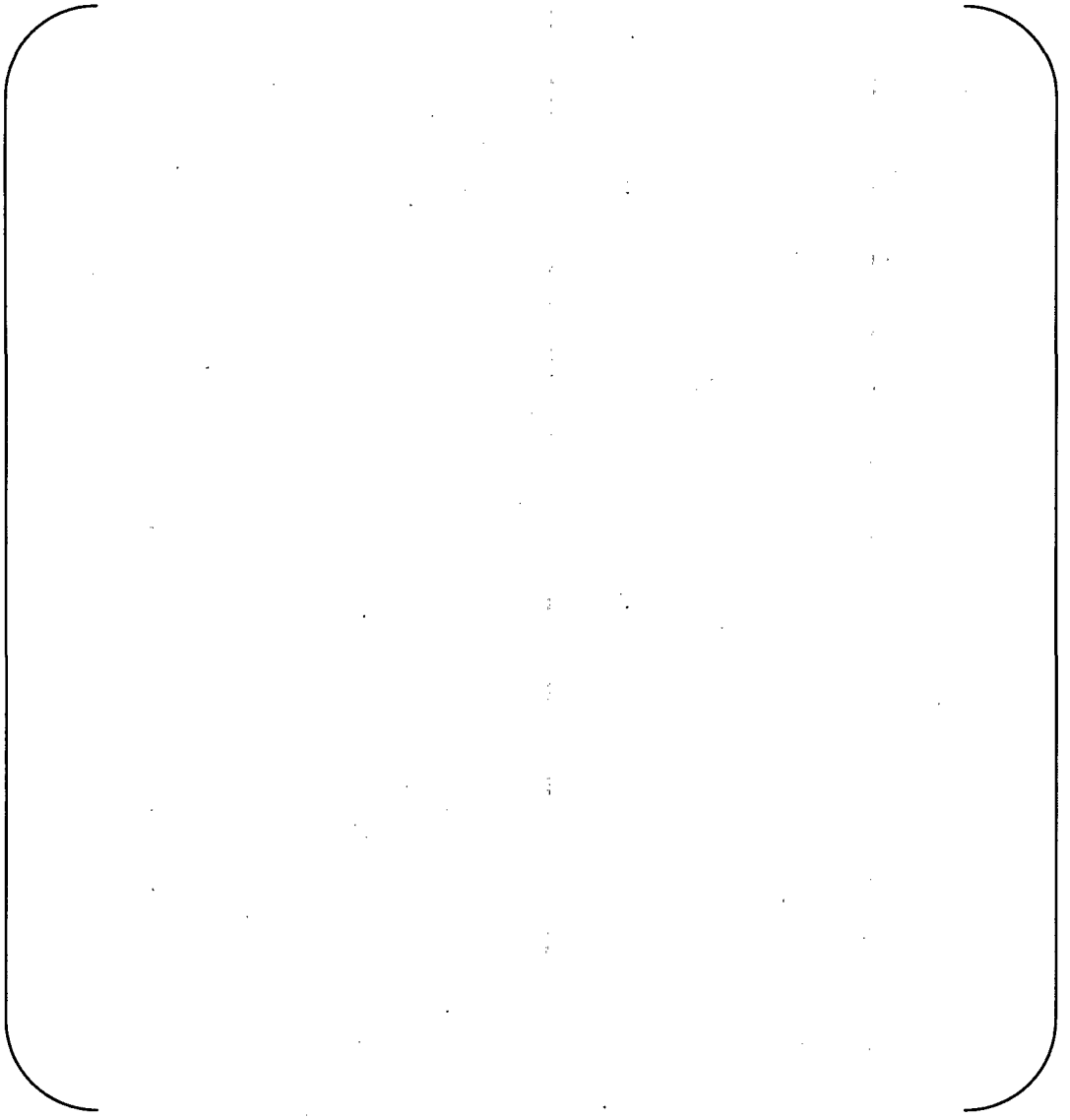

Fig. 6.2.2-1 Load sequence for Shop Rolling

6.2.3 Simulation of Hydrostatic Pressure Testing

To evaluate difference of the tube-to-AVB gaps increment around the center column, where many wears have occurred, between Unit-2 and 3, due to the number of pressure testing, simulation of pressure testing is performed.

The weight of the tube bundle increases by the weight of water inside the tubes during the primary hydrostatic pressure test. The orientation of the tube bundle during pressure testing is with the tube lane inclined at an angle of 45 degrees – but is simulated with tube bundle in the out-of-plane orientation. The test sequence is adding water, pressurization, depressurization, and draining water. The tube mass is increased by a factor of 1.5 to account for the added weight of water. Although gravity is oriented at 45-degree orientation the simulation is run with the bundle in the out-of-plane direction. The out-of-plane equivalent loading for the hydrotest is $+1G/\sqrt{2} \times 1.5 = +1G$. A 0.7G loading is used to represent the draining / depressurization step. The following load sequence is used to model two hydrotests.

0G → +1G (adding water / pressurization) → +0.7G (draining water) → +1G (adding water / pressurization) → +0.7G (draining water) → 0G

7. Results

7.1 Validation of analysis model

Measurement points of AVB #41 and #69 for sagging during fabrication are shown in Figure 7.1-1. Measurement and analysis results are compared in Table 7.1-1. The calculated sag is slightly less than what was actually measured, but is considered to be close enough to validate the model.

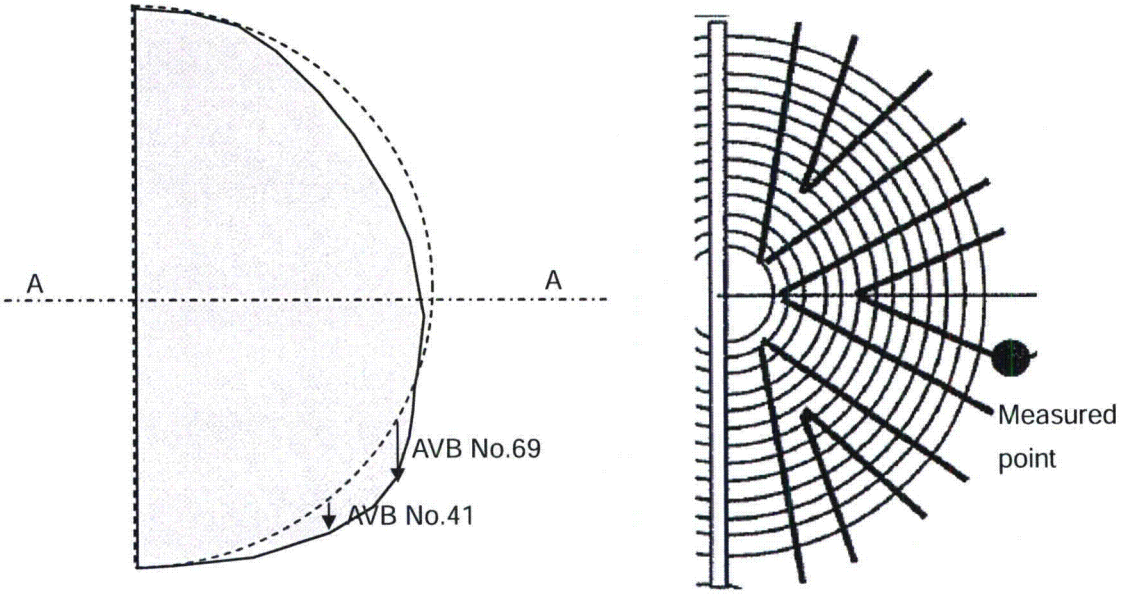

(1) Out-of-Plane Deformation (2) Section A-A

Fig. 7.1-1 Out-of-Plane Deformation due to Sagging

Table 7.1-1 Comparison Result of Out-of-plane Displacement during Sagging

Case	AVB−Tube	Displacement (mm)	
		AVB No.41	AVB No.69
Analysis	None (Retaining bars are not modeled)	[ ]	
Measurement	Fastened	[ ]	

7.2 Simulation of SG rotation

7.2.1 Deformation and Gaps during SG rotation

The deformation of tube bundle and the tube-to-AVB gaps during SG rotation are analyzed step by step, as follow.

(1) Step 0: Initial Condition

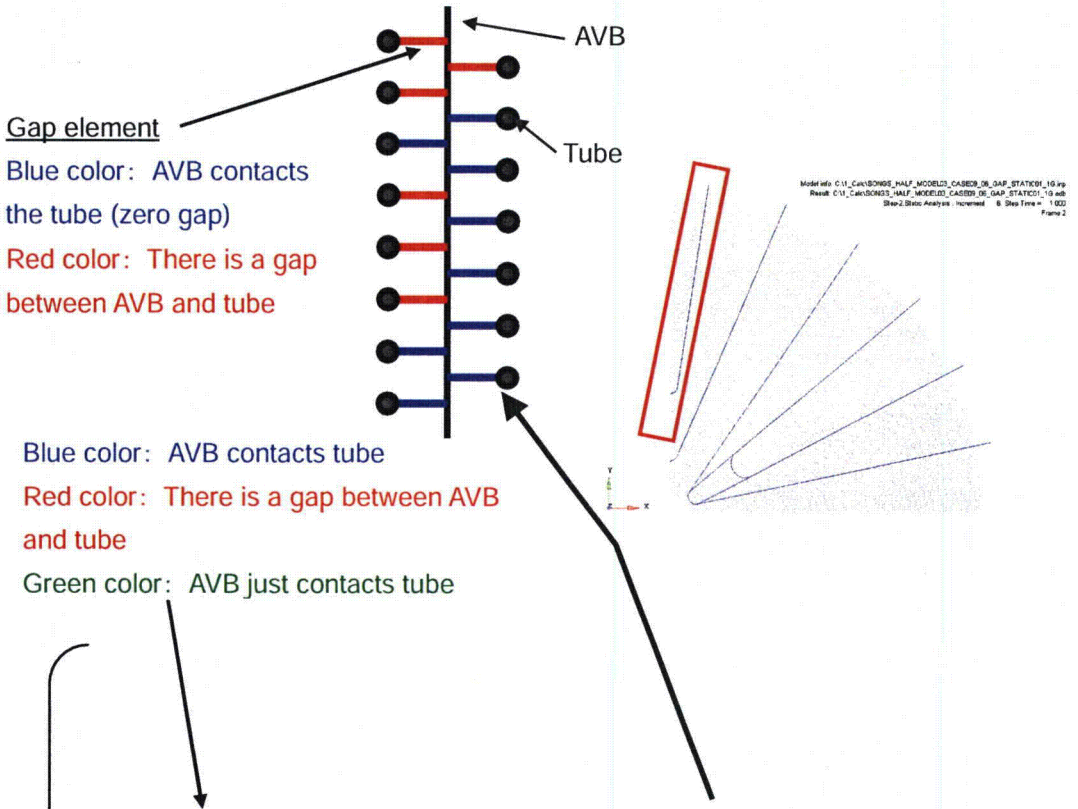

Fig. 7.2.1-1 AVB-Tube Gap contour for initial condition

(2) Step 1: +1G acting (1st turn)

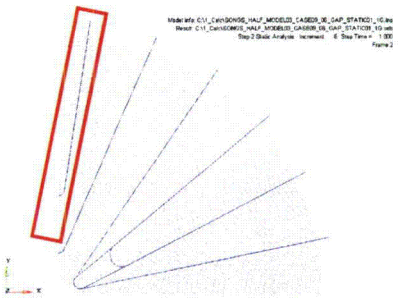

Sagging of retaining bar depends on sagging of tubes in center columns. Retaining bar and AVBs push tubes down, because sagging of retaining bar is larger than gravity deformation of tubes near both ends of retaining bars.

Tubes gravity deformation is different in each column, because gravity deformation is proportional to 4th power of tube radius.

No gap is generated, because retaining bar pull AVBs down

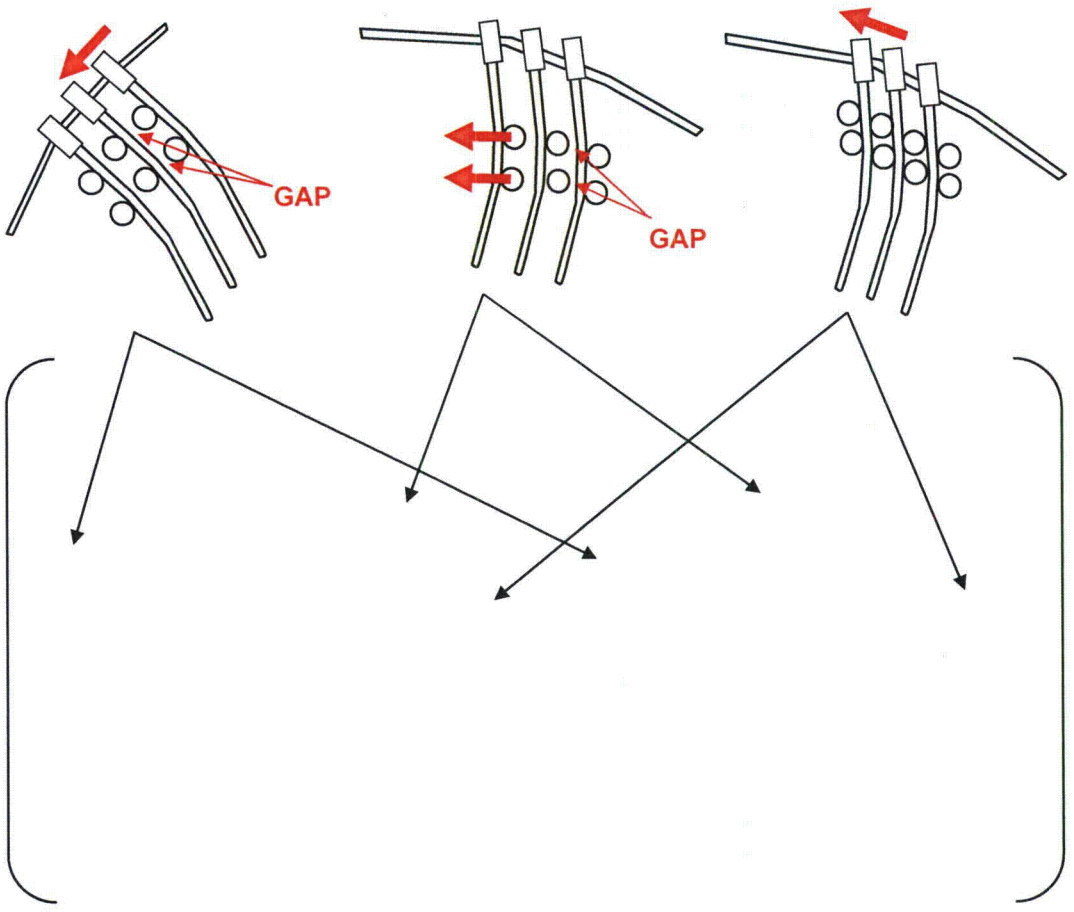

Fig. 7.2.1-2 AVB-Tube Gap contour for +1G condition of first turn

(3) Step 2: 0G condition

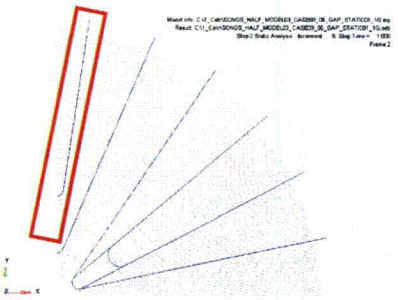

It appears that the gaps generated by ±1G remain because AVB cannot move into tube bundle due to friction force.

Fig. 7.2.1-3 AVB-Tube Gap contour for 0G condition of first turn

(4) Step 3: -1G acting (1st turn)

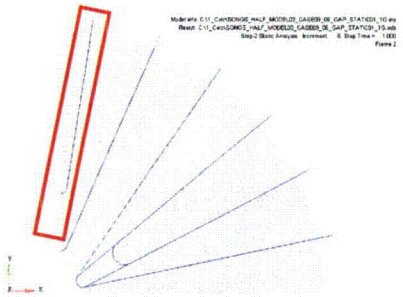

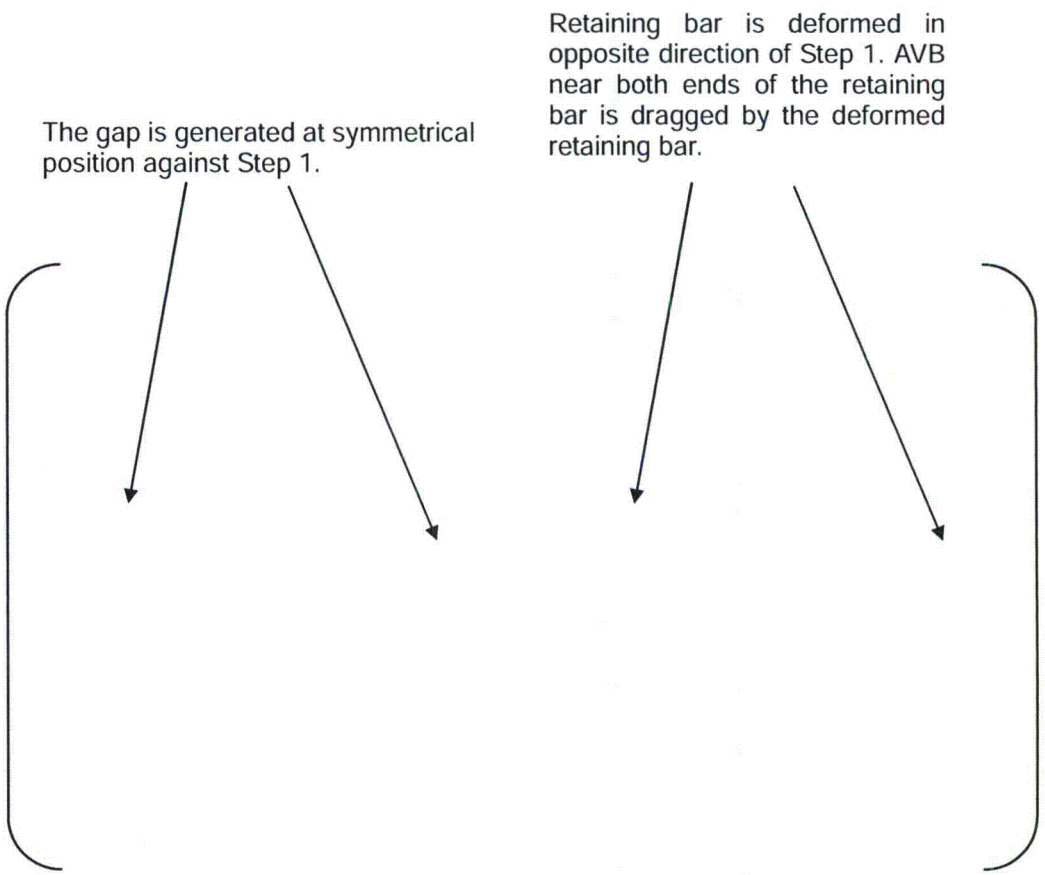

Fig. 7.2.1-4 AVB-Tube Gap contour for -1G condition of first turn

(5) Step 4: Gravity free (After 1st turn)

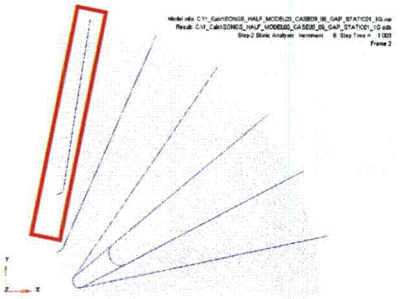

The gaps generated by the gravity on Step 3 remain.
The gaps generated by the gravity on Step 1 don't remain.
(The gaps contour is determined by the last gravity.)

The deformations of the retaining bar and AVB remain. It would appear that the AVB cannot move into the tube bundle due to friction force.

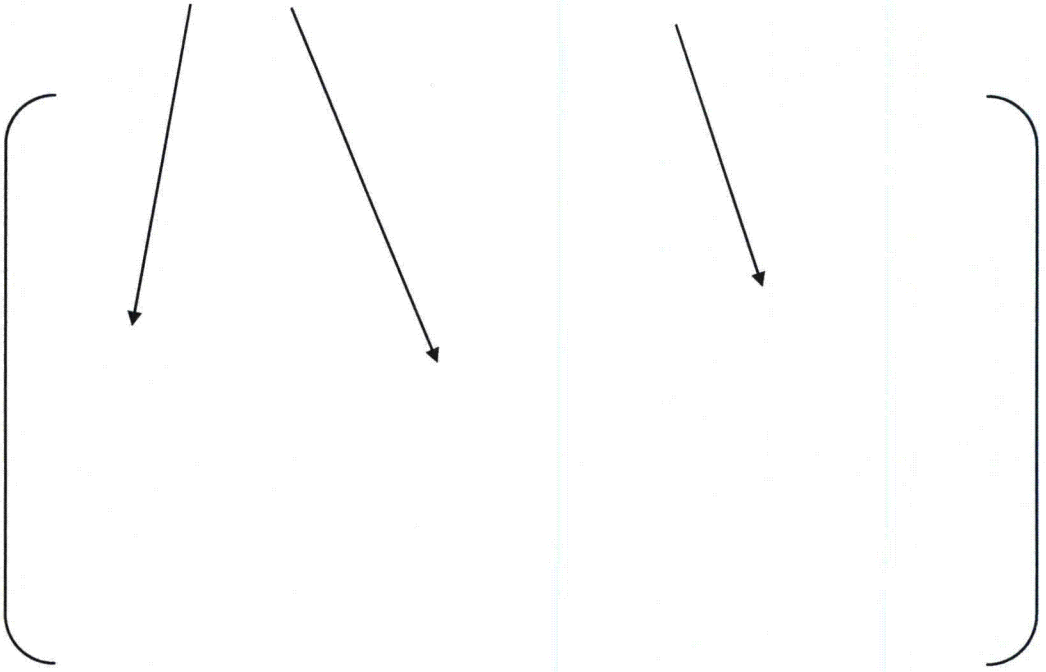

Fig. 7.2.1-5 AVB-Tube Gap contour for 0G condition of first turn

(6) Step 25-28 7th turn

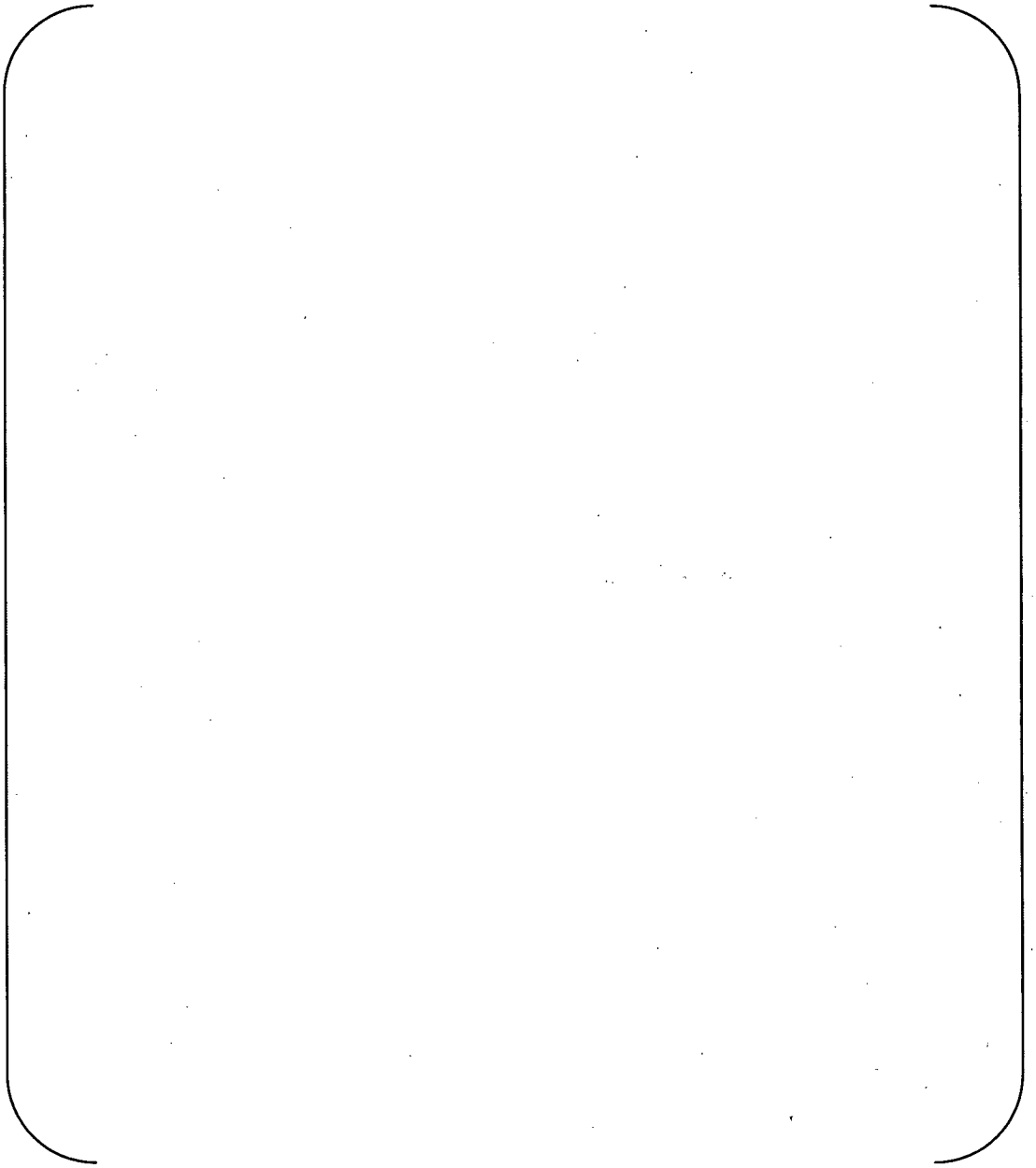

Fig. 7.2.1-6 AVB-Tube Gap contour of 7th turn

(7) Step 28 Gravity free (after 7th turn)

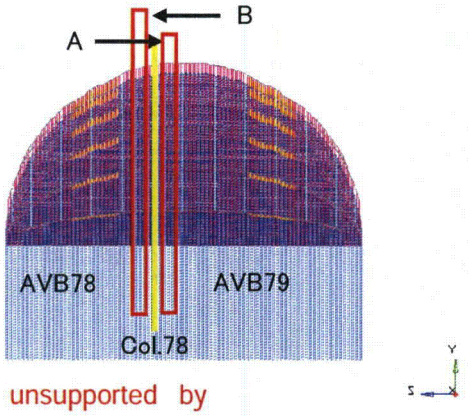

For one surface, there are some unsupported points in one tube. On the other hand, for the opposite surface, the tube contact with the AVB at all points.

These tubes are unsupported by AVBs continuously.

There are consecutive small gaps at AVB support points. However, the increases of gaps are negligibly small.

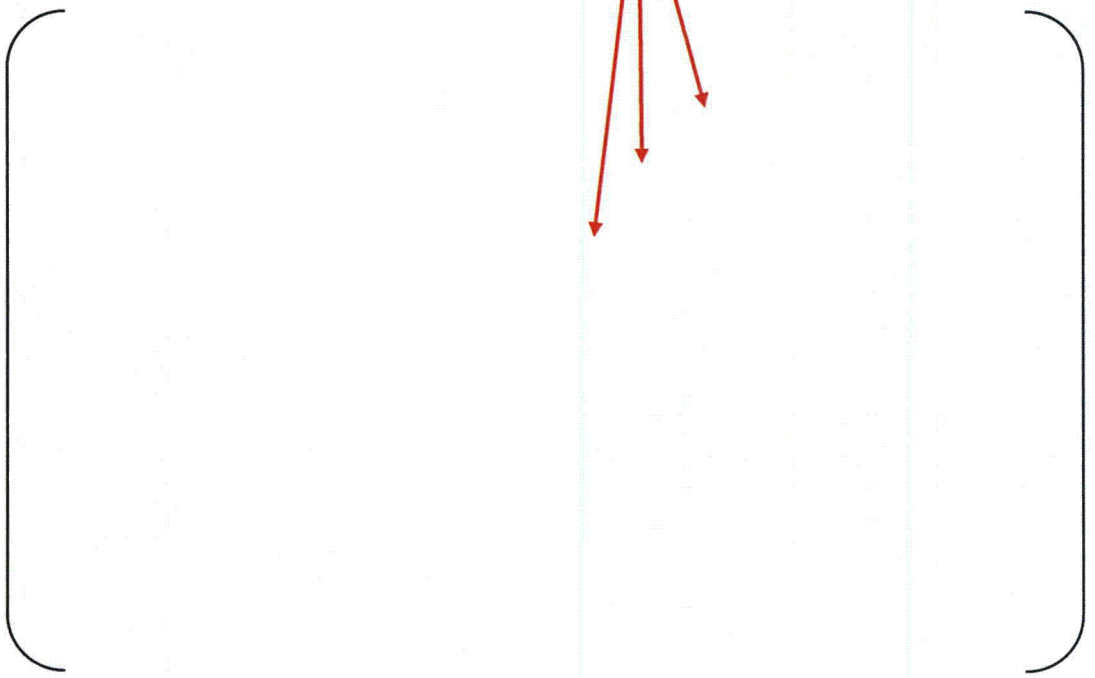

Fig. 7.2.1-7 AVB-Tube gap contour in Column 78

7.2.2 Enlargement of tube bundle width

Enlargement of tube bundle width (cross sections α1, α2, and α3) is calculated from 1st to 7th turn at the points shown in Fig. 7.2.2-1.

The width of the tube bundle is not changed after the 3rd turn as shown in Fig. 7.2.2-2. The maximum change of the width is[ ] mm at cross-section α3. The expansion is caused by the AVB-Tube gaps near the edges at the retaining bars. It is theorized that during operation, the fluid hydrodynamic pressure might shift the gaps from the edges to the center. This would equate to a widening of [ ] near the center column.

Fig. 7.2.2-1 Evaluated points of expansion

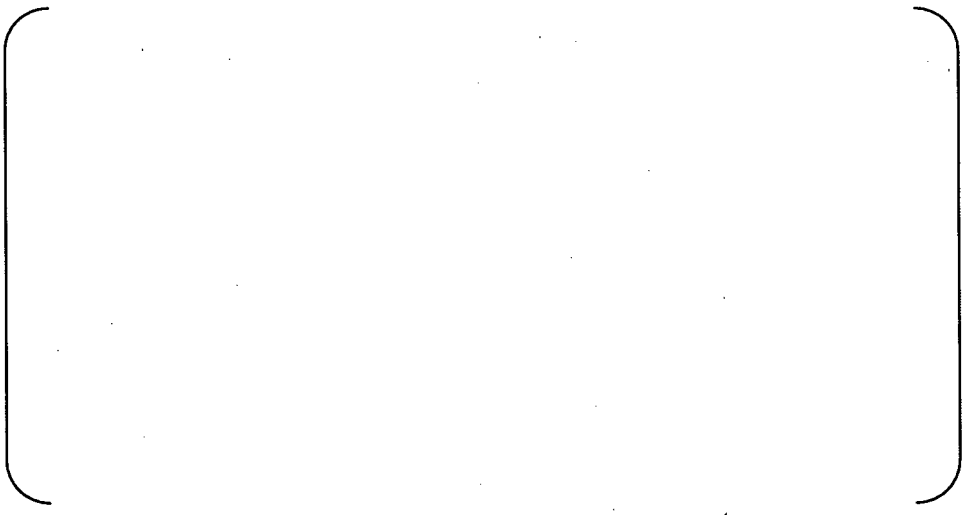

Fig. 7.2.2-2 Change per rotation of tube bundle width (first 7 rotations)

7.2.3 Change of the Tube-to-AVB gaps

Changes of the AVB-tube gaps from 1st to 7th turn are investigated. Changes near Col90, 135, and 160 are shown in Fig. 7.2.3-1. Although the small gaps (about [ ] mm gaps) are generated near Col.90, the large gaps (about [ ] mm) are generated near the retaining bars. It suggests possibility of the larger gaps (about [ ] mm) near the center column by redistribution during operation.

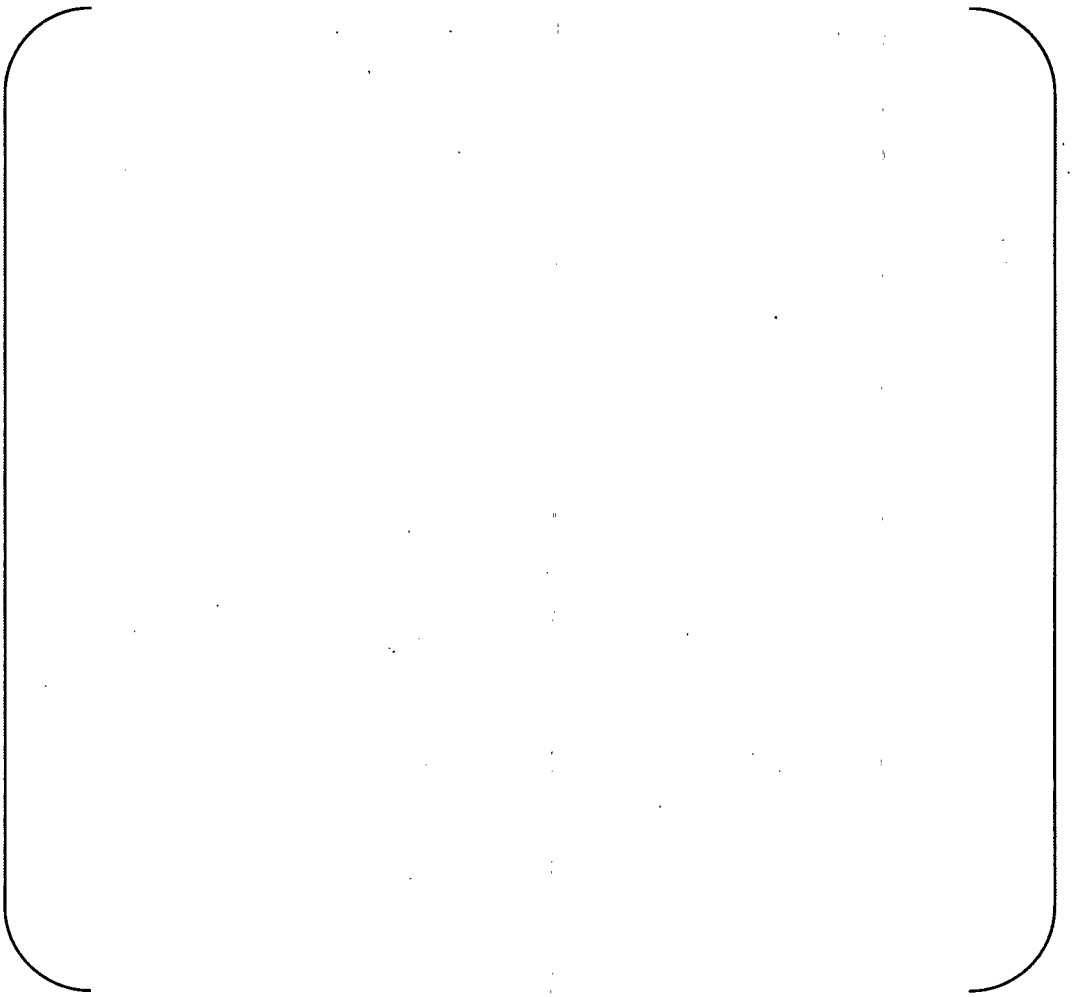

Fig. 7.2.3-1 Change of the AVB-Tube gap between 1st turn through 7th turn

7.3 Simulation of Hydro Test

7.3.1 Deformation and Gaps due to pressure testing

The load direction and deformation during pressure testing is shown in Fig. 7.3.1-1. The tube-to-AVB gaps during pressure testing are shown in Fig. 7.3.1-2 and 7.3.1-3. The tube-to-AVB gaps generated by pressure testing are around [ ] mm, and are negligibly small.

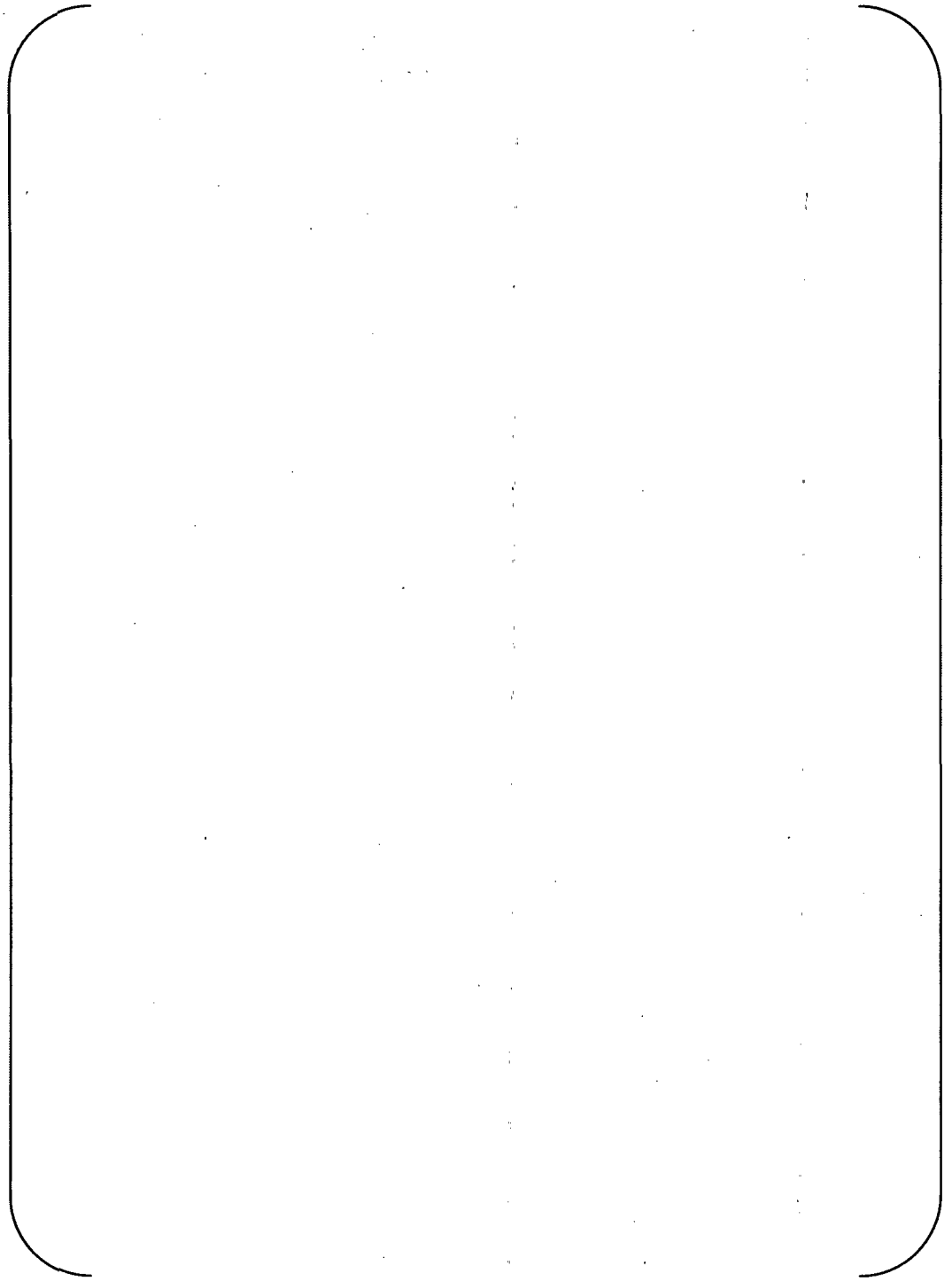

Fig.7.3.1-1 Load direction and deformation during pressure testing

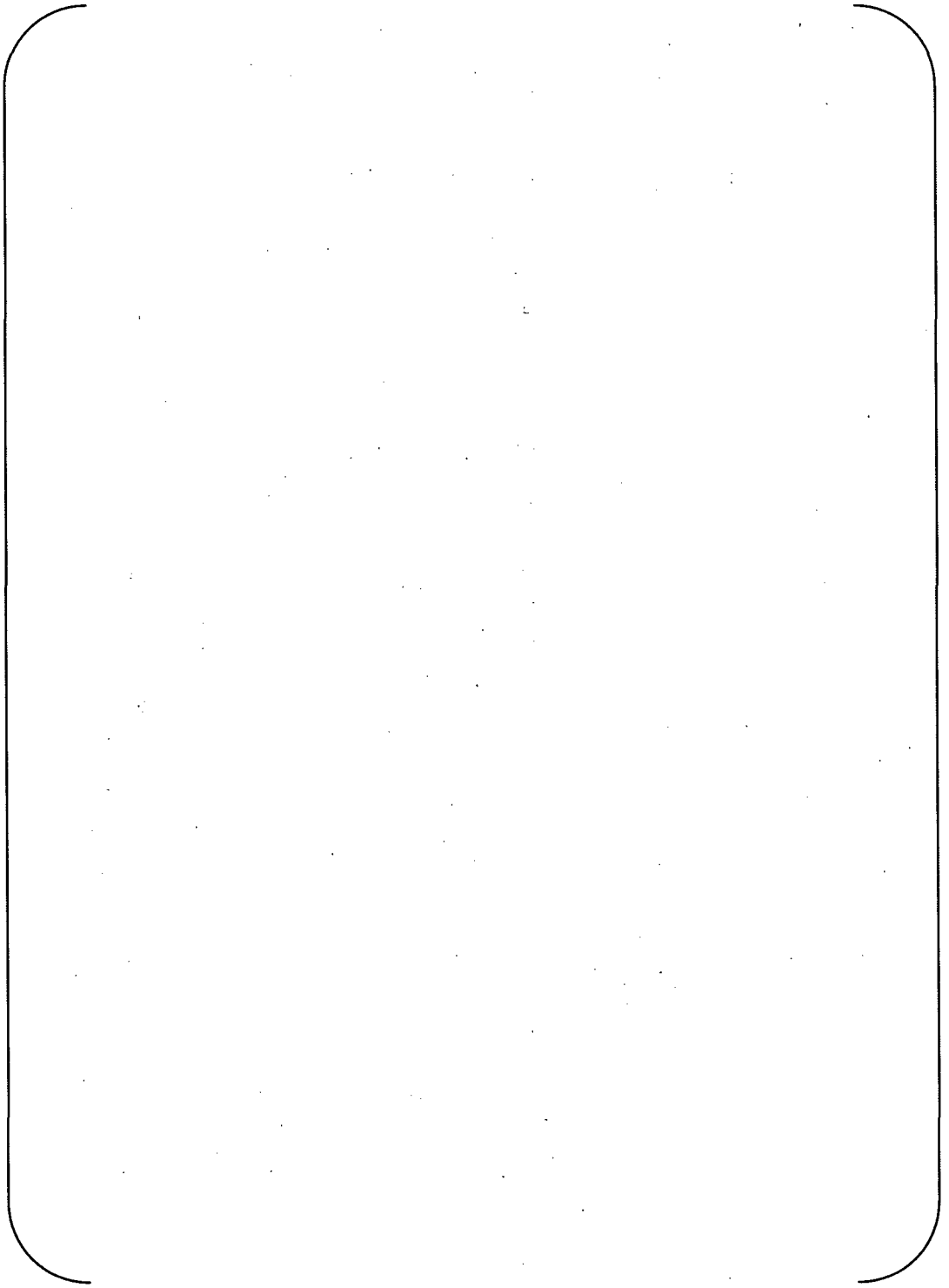

Fig. 7.3.1-2 AVB-Tube Gap Contour in 1st Pressure Testing

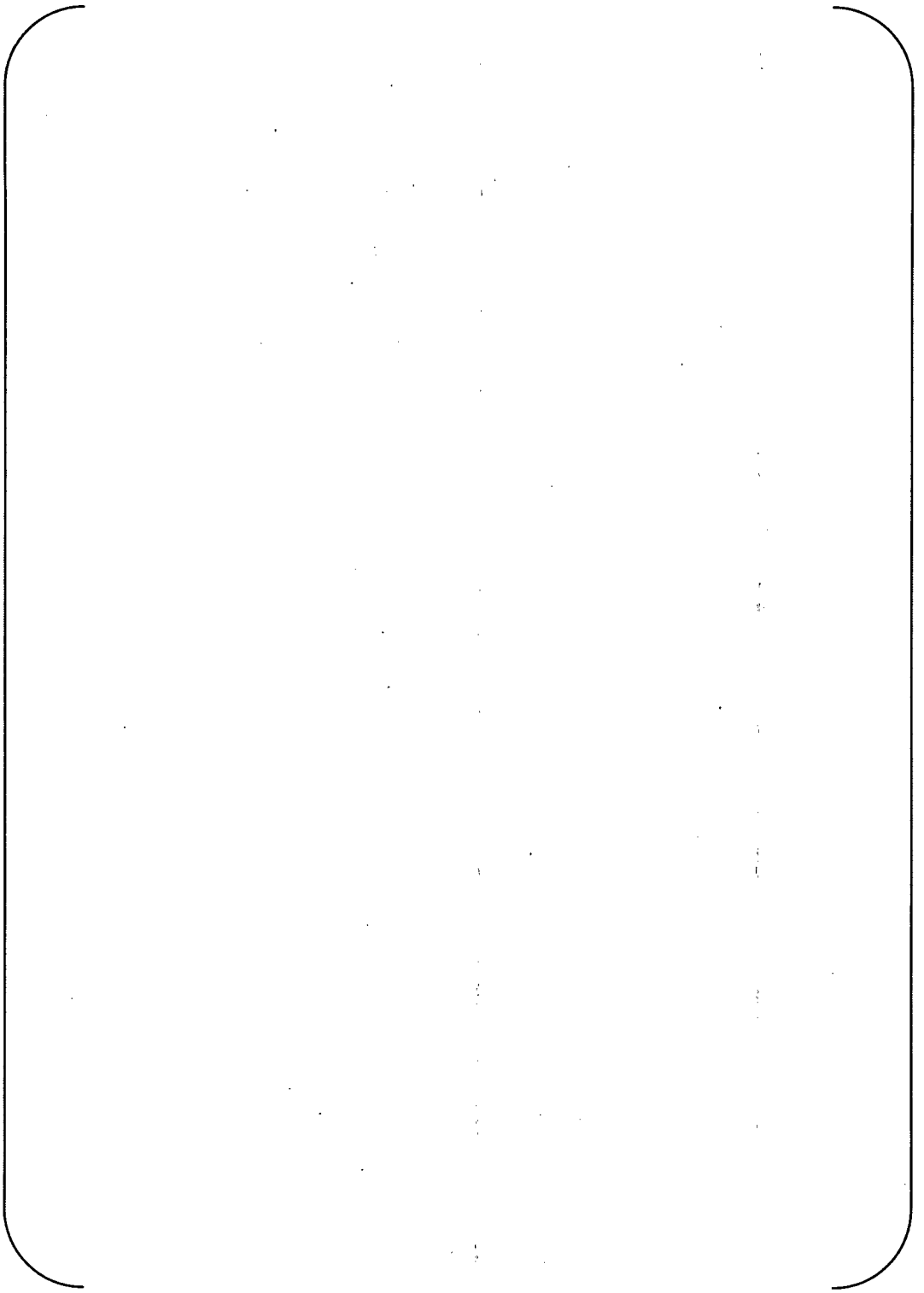

Fig. 7.3.1-3 AVB-Tube Gap Contour in 2nd Pressure Testing

Appendix-6
Investigation of ISI ECT Data for AVB Support Condition for Unit-2/3

1. Tube to AVB gap evaluation

1.1 Introduction

ECT data was used to evaluate the tube-to-AVB gap sizes in the Unit 2 and Unit 3 SGs after 22 months and 11 months of operation, respectively.

Bobbin probe was used for the evaluation.

1.2 Evaluation method

Effort was made to eliminate or minimize sources of error in the ECT data shown in Table 1. Table 2 describes the countermeasures taken in this evaluation.

Table 1 The factors which influence the gap evaluation

	140kHz Abs. Peak-to-peak amplitude		140kHz abs Integral Amplitude	
Thickness reduction or dent of tube	X	L	X	L
Misalignment of AVB	X	L	-	-
Dimensional error on calibration notch	X	M	X	M
Variation of scanning speed of probe	-	-	X	M
Scale on tube outer surface	X	S	X	S
Thickness of tube	X	S	X	S
Width of AVB	X	S	X	S

Note: "L","M" and "S" show the degree of influence on the evaluation.
L: Large, M: Medium, S: Small

Table 2 Significant error factor and countermeasure

Error factor	Correction
Misalignment of AVB	Differential channel is sensitive to the misalignment factor. Absolute channel and the absolute amplitude integral method can reduce the factor. These two methods are adopted. (Attachment 2)
Dimensional error on Calibration notch	Each of Cal std variability is corrected.

1.3 Tube-to-AVB Gap Evaluation

Color maps that show the bobbin absolute AVB signal amplitude for each tube at each AVB in each of the 4 SGs (refer to Attachment 1). Measurements of larger amplitudes are associated with smaller gaps.

The large green areas of the Attachment 1 plots indicate gaps of [ ] or less (approximate). The amplitudes in B01, B12 of SG-3B around Row 50 are slightly smaller than what is present in other SGs in the region, which potentially indicates larger gaps along Row 50.

Figure 1 shows an evaluation of average amplitude at each AVB of the four steam generators. In this figure the ranking of SGs by average amplitude from large to small is 2B, 2A/3B, 3A - where the larger amplitude is associated with smaller tube-to-AVB gaps. This indicates that (slightly) larger average gaps are present in the Unit-3 SGs than in the Unit-2 SGs. It is also noted that Figure 1 shows smaller gaps (larger amplitudes) in the region of the tubes that are closest to the top TSP. This may be related to the uniform tube support plate hole spacing. Figure 2 shows the maximum gap, minimum gap and distribution of ECT amplitude value.

Mock up test results of tube-to-AVB gaps and AVB misalignment are shown in Attachment 2. These results provide insight into the accuracy of the data.

※Remarks for Attachment 1: The white color in 2A and 2B means that ECT data is missing at that location.

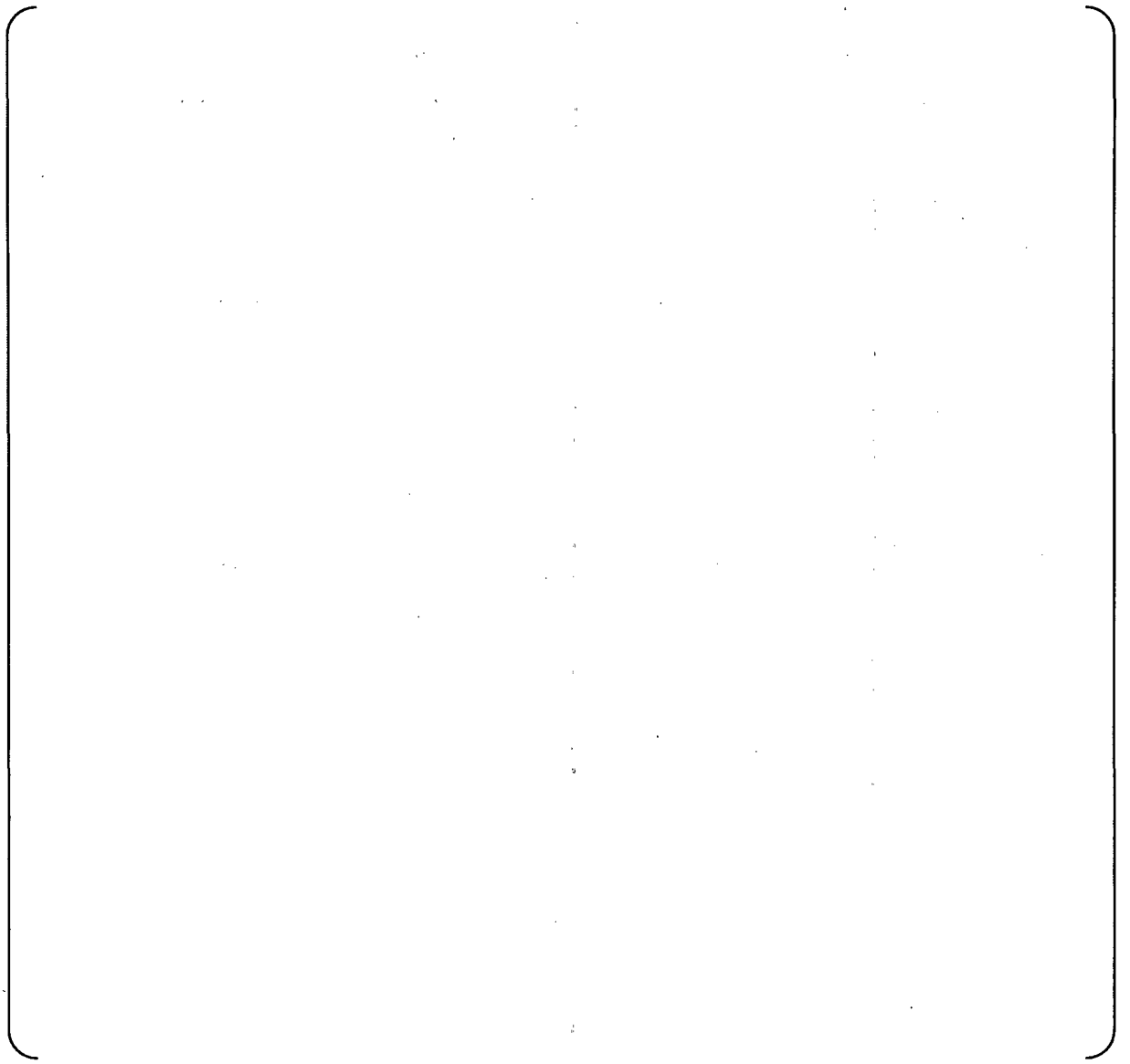

Fig.2 Distribution of ECT amplitude value (140kHz-Abs,integral)

4 Conclusion

The results of this evaluation show that the Unit-3 SGs have slightly larger average tube-to-AVB gaps than the Unit-2 SGs, with the largest in SG-3A. This trend indicates the tube-to-AVB contact force of Unit-3 SGs are smaller than that of Unit-2 SGs.

Attachment 1: Amplitude integral color map of Bobbin probe (Abs)
Attachment 2: Mock up test result of gap and misalignment evaluation

Amplitude integral color map ( ) (1/2)

Amplitude integral color map ([ ]Abs) (2/2)

Amplitude of Bobbin coil probe v.s. gap and misalignment (Mock-Up)

2. AVB insertion depth evaluation

Evaluation of as-built insertion depth of AVBs was conducted by the bobbin ISI-ECT data for representative columns for 3B-SG.

2.1 Sample tubes and AVBs used for evaluation

See Table-1, 2, 3, 4 and 5.

2.2 Evaluation method

Each AVB location on representative tubes is evaluated by estimating the arch length on tubes by ISI-ECT signal interval from #7 TSP. And these locations are plotted on the drawing for comparison with the design-based locations. (See Table-1, 2, 3, 4 and 5.)

2.3 Result

ECT-based AVB locations are compared with design-based locations as shown in Fig.1, 2, 3, 4 and Fig.5. It is evaluated that AVB insertion depth in actual SG is not changed compared with the design-based location, where the measurement uncertainty of AVB position due to the difference of the scanning speed is considered approximately [ ].

Table-1 Distance between the center of #7TSP thickness and AVB position (3B-SG)

<Column 9>

Row	B01	B02	B03	B04	B05	B06	B07	B08	B09	B10	B11	B12
1												
3												
5												
7												
9												
11												
13												
15												
19												
23												
27												
29												
31												
33												
35												
37												
41												
43												
47												
49												
51												
53												
55												

(unit ; mm)

Table-2 Distance between the center of #7TSP thickness and AVB position (3B-SG)

<Column 10>

Row	B01	B02	B03	B04	B05	B06	B07	B08	B09	B10	B11	B12
2												
4												
6												
8												
10												
12												
14												
16												
18												
20												
22												
24												
26												
28												
30												
38												
48												
50												
52												
58												

(unit ; mm)

Table-3 Distance between the center of #7TSP thickness and AVB position (3B-SG)

<Column 11>

Row	B01	B02	B03	B04	B05	B06	B07	B08	B09	B10	B11	B12
1												
3												
5												
7												
9												
11												
13												
15												
17												
19												
23												
27												
29												
37												
47												
49												
51												
57												
63												

(unit ; mm)

Table-4 Distance between the center of #7TSP thickness and AVB position (3B-SG)

<Column 77>

ROW	B01	B02	B03	B04	B05	B06	B07	B08	B09	B10	B11	B12
3												
7												
15												
17												
19												
21												
23												
25												
27												
37												
47												
67												
87												
107												
127												
141												

(unit ; mm)

Table-5 Distance between the center of #7TSP thickness and AVB position (3B-SG)

<Column 89>

Row	B01	B02	B03	B04	B05	B06	B07	B08	B09	B10	B11	B12
1												
3												
5												
7												
9												
11												
13												
15												
19												
21												
23												
27												
29												
33												
37												
39												
43												
47												
67												
85												
103												
107												
109												
113												
125												
137												

(unit ; mm)

Fig.1 Column9 AVB Position
(solid line ; design, broken line ; ISI-ECT)

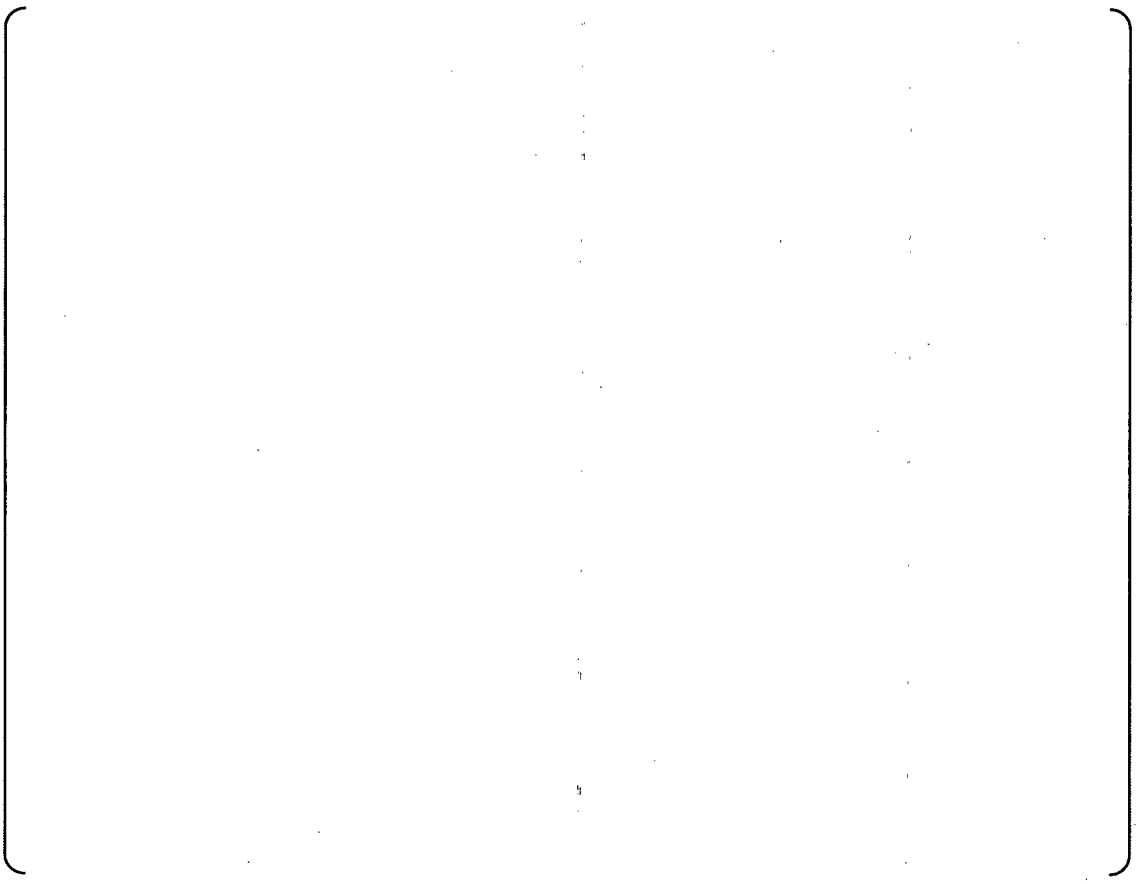

Fig.2 Column10 AVB Position
(solid line ; design, broken line ; ISI-ECT)

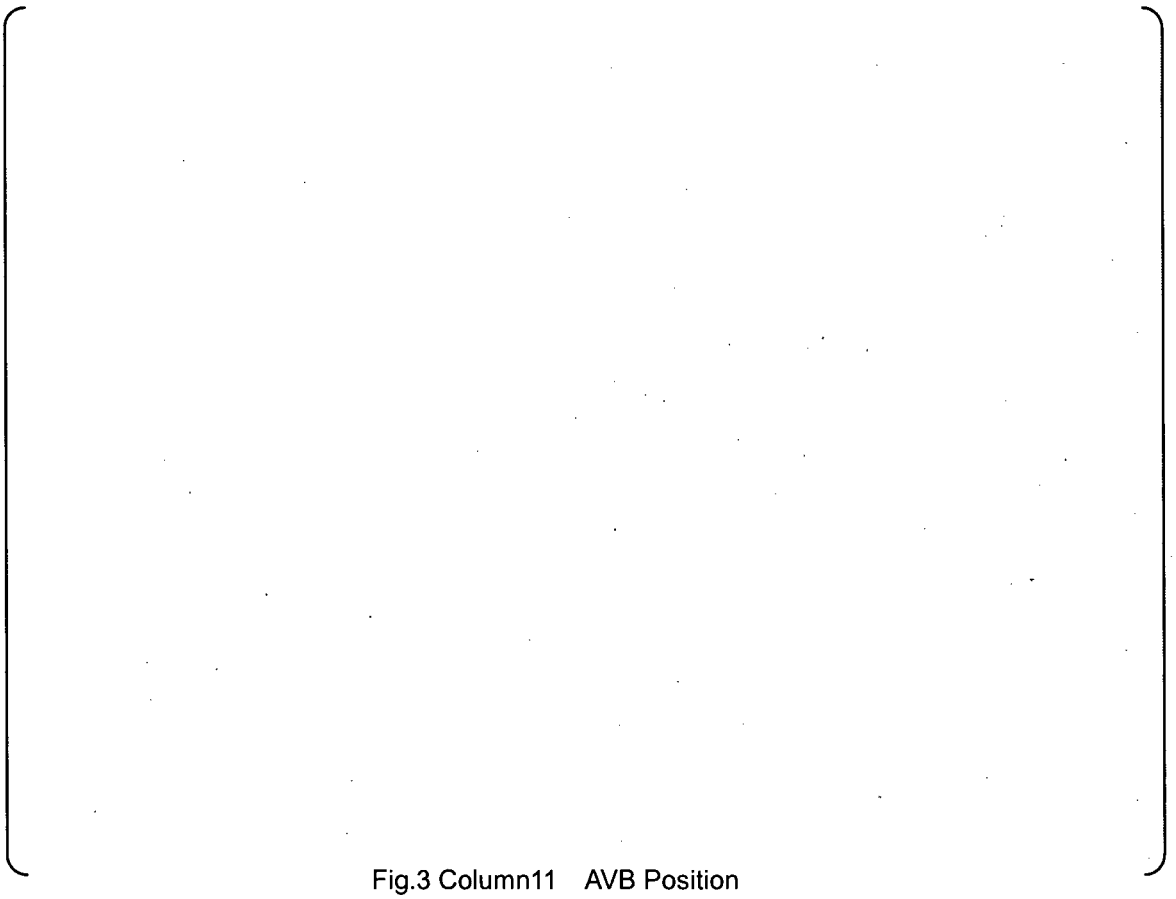

Fig.3 Column11 AVB Position
(solid line ; design, broken line ; ISI-ECT)

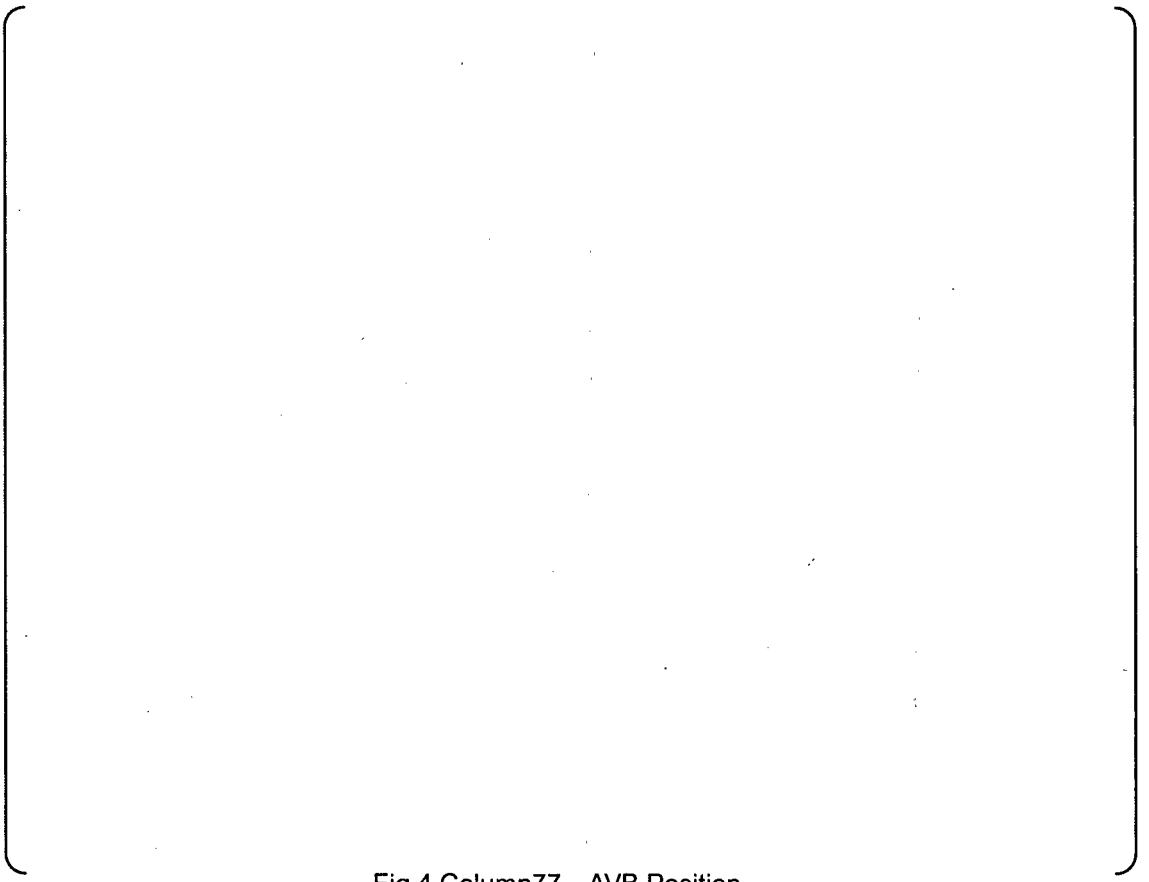

Fig.4 Column77 AVB Position
(solid line ; design, broken line ; ISI-ECT)

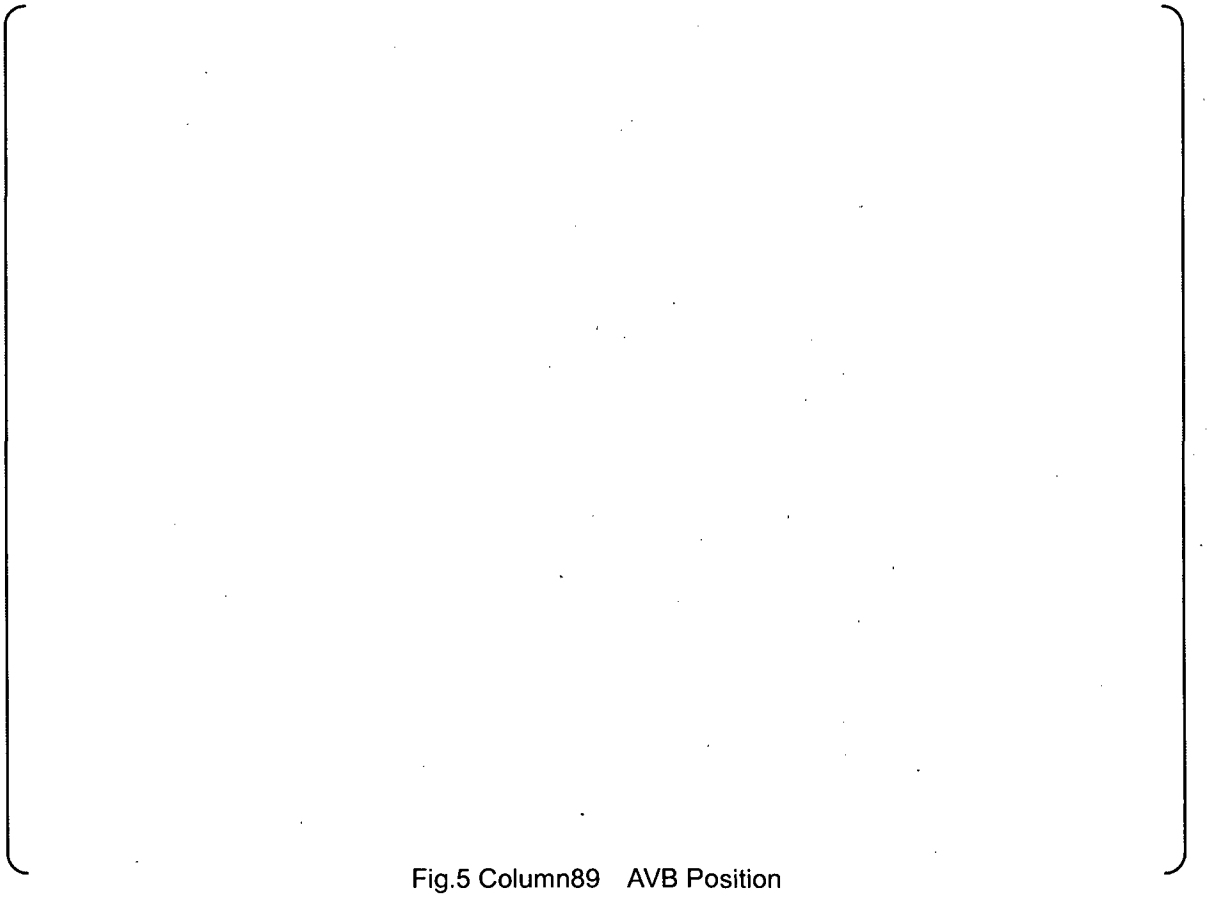

Fig.5 Column89 AVB Position
(solid line ; design, broken line ; ISI-ECT)

Appendix-7
Visual Inspection Results for U-Bend Region for Unit-2/3

1. Purpose

This appendix shows the visual inspection result of the tubes and AVBs in U-bend region of SONGS Unit 2 / Unit-3. These visual inspections were performed using a CCD camera inserted into the U-bend region and recorded on DVD by AREVA.

2. Location Inspected

The locations inspected are shown below.

Unit-3

Unit-3A: AVB 04	Col. 87/86 → 84/83 (4 columns)	
Unit-3A: AVB 09	Col. 86/87 → 80/81 (7 columns)	
Unit-3B: AVB 04	Col. 82/81 → 75/74 (8 columns)	
Unit-3B: AVB 04	Col. 61/60 → 50/49 (12 columns)	Total 31 columns

Unit-2

Unit-2A: AVB 04	Col. 88/87 → 73/72 (16 columns)	
Unit-2B: AVB 04	Col. 87/86 → 76/75 (12 columns)	Total 28 columns

3. Wear Patterns and Characteristics

Two wear patterns were observed at the tube-to-AVB intersections. The wear patterns are described as follows.

3.1 Wear Pattern-1 (Regional Wear on Tube Surface)

Characteristics

① Tube wear scar indicates in-plane motion or vibration

② Evidence of both parallel and perpendicular movement relative to the AVB

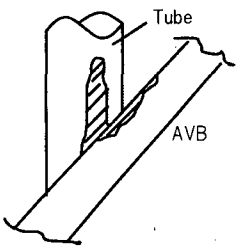

Fig-1 Wear Pattern 1

3.2 Wear Pattern-2 (Local Wear on Tube Surface)

Characteristics

① Local wear occurs on the tube but the wear surface is not exposed (cannot be seen)
② Unable to determine if wear occurs on tube or AVB or both
③ Unable to determine the direction of motion or vibration
④ An extreme interpretation is that both tube and AVB are worn into each other.

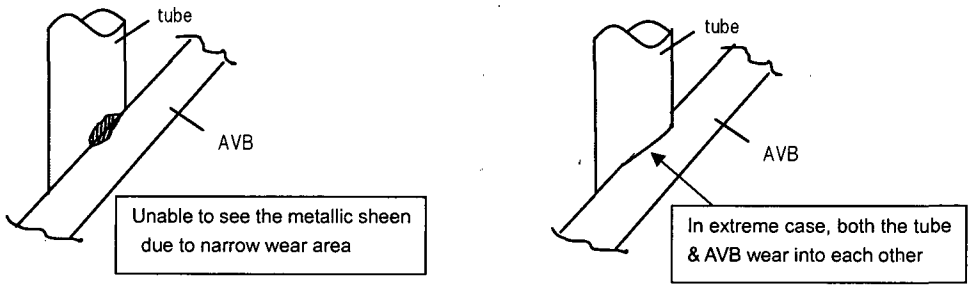

(a) Case 1 (b) Case 2

Fig-2 Wear Pattern 2

4. Results of Visual Inspection of Unit-2 / Unit-3

4.1 Common Observations from Unit-2 and Unit-3 (See Photo-1 to Photo-8)

- No large gaps between the AVBs and tubes
- AVBs appeared to be straight, no detectable abnormalities
- No abnormality in the orientation between the AVBs and tubes
- No abnormality in AVB positions or end cap-to-retaining bar welds

4.2 Unit-3

- Pattern-1 wear due to high amplitude in-plane vibration, as shown in Photo-9 and Photo-10, were found in the free span region.
- Pattern-2 wear as shown in Photo-11 and Photo-12 was found near where Pattern-1 occurred.
- There is some Pattern-1 wear identified by visual inspection , for which Bobbin ECT was not able to detect as this type of wear. (See Table-1～Table-4)

2) Unit-2

- As shown in Photo-13, Photo-14, Pattern-2 wear, which was found in Unit-3, was also found in Unit-2. However, no Pattern-1 wear was found.

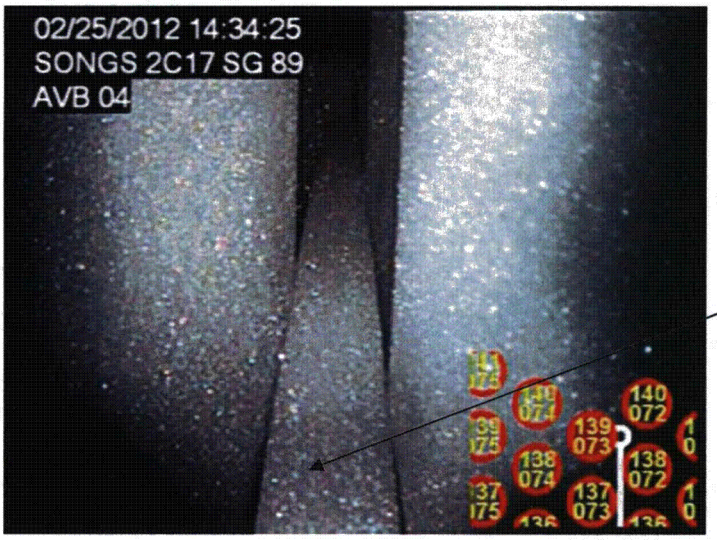

Photo-1 Visual Inspection Image of Outermost Tube Region [Unit-2A]

Image of Unit-2A Col. 72/73 tubes at AVB 04

Left side is Row 139, right side's far end is Row 140 and right side's closer end is Row 138.

The bottom of the End Cap is seen over the outermost tube.

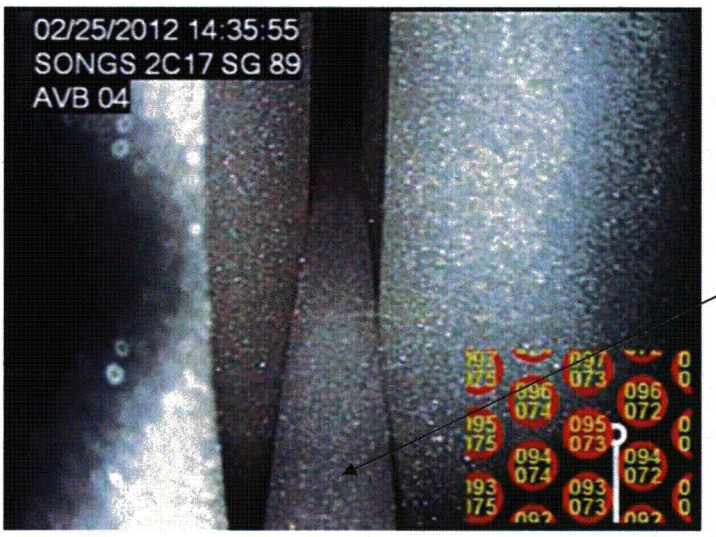

Photo-2 Tube Bundle Visual Inspection Image [Unit-2A]

Image of Unit-2A Col. 72/73 tubes around Row 95 at AVB 04 (Sample).

No gaps between the tube and AVB beyond 0.1mm and no twisting and bending on the AVB are observed.

Photo-3 Visual Inspection Image of Outermost Tube Region [Unit-2B]

Image of Unit-2B Col. 78/79 tubes at AVB 04

Left side is Row 141, right side's far end is Row 142 and right side's closer end is Row 140.

The bottom of the End Cap is seen over the outermost tube.

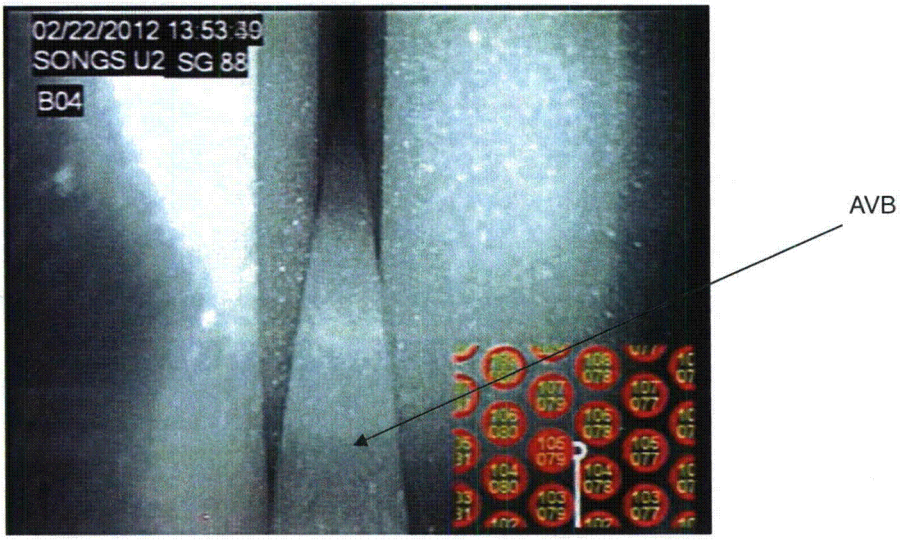

Photo-4 Tube Bundle Visual Inspection Image [Unit-2B]

Image of Unit-2B Col. 78/79 tubes around Row 105 at AVB 04 (Sample).

No gaps between the tube and AVB beyond 0.1mm and no twisting and bending on the AVB are observed.

Photo-5 Visual Inspection Image of Outermost Tube Region [Unit-3A]

Image of Unit-3A Col. 84/83 tubes at AVB 04

Left side's far end is Row 142, right side is Row 141 and left side's closer end is Row 140.

The bottom of the End Cap is seen over the outermost tube.

Photo-6 Tube Bundle Visual Inspection Image [Unit-3A]

Image of Unit-3A Col. 84/83 tubes around Row 125 at AVB 04 (Sample).

No gaps between the tube and AVB beyond 0.1mm and no twisting and bending on the AVB are observed.

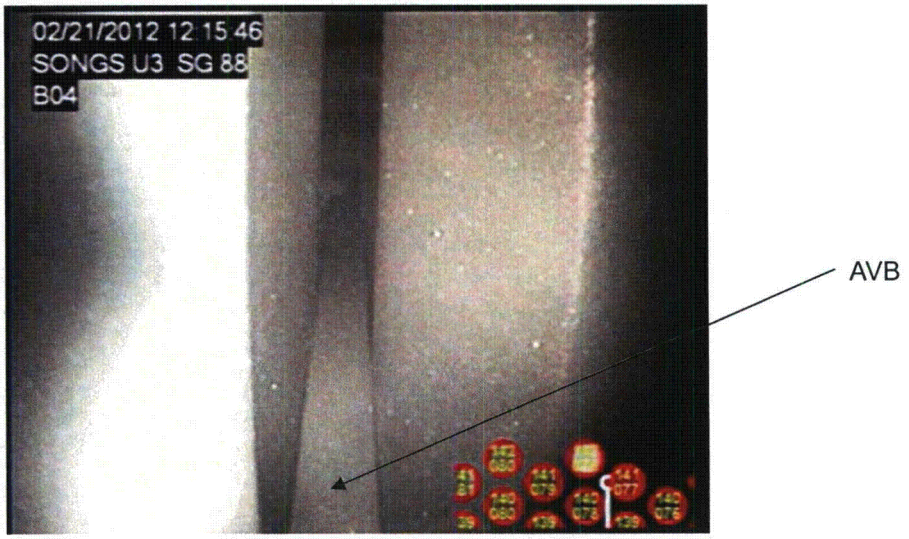

Photo-7 Visual Inspection Image of Outermost Tube Region [Unit-3B]

Image of Unit-3B Col. 78/77 tubes at AVB 04

Left side's far end is Row 142, right side is Row 141 and left side's closer end is Row 140.

The bottom of the End Cap is seen over the outermost tube.

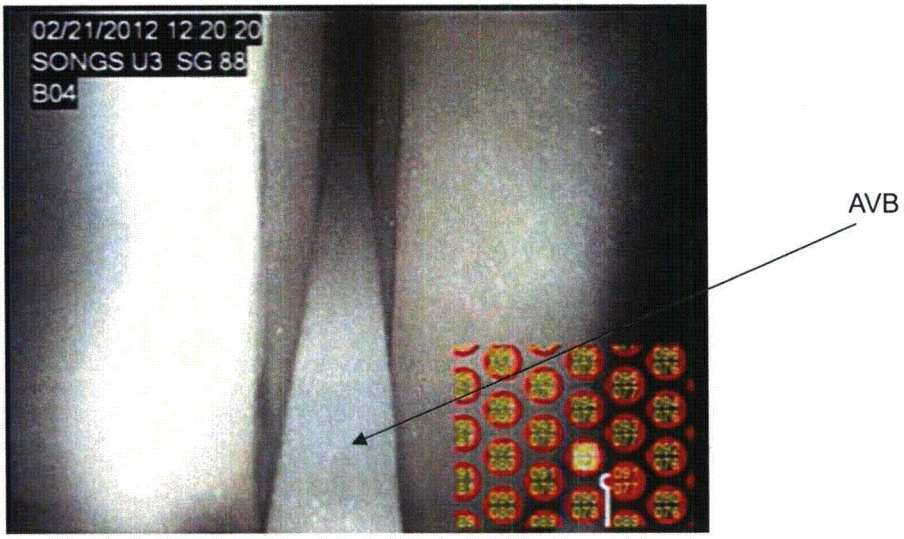

Photo-8 Tube Bundle Visual Inspection Image [Unit-3B]

Image of Unit-3B Col. 78/77 tubes around Row 90 at AVB 04 (Sample).

No gaps between the tube and AVB beyond 0.1mm and no twisting and bending on the AVB are observed.

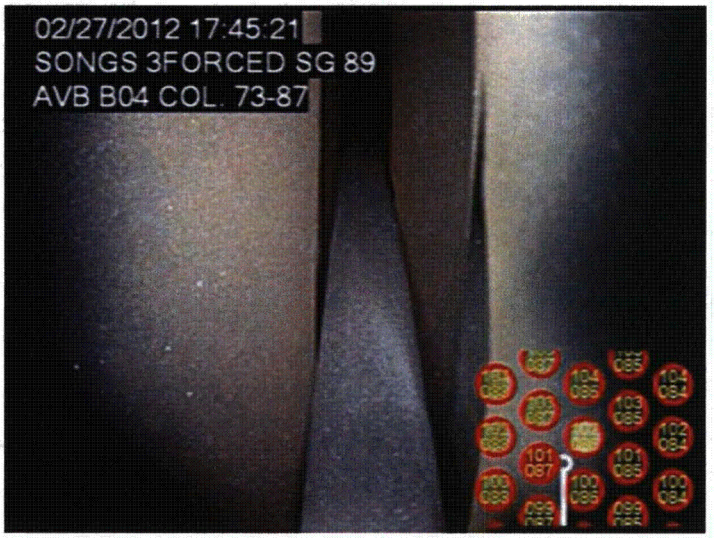

Photo-9 Sample of Pattern-1 [Unit-3A]

Image of Unit-3A Col. 87/86 shows a sample of Pattern-1 wear.

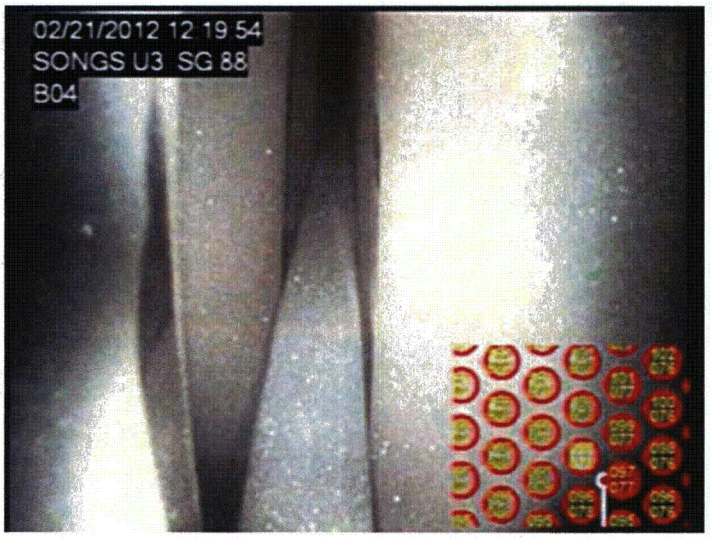

Photo-10 Sample of Pattern-1 [Unit-3B]

Image of Unit-3B Col. 78/77 shows a sample of the Pattern-1 wear.

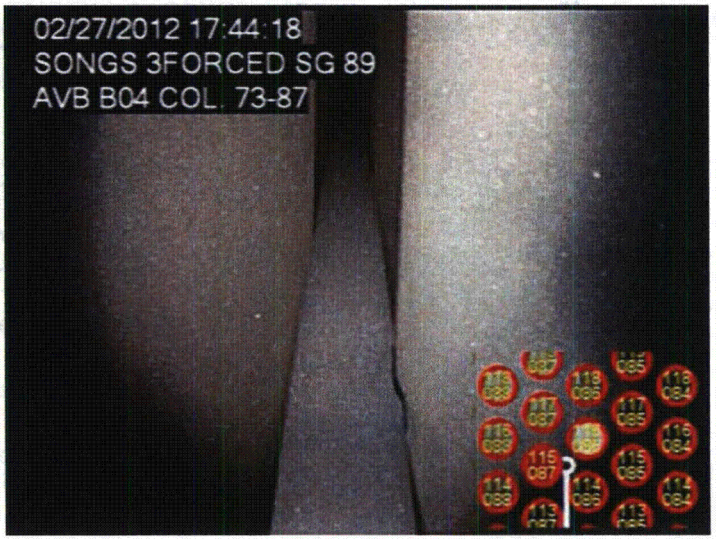

Photo-11 Sample of Pattern-2 [Unit-3A]

Image of Unit-3A Col. 87/86 shows a sample of Pattern-2 wear, where wear between tube and AVB cannot be distinguished.

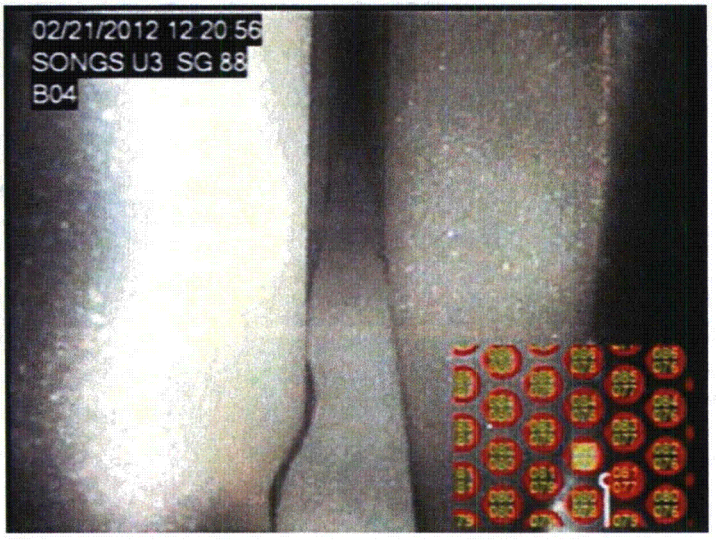

Photo-12 Sample of Pattern-2 [Unit-3B]

Image of Unit-3B Col. 78/77 shows a sample of the most typical Pattern-2 wear, where wear between the tube and AVB cannot be distinguished.

Photo-13 Sample of Pattern-2 [Unit-2A]

Image of Unit-2A Col. 88/87 shows a sample of Pattern-2 wear.

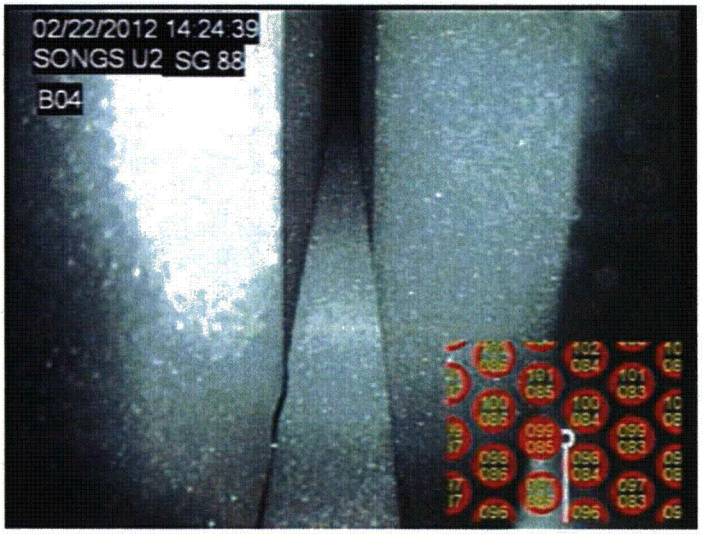

Photo-14 Sample of Pattern 2 [Unit-2B]

Image of Unit-2B Col. 85/84 shows a sample of Pattern-2 wear.

Table-1 SONGS Unit-3A AVB 04 Visual inspection result

Col. 87	Col.87/86				Col. 86	Col.86/85				Col. 85	Col.85/84				Col. 84	Col.84/83				Col. 83
TWD (%)	Row	Col.87	Row	Col.86	TWD (%)	Row	Col.86	Row	Col.85	TWD (%)	Row	Col.85	Row	Col.84	TWD (%)	Row	Col.84	Row	Col.83	TWD (%)
	141		142			142		141			141		142			142	?	141		
	139		140			140		139			139		140			140		139		
	137	P2	138			138		137	P2(minor)		137		138			138		137		
	135		136	P1	6	136	P1	135	P2(minor)		135		136		12	136		135		
	133		134	P1		134	P1?	133	P2(minor)		133		134		8	134		133		5
	131		132	P2(minor)	7	132	P1?	131	P2(minor)		131	P1	132			132		131		
	129		130	P2		130		129	P2(minor)		129		130	P2(minor)		130		129		
	127	P2(minor)	128	P2(minor)	6	128		127	P1?		127		128			128		127		
	125		126			126		125	P2(minor)		125		126			126		125		
	123		124			124		123			123		124			124		123		
	121	P2(minor)	122	P2(minor)	11	122		121		6	121	P2(minor)	122	P2(minor)	6	122		121		
6	119	P2(minor)	120	P2	6	120		119	P2		119	P2(minor)	120	P2(minor)		120		119		8
	117	P2(minor)	118	P1	9	118	P2(minor)	117	P1		117	P1?	118	P1	9	118		117		7
8	115		116	P1	12	116	P1	115	P1	10	115		116	P1	13	116		115		
8	113		114	P2	19	114	P2?	113	P2(minor)	17	113		114	P1	8	114		113		11
12	111		112	P1	9	112	?	111	P1	13	111		112	P1	23	112		111		23
11	109		110	P2	11	110		109	P1	12	109	P2(minor)	110	P1	14	110		109		
17	107	P1	108	P1	11	108	?	107	P1	15	107	P1	108	P1	16	108		107		16
9	105	P1	106	P1	25	106	P1	105	P1	22	105	P1	106	P1	16	106		105	P2?	22
13	103	P1	104	P1	22	104	P1	103	P1	15	103	P1	104	P1	17	104		103		17
13	101	P1	102	P1	25	102	P1	101	P1	21	101	P1	102	P1		102		101	P2(minor)	18
15	99	P1	100	P1	25	100	P1	99	P1	24	99	P1	100	P1	12	100		99		9
12	97	P1	98	P1	24	98	P1	97	P1	22	97	P1	98	P1	18	98		97	P2(minor)	18
12	95	P1	96	P1	20	96	P1	95	P1	21	95	P1	96	P1	12	96	P2(minor)	95	P2(minor)	5
27	93	P1	94	P1	22	94	P1	93	P1	20	93	P1	94	P1	21	94	P2(minor)	93		16
12	91	P1	92	P1	20	92	P1	91	P1	17	91	P1	92	P1	18	92		91	P2(minor)	11
	89	P1?	90	P1	23	90	P1	89	P1	10	89	P1	90	P1	7	90		89	P2(minor)	10
13	87	P1?	88	P1	18	88	P1	87	P1	18	87	P1	88	P1	13	88		87		
	85		86	P1	12	86	P1	85	P1	12	85	P1	86	P1	7	86		85		10
	83	P2(minor)	84	P1	12	84		83	P1	18	83	P2(minor)	84	P2	7	84		83		11
	81		82	P2	8	82		81	P2(minor)		81		82	P2	10	82	?	81	?	
	79		80	P2		80		79	P2(minor)		79		80	P2(minor)		80	?	79	?	
11	77		78	P2	11	78		77	P2(minor)	6	77		78	P2(minor)	5	78	?	77	?	
	75		76	P2(minor)		76		75	P2(minor)		75		76	Stay rod		76	Stay rod	75	?	
	73		74	P2(minor)		74		73	P2(minor)		73		74	P2(minor)	6	74	?	73	?	
	71		72	P2(minor)		72		71	P2(minor)		71		72	P2(minor)		72	?	71	?	
			70	P2(minor)		70							70	P2(minor)		70	?			

: Free span indication by ECT

Table-2(1/2) SONGS Unit-3A AVB 09 Visual inspection result

Col. 80	Col.80/81				Col. 81	Col.81/82				Col. 82	Col.82/83				Col. 83	Col.83/84				Col. 84
TWD (%)	Row	Col.80	Row	Col.81	TWD (%)	Row	Col.81	Row	Col.82	TWD (%)	Row	Col.82	Row	Col.83	TWD (%)	Row	Col.83	Row	Col.84	TWD (%)
	142		141			141		142			142		141			141		142		
	140		139			139		140			140		139			139		140		
	138		137	P2(minor)		137		138	P2(minor)		138		137	P2(minor)		137		138		
	136		135	P2(minor)	14	135		136	P1?		136	P2(minor)	135			135		136		
	134		133	P2(minor)		133		134			134		133	P2(minor)		133		134	P2(minor)	
	132		131			131		132	P2(minor)		132	P2(minor)	131			131		132	P1	
	130		129		5	129		130	P2(minor)		130	P2(minor)	129	P2(minor)		129		130	P2(minor)	
	128		127			127		128	P2(minor)	7	128		127	P1		127		128	P2	
7	126		125		8	125		126			126	P2(minor)	125	P2(minor)	6	125		126	P2(minor)	
	124		123			123		124			124	P2(minor)	123			123		124	P2(minor)	
	122		121			121		122	P2(minor)		122		121	P1		121		122	P2(minor)	
	120		119			119		120		8	120		119	P1	16	119		120	P2(minor)	
	118		117	P1		117		118	P2(minor)	11	118		117	P1		117		118	P2(minor)	15
	116		115	P1	11	115		116		11	116		115	P1		115		116	P2(minor)	14
10	114		113	P2(minor)		113		114	P2(minor)	8	114		113	P1	10	113		114	P2(minor)	
	112		111	P2(minor)	9	111		112	P2(minor)	10	112		111	P2(minor)	13	111		112	P2(minor)	11
15	110		109		11	109		110			110		109	P2(minor)		109		110	P2(minor)	16
17	108		107	P1	12	107		108	P1	7	108		107	P1	19	107	P2(minor)	108	P1	
17	106		105	P1	10	105		106	P1	21	106		105	P1	19	105	P2(minor)	106	P1	13
9	104		103	P1	16	103		104	P1	20	104		103	P1	10	103	P2(minor)	104	P1	11
28	102		101	P1	23	101		102	P1	14	102		101	P1	26	101	P1?	102	P1	8
29	100		99	P1	28	99	P2(minor)	100	P1	14	100		99	P1	26	99	P1?	100	P1	31
41	98		97	P1	15	97		98	P1	39	98		97	P1	15	97	P1?	98	P1	30
29	96		95	P1	15	95		96	P1	43	96		95	P1	14	95	P1?	96	P1	12
30	94		93	P1	15	93		94	P1	14	94		93	P1	10	93	P1?	94	P1	26
	92		91	P1	18	91		92	P1	34	92		91	P1	10	91	P2(minor)	92	P1	27
	90		89	P1	18	89		90	P1	34	90		89	P1		89	P2(minor)	90	P1	
	88		87	P1?	11	87		88	P1?		88		87	P1	13	87	P2(minor)	88	P1	9
	86		85	P2(minor)	10	85		86	P2(minor)	7	86		85	P2	13	85		86	P1	9
	84		83	P2(minor)	13	83		84	P2(minor)	10	84		83	P2(minor)	12	83		84	P2(minor)	
9	82		81			81		82	P2(minor)		82		81	P2(minor)	9	81		82		9
	80		79			79		80	P2(minor)		80		79	P2(minor)		79		80		
	78		77	P2(minor)	10	77		78	P2(minor)		78		77	P2(minor)		77		78		
	76		75		7	75		76	P2(minor)		76		75	P2(minor)	5	75	P2(minor)	76	Stay rod	
	74		73	P2(minor)		73		74	P2(minor)		74		73	P2(minor)		73	P2(minor)	74		
	72		71			71		72			72		71			71	P2(minor)	72		
	70							70			70							70	P2(minor)	

: Free span indication by ECT

Table-2(2/2) SONGS Unit-3A AVB 09 Visual inspection result

Col. 84	Col.84/85				Col. 85	Col.85/86				Col. 86	Col.86/87				Col. 87
TWD (%)	Row	Col.84	Row	Col.85	TWD (%)	Row	Col.85	Row	Col.86	TWD (%)	Row	Col.86	Row	Col.87	TWD (%)
	142		141			141		142			142		141		
	140		139			139		140			140		139		
	138		137	P2(minor)		137		138			138		137		
	136		135	P2(minor)		135	P2(minor)	136			136		135		
	134		133	P2(minor)		133		134			134		133	P2(minor)	
	132		131	P2(minor)		131		132			132		131	P1	11
	130		129		8	129		130			130		129	P2(minor)	
	128		127		9	127		128			128		127	P1	16
	126		125		7	125	P2(minor)	126			126		125	P2(minor)	6
	124		123	P2(minor)	7	123		124	P2(minor)		124		123	P2(minor)	
	122		121	P2(minor)	9	121		122			122		121	P2(minor)	
	120		119		6	119		120			120		119	P1	5
15	118		117	P2(minor)	14	117		118			118		117	P1	13
14	116		115	P1	11	115		116		9	116		115	P1	9
	114		113	P1	18	113		114			114		113	P1	10
11	112		111			111		112			112		111		
16	110		109	P1?		109		110			110		109		
	108	P2(minor)	107	P1?	24	107	P2(minor)	108			108	P2(minor)	107		11
13	106	P2(minor)	105	P1	25	105	P2(minor)	106	P1	18	106	P2(minor)	105	P1	
11	104	P1	103	P1	16	103	P2(minor)	104	P1	17	104		103	P1	23
8	102	P1	101	P1	6	101	P1?	102	P1	11	102		101		22
31	100	P1	99	P1	11	99	P1	100	P1	12	100	P2(minor)	99		17
30	98	P1	97	P1	21	97	P1?	98	P1	17	98		97	P1	10
12	96	P1	95	P1	16	95	P1?	96	P1	9	96	P1	95	P1	10
26	94	P1	93	P1	9	93	P1 H6	94	P1	33	94	P1?	93	P1	7
27	92	P1?	91	P1	16	91	P1	92	P1	31	92		91	P1	7
	90	P2(minor)	89		11	89	P1	90	P1	9	90	P1?	89	P1	15
9	88	P2(minor)	87	P1	9	87	P1	88	P1	7	88		87	P1	6
9	86	P2(minor)	85	P1		85	P1?	86	P1		86		85	P1	9
	84	P2(minor)	83	P1	8	83		84	P2(minor)	10	84		83	P1	14
9	82	P2(minor)	81		9	81		82			82	P2(minor)	81	P2(minor)	
	80	P2(minor)	79			79	P2(minor)	80			80	P2(minor)	79		10
	78		77			77		78			78	P2(minor)	77	P2(minor)	6
	76	Stay rod	75	P2(minor)		75	P2(minor)	76			76		75	P2(minor)	
	74	P2(minor)	73	P2(minor)		73	P2(minor)	74	P2(minor)		74	?	73	?	5
	72		71	P2(minor)		71		72			72	?	71	?	
	70							70			70	?			

: Free span indication by ECT

Table-3(1/5) SONGS Unit-3B AVB 04 Visual inspection result

Col. 82	Col.82/81				Col. 81	Col.81/80				Col. 80	Col.80/79				Col. 79	Col.79/78				Col. 78
TWD (%)	Row	Col.82	Row	Col.81	TWD (%)	Row	Col.81	Row	Col.80	TWD (%)	Row	Col.80	Row	Col.79	TWD (%)	Row	Col.79	Row	Col.78	TWD (%)
	142		141			141	?	142	?		142		141			141		142	?	
	140		139			139	?	140	?		140		139			139		140		
	138		137			137	?	138	?		138		137			137		138		
	136	P2(minor)	135		6	135	?	136	?		136		135	P2(minor)		135	P2(minor)	136		
	134	?	133	?	12	133	?	134	?		134		133		14	133	P2	134		5
10	132	?	131	P2(minor)		131	?	132	?	9	132	P2(minor)	131	P2(minor)	5	131	P2	132	P2(minor)	
8	130	P2(minor)	129			129	?	130	?	5	130		129			129	P2	130		9
	128	?	127	P2(minor)	12	127	?	128	?	10	128		127	P2(minor)		127	P2	128		15
	126		125			125	?	126	?	6	126	P2(minor)	125		12	125	P2	126	P2(minor)	
22	124	P2	123			123	?	124	?	25	124	P2(minor)	123		9	123	P2	124		19
	122	P2(minor)	121		14	121	?	122	?	28	122	?	121	P1?	17	121	P1	122	P1	18
	120	?	119	P2	27	119	?	120	?	15	120	P1	119	P1	19	119	P1	120		17
	118	?	117	P1?	12	117	?	118	?	21	118	P1	117	P1	15	117	P1	118	P1	18
24	116	?	115	P1	14	115	?	116	?	20	116	P1	115	P1	17	115	P1	116	P1	10
15	114	P1	113	P1	27	113	P1	114	?	29	114	P1	113	P1	19	113	P1	114	P1?	17
14	112	P1	111	P1	14	111	P1	112	P1	22	112	P1	111	P1	15	111	P1	112	P1	
9	110	P1	109	P1	18	109	P1	110	?	16	110	P1	109	P1	16	109	P1	110	P1?	17
12	108	P1	107	P1	16	107	P1	108	P1	22	108	P1	107	P1	14	107	P1	108	P1	10
16	106	P1	105	P1	21	105	P1	106	P1	18	106	P1	105	P1	20	105	P1	106	P1	
21	104	P1	103	P1	17	103	P1	104	P1	23	104	P1	103	P1	22	103	P1	104	P1	23
16	102	P1	101	P1	25	101	P1	102	P1	19	102	P1	101	P1	13	101	P1	102	P1?	13
16	100	P1	99	P1	20	99	P1	100	P1	14	100	P1	99	P1	11	99	P1	100	P1?	16
20	98	P1	97	P1	19	97	P1	98		26	98	P1	97	P1	15	97	P1	98	P1?	
27	96	P1	95	P1	20	95	P1	96	P1?	21	96	P1?	95	P1	14	95	P1	96		37
18	94	P1	93	?	12	93		94	P2		94		93	P2	13	93	P2	94	P2	17
12	92		91	P2	23	91		92	P2	10	92		91	P2	13	91	P2	92	P2	10
	90		89	P2	15	89	P2	90	P2	18	90		89	P2	25	89	P2	90		11
10	88	P2	87	P2(minor)	6	87		88	P2	14	88		87	P2	16	87	P2(minor)	88		7
10	86	P2	85	P2	12	85	P2(minor)	86	P2	14	86		85	P2	20	85		86	P2(minor)	7
6	84	P2(minor)	83	P2	8	83	P2(minor)	84	P2	25	84		83	P2	12	83	P2(minor)	84	P2	17
12	82	P2(minor)	81	P2(minor)	9	81	P2	82	P2	16	82		81	P2	20	81		82	P2(minor)	11
14	80		79		5	79	P2(minor)	80	P2(minor)	13	80	P2(minor)	79	P2		79	P2(minor)	80	P2(minor)	21
9	78	P2	77	P2(minor)		77	P2(minor)	78	P2(minor)	8	78	P2	77			77	P2	78		
	76	P2(minor)	75	P2(minor)		75	P2	76			76	P2	75			75	P2	76	P2	
	74		73			73	P2	74			74	P2	73	P2(minor)		73	P2(minor)	74	P2	
	72		71			71	P2	72	P2(minor)		72	P2	71			71	P2	72		
	70							70			70							70		

: Free span indication by ECT

Table-3(2/5) SONGS Unit-3B AVB 04 Visual inspection result

Col. 78	Col.78/77				Col. 77	Col.77/76				Col. 76	Col.76/75				Col. 75	Col.75/74				Col. 74
TWD (%)	Row	Col.78	Row	Col.77	TWD (%)	Row	Col.77	Row	Col.76	TWD (%)	Row	Col.76	Row	Col.75	TWD (%)	Row	Col.75	Row	Col.74	TWD (%)
	142		141			141							141	?		141				
	140		139	?		139		140			140	?	139	?		139		140		
	138	?	137			137		138			138	?	137	?		137		138		
	136		135			135	P2(minor)	136	P2(minor)		136	?	135	?		135		136		
5	134	P2(minor)	133	P2(minor)		133		134	P2(minor)		134	?	133	?		133		134		
	132		131	P2(minor)		131	P2(minor)	132	P2(minor)		132	?	131	?		131	P2(minor)	132	P2(minor)	
9	130	P2	129	?		129		130	P2(minor)		130	P2?	129			129		130		7
15	128	?	127		9	127		128	P2(minor)	6	128	P2(minor)	127		10	127	P2	128	P2(minor)	
	126	P2(minor)	125	?		125	P2(minor)	126	P2(minor)	9	126	?	125			125	P2(minor)	126	P2	12
19	124	?	123		8	123	P2(minor)	124	P2	14	124	P2(minor)	123	P2(minor)		123	P2(minor)	124	P2(minor)	
18	122	P2	121		24	121	P1	122	P1	11	122	P1	121	P2(minor)	14	121		122		11
17	120	P1	119	P1	19	119	P1	120	P1	20	120	P1	119	P2(minor)	6	119		120		15
18	118	P1	117	P2?	17	117	P1	118	P1	6	118	P1	117	P2(minor)	17	117	P2(minor)	118		10
10	116	P1	115	?	15	115	P1	116	P1	18	116	P1	115	P2(minor)	16	115	P1	116		
17	114	P1	113	P1	21	113	P1	114	P1	10	114	P1	113	P1		113	P1	114	P2(minor)	13
	112	P1	111	P1	17	111	P1	112	P1	14	112	P1	111	P1	10	111	P1	112	P2?	
17	110	P1	109	P1	20	109	P1	110	P1	11	110	P1	109	P1		109	P1	110	P1?	13
10	108	P1	107	P1	20	107	P1	108	P1	13	108	P1	107	P1		107	P1	108	P1?	9
	106	P1	105	P1	20	105	P1	106	P1	24	106	P1	105	P1	8	105	P1	106	P1	10
23	104	P1	103	P1	15	103	P1	104	P1	10	104	P1	103	P1	15	103	P1	104		
13	102	P1	101	P1		101	P1	102	P1?	13	102	P1	101	P2?	8	101	P1	102		7
16	100	P1	99	P2	12	99	P1	100	P1?	8	100	P1	99	P2(minor)	8	99	P2(minor)	100		14
	98	P1	97	P2	17	97	P1	98			98	P1?	97	P2(minor)		97	P2(minor)	98		7
37	96	P2	95	P2	11	95	P2(minor)	96	P2	18	96		95	P2	18	95		96		
17	94		93	P2	12	93		94	P2	9	94	P2(minor)	93	P2(minor)	10	93	P2	94	P2(minor)	10
10	92		91	P2(minor)	14	91		92	P2(minor)	13	92	P2(minor)	91	P2	8	91	P2(minor)	92	P2	13
11	90	P2(minor)	89	P2(minor)	8	89	P2(minor)	90	P2(minor)	11	90		89	P2	10	89		90	P2(minor)	8
7	88	?	87	?	14	87	?	88	P2(minor)	6	88	P2(minor)	87	P2	12	87		88		
7	86	?	85	P2(minor)	9	85		86	P2	19	86		85	P2(minor)	7	85		86	P2(minor)	
17	84	?	83	P2(minor)	6	83	P2(minor)	84	P2(minor)	6	84		83	P2(minor)	8	83	P2(minor)	84	P2(minor)	6
11	82		81	P2(minor)	13	81	P2(minor)	82	P2(minor)	8	82		81	P2(minor)	7	81	P2(minor)	82		
21	80	?	79	P2(minor)	6	79	P2(minor)	80	P2(minor)	11	80		79	P2	7	79		80		
	78	P1?	77	P2(minor)		77	P2(minor)	78	P2(minor)		78		77	P2		77		78		
	76	P2(minor)	75			75	?	76	P2(minor)		76		75			75		76		
	74	P2	73			73	P2(minor)	74			74		73	?		73	P2(minor)	74	P1?	
	72	?	71			71	P2(minor)	72			72	?	71	?		71	P2(minor)	72	Stay rod	
	70	P2(minor)						70			70	?						70		

: Free span indication by ECT

Table-3(3/5) SONGS Unit-3B AVB 04 Visual inspection result

Col. 61	Col.61–60				Col. 60	60–59				Col. 59	59–58				Col. 58	58–57				Col. 57
TWD (%)	Row	Col.61	Row	Col.60	TWD (%)	Row	Col.60	Row	Col.59	TWD (%)	Row	Col.59	Row	Col.58	TWD (%)	Row	Col.58	Row	Col.57	TWD (%)
	135																			
	133	P2(minor)	134			134		133			133									
	131		132			132	?	131			131		132			132		131		
	129		130	?		130		129			129	?	130	?		130		129		
	127	?	128			128		127			127	P2(minor)	128	?		128		127		
	125	P2(minor)	126	?		126	P2(minor)	125			125		126			126		125		
	123	P2(minor)	124	P2(minor)		124		123	?		123	P2(minor)	124			124		123		
	121	P2(minor)	122	?		122	P1	121			121	P2(minor)	122	P1		122	?	121		
	119	?	120	?		120	P1?	119	?		119	P1	120	P1		120	?	119		
	117	P2(minor)	118	?		118		117	?		117		118	P1		118	P2(minor)	117		
	115	?	116	?		116	P1	115			115	P1?	116	P1?		116		115		
	113	P2(minor)	114	?		114	P1	113			113	?	114	P1?		114		113		
	111	?	112	P2(minor)		112	P1?	111	?		111	P1?	112	P2(minor)		112		111		
	109	P2(minor)	110			110	P1	109			109	P2(minor)	110	P1?		110	?	109		
	107	P2(minor)	108	?		108	P2(minor)	107			107	P2(minor)	108			108		107	?	
	105	?	106	?		106	P2(minor)	105	P2(minor)		105	P2(minor)	106			106	P2(minor)	105		
	103	?	104	?		104	P2(minor)	103	?		103	P2(minor)	104			104		103		
	101	?	102	?		102	?	101			101	P2(minor)	102			102		101	P2(minor)	
	99	?	100			100	?	99	P2(minor)		99		100			100	?	99		
	97	P2(minor)	98	P2(minor)		98	P2(minor)	97			97		98			98	P2(minor)	97		
	95	?	96	P2(minor)		96	P2(minor)	95			95	P2(minor)	96			96	?	95	?	
	93		94			94	?	93	?		93	P2(minor)	94	P2(minor)		94	?	93		
	91	P2(minor)	92	P2(minor)		92	?	91	?		91		92	P2(minor)		92	P2(minor)	91		
	89	P2(minor)	90			90		89			89		90			90	P2(minor)	89		
	87	P2(minor)	88			88	P2(minor)	87			87		88			88	P2(minor)	87	?	
	85		86			86	P2(minor)	85			85		86			86		85		
	83	P2(minor)	84			84		83			83		84			84		83		
	81		82	?		82		81			81		82			82		81		
	79	?	80			80		79	P2(minor)		79		80			80		79		
	77	?	78	?		78		77	?		77		78			78		77		
	75		76			76		75			75	?	76			76		75		
	73	?	74	?		74		73			73		74			74		73		
	71	P2(minor)	72			72		71			71		72			72		71		
			70			70							70			70				

: Free span indication by ECT

Table-3(4/5) SONGS Unit-3B AVB 04 Visual inspection result

Col. 57	Col.57/56				Col. 56	Col.56/55				Col. 55	Col.55/54				Col. 54	Col.54/53				Col. 53
TWD (%)	Row	Col.57	Row	Col.56	TWD (%)	Row	Col.56	Row	Col.55	TWD (%)	Row	Col.55	Row	Col.54	TWD (%)	Row	Col.54	Row	Col.53	TWD (%)
	131		132	?		132	?	131	?		131	?								
	129		130			130		129			129		130	?		130	?	129	?	
	127		128			128		127			127		128			128		127		
	125		126			126		125			125	P2(minor)	126			126		125		
	123		124			124		123			123	P2(minor)	124			124	P1	123		
	121		122			122		121			121		122			122	P1	121	?	
	119	P2(minor)	120	P1		120		119			119	P2(minor)	120			120	P2(minor)	119	P2(minor)	
	117	P2(minor)	118	P1		118	P1	117	?		117	P2(minor)	118	P1		118	P2(minor)	117		
	115	P2(minor)	116	P2(minor)		116		115			115		116	P1		116	P2(minor)	115		
	113	P2(minor)	114	P1		114	P1	113	P2(minor)		113	P2(minor)	114			114	P2(minor)	113		
	111	P2(minor)	112	P2(minor)		112	P1	111	P2(minor)		111	P1	112			112	P2(minor)	111		
	109	P2(minor)	110	P2(minor)		110	P2(minor)	109	P2(minor)		109	P2(minor)	110			110	P1	109		
	107	P2(minor)	108			108	P1	107	P2(minor)		107	P1	108			108		107		
	105	P2(minor)	106	P2(minor)		106	P1	105	P2(minor)		105	P2(minor)	106	P2(minor)		106	P1	105		
	103		104			104	P1	103	P2(minor)		103	P1	104			104	P2(minor)	103		
	101	P2(minor)	102			102	P1	101	P2(minor)		101		102	P2(minor)		102	P2(minor)	101	P2(minor)	
	99		100			100	P2(minor)	99	P2(minor)		99	P1	100	P2(minor)		100	P2(minor)	99	?	
	97	P2(minor)	98			98	P1	97			97	P2(minor)	98			98	P2(minor)	97	P2(minor)	
	95	P2(minor)	96	P2(minor)		96	P2(minor)	95			95	P2(minor)	96			96	P2(minor)	95		
	93	P2(minor)	94	P2(minor)		94	P2(minor)	93	P2(minor)		93	P1	94			94	P1	93		
	91	P2(minor)	92			92	P2(minor)	91	P2(minor)		91	P2(minor)	92			92	P2(minor)	91		
	89	P2(minor)	90			90	P2(minor)	89			89	P2(minor)	90			90	P2(minor)	89		
	87	P2(minor)	88			88	P2(minor)	87			87	P2(minor)	88			88	P2(minor)	87		
	85	P2(minor)	86			86	P2(minor)	85			85	P2(minor)	86			86	P2(minor)	85		
	83	P2(minor)	84	P2(minor)		84	P2(minor)	83			83	P2(minor)	84			84	P2(minor)	83		
	81	P2(minor)	82	P2(minor)		82	P2(minor)	81			81	P2(minor)	82			82	P2(minor)	81		
	79	P2(minor)	80			80		79			79	P2(minor)	80			80	P2(minor)	79		
	77		78			78		77			77		78			78		77		
	75		76			76	P2(minor)	75			75	P2(minor)	76			76		75		
	73		74			74		73			73		74			74		73		
	71		72			72		71			71		72			72		71		
			70			70							70			70				

: Free span indication by ECT

Table-3(5/5) SONGS Unit-3B AVB 04 Visual inspection result

Col. 53	Col.53/52				Col. 52	Col.52/51				Col. 51	Col.51/50				Col. 50	Col.50/49				Col. 49
TWD (%)	Row	Col.53	Row	Col.52	TWD (%)	Row	Col.52	Row	Col.51	TWD (%)	Row	Col.51	Row	Col.50	TWD (%)	Row	Col.50	Row	Col.49	TWD (%)
	129	?																		
	127		128	?		128	?	127	?		127	?								
	125		126			126		125			125		126	?		126	?	125	?	
	123	P2(minor)	124			124		123			123		124			124		123		
	121		122			122		121			121		122	P1		122		121		
	119	P2(minor)	120	P2(minor)		120	P1	119			119	P1	120	P1		120		119		
	117	P1	118	P2(minor)		118	P1	117			117		118	P2(minor)		118	P2(minor)	117		
	115	P2(minor)	116			116	P2(minor)	115			115		116			116	P2(minor)	115		
	113	P1	114			114	P2(minor)	113	P2(minor)		113	P1	114	P2(minor)		114	P2(minor)	113		
	111	P1	112			112	P1	111			111		112			112	P2(minor)	111		
	109	P2(minor)	110			110		109			109	P2(minor)	110	P2(minor)		110	P2(minor)	109		
	107	P2(minor)	108			108	P1	107			107		108			108	P2(minor)	107		
	105	P2(minor)	106			106	P2(minor)	105			105	P2(minor)	106			106	P2(minor)	105		
	103	P2(minor)	104			104	P2(minor)	103			103		104			104	P2(minor)	103		
	101	P2(minor)	102			102	P2(minor)	101	P2(minor)		101	P2(minor)	102			102		101	P2(minor)	
	99	P2(minor)	100			100		99			99	P2(minor)	100			100		99		
	97	P1	98			98	P2(minor)	97			97		98			98	P2(minor)	97		
	95		96			96	P2(minor)	95			95	P1	96			96		95		
	93	P2(minor)	94			94	P2(minor)	93			93	P2(minor)	94			94	P2(minor)	93		
	91	P2(minor)	92			92	P2(minor)	91			91		92	P2(minor)		92		91		
	89	P2(minor)	90			90		89			89		90			90		89		
	87		88			88	P2(minor)	87			87	P2(minor)	88			88		87		
	85		86			86	P2(minor)	85			85	P2(minor)	86			86	P2(minor)	85		
	83		84			84	P2(minor)	83			83	P2(minor)	84	P2(minor)		84		83		
	81		82			82	P2(minor)	81			81	P2(minor)	82			82		81		
	79	P2(minor)	80			80	P2(minor)	79			79		80			80		79		
	77	P2(minor)	78			78	P2(minor)	77			77	P2(minor)	78			78	P2(minor)	77		
	75		76			76	P2(minor)	75			75	P2(minor)	76			76	P2(minor)	75		
	73		74			74		73			73	P2(minor)	74			74		73		
	71		72			72		71			71	P2(minor)	72			72		71		
			70			70							70			70				

: Free span indication by ECT

Table-4 Description of the abbreviations in Table-1～Table-3

Abbreviation	Description
P1	Tube Confirmed with Wear Pattern-1
P1?	Tube Suspected with Wear Pattern-1
P2	Tube Confirmed with Wear Pattern-2
P2 (minor)	Tube Confirmed with Minimal Wear Pattern-2
P2?	Tube Suspected with Wear Pattern-2
? (Unjudgeable)	Tube that cannot be determined due to the inspection rate in the video, etc

Appendix-8
SG Tube Flowering Analysis for Unit-2/3

1. Purpose

There are many instances of tube wear in the central part of the Unit-2 and Unit-3 U-bends. This wear should not be possible if the tubes were fully supported. This appendix contains an evaluation of the possible effects of fluid flow on the tubes and their support condition to determine how much influence they have on the tube support conditions.

2. Conclusion

The analyses results are the following.

- ✓ The distance between tubes within columns increases due to thermal elongation and dynamic pressure by a small amount relative to their nominal spacing (maximum change: [ ]
- ✓ The tube-to-AVB gaps in the center columns increase due to hydrodynamic pressure by [ ] when the manufacturing tolerance dispersion is not taken into account (Case C3A').
- ✓ The tube-to-AVB gap increase due to hydrodynamic pressure is small when the manufacturing tolerance dispersion is taken into account (Case D1).
- ✓ The area where the largest gaps are generated, correlates with the area with the most tube wear.
  - ➢ In the center columns and the outer rows the analysis shows that there are many AVB intersections with gaps on both sides of the AVBs (inactive supports).
  - ➢ There are many instances of consecutive inactive supports along tubes in the region.
- ✓ Increasing the retaining bar stiffness provides only a modest reduction in the gaps due to the hydrodynamic pressure. Such a change is not judged to be an effective countermeasure.

3. Methodology and Assumptions

1) Analysis model

The ABAQUS finite element program is used to model the U-bend. The tube bundle is symmetric about the central plane perpendicular to the tubelane, so a half-symmetry model is assumed. All of the U-tubes, AVBs, retaining bars, retainer bars, and bridges are modeled using beam elements. The model includes the U-bend and the straight leg of the tubes down to the elevation of the 6th TSP. The model is shown in Figure 3-1. Nominal dimensions are used. Manufacturing tolerances are not considered.

The two TSPs are represented as pinned supports. All tubes at the TSP#6 elevation are prevented from displacing in the lateral and axial directions but are free to rotate. All tubes at the TSP#7 elevation are restrained against lateral displacement but are free to displace axially and to rotate. Modeling the top two TSPs is sufficient to produce a reasonable structural representation of the U-bend portion of the tube bundle.
In Case C3A', all tubes at the TSP#6 elevation are able to displace in the lateral within gap range and free to rotate but axially fixed. All tubes at the TSP#7 elevation are restrained against lateral displacement by gap elements but are free to displace axially and to rotate.

Additional modeling details:

- Water mass inside (and outside) the tubes is simulated by an increase in tube density.
- Contact between tubes and AVBs is simulated by gap elements.
- The tube stiffness in compression is [ ] which is the spring stiffness of the gap elements under compression when the tube-to-AVB gap is zero.
- The initial tube-to-AVB gaps are set to zero. The gap elements exert a force on the tube when in compression, but displace freely under tension.
- A[ ]coefficient of friction for lateral movement between tubes and AVB is assumed. Tube can slide along the AVB, if slide force is larger than the force multiplying the compression force by[ ]
- The tube and AVB Modulus of Elasticity is specified based on operating temperature.
- Elastic material behavior is assumed for all parts.

2) Loading conditions

The hydrodynamic pressure across each tube is obtained from the ATHOS thermal hydraulic analysis and is applied to the tubes.

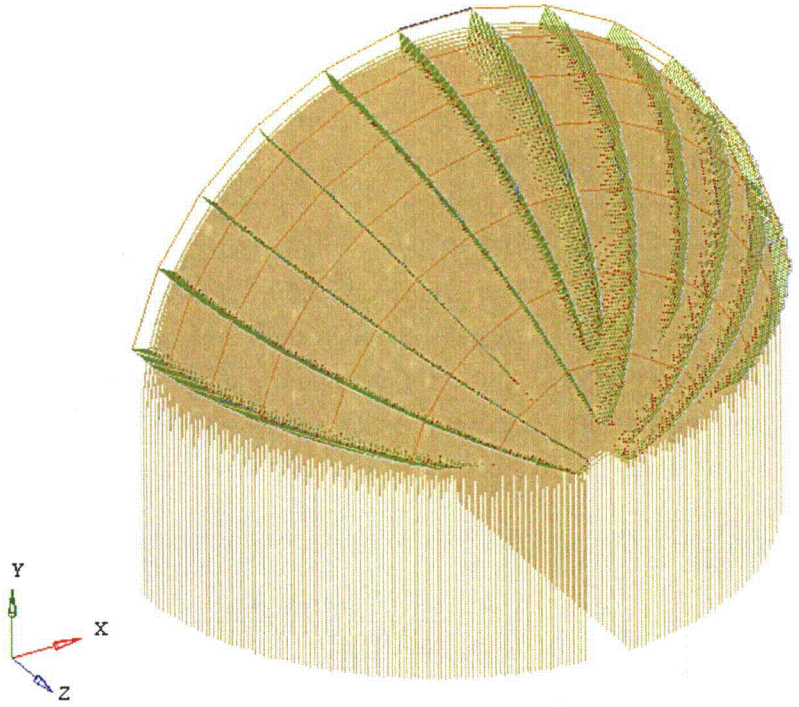

(i) Bird's-eye View of the Model

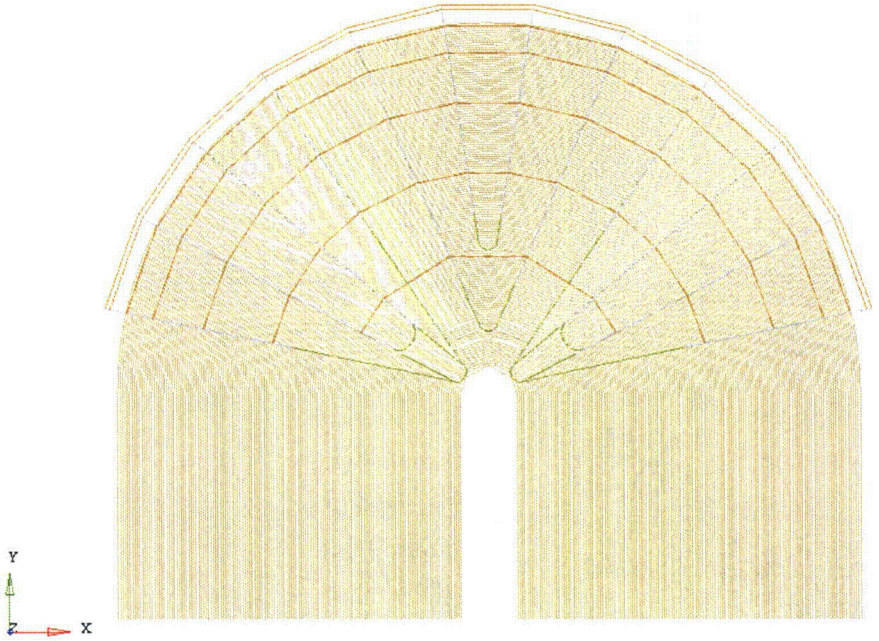

(ii) Side View of the Model

Fig. 3-1 ABAQUS model

4. Analysis cases

Table 4.1 describes the five cases that were analyzed. Cases C1 and C2 are used to confirm the influence of thermal elongation and hydrodynamic force on the tubes without any AVB supports. In these two cases the AVBs are not included so that the tubes can deform freely and so that the response of each tube can be evaluated independently. Cases C3A and C3B are used to evaluate the tube-to-AVB gap behavior. In Case C3A the hydrodynamic force produced by ATHOS (both in-plane and out-of-plane) is applied to the tubes. In Case C3B, only the hydrodynamic forces in the out-of-plane direction are applied. Case-C3C is a repeat of Case C3A but with much stiffer retaining bars ([ ]). This case was run to quantify its effectiveness as a countermeasure to prevent further tube wear.
In Case C3A', the latest ATOHS output is applied from Appendix-12. Additionally, Case D1 is used to evaluate effects the hydrodynamic force and manufacture dispersion, which is applied from Appendix-9 Case 2-1 analysis condition.

Table 4.1 analyses cases

<table>
<tr><th colspan="2" rowspan="2">Analysis Case</th><th colspan="4">Analysis Model</th><th rowspan="2">Load</th></tr>
<tr><th>Model Region</th><th colspan="2">AVB Assembly</th><th>Friction Factor</th><th>Method</th></tr>
<tr><td colspan="2">C1</td><td rowspan="2">Only tubes with water</td><td colspan="2" rowspan="2">No AVB
(Tubes only)</td><td rowspan="8">[ ]</td><td rowspan="8">Elastic Analysis</td><td>Temperature distribution</td></tr>
<tr><td colspan="2">C2</td><td>Dynamic Pressure (in-plane & out)</td></tr>
<tr><td rowspan="4">C3</td><td>A</td><td rowspan="6">AVBs, Retaining bars, Bridges, Retainer bars, and tubes with water</td><td rowspan="3">Gap elements for contact between AVBs and tubes (Contact spring : [ ][N/mm])</td><td rowspan="2">Original Retaining Bar</td><td>Dynamic Pressure (in-plane & out)</td></tr>
<tr><td>B</td><td>Dynamic Pressure (out of plane)</td></tr>
<tr><td>C</td><td>Retaining Bar stiffness =[ ] (Twice diameter)</td><td>Dynamic Pressure (in-plane & out)</td></tr>
<tr><td>A'</td><td>Gap elements for contact between TSP and tubes (Contact spring : [ ][N/mm])</td><td rowspan="2">Dynamic Pressure (in-plane & out) From Appendix-12 Dynamic Pressure (in-plane & out)</td></tr>
<tr><td colspan="2">D1</td><td>Manufacturing Dispersion From Appendix-9 Case2-1 for Unit-3</td></tr>
</table>

5. Results of analyses

5.1 Case-C1: Vertical Thermal Expansion Analysis (no AVB contact)

The total and vertical tube deformations of the tube bundle are shown in Figure 5.1-1. The top of the outermost tube grows by [ ] from the tubesheet surface. The vertical growth and total growth are essentially the same because the difference in the hot and cold side tube temperatures is small. This is because the average tube wall temperature is used, which is mid-way between the primary and secondary side temperatures.

Figure 5.1-2 shows the change in distance between tube rows in column 78 due to thermal expansion. The nominal distance of [ ]grows [ ] to a value of[ ]

The change in distance between tubes of the same column, due to tube thermal expansion from room temperature to operating temperature is negligible.

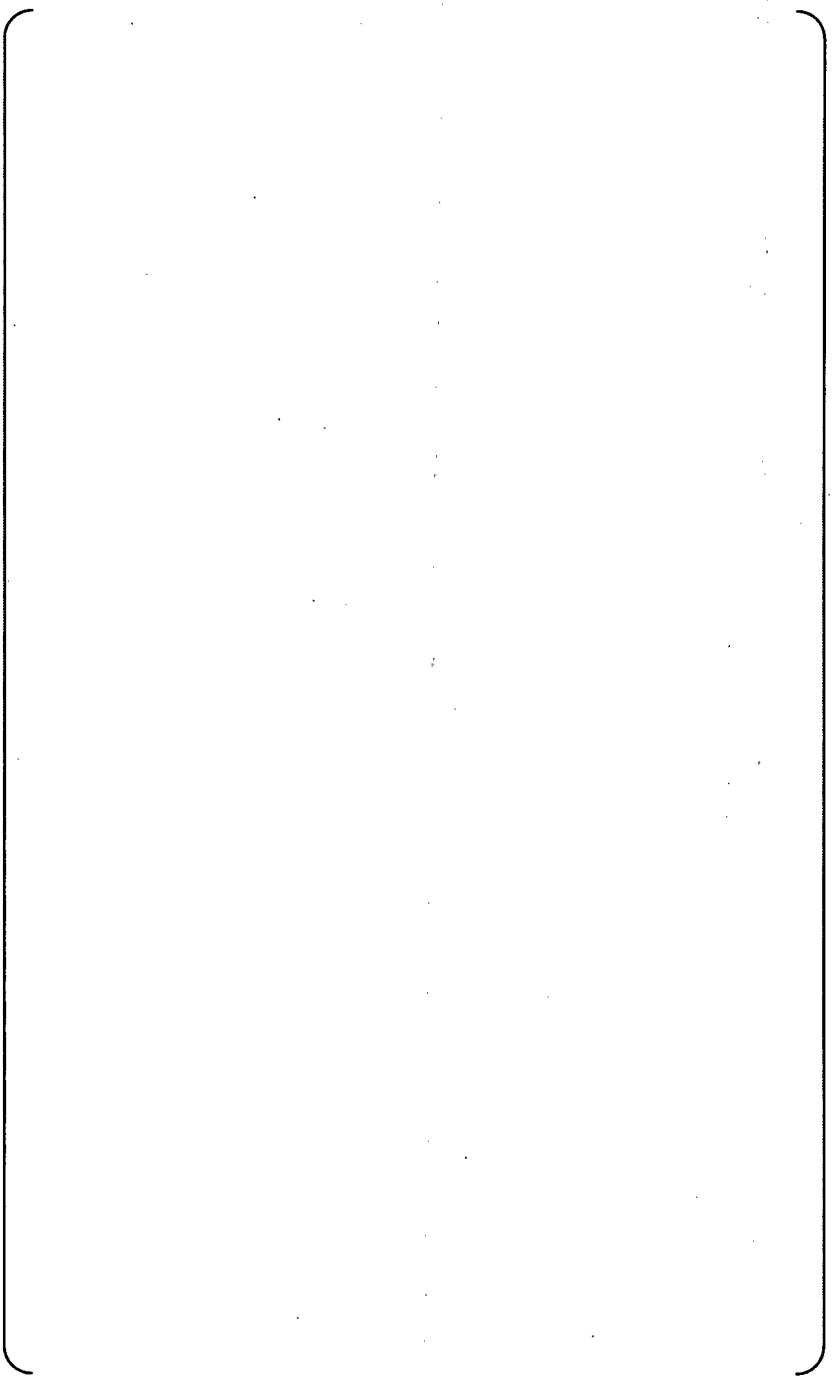

Fig. 5.1-1 Case-C1: Thermal expansion due to tube temperature (ave. wall temp.)

Fig. 5.1-2 Case-C1: Distance between adjacent tubes in Col.78 after thermal elongation

5.2 Case-C2: Tube Deformation from Hydrodynamic Force (no AVB contact)

In the U-bend at operating conditions (without any friction or restraint from the AVBs) the hydrodynamic forces cause the tubes to deform as shown in Figures 5.2-1 and 5.2-2. Figure 5.2-1 shows the overall displacement of the U-bend at operating conditions. The hydrodynamic forces cause the tube columns to spread apart (view i) with the maximum out-of-plane displacement of [ ]Note that this view of the U-bend does not show the hot and cold sides. This will be important when visualizing the behavior of later load cases.

In the in-plane direction (views ii and iii) the bundle displaces (horizontally) toward the hot side because the hot side hydrodynamic forces are larger than the cold side forces. The outermost, central tube, R142C86, displaces downward by[ ]at the apex and at about 45° off vertical on the hot side, where the hydrodynamic force is largest, it displaces upward by [ ] In view ii at this same 45° zone, R142C86 displaces horizontally by[ ]

Figure 5.2-2 displays the change in spacing between adjacent tubes within column 78 in response to the hydrodynamic forces. At the top of the bundle, the tube-to-tube spacing decreases by a maximum of [ ]as the U-tubes are pulled downward. The tube-to-tube spacing on the hot side (45° off the vertical) has a greater increase in tube spacing than occurs on the cold side. The greater hydrodynamic force on the hot side has a greater effect than that of the cold side. The larger radius tubes have the greatest increases in spacing.

This case (C2) has no AVBs in it and helps understand how the fluid forces push the tubes and how the tubes deform at operating conditions. Case C3A is a repeat of this case, but with the effects of the AVBs, retaining bars, retainer bars, and bridges included.

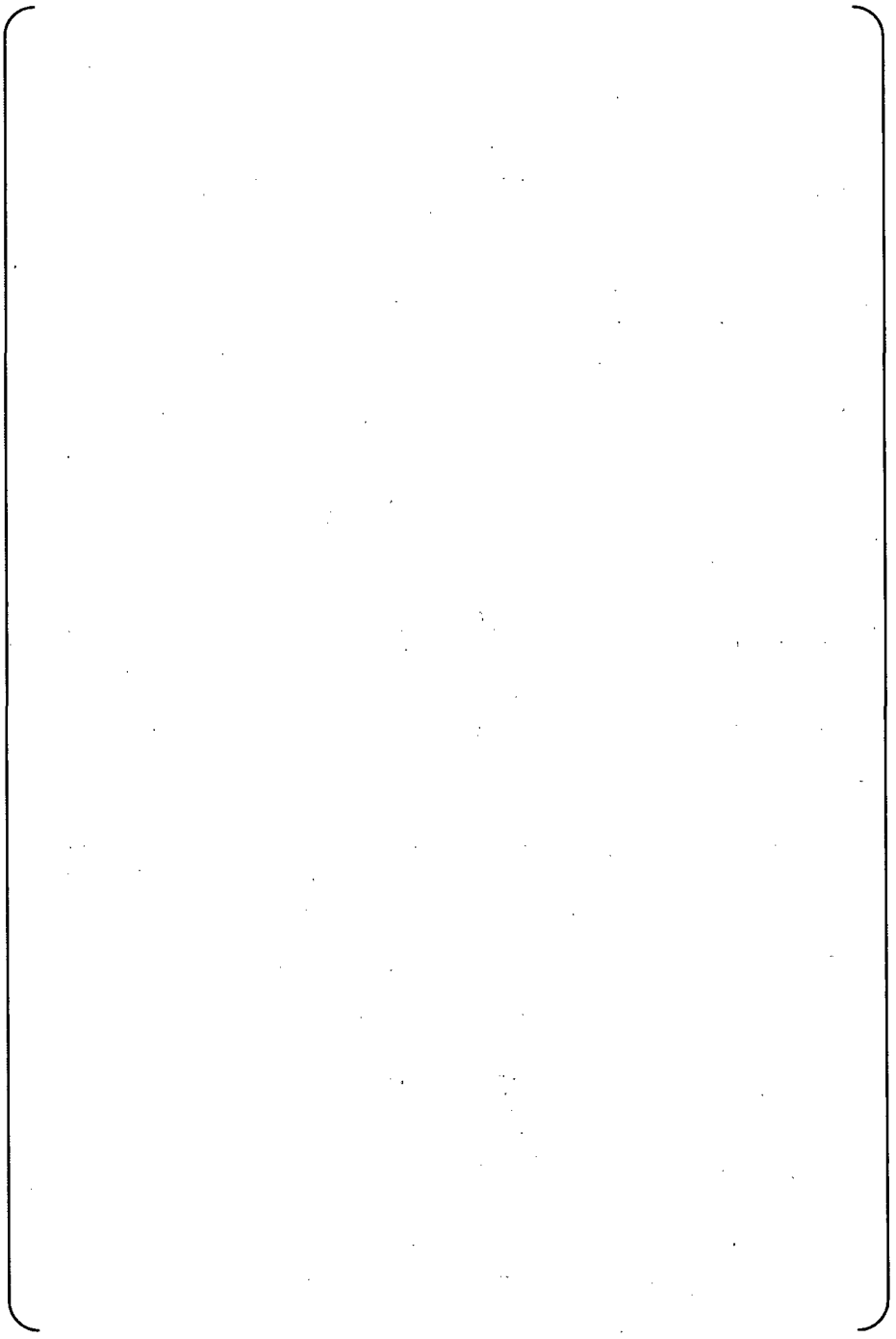

Fig. 5.2-1 Case-C2: Deformation due to dynamic pressure (no AVBs)

Fig. 5.2-2 Case-C2: Distance between adjacent tubes in Col.78 due to dynamic pressure

5.3 Case-C3A: Tube Deformation from Hydrodynamic Force (AVB assembly in)

Figure 5.3-1 (top 3D view) shows a similar overall displacement pattern for Case C3A and Case C2 (i.e. contraction on top and expansion on the hot and cold sides). Figure 5.3-1 (bottom view) shows the "total" tube deformation, which is the combination of the horizontal and vertical displacements. This view was not plotted for Case C2.

Figure 5.3-2 shows how the total deformation relates to the displacement in the vertical direction (top view) and in the horizontal direction (bottom view). The general trend seen in Case C2 where the hydrodynamic forces caused the bundle to displace toward the hot side and for the top of the bundle to move downward is also evident in Case C3A. However, the influence of the AVBs, retaining bars, and retainer bars produces some added effects. Figure 5.3-2 (bottom view) shows that the maximum out-of-plane deformation occurs near Col.10 at the ends of the retaining bars, even though the maximum dynamic pressure is located above Col.30. The maximum out-of-plane deformation is[ ]

Figure 5.3-2 (top view) shows the retaining bar deflection. As the pressure pushes the tubes away from the bundle central plane, they take the AVBs and retainer bars with them – and stretch the retaining bars. This stretching of the retaining bars causes them to flatten out (displace downward) at the top of the bundle (in the center columns). The hot side / cold side hydrodynamic forces also cause the tubes to displace downward (at the top of the bundle). The maximum downward deformation is[ ]

Figure 5.3-3 shows AVB and retaining bar deformation along AVB-B06. The bottom view with 100x magnification shows the downward displacement of the retaining bar at the center columns and shows AVB bending.

Figures 5.3-4 and 5.3-5 show the gap distributions between tubes and AVBs at cross sections along AVBs B06 and B05. The largest gaps are found in the zone bounded by Columns 77 to 81 and Rows 104 to 122. This zone corresponds to the region with the most severe wear in Unit-2 and Unit-3. The largest increase in tube-to-AVB gap in this region is[ ]for Section B6 and[ ]for Section B5. Figure 5.3-6 contains another display of the change in tube-to-AVB gaps within Section B5.

Figure 5.3-7 shows the regions along the AVBs in Column 78 where there is tube contact or a gap. On the side of the AVB in the A-direction (view i) there are gaps on the full population of tubes between Row 80 and Row 112. In the B-direction (view ii) there is intermittent contact. Support by an AVB on a single side of the tube is considered to be an

"active" support. Tubes with no AVB contact on either side are considered to be "inactive" supports. Within the Figure 5.3-7 population there are many tubes with consecutive inactive supports. The largest number of consecutive inactive supports in this figure is six. Such an unsupported tube span would have a low natural frequency and would exhibit unstable vibration characteristics under normal operating conditions.

Figure 5.3-8 shows that the distance between Column 78 tubes increases the most on the hot side where the hydrodynamic force is largest. The increase is greatest between the largest radius tubes. Elastic tube bending produces the reduction in spacing on the cold side.

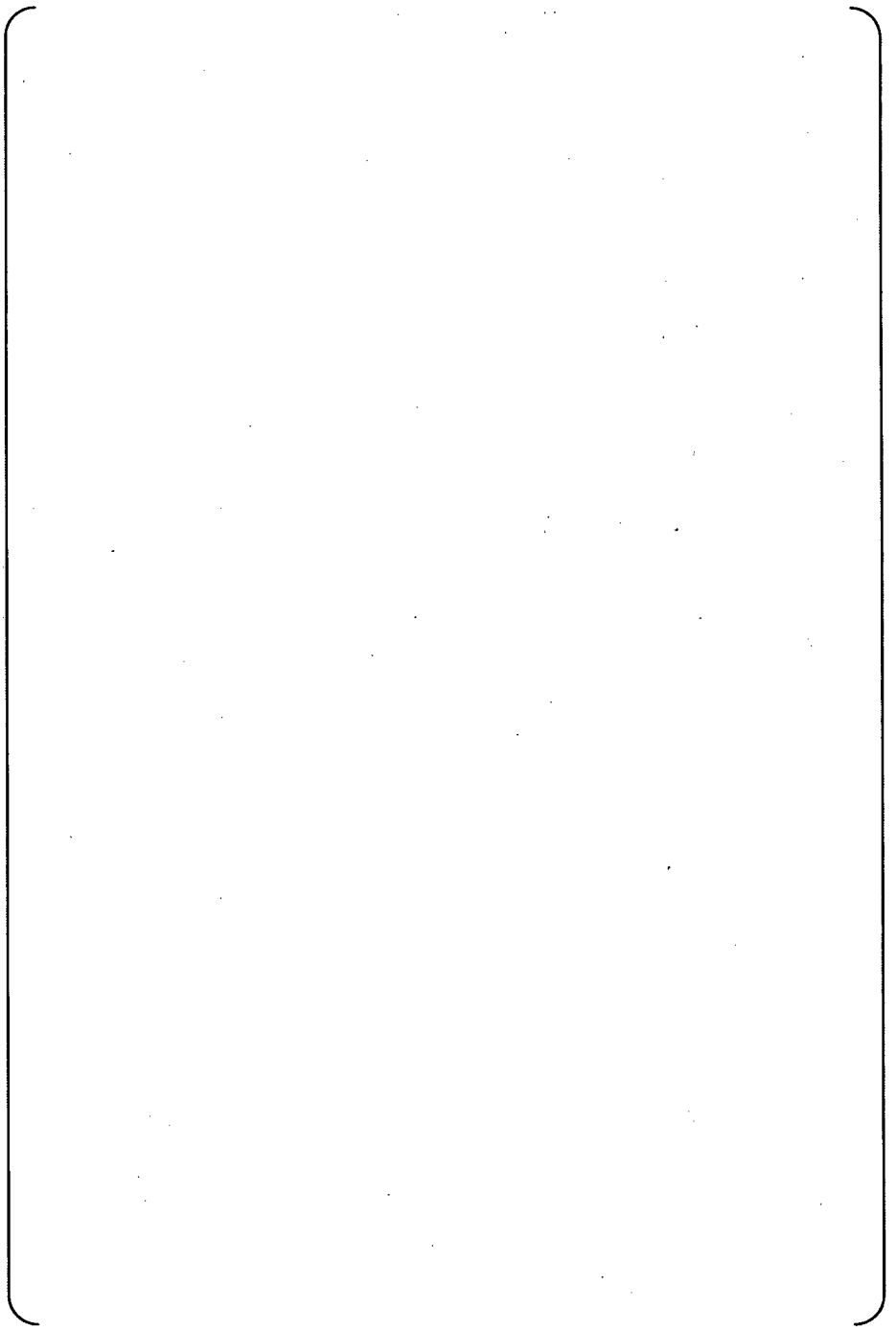

Fig. 5.3-1 Case-C3A: Total deformation due to dynamic pressure (with AVB contact)

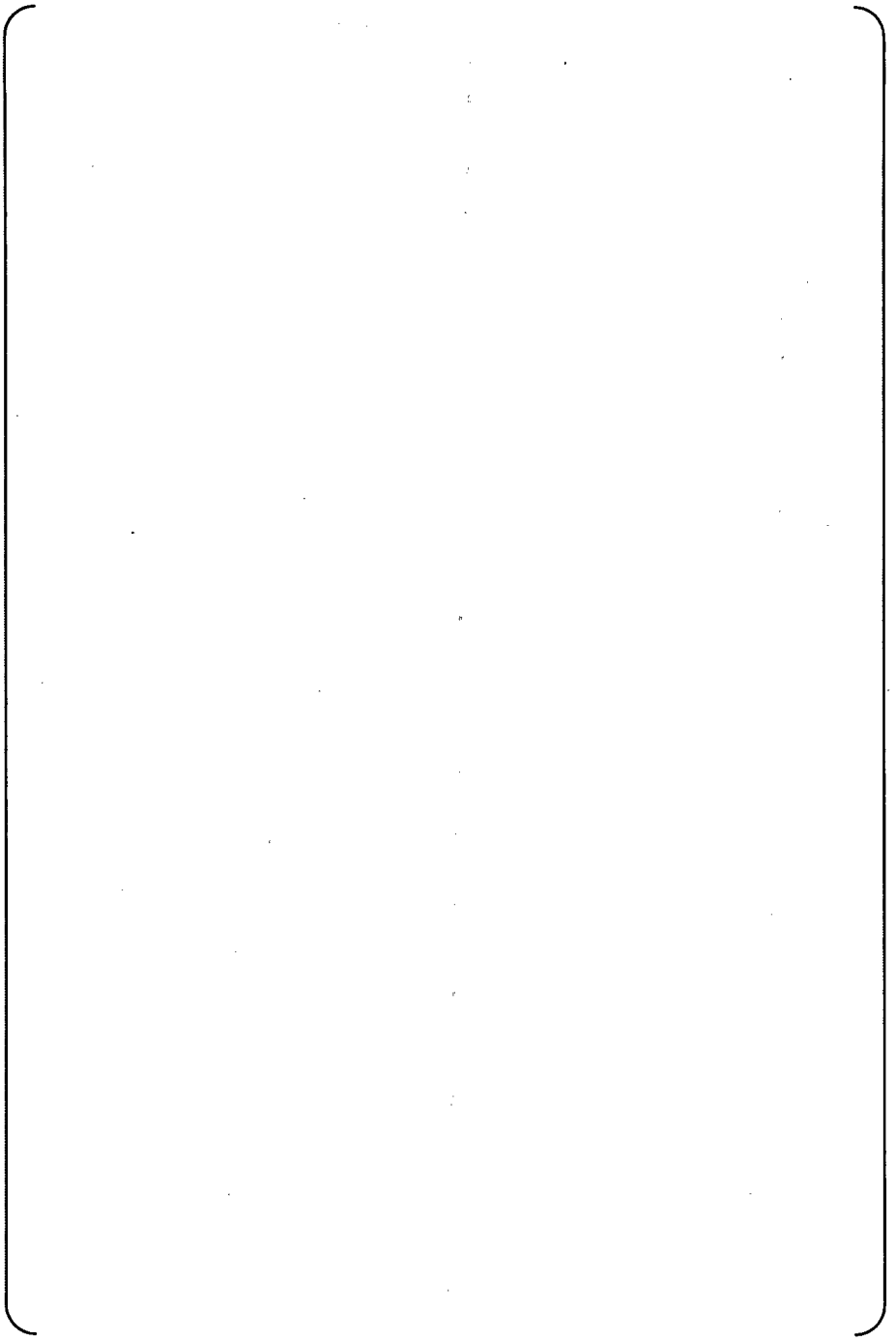

Fig. 5.3-2 Case-C3A: Deformation contour due to dynamic pressure (tubes-AVBs contact)

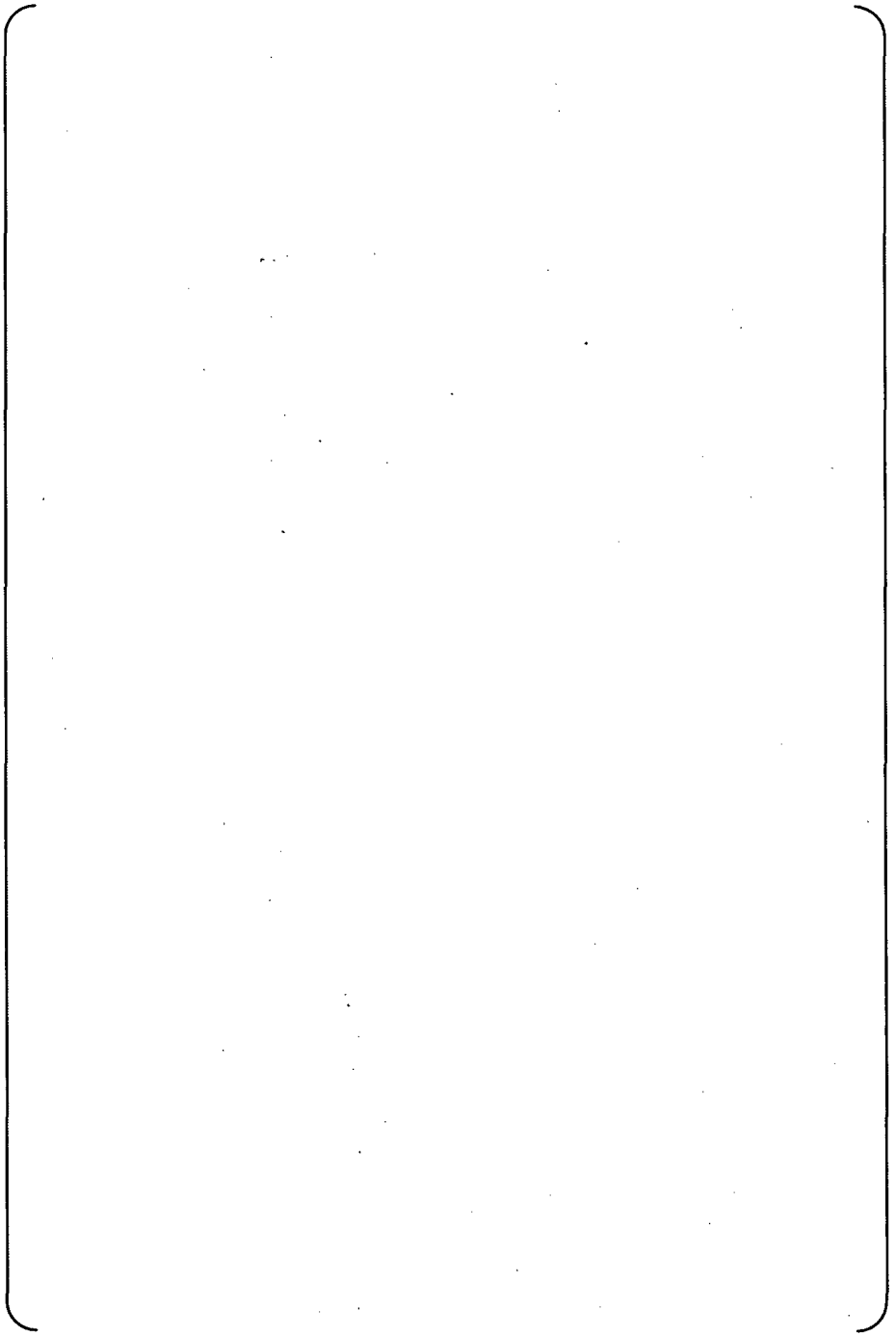

Fig. 5.3-3 Case-C3A: Deformation due to dynamic pressure (tubes-AVBs contact)

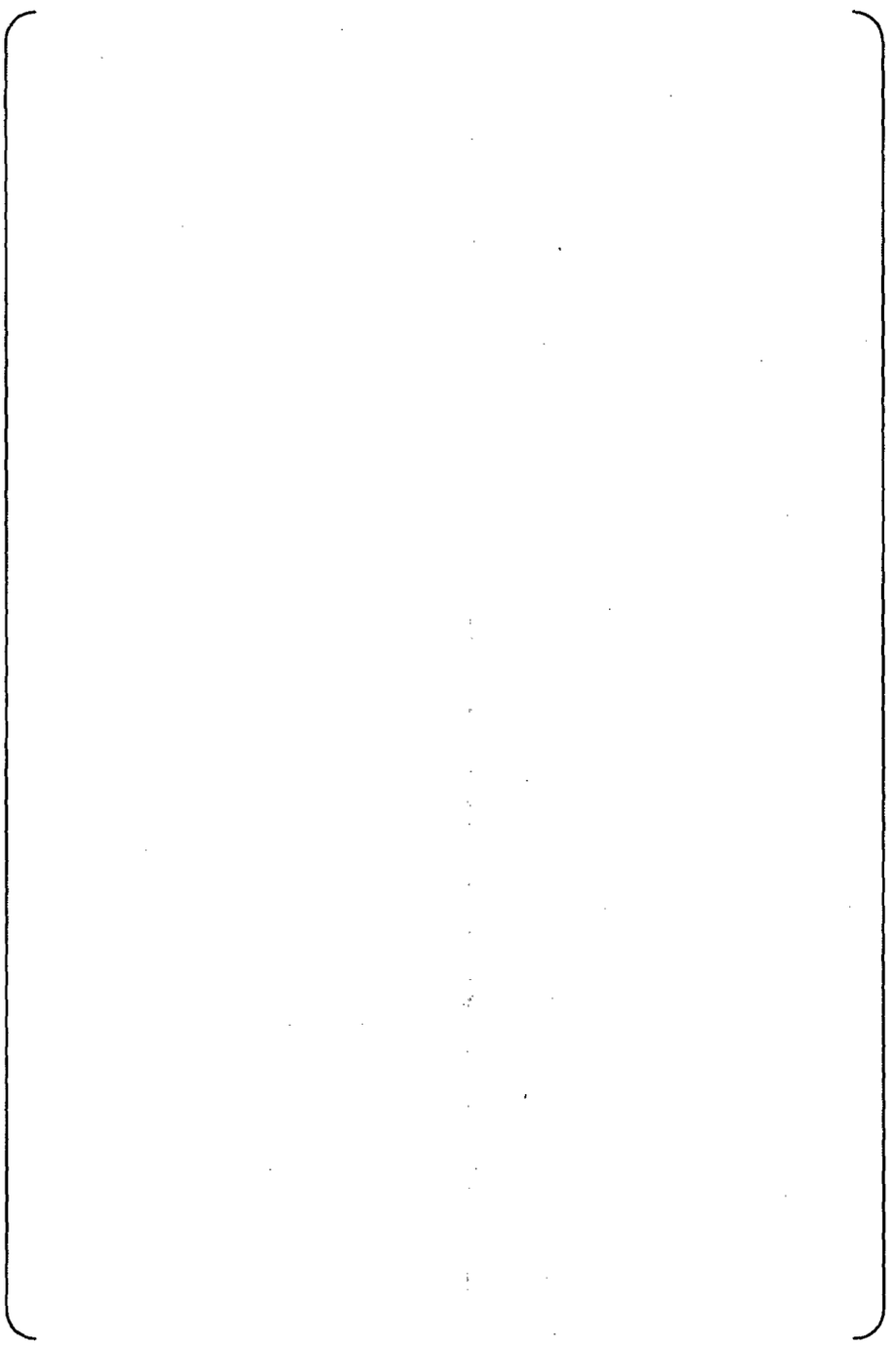

Fig. 5.3-4 Case-C3A: Gap distribution between AVBs and tubes in B6 section

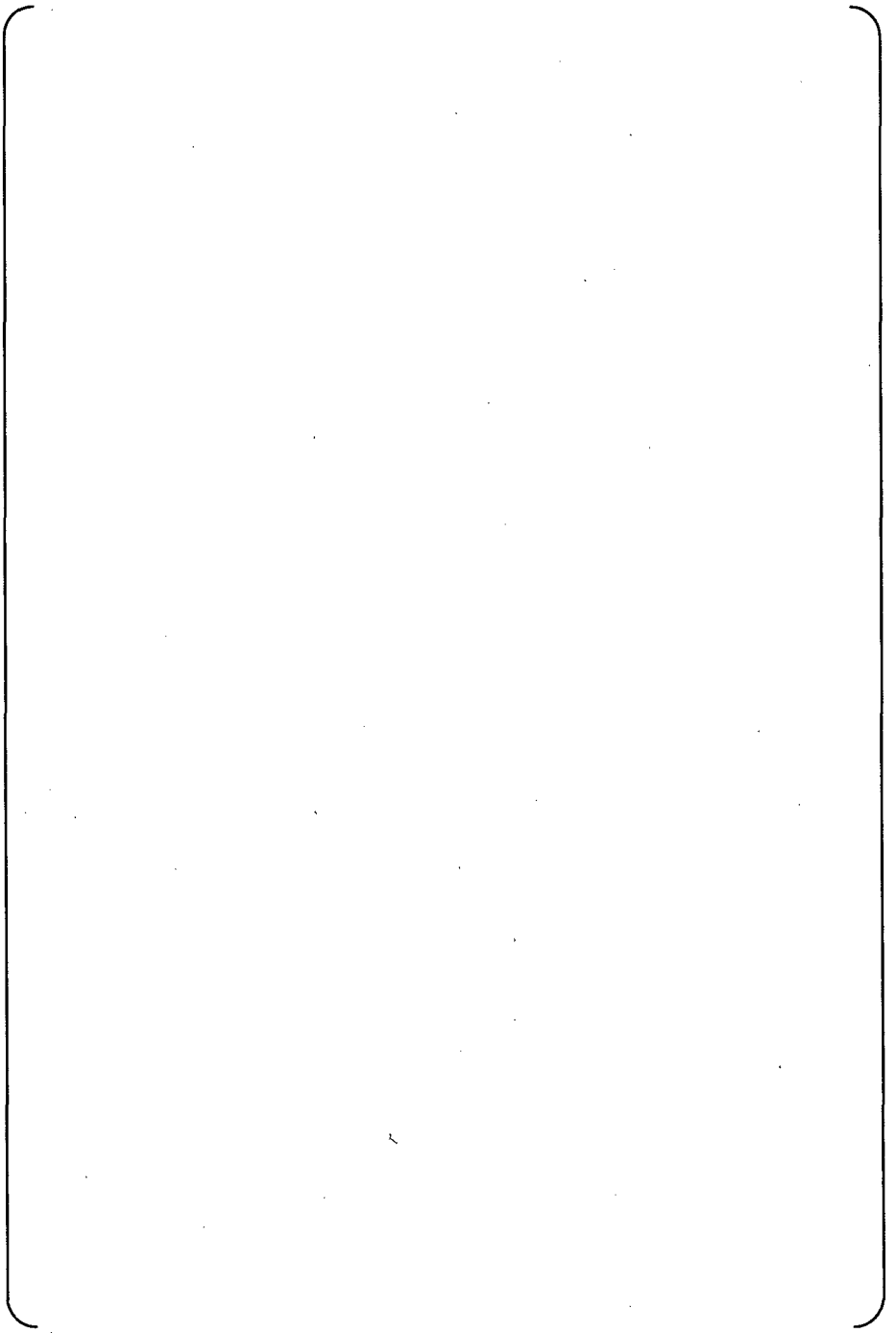

Fig. 5.3-5 Case-C3A: Gap distribution between AVBs and tubes in B5 section

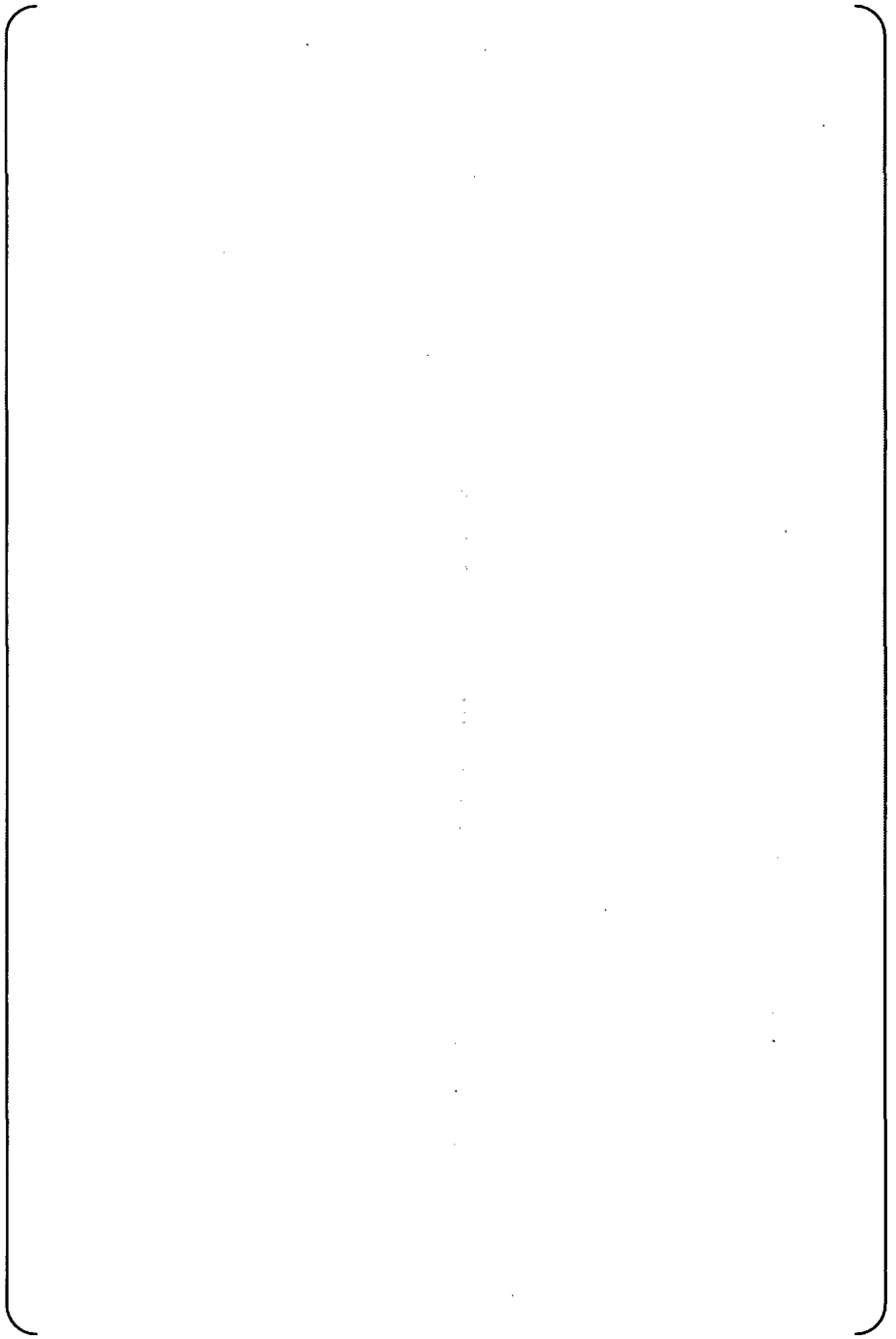

Fig. 5.3-6 Case-C3A: Gaps between AVBs and tubes in each Column in B5 section

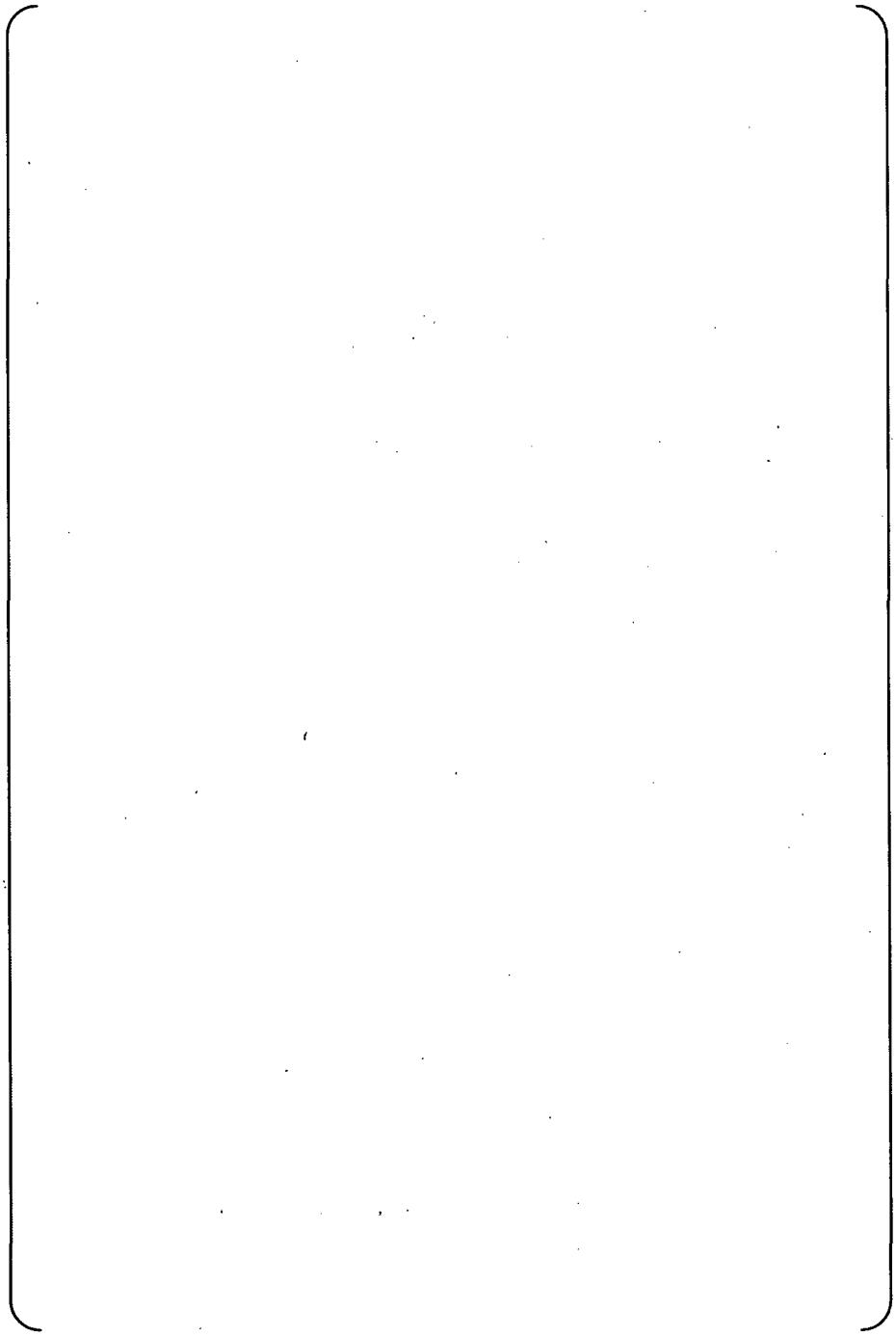

Fig. 5.3-7 Case-C3A: Gaps of tubes in Col.78 to adjacent AVBs

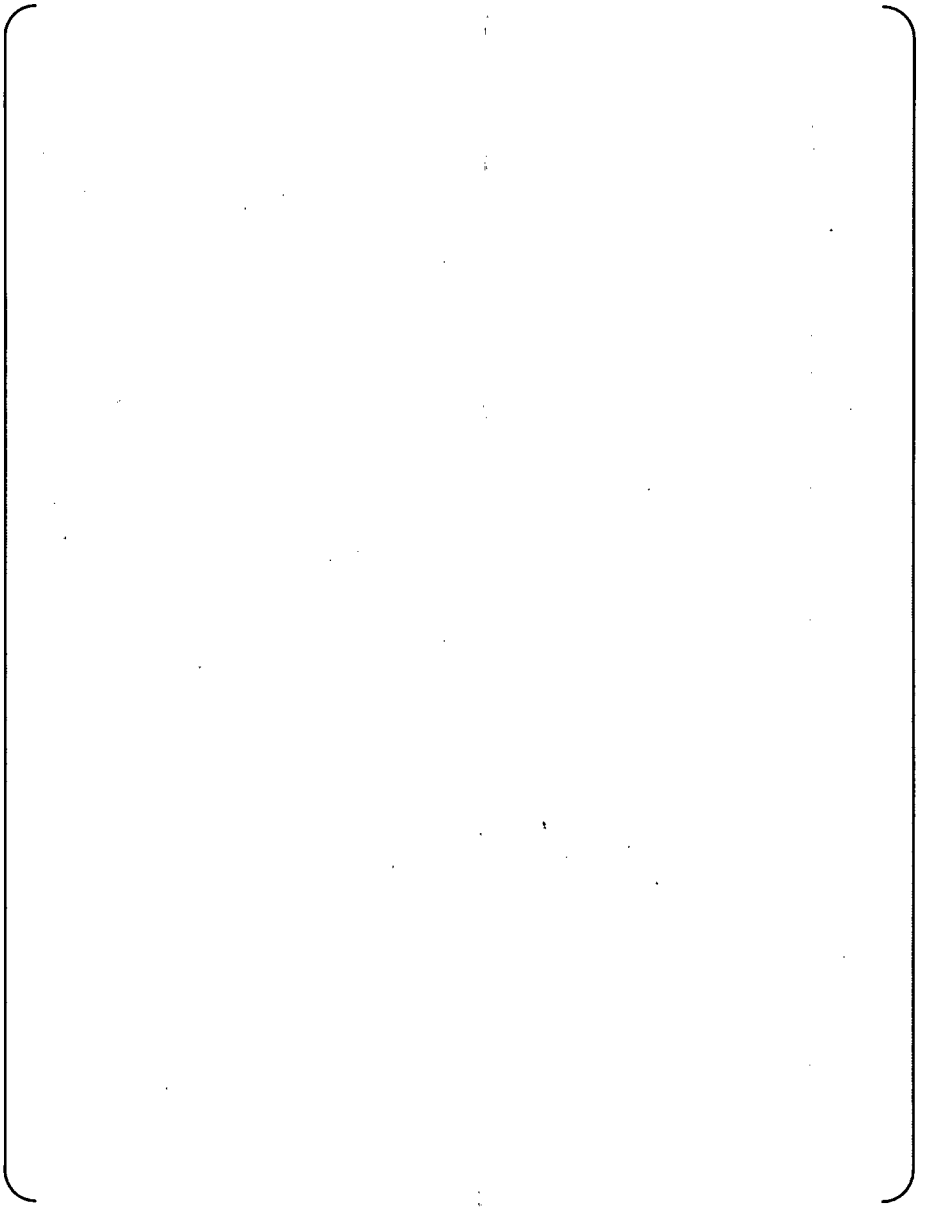

Fig. 5.3-8 Case-C3A: Gap between adjacent tubes in Col.78 under dynamic pressure

5.4 Case-C3B: Tube deformation – Out-of-Plane Hydrodynamic Force Alone

Case-C3B considers only the hydrodynamic pressure effects in the tube out-of-plane direction. Figure 5.4-1 shows a comparison of the horizontal tube displacement from Cases C3A and C3B. The Case C3B out-of-plane maximum displacement is [ ] [ ] and for Case C3A the result is [ ] This indicates that the out-of-plane hydrodynamic pressure without the vertical, in-plane component produces a larger out-of-plane displacement.

Figure 5.4-2 compares the vertical displacements for these two cases. The maximum downward deflection at the top of the tube bundle for Case C3B is [ ] and for Case C3A it is [ ] So, the out-of-plane load case has less downward displacement at the top of the bundle.

Figures 5.4-3 and 5.4-4 display the gap distributions between tubes and AVBs in cross sections along AVBs B06 and B05. These results are quite similar for both the C3A and C3B cases.

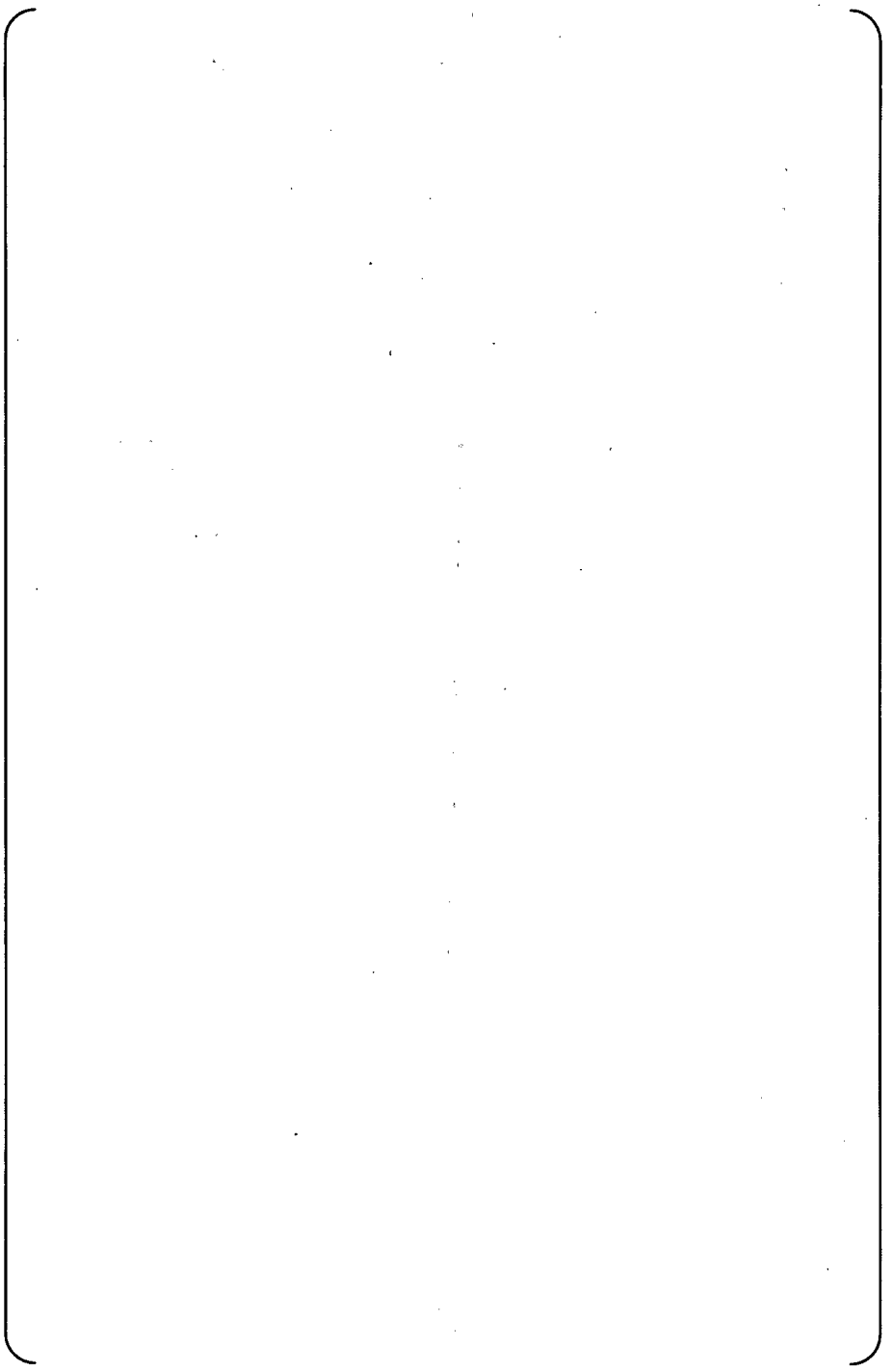

Fig. 5.4-1 Case-C3B: Deformation out of plane contour

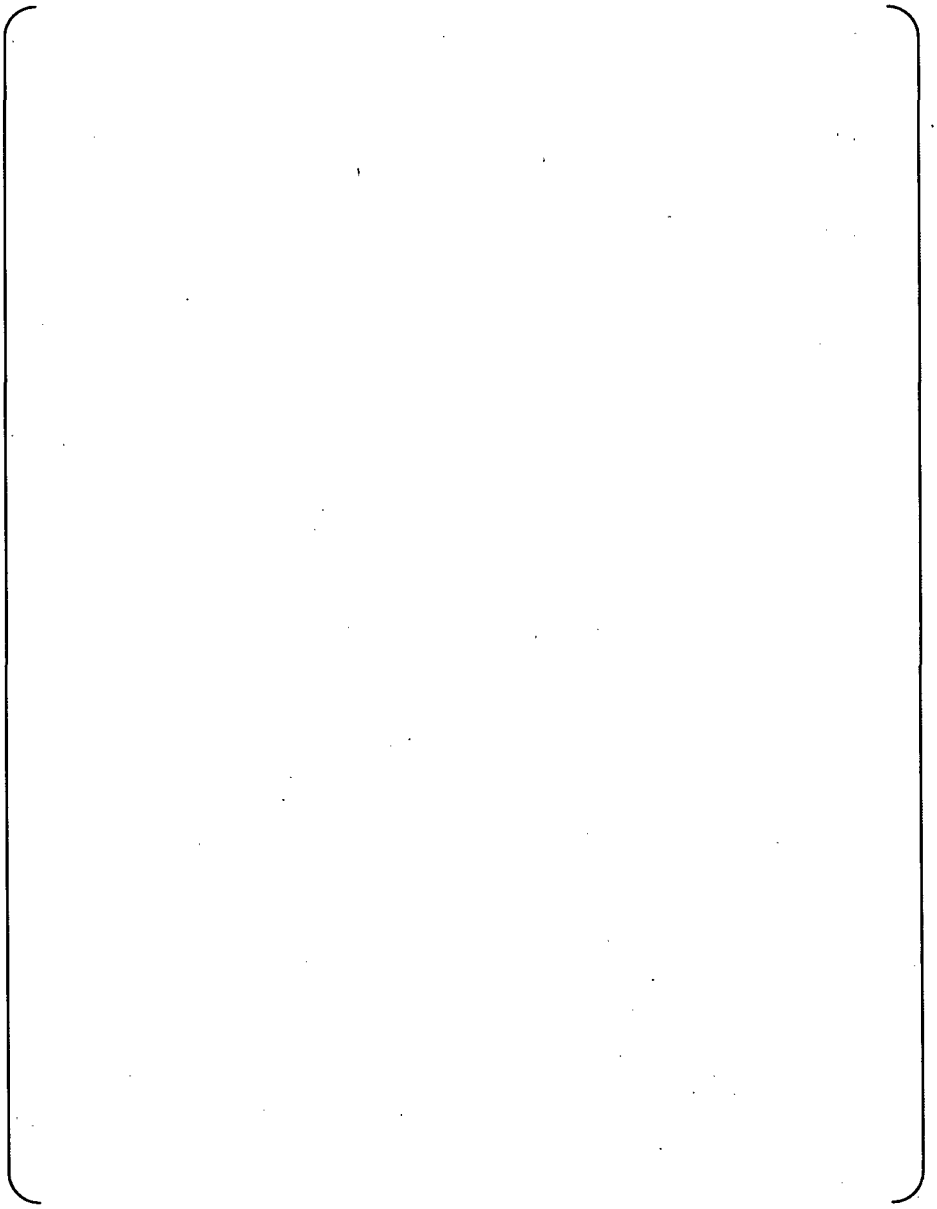

Fig. 5.4-2 Case-C3B: Vertical deformation contour

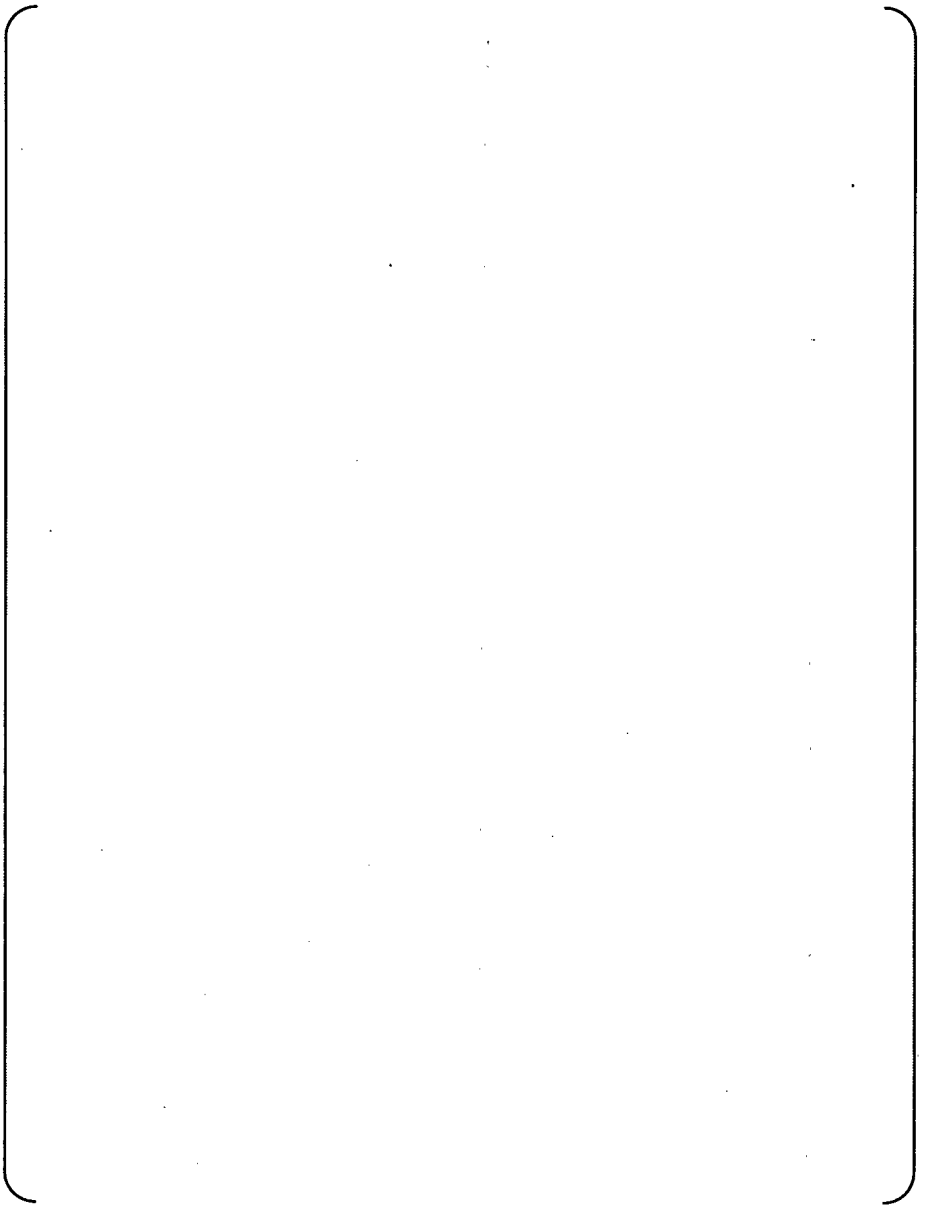

Fig. 5.4-3 Case-C3B: Gap distribution between AVBs and tubes in B6 section

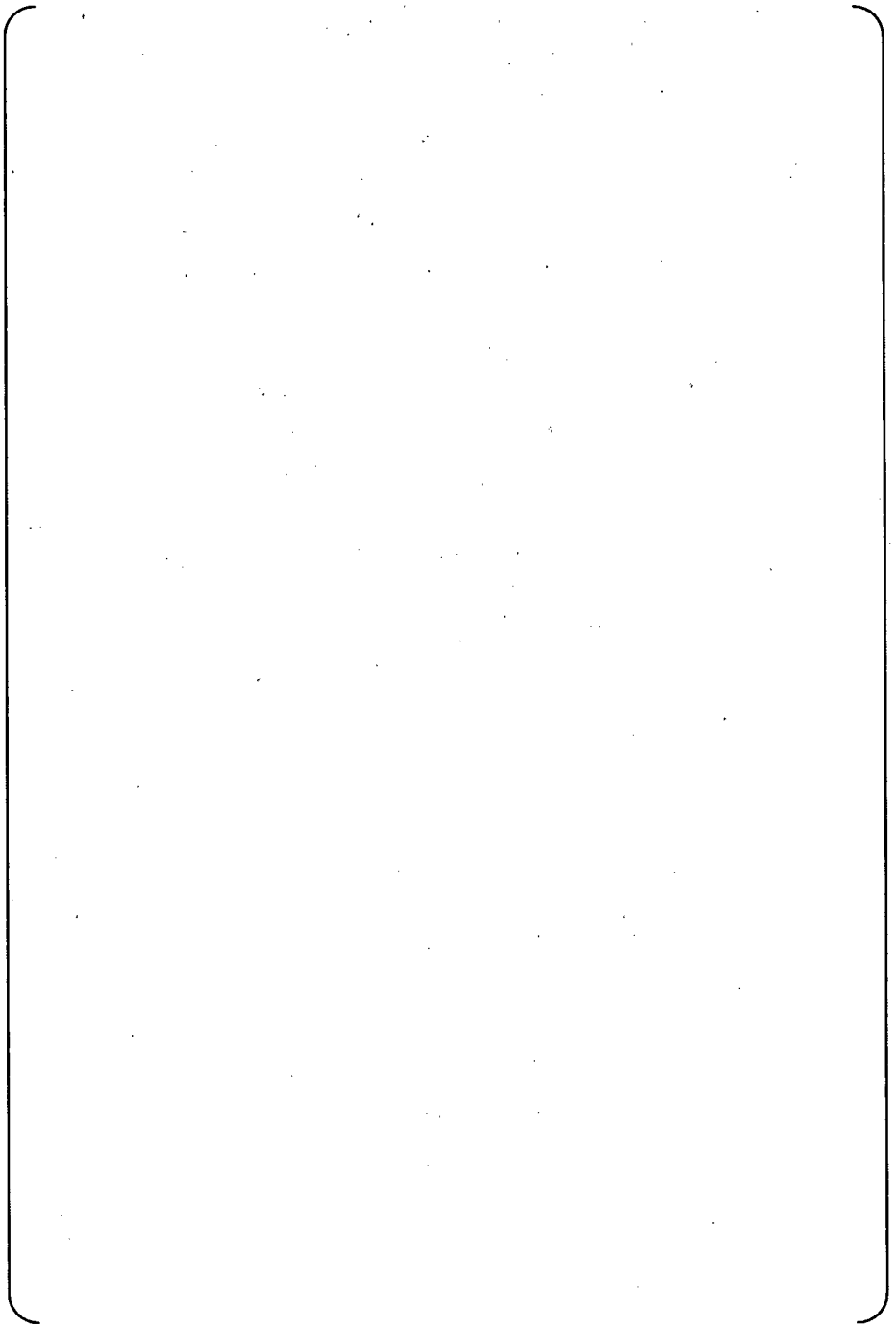

Fig. 5.4-4 Case-C3B: Gap distribution between AVBs and tubes in B5 section

5.5 Case-C3C: Tube deformation with Stiffer Retaining Bars

Case C3C is the same as case C3A, except that it has stiffer retainer bars. The retaining bar stiffness used in case C3C is 16 times larger than that of the actual bar. The factor of 16 results from doubling the retaining bar diameter based on the moment of inertia expressed by $\pi/64 \times d^4$.

Figures 5.5-1 and 5.5-2 show a comparison of the out-of-plane displacement and the vertical displacement for cases C3A and C3C. Stiffening the retainer bar by a factor of 16x produces a 15% reduction in deflection, which is small.

Figure 5.5-3 shows that the retaining bar and AVB deflection shapes are nearly the same. This further demonstrated in Figures 5.5-4 and 5.5-5 show the tube-to-AVB gap distributions at Sections B6 and B5 for cases C3A and C3C. All four cases have a maximum gap change of [ ](when rounded off to the nearest mil). If the analytical results are used with their reported number of digits, it might be concluded that there is a 20% reduction in gaps due to the stiffening of the retaining bars.

It is concluded that increasing the retaining bar stiffness is not an effective way to reduce the tube-to-AVB gaps.

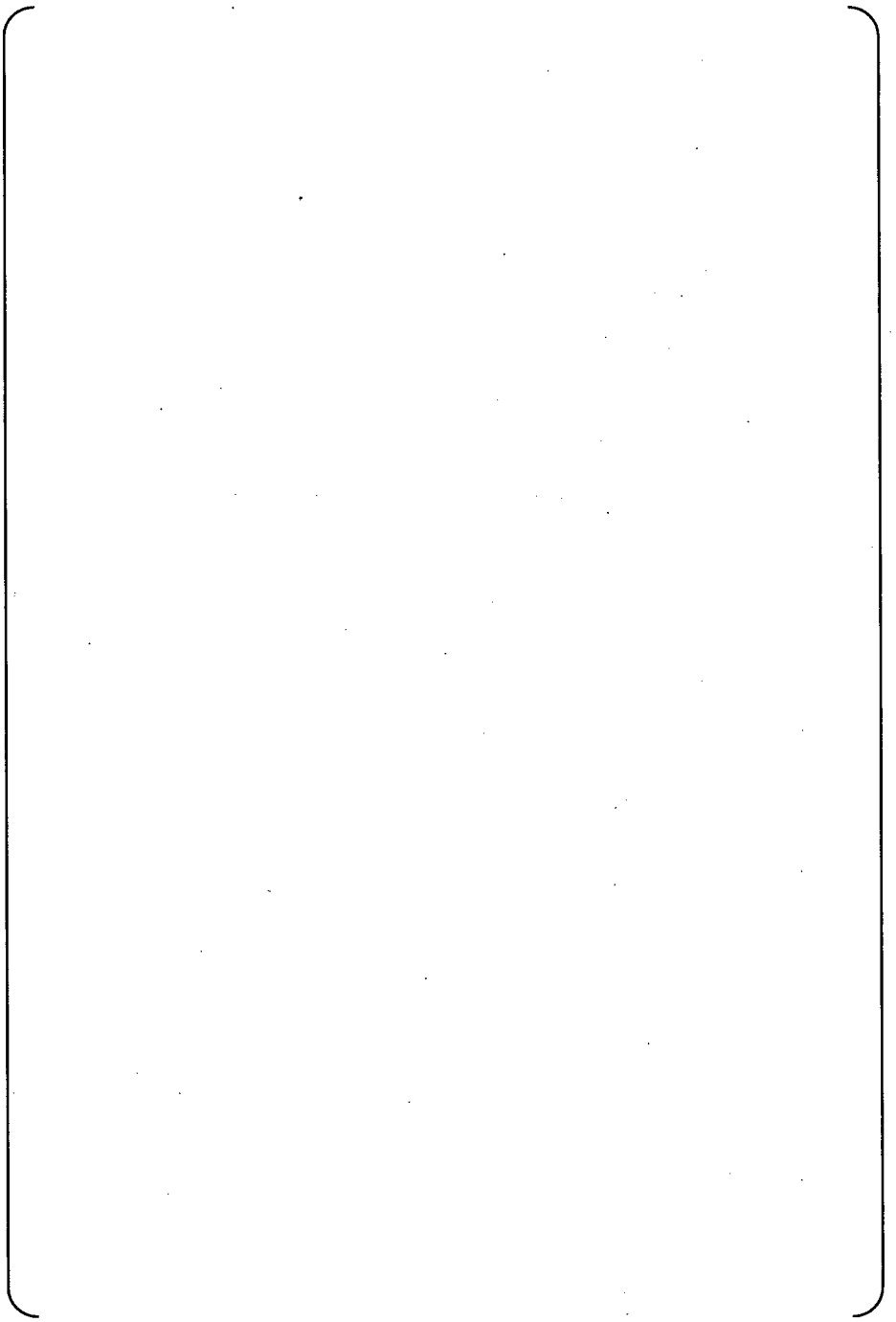

Fig. 5.5-1 Case-C3C: Out-of-Plane Deformation based on Retainer Bar Stiffness

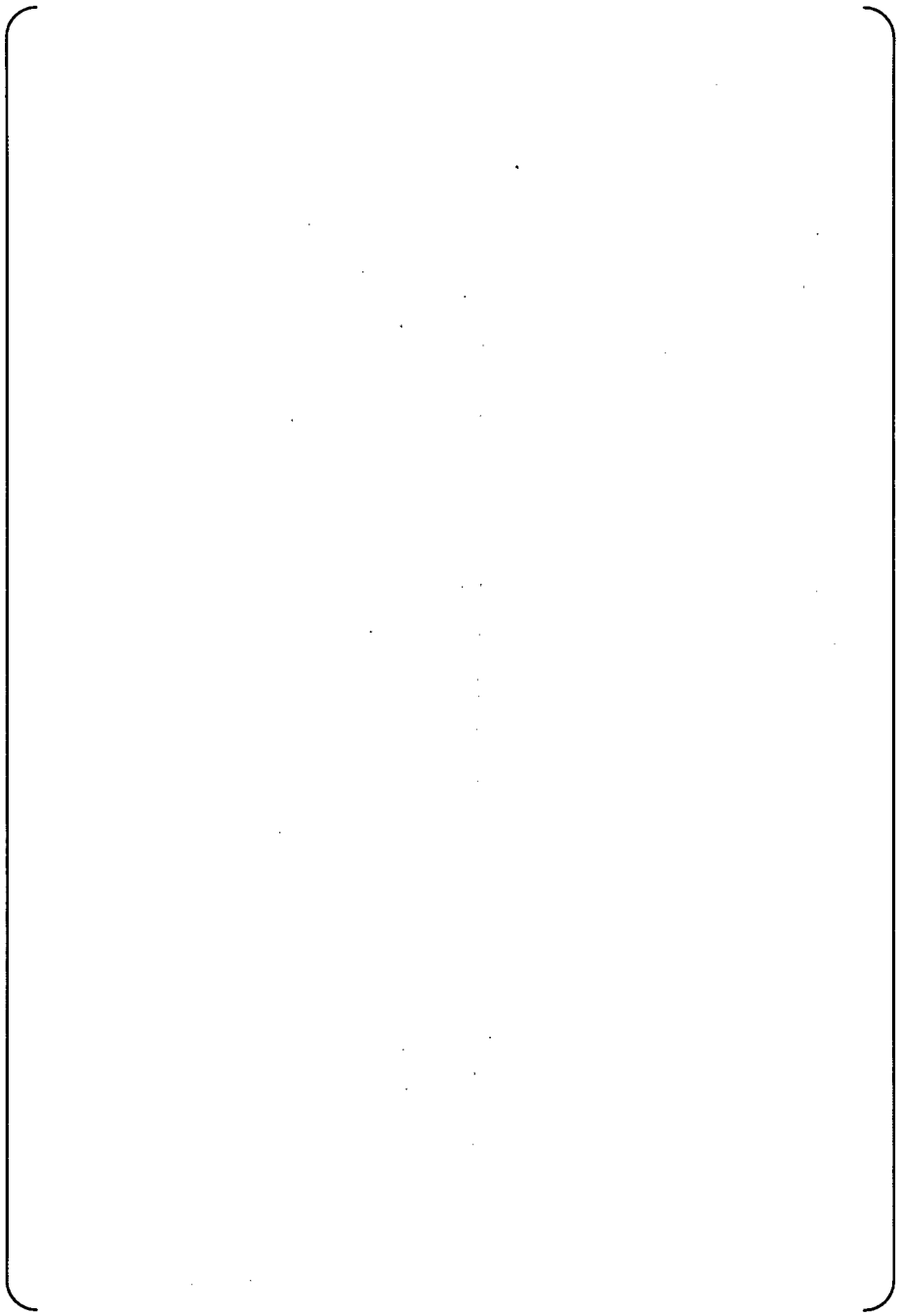

Fig. 5.5-2 Case-C3C: Vertical Displacement based on Retainer Bar Stiffness

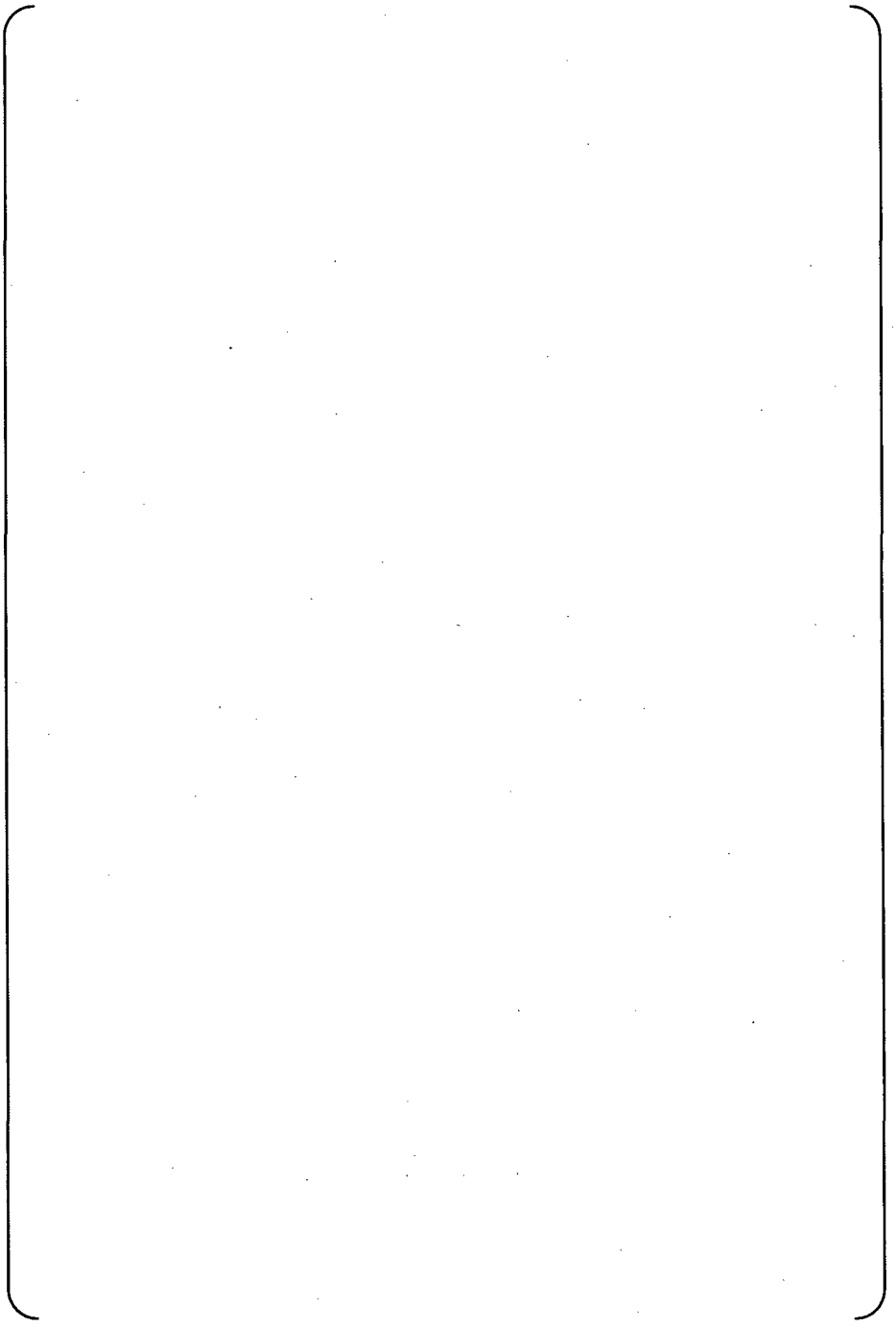

Fig. 5.5-3 Case-C3C: Deformation mode due to dynamic pressure

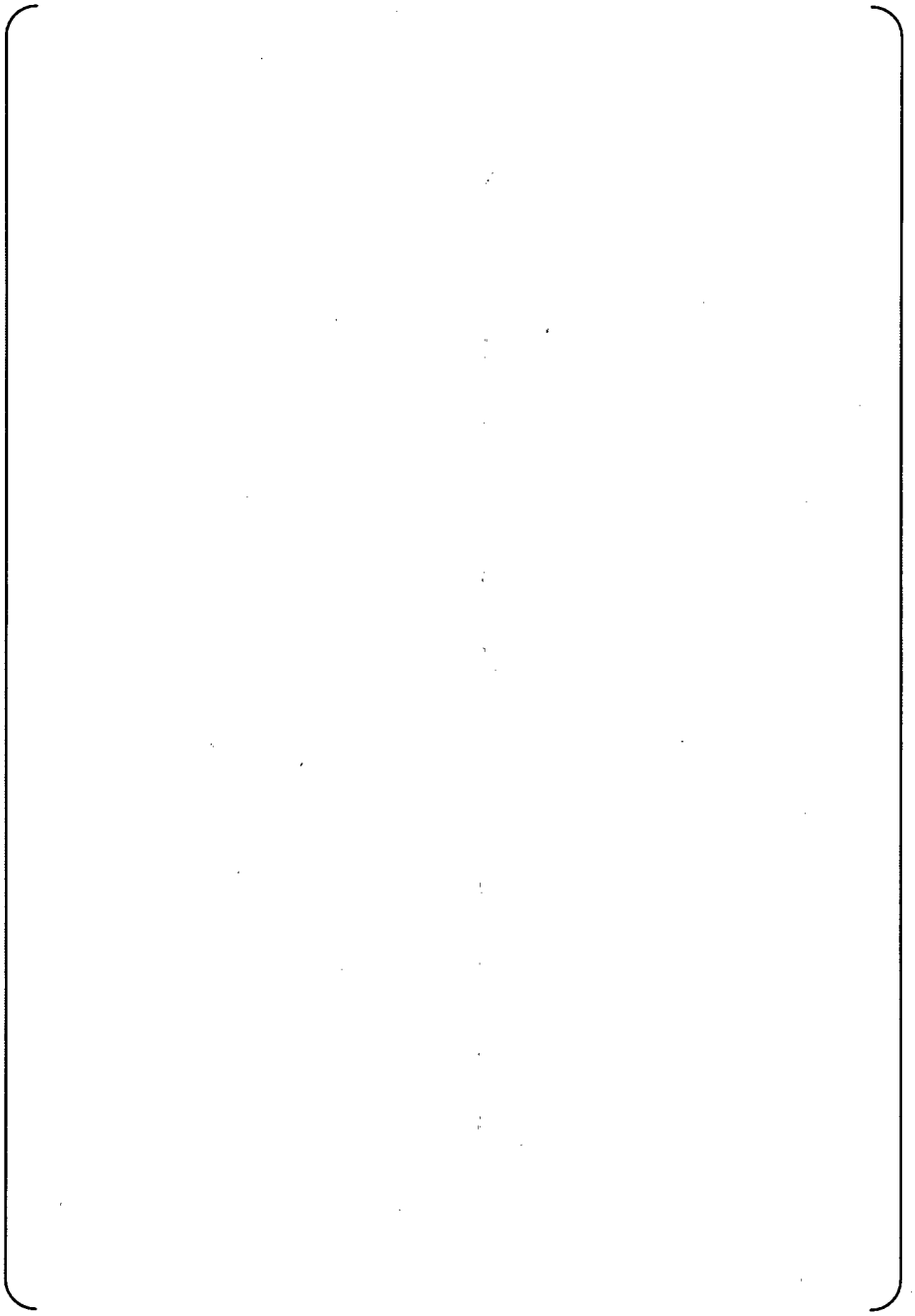

Fig. 5.5-4 Case-C3C: Gap distribution between AVBs and tubes in Section B6

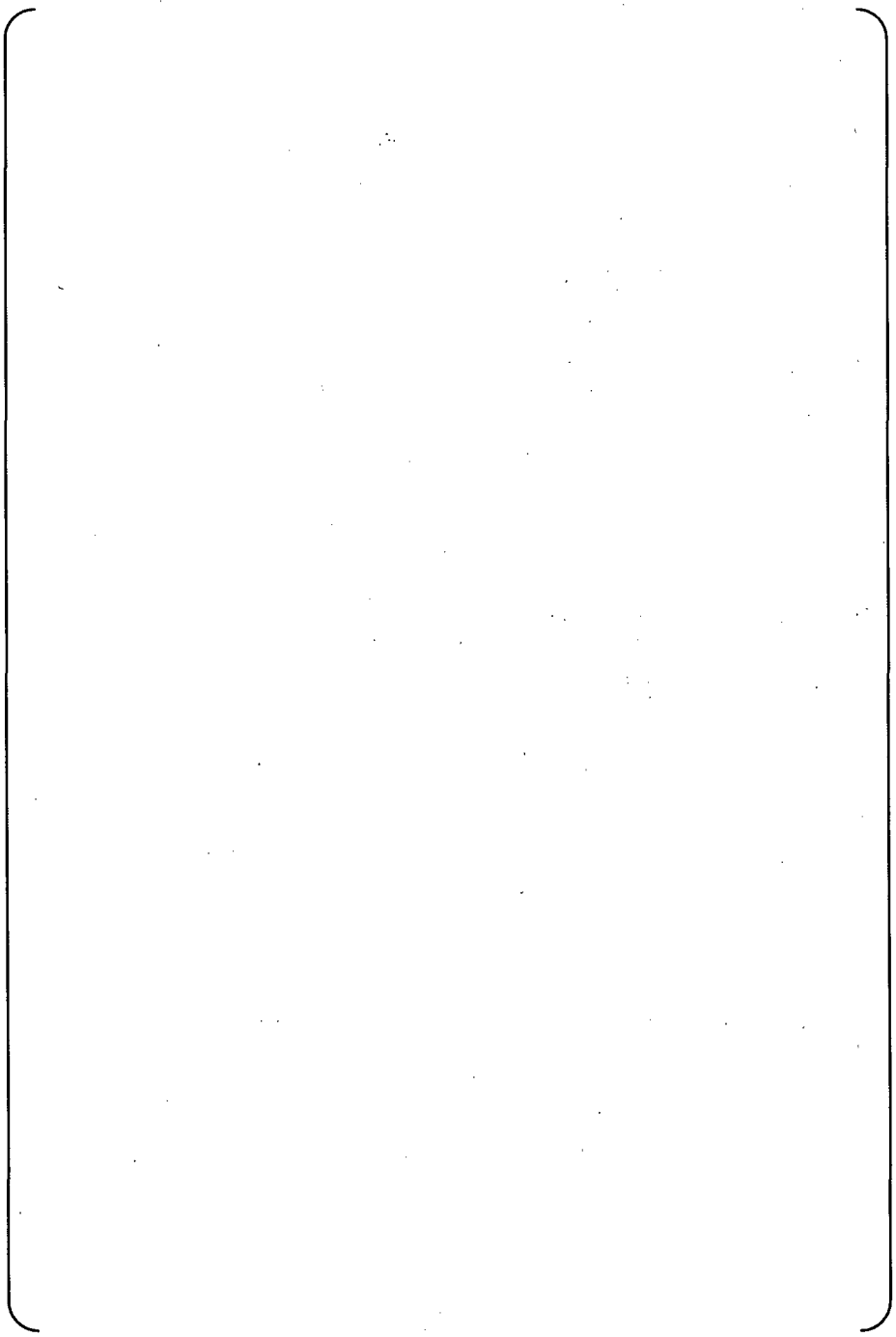

Fig. 5.5-5 Case-C3C: Gap distribution between AVBs and tubes in Section B5

5.6 Case-C3A': Tube Deformation from the latest Hydrodynamic Force (AVB assembly in)

Figure 5.6-1 shows the "total" tube deformation, which is the combination of the horizontal and vertical displacements. Horizontal deformation is dominant to total. The large hydrodynamic force in HOT side makes this horizontal displacement.

Figure 5.6-2 shows how the total deformation relates to the displacement in the vertical direction (top view) and in the horizontal direction (bottom view). The general trend is almost same as Case C3A. The hot side / cold side hydrodynamic forces also cause the tubes to displace downward (at the top of the bundle). The maximum downward deformation is [ ]

Figure 5.6-3 shows AVB and retaining bar deformation along AVB-B06. The deformation trend is same as Case C3A.

Figures 5.6-4 and 5.6-5 show the gap distributions between tubes and AVBs at cross sections along AVBs B06 and B05. The largest gaps are found in the center column and high row zone. This zone corresponds to the region with the most severe wear in Unit-2 and Unit-3. The largest increase in tube-to-AVB gap in this region is [ ] for Section B6 and B5.

Figure 5.6-6 shows the regions along the AVBs in Column 78 where there is tube contact or a gap. In Case C3A', there are many tubes with consecutive inactive supports as same as Case C3A. Such an unsupported tube span would have a low natural frequency and would exhibit unstable vibration characteristics under normal operating conditions.

Figure 5.6-7 shows the distribution of contact forces between tubes and AVBs. This contour just express compression magnitude, however contact forces can be obtained by multiplying by compression spring stiffness[.] In the center column and high Row area, where severe wear occurred, the contact forces are around [ ]This small force hardly supports and fixes a tube.

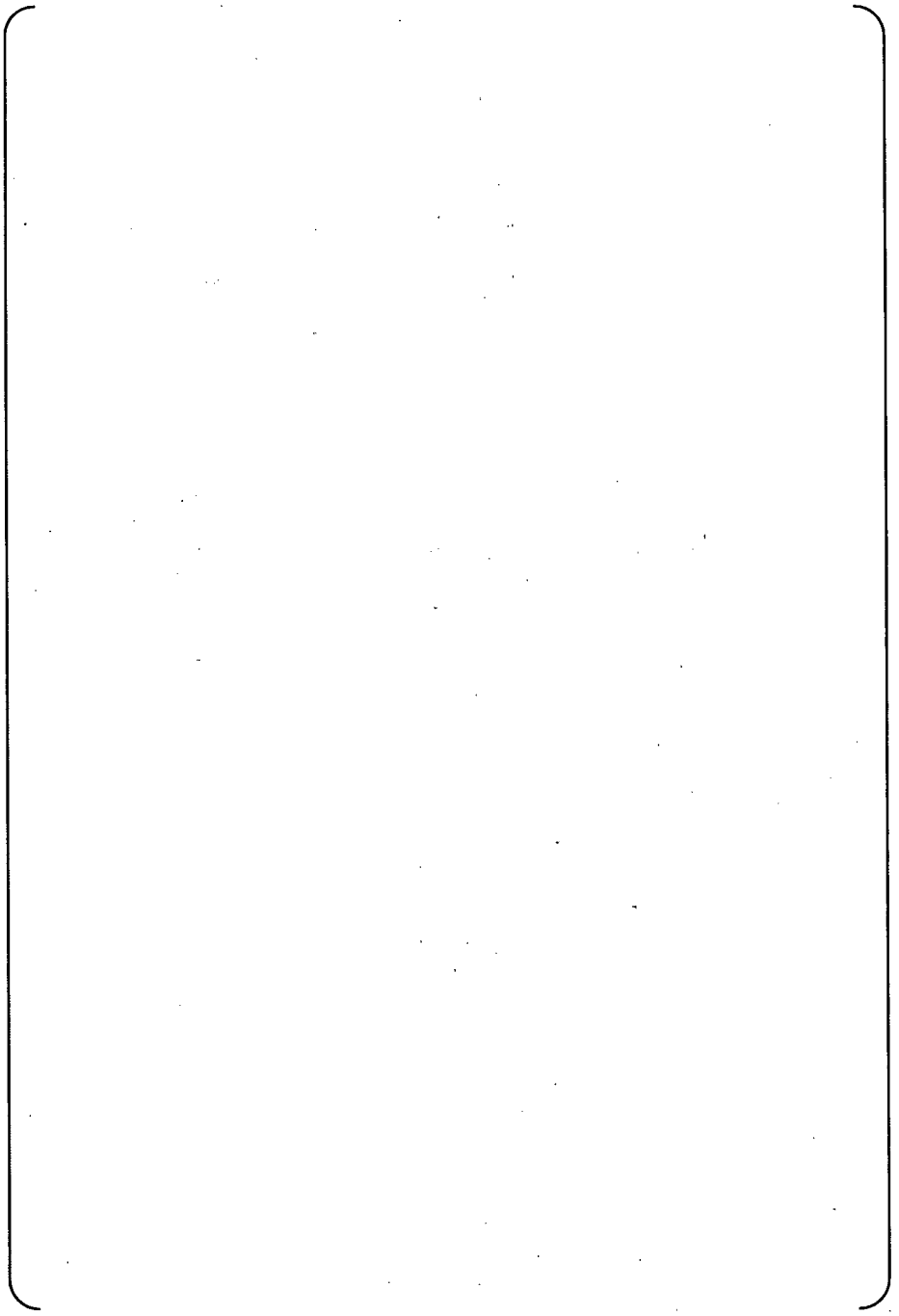

Fig. 5.6-1 Case-C3A': Total deformation due to dynamic pressure (with AVB contact)

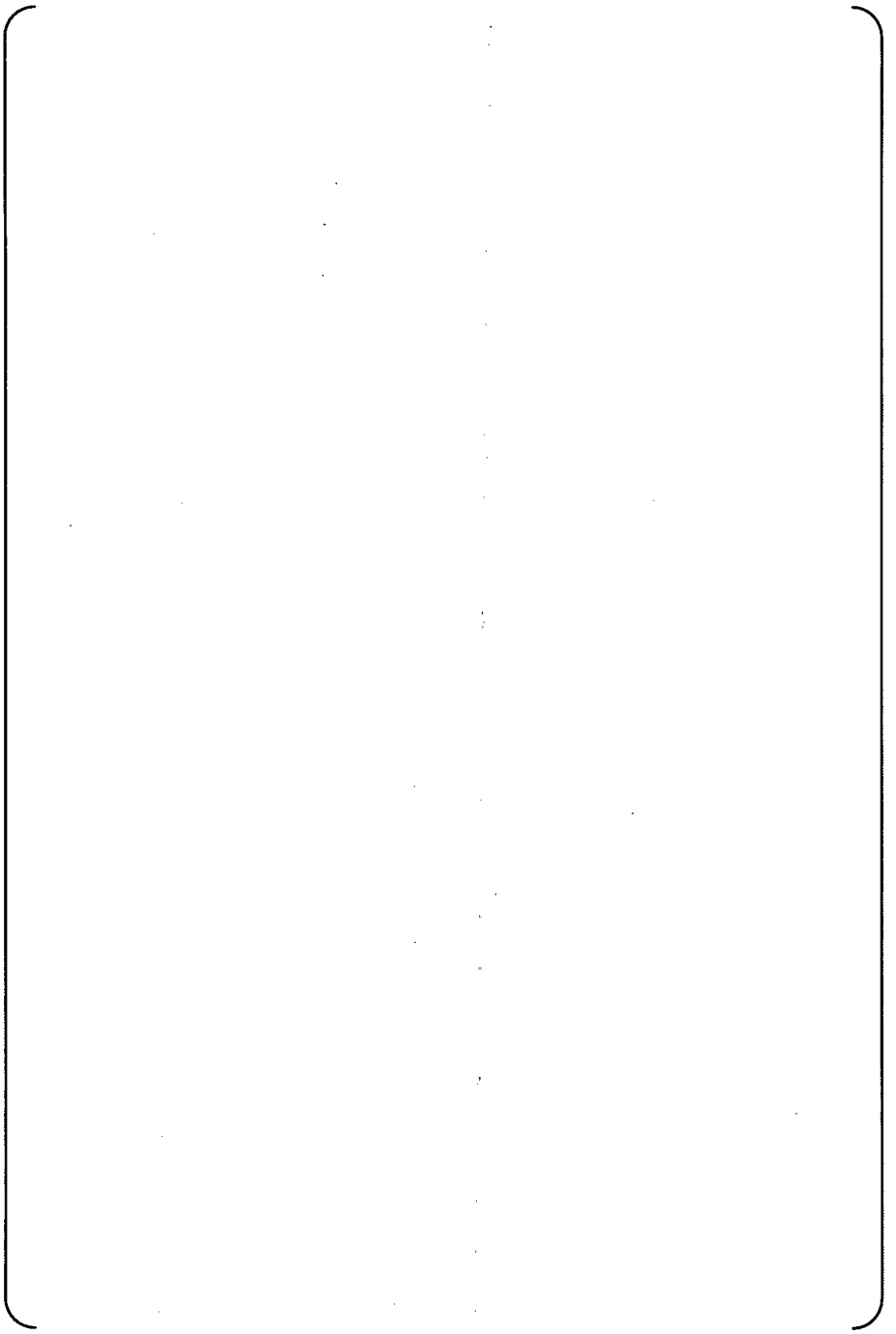

Fig. 5.6-2 Case-C3A': Deformation contour due to dynamic pressure (tubes-AVBs contact)

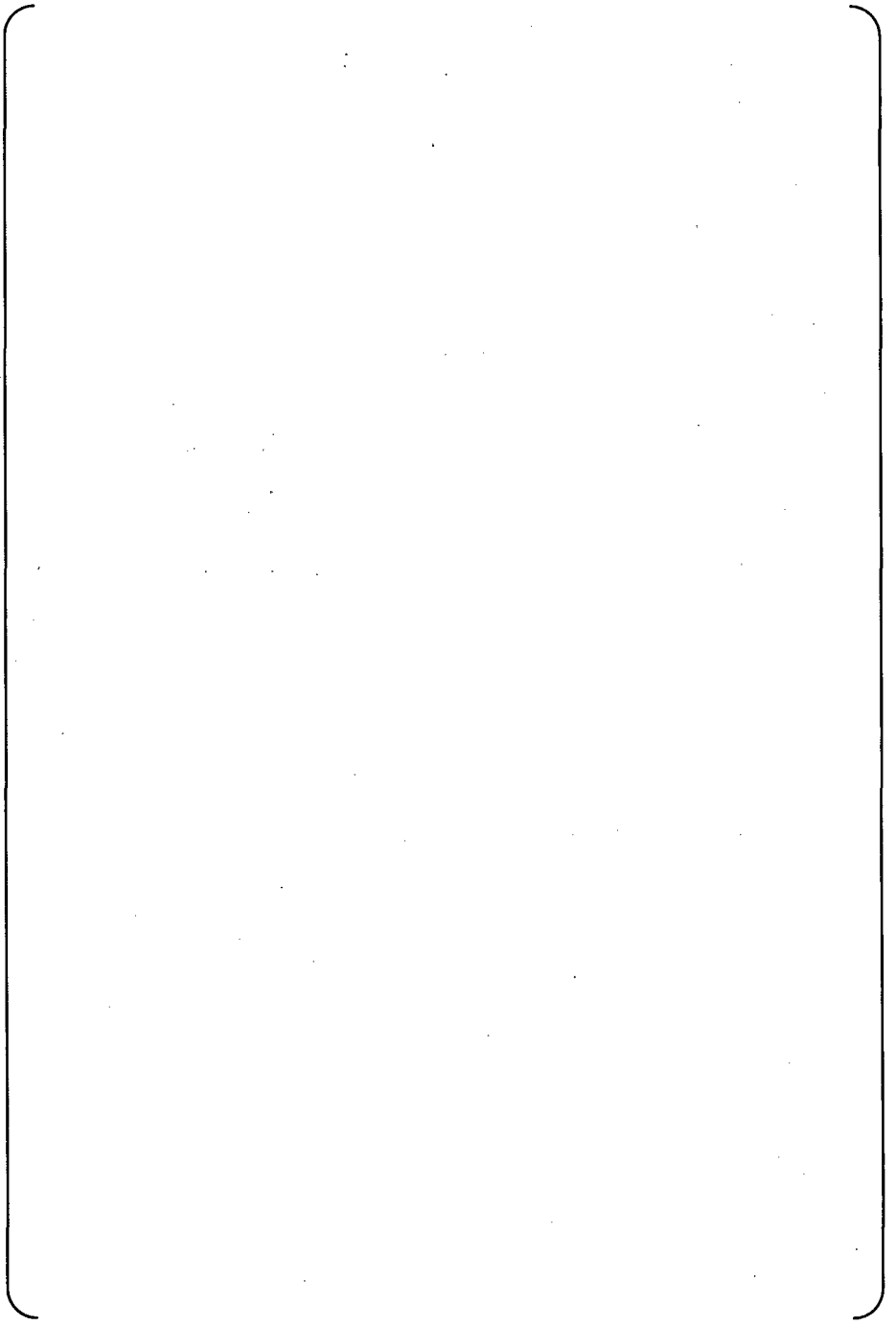

Fig. 5.6-3 Case-C3A': Deformation due to dynamic pressure (tubes-AVBs contact)

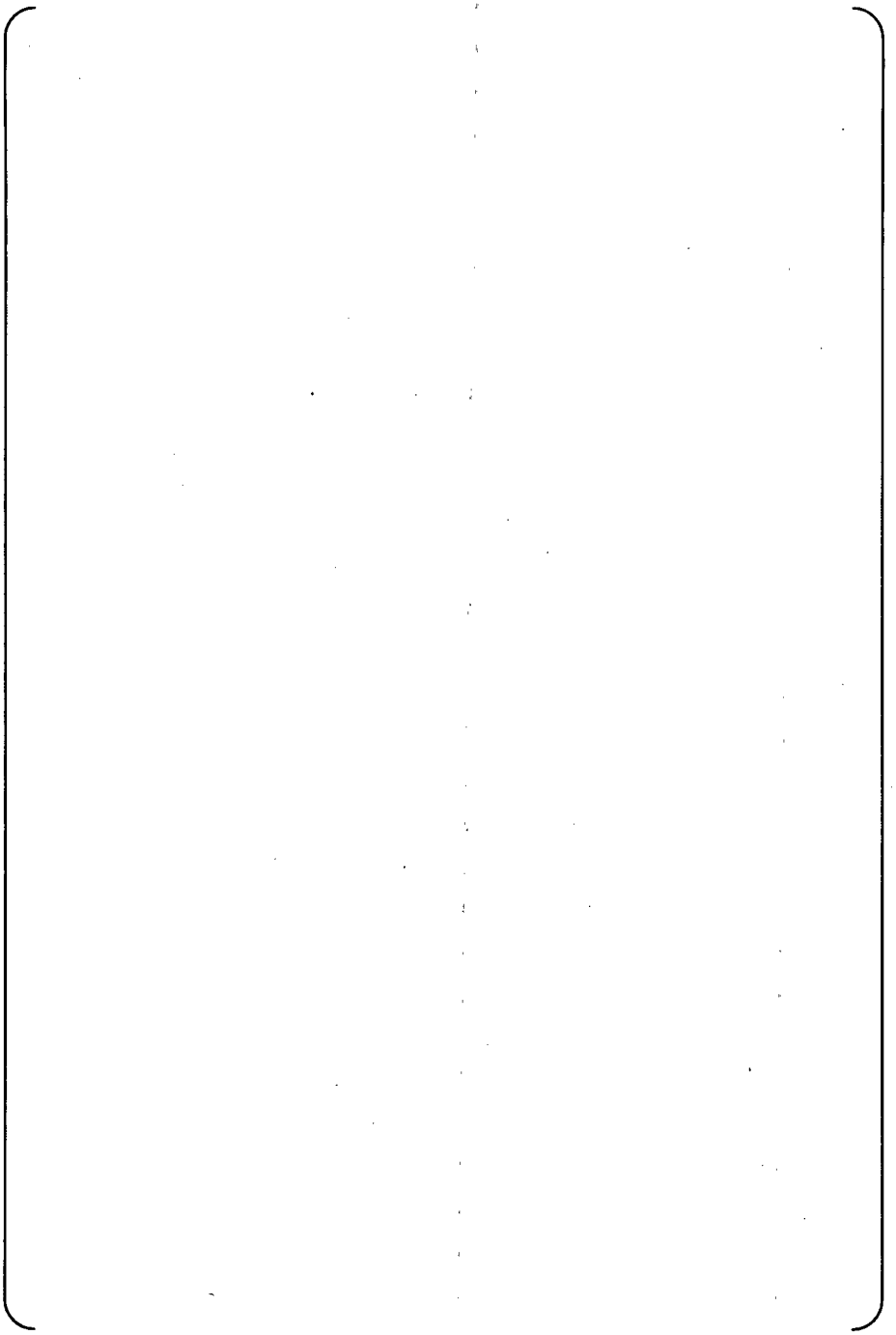

Fig. 5.6-4 Case-C3A': Gap distribution between AVBs and tubes in B6 section

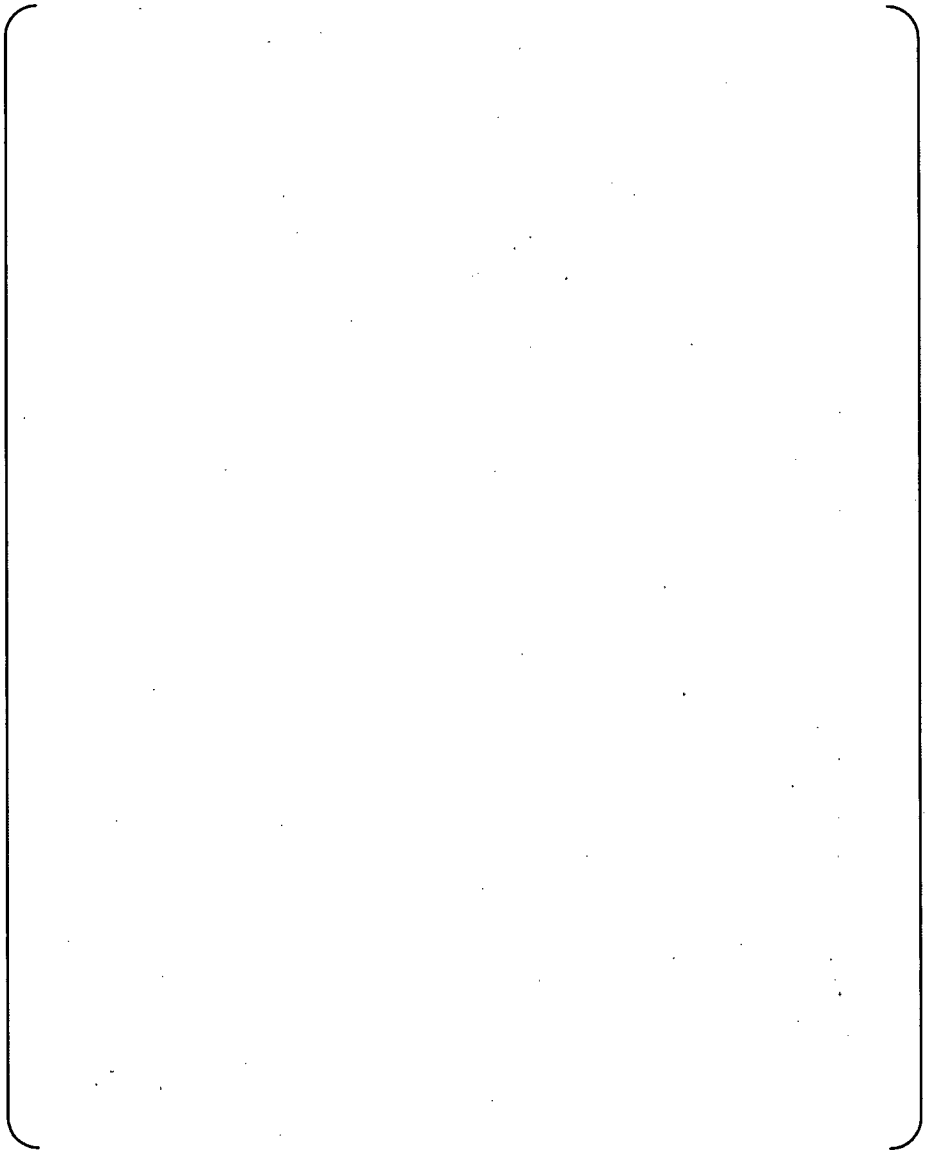

Fig. 5.6-5 Case-C3A': Gap distribution between AVBs and tubes in B5 section

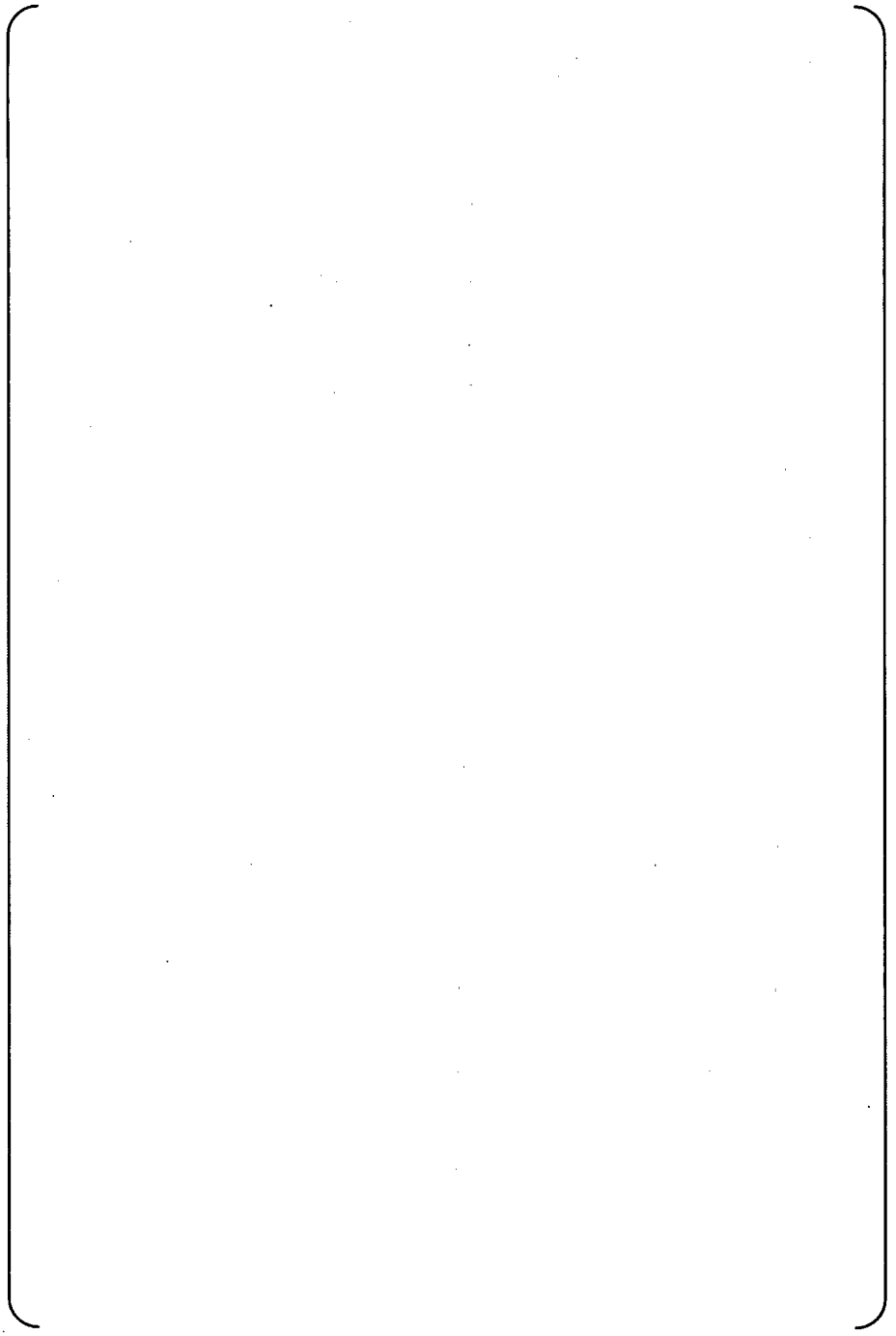

Fig. 5.6-6 Case-C3A': Gaps of tubes in Col.78 to adjacent AVBs

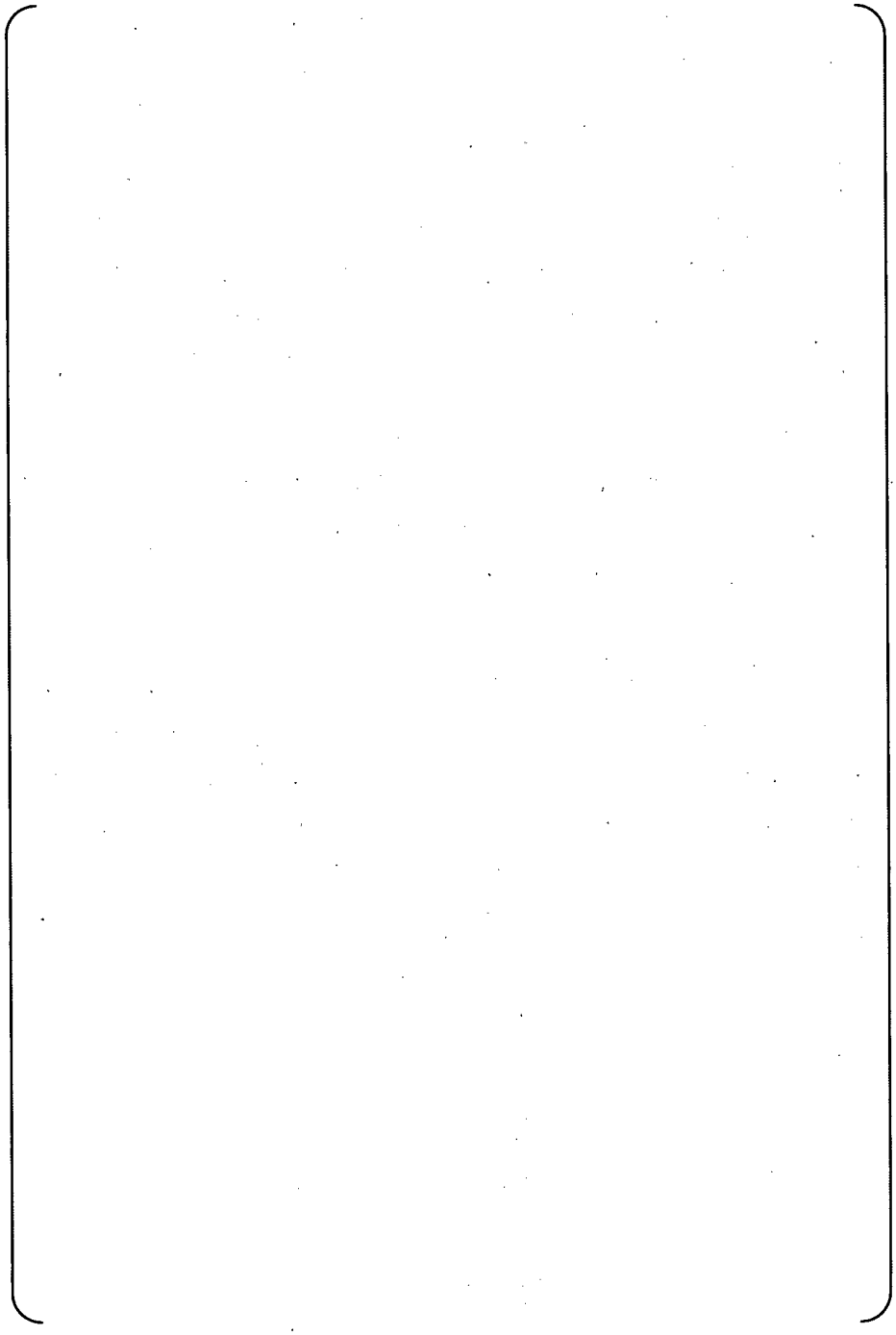

Fig. 5.6-7 Case-C3A': Distribution of contact forces between tubes and AVBs

5.7 Case-D1: Tube Deformation with manufacturing dispersion and the latest Hydrodynamic Force (AVB assembly in)

Figure 5.7-1 shows the "total" tube deformation. Tube bundle expands by manufacturing dispersion. Color counter shows no tendency of hydrodynamic force such as Case C3 series. This indicates that manufacturing dispersion is dominant for tube deformation and prevents hydrodynamic deformation due to large friction force.

In Case C3A', out-of-plane tube displacement pulls AVBs and retainer bars outward. In the center columns, this causes the retaining bars to displace downward. Figure 5.7-2 presents the displacement in vertical direction in Case D1. The center column AVBs in Case D1 seem to be fixed because friction force due to manufacturing dispersion is higher than Case C3A'.

Figure 5.7-3 shows AVB and retaining bar deformation mode along AVB-B06. The deformation mode is different from Case C3 series. The center column AVBs are fixed by high friction force. Outer column AVBs are moved up due to outer column tubes outward displacement.

Figures 5.7-4 shows the gap distributions between tubes and AVBs at cross sections along AVBs B01, B02, and B05. The gaps are scattering by manufacturing dispersion distribution. The color contour in section B1 and B2 includes many blue (compression) plots than section B5. This indicates that reaction forces at B1 and B2 are larger than B5.

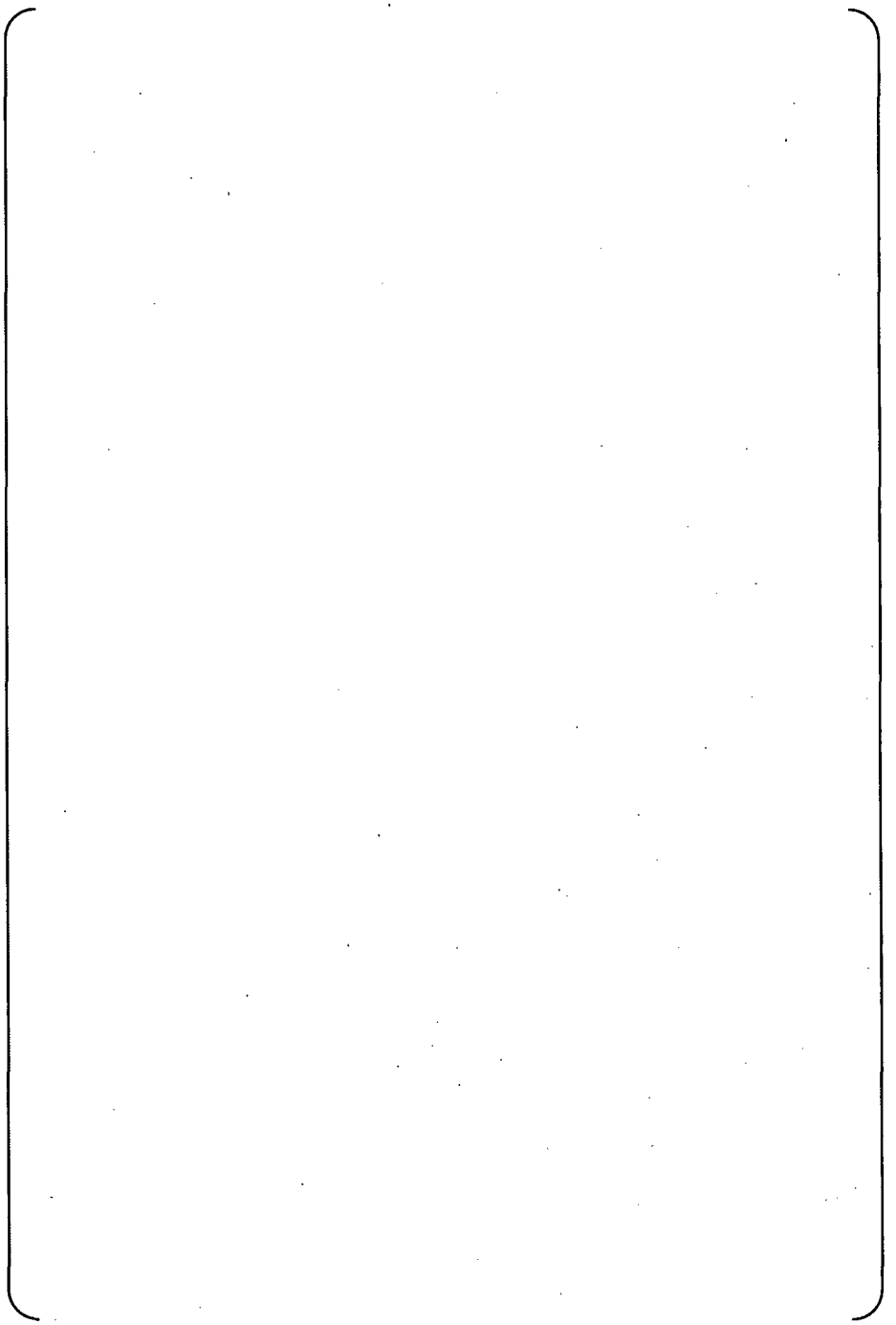

Fig. 5.7-1 Case-D1: Deformations due to dynamic pressure and manufacturing dispersion

Fig. 5.7-2 Case-D1: Vertical deformation contour due to dynamic pressure and manufacturing dispersion

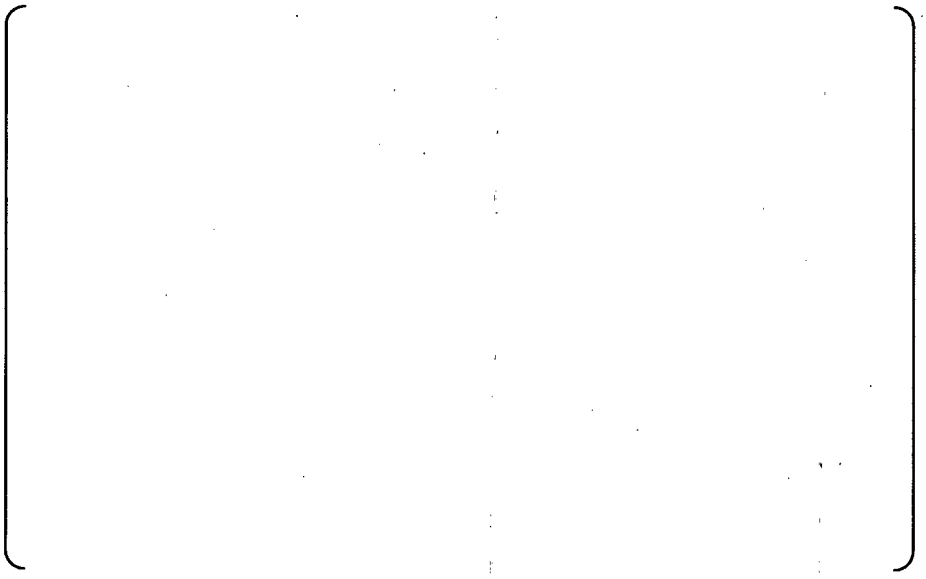

Fig. 5.7-3 Case-D1: Deformation mode due to dynamic pressure and manufacturing dispersion

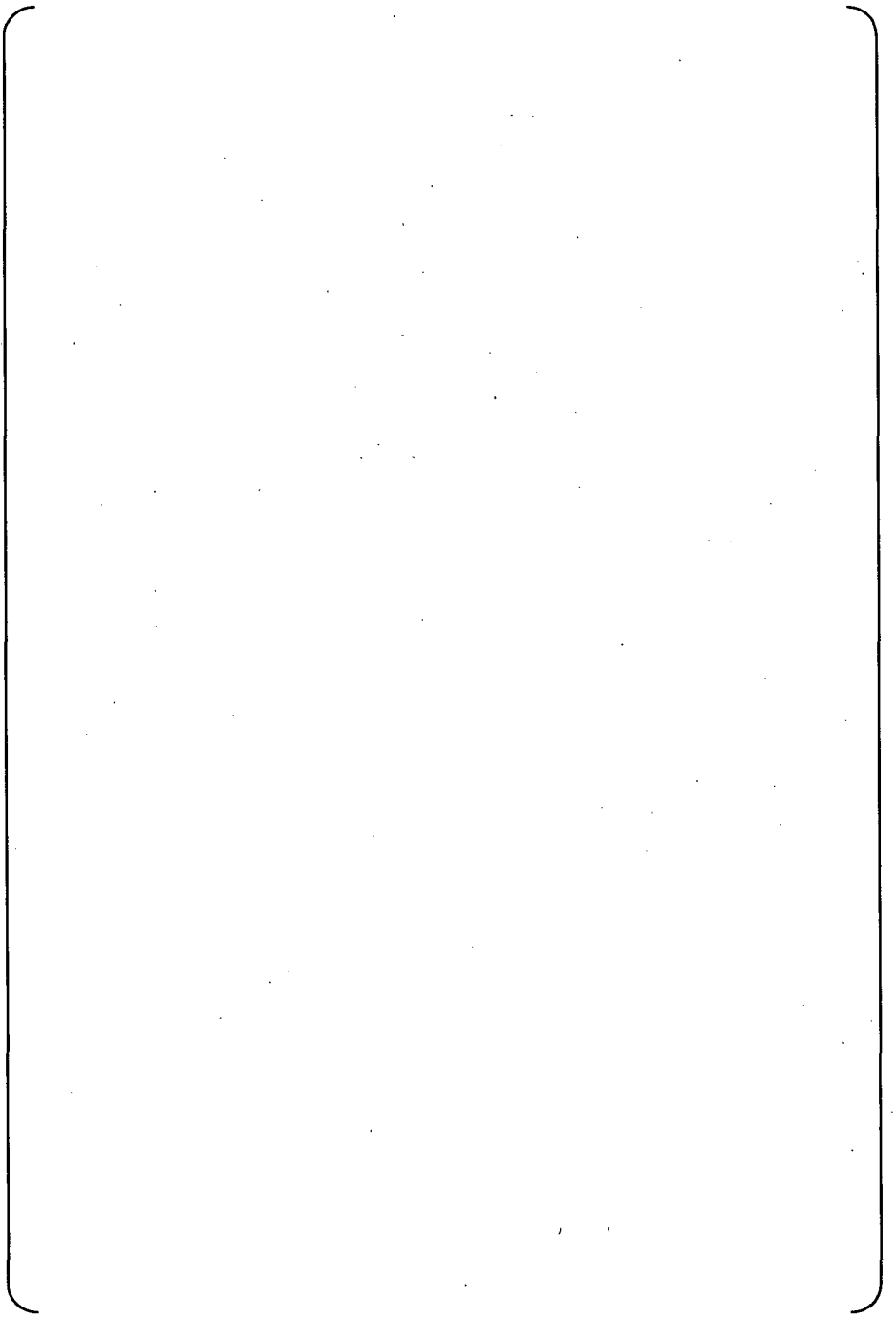

Fig. 5.7-4 Case-D1: Gap distribution between AVBs and tubes in B1, B2, and B5 section

Appendix-9
Simulation of Manufacturing Dispersion for Unit-2/3

1. Purpose

The wear in Unit-3 is more severe than Unit-2. This seems to be caused by difference of AVB-tube contact forces between Unit-2 and Unit-3. The contact force is generated by manufacturing dispersion; tube ovality, tube flatness, tube true position, AVB thickness deviation, AVB flatness, AVB twist. This appendix contains the evaluation of contact forces due to manufacturing dispersion between Unit-2 and Unit-3, and simulation of Ding signals in Unit-2. Fig.2-1 Distribution of contact forces in manufacturing dispersion analysis

2. Conclusion

The analyses results show a consistent with the Ding signal distributions (as shown in Fig.2-1) and trend that contact forces between tube and AVB in Unit-3 are less than half of Unit-2 contact force (as shown in Fig.2-2).

Unit-2 Unit-3

Fig.2-1 Distribution of contact forces in manufacturing dispersion analysis

Unit-2 Unit-3

Fig.2-2 Distribution of contact forces in manufacturing dispersion analysis

3. Assumption

1) The manufacturing dispersion of Unit-2 A-SG (E089) represents Unit-2, and Unit-3 A-SG(E089) represents Unit-3.

2) Tube G value, tube pitch, tube flatness, AVB thickness and AVB twist deviations are considered as manufacturing dispersion. AVB flatness regards as 0, because AVB flatness means not micro winding beyond each row but macro winding beyond scores rows, and this macro winding makes negligible small contact force due to less stiffness of AVB beyond scores rows. The initial gap between tube and AVB is nominal gap [ ] in cold condition, and this gap is changed according to deviation of above values. Each deviation is randomly given to the gap in the analysis model. The contact force of tube to AVB is generated as reaction force due to accumulation of each deviation.

3) The manufacturing deviation is assumed to follow normal distribution, so the standard deviation is adopted in the analysis. The actual standard deviation is used for measured dimensions. AVB twist is deviates based on the actual distribution in the verification test for AVB press load (refer to Attachment 9-1) in this study.

4) AVB nose thickness and twist for Unit-3 are assumed to be smaller than Unit-2 as shown in Table 6-1. In a process of AVB making up in shop, AVB nose area is pressed in order to flattening increased inside thickness due to bending. The press load was [ ] [N] for Unit-2 and [ ] [N] for Unit-3. The reason of this change is to improve AVB thickness and twist accuracy. All AVB twists for both Unit-2 and Unit-3 are satisfied with the tolerance specified in the design drawing, however checked by Go/No-go. Before adopting [ ] [N] pressing for Unit-3, a verification testing was performed. Attachment 9-1 shows a summary of the test results and AVB twist in [ ] [N] press is better than [ ] [N].

5) ECT ding signals are supposed to indicate elastic ding by reaction force due to manufacturing dispersion. [ ] [N] is a threshold of elastic ding as a result of ding testing. [ ] [N] is necessary to make plastic ding on tube, however such high reaction force is hardly generated in bundle rotation analysis and flowering analysis. Attachment 9-2 presents a result of simple ding testing.

4. Acceptance criteria

There are no acceptance criteria associated with this report since this evaluation is performed to compare the trend of the tube-to-AVB contact force in Unit-2 and Unit-3.

5. Design Inputs

5.1 Geometry

The nominal dimensions are obtained from the design drawings (Ref.1 to 7).

5.2 Manufacturing dispersion and tolerances

Tube G value, tube pitch, tube flatness, AVB thickness deviation, AVB twist, and AVB flatness are considered in manufacturing dispersion analysis. Figure 5.2-1 shows image of each deviation. Table 5.2-1 shows the manufacturing dimensions and tolerances. Table 5.2-2 presents measurement results of the dimensions. AVB thickness in bending portion is measured separately from straight bar, because AVB bending process makes AVB inside thickness increase.

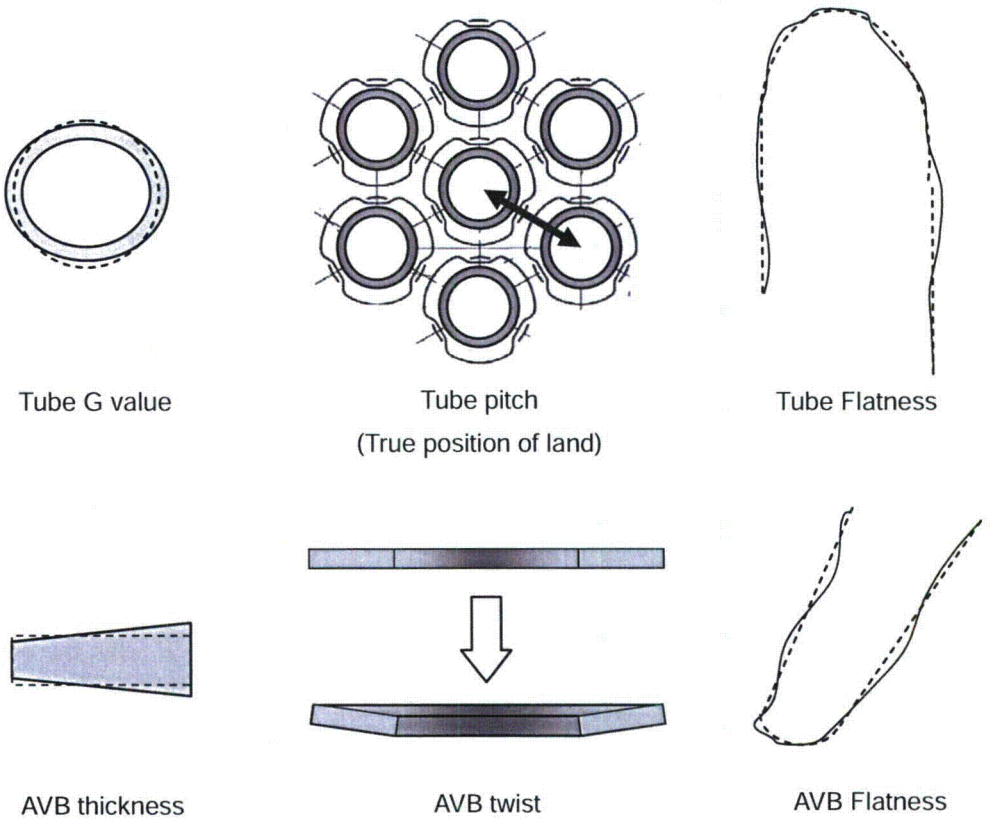

Figure 5.2-1 Image of manufacturing dispersion

Table 5.2-1 Dimensions and tolerances

	AVB			Tube		
	Thickness	Twist	Flatness	G value	Pitch	Flatness
Nominal	[					]
Tolerance						
Note	Measured	Go/No-go checked	Go/No-go checked	Measured	–	Go/No-go checked

Note: The tolerances are specified in the design drawings (Ref.4 and 7) and material specification (Ref.8)

Table 5.2-2 Measurement results of the dimensions

	AVB thickness change from nominal δ_A		Tube ovality δ_H	Standard deviation		
				AVB thickness change from nominal σ_A		Tube ovality σ_H
	Bending portion	Straight Bar		Bending portion	Straight Bar	
2A	[					]
2B						
Average in Unit-2						
3A						
3B						
Average in Unit-3						

6. Methodology

6.1 Analysis model

All parts of the U-bend assembly above the #6 TSP (Tubes, AVBs, Retaining bars, Retainer bars and Bridges) are modeled as beam elements. Figure 6.1-1 shows overview of the analysis model. The model area is a quarter by taking into account symmetry. The contact points between tube to AVB, and tube to TSP are modeled as gap elements, which show spring property in compression. This model is same as the flowering analysis model in Appendix-6. FEA code used is ABAQUS.

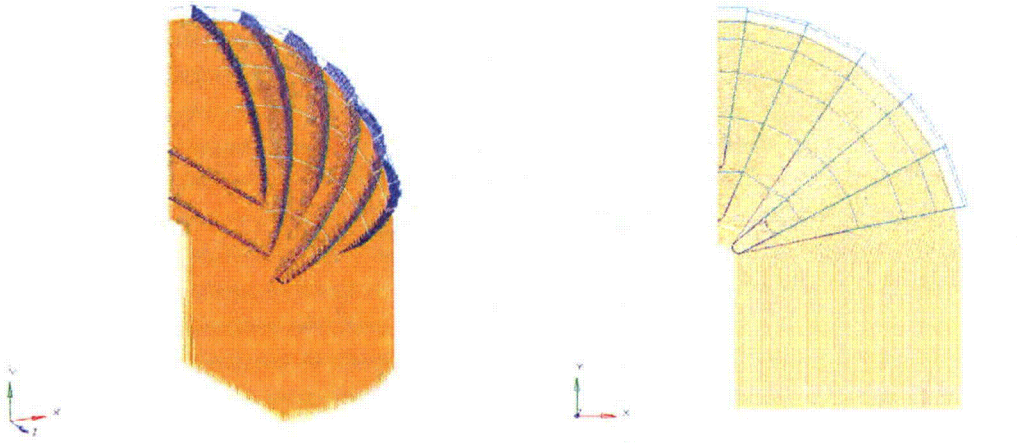

Bird's-eye View of the Model　　Front View of the Model

Figure 6.1-1 Analysis model

6.2 Inputs of manufacturing dispersion

6 types of the manufacturing dispersion introduced in Section 5.2 are considered in the analysis model. The deviation is generated according to random number and inputted to the gap elements in the analysis model. The random number dispersion follows normal distribution. Figure 6.2-1 indicates how to input the deviation to gap element in the analysis model. Especially for AVB twist, AVB twist factor in consideration of torsion stiffness is defined as a decrease function of distance from AVB bending peak, because the more contact points leave from AVB nose, the less AVB torsion stiffness is. Figure 6.2.2 shows AVB twist factor. In AVB nose area, the factor is always 1, because increased twist from nose tip and decreased stiffness from nose tip cancel each other. On the other hands, AVB twist is considered to be kept along the straight bar, so the factor decreases according to far from AVB nose.

Table 6.2-1 shows inputs used as manufacturing dispersion for the analysis model.

Total deviation = $\delta_0 + (\delta_A \pm 3\sigma_A)/2 + (\delta_H \pm 3\sigma_H)/2 + (\pm 3\sigma_S) + |\pm 3\sigma_{TA}|/2 + (\pm 3\sigma_{BA})/2 + (\pm 3\sigma_B)/2$

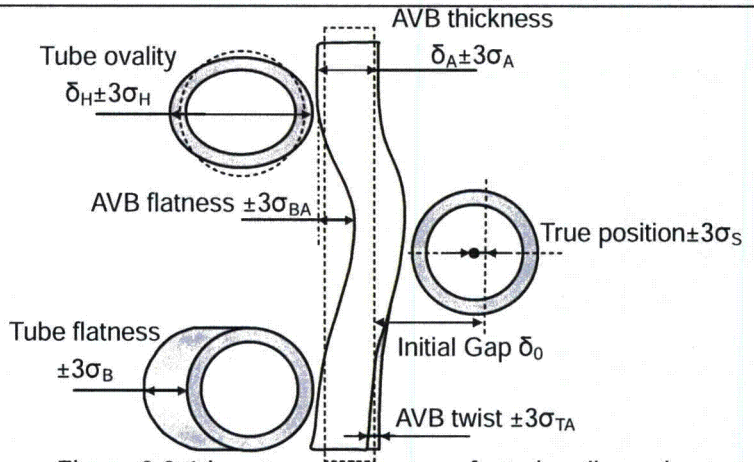

Figure 6.2-1 how to consider manufacturing dispersion

AVB nose

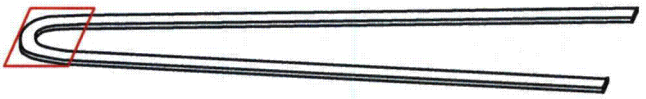

[ ]

Figure 6.2-2 how to consider manufacturing dispersion

6.3 Analysis cases

The manufacturing dispersion analyses are performed for the cases as shown in Table 6.2-1.

Table 6.2-1 Measurement results of the dimensions Unit: mm (mils)

Unit	AVB thickness change from nominal δ_A		Tube ovality δ_H	Standard deviation σ					
				AVB thickness change from nominal σ_A		Tube ovality σ_H	AVB twist*2 σ_{TA}	AVB Flatness*3 σ_{BA}	Tube Flatness σ_B
	Bending portion*1	Straight Bar		Bending portion	Straight Bar				
Case 1 Unit-2A (U2-E089)	[								]
Case 2 Unit-3A (U3-E089)									
Note	Measured*1	Measured	Measured	Measured	Measured	Measured	Go/No-go checked	Go/No-go checked	Go/No-go checked

Note)*1:AVB thickness of bending portion is assumed based on the fact obtained by the AVB pressing test results(See Attachment 9-2 for details), which indicated that AVB nose thicknesses of Unit-2 SGs are larger than Unit-3 SGs due to the difference of AVB pressing load ([ ] N for Unit-2 SGs and [ ] N for Unit-3 SGs) and the side wide AVBs of Unit-2 are thinner than other types of AVBs.

*2:AVB twist probability distributions are assumed based on the AVB pressing test results(See Attachment 9-2 for details). The probability distribution multiplied by the factor of each AVB type, shown in this table, is assumed.

*3: AVB Flatness is judged as 0, because AVB flatness is assumed macro distortion.

7. 7. Results

7.1 Simulation of Ding signals

Figure7.1-1 shows the distribution of contact forces over[ ][N], that is threshold of Ding signal, of Case1 and Figure7.1-2 shows the result of Case2. Case1 simulates Unit-2 and Case2 simulates Unit-3. The results are similar to Fig 1 of Attachment 9-3 of Ding signals distributions on PSI-ECT.

The manufacturing dispersion makes a lot of off-set points between tubes and AVBs. The higher force is generated at stiffer portion of tube and AVB, because the off-set is displacement control type loading. In AVB bending portion, AVB and tube (support span is shorter) are stiffer than straight bar region, so that much higher forces are generated at around Row 15(Center Wide AVBs nose), around Row 30(Side Narrow AVBs nose) and around Row 50(Center narrow AVBs nose). In the manufacturing dispersion analyses, much higher reaction forces are generated at AVB bending portion in Unit-2 than Unit-3, because AVB nose thickness and twist for Unit-2 is larger than those of Unit-3 due to difference of the press loads for flattening. This is assumed to be a mechanism of Ding signals and a cause of Ding signals difference between Unit-2 and Unit-3. Also, the assumptions in this study are supposed to be adequate by showing the similar contact force distributions to Ding signals.

7.2 Contact forces

Figure 7.2-1 and 7-2-2 present the distributions of the average contact forces of each row are shown for both Units and indicate that Unit-3 has smaller contact forces at AVB supports than Unit-2. This difference is one of causes that Unit-3 has more severe wears, because contact forces have a role to restrict tube vibration.

Fig.7.2-3 presents the displacement tendency of a representative tube (Row100) in Unit 3 and shows tube bundle expansion at each AVB contact point due to the dimensional variation. The displacements of tubes in outer columns and center AVB support points are larger than those in center columns and side AVB points. This tendency can be explained by Fig.7.2-4 that shows the image that tubes displacement is restricted by TSP.

This tube displacement means bundle expansion, and the equivalent average gap per each column in each AVB support point is found by dividing the expansion by the number of column. Fig.7.2-5 shows inverse of the average gap at each AVB support point. The inverse of the gap corresponds with ECT Voltage, because if gap increase, ECT voltage will decrease. Fig.7.2-5 is similar to the distribution of ECT signals shown in Fig.1 of Appendix-6.

Fig.7.1-1 distribution of contact forces in Case 1 [Unit-2]

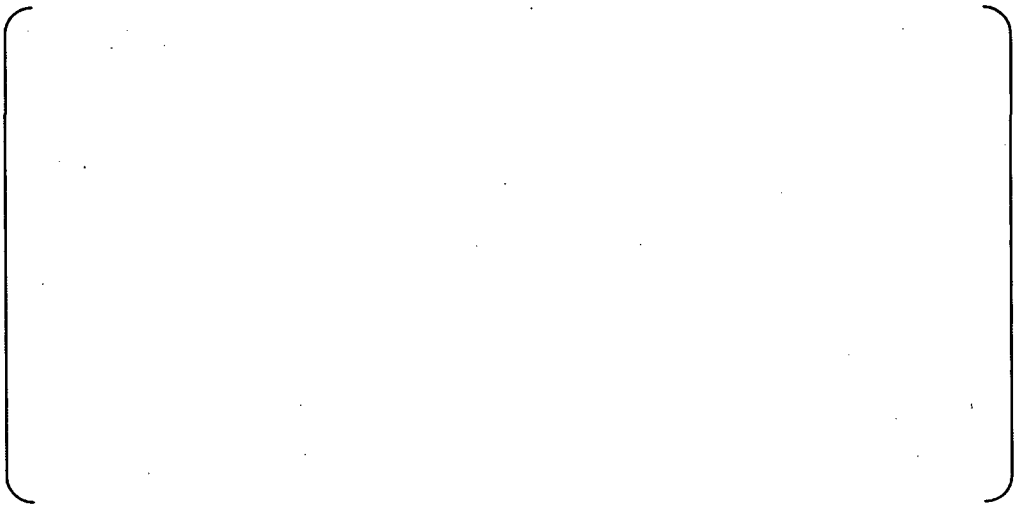

Fig.7.1-2 distribution of contact forces in Case 2 [Unit-3]

Fig.7.2-1 Distributions of the average contact forces of each row in Case 1
[Unit-2]

Fig.7.2-2 Distributions of the average contact forces of each row in Case 2
[Unit-3]

Fig.7.2-3 Displacement tendency at each AVB contact point of Row100 tubes in Case 2 [Unit-3]

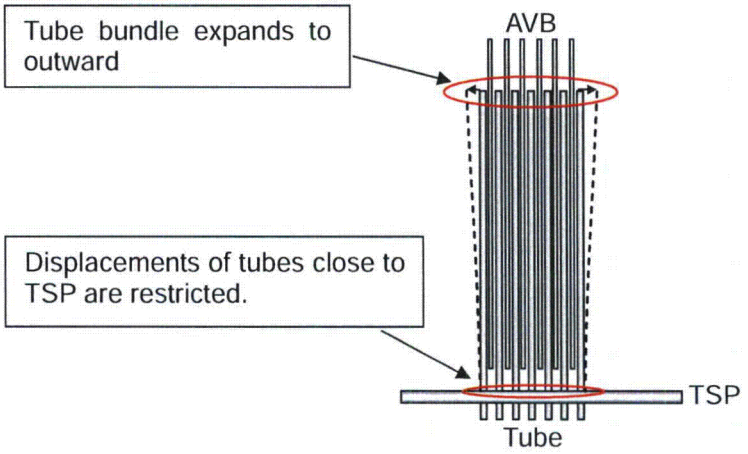

Fig.7.2-4 Interaction of TSP to tube displacement

Fig.7.2-5 Inverse of average gap at each AVB point Row100 tubes in Case 2 [Unit-3]

8. References

1) L5-04FU051 Rev.1 Design drawing of Tube Bundle 1/3
2) L5-04FU052 Rev.1 Design drawing of Tube Bundle 2/3
3) L5-04FU053 Rev.3 Design drawing of Tube Bundle 3/3
4) L5-04FU108 Rev.3 Design drawing of Tube Support Plate Assembly 3/3
5) L5-04FU111 Rev.2 Design drawing of Anti-Vibration Bar Assembly 1/9
6) L5-04FU112 Rev.1 Design drawing of Anti-Vibration Bar Assembly 2/9
7) L5-04FU118 Rev.3 Design drawing of Anti-Vibration Bar Assembly 8/9
8) L5-04FZ014 Rev.4, Purchase specification of heat transfer tubing

Attachment 9-1 Summary of verification test for AVB press load improvement

There is an AVB bending process in shop for AVB making up. In this process, AVB inside thickness increases due to bending. If as bent, AVB bending portion thickness deviate from the maximum tolerance specified in design drawing, so MHI presses AVB bending portion for flattening. In Unit-2, the press load is[ ], and it is necessary to touch up AVB bending inside portion after bending, because press load is insufficient to make the thickness within the maximum tolerance. In Unit-3, the press load is changed from[ ][N] to[ ][N] in order to improve AVB bending portion accuracy.

This attachment introduces the result of verification test for AVB press load change performed at that time.

- press load:[ ] [N],[ ][N],[ ][N]
- AVB twist measurement area

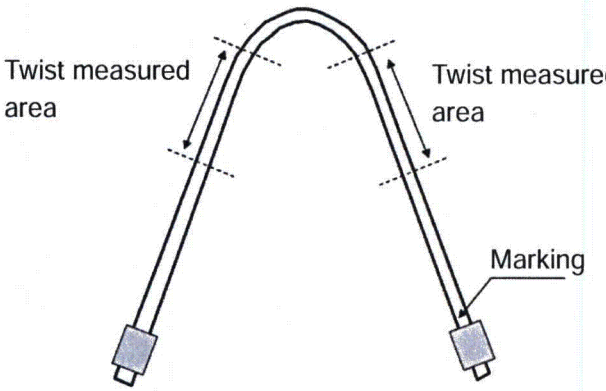

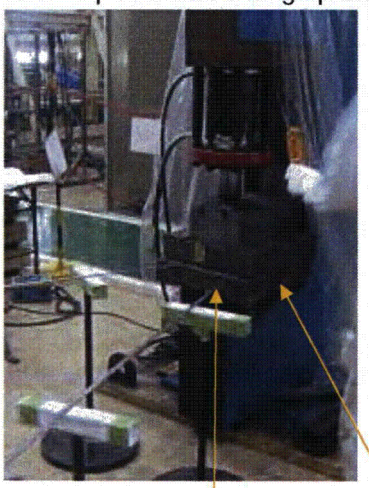

- Twist results

[ ]

- Summary
  - In Unit-2, AVB which twist deviates from the tolerance is needed to be flattened and touched up by hand, so that AVB twist satisfies the tolerance. In Unit-3, it comes to be not necessary to touch up after the[ ][N] press adopted.
  - The standard deviation of [ ][N] press is supposed to be about a half of [ ][N] press.

Attachment 9-2 Confirmation test for Ding load

There are a lot of Ding ECT signals indicated in Unit-2. The distribution trends of Ding signals are quite different between Unit-2 and Unit-3. So, MHI performed a simple mechanical load test in order to confirm that how much load was necessary to make Ding ECT signal (>[ ]V). This attachment provides the summary of the confirmation test.

➢ The correlation between load and ECT Ding signal is achieved by ECT testing at each load step.

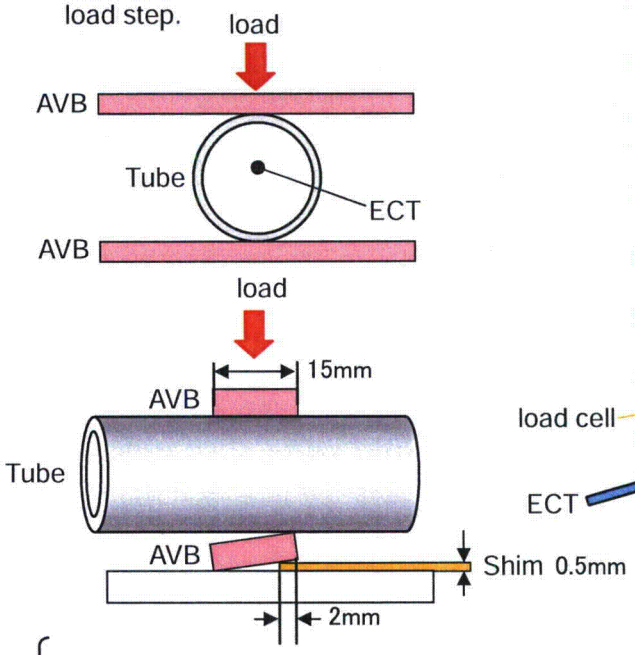

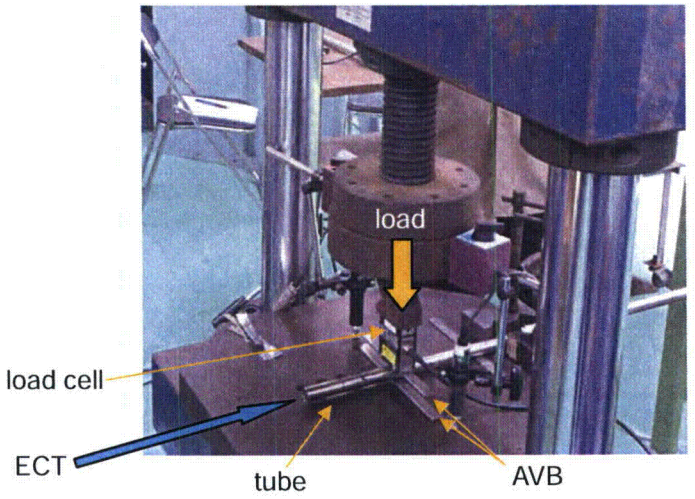

[ ]

➢ Summary

- In the case that[ ]V Ding signal means elastic ding, the minimum load is [ ][N]. If [ ] Ding signal means plastic ding, the minimum load[ ] [N] will be necessary.

Attachment 9-3 Ding Signals at U-bend Region from PSI

The PSI-ECT inspection was performed with all four SGs in the horizontal position. The Unit-2 SG inspection was performed at the SONGS site and the Unit-3 SG inspection was performed in the MHI shop prior to shipment. Analysis of the PSI data shows a distinct difference between the Unit-2 and Unit-3 SG. In the Unit-2 SGs there were many ding signals at the AVB tips that were not evident in the Unit-3 SGs as shown in Fig.1. The greater number of dings implies more interference between the tubes and AVBs, which correlates with a larger variation in gaps and presumably greater average tube-to-AVB contact force during operation. This is consistent with the finding that the tube-to-AVB gaps in the Unit-3 SG are slightly larger and that the average contact force is smaller in the Unit-3 SGs than in the Unit-2 SGs (refer to Appendix-6).

(a) Unit-2

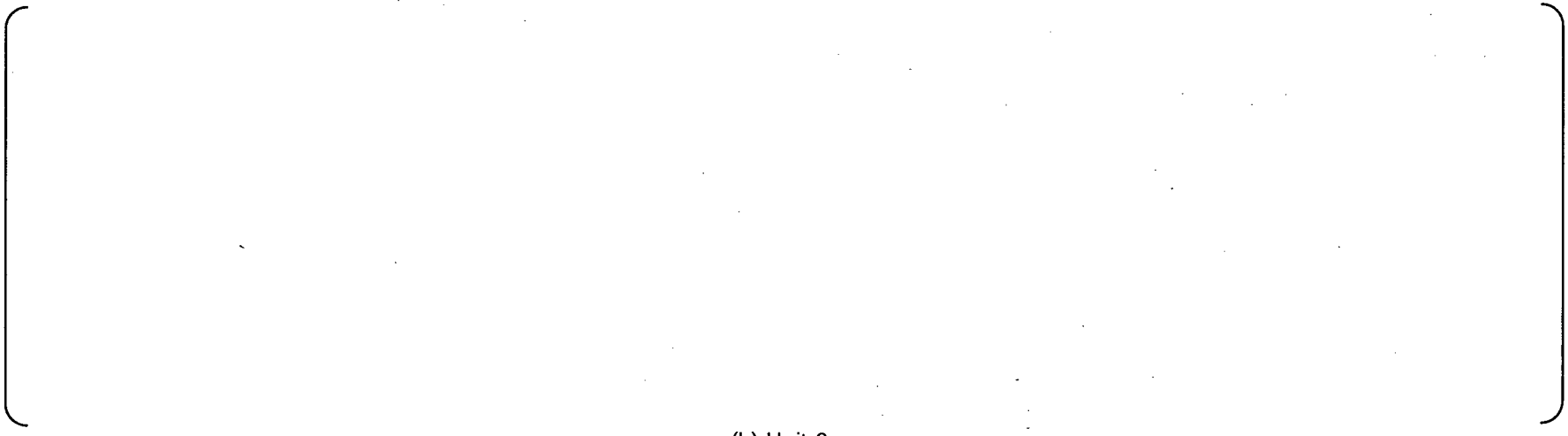

(b) Unit-3

Fig 4.1.2-3 Ding signals at U-bend region from PSI ECT